

Polysulfone Nanocomposites for Electrochemical Screening of Antibiotic Residues

By

LISEBO PHELANE



UNIVERSITY *of the*

A thesis submitted in fulfilment of the requirements for the degree of

Doctor of Philosophy

In the Department of Chemistry, Faculty of Science
University of the Western Cape
Bellville, Cape Town, South Africa

Supervisor: Prof Priscilla Baker
Co-Supervisor: Prof Emmanuel Iwuoha

April, 2017

ABSTRACT

Antibiotics are defined as any class of organic molecule that kills or inhibits microbes by specific interactions with bacterial targets. Antibiotics may be classified based on bacterial spectrum (broad versus narrow), route of administration, type of activity (bactericidal versus bacteriostatic), and origin (natural versus synthesized), and can also be classified based on their chemical structure. The intensive use of antibiotics for human (domestic and hospital use), veterinary and agriculture purposes, these compounds are continuously released into the environment from anthropogenic sources, such as wastewater treatment plants which are considered as one of the major source of evolution and spreading of antibiotic resistance into the environment.

In this study chemical sensors based on polysulfone nanocomposites were developed for the detection of antibiotic residues. Polysulfone (PSF) was prepared by dissolving polysulfone beads in N,N-dimethylacetamide. Graphene oxide (GO) was synthesized using the Hummers method which involves the oxidation of graphite to graphene oxide. The composite material was prepared by incorporating graphene oxide into the polysulfone matrix. Chemical sensors prepared from novel homogeneously blended polysulfone and graphene oxide suspensions, were characterised by cyclic voltammetry (CV), and electrochemical impedance spectroscopy (EIS), to determine formal potential, diffusional and interfacial charge transfer properties. Raman spectroscopy, fourier-transform infrared spectroscopy (FTIR) and scanning electron microscopy (SEM) were used to evaluate chemical composition of material and surface morphology. The qualitative analytical performance of the polymer nanocomposite sensors towards the selected antibiotic residues are reported here.

The spectroscopic techniques used confirmed successful synthesis of graphene oxide by the presence of graphene oxide spectral bands. The incorporation of graphene oxide into the polysulfone matrix was evident in the SEM image of the composite and also the improved contact angle value of the composite. Graphene oxide improved the electrochemical behaviour of polysulfone confirmed by the diffusion coefficient obtained from the cyclic voltammetry which was the highest when compared to that of the unmodified polysulfone. The polysulfone film introduced a blocking layer which reduced the electron transfer in the redox reaction of $K_3[Fe(CN)_6]$. PSF/GO showed enhanced electron transfer when compared

to bare BDDE. The diffusion coefficient and sensitivity for PSF-GO/BDD electrode was calculated to be $2.660 \times 10^{-4} \text{ cm}^2 \text{ s}^{-1}$ and $6.7587 \times 10^{-6} \text{ mV s}^{-1} / \text{A}$, respectively.

The analytical performance of the electrochemical sensors was measured by SWV, UV/Vis and EIS for the detection of the three antibiotic residues (norfloxacin, neomycin and penicillin G). SWV LODs were $4.92 \times 10^{-6} \text{ M}$, 8.85×10^{-6} and $9.62 \times 10^{-6} \text{ M}$ for norfloxacin, neomycin and penicillin G respectively. LOD results from EIS measurements were $3.13 \times 10^{-6} \text{ M}$, $3.69 \times 10^{-6} \text{ M}$ and $5.83 \times 10^{-6} \text{ M}$ for penicillin G, norfloxacin and neomycin, respectively. EIS results revealed that PSF-GO/BDD electrode showed the best quantitative response and highest sensitivity towards neomycin. The electrochemical sensors developed in this work showed very good analytical performance compared to literature reports, for these antibiotics. Complimentary calibration curves by UV/Vis spectroscopy was done for appreciation of the sensitivity of spectroscopy methods versus electrochemical methods.



KEYWORDS

Antibiotics

Norfloxacin

Penicillin G

Neomycin

Graphene Oxide

Chemical sensor

Polysulfone

Cyclic Voltammetry

Electrochemical Impedance Spectroscopy

Square Wave Voltammetry

UV/Vis spectroscopy



DECLARATION

I declare that **Polysulfone nanocomposites for electrochemical screening of antibiotic residues** is my own work, that it has not been submitted for any degree or examination in any other university, and that all sources I have used or quoted have been indicated and acknowledged by means of complete references.

Lisebo Phelane



April 2017

Signed.....

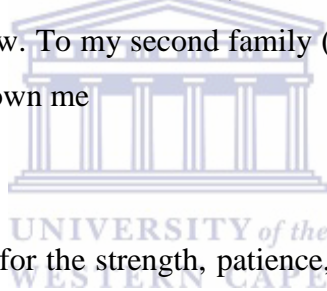
ACKNOWLEDGEMENTS

A big thank you to SensorLab management, more especially to my supervisors, Professor Priscilla G.L Baker and Professor Emmanuel Iwuoha, for the opportunity you given me to further my studies, your excellent supervision, support and encouragement during this period.

To all SensorLab researchers, I thank you for welcoming me and becoming my second family. Your help academically and your willingness to help is highly appreciated. A special thanks to Dr Brett Kuyper for helping me with the thesis write-up.

To my family: my father Thabang Phelane, Tlalane Phelane, Ntsoaki Phelane, Moleleki Phelane and Mamorena Phelane. My cousins: Nthabiseng Phelane, Mamokete Phelane, Thabiso Phelane and Rethabile Mdweksha. A big thank: you for your love, support, care, upbringing and your prayers through this difficult journey.

Lastly to my baby boy Reitumetse Mokete Phelane, mommy loves you so much. You are the reason I kept on pushing until now. To my second family (the Kgotlele's) I thank you all for the love and support you have shown me



All thanks to the Lord Almighty for the strength, patience, guidance and the will to keep on moving forward and reaching my goal.

DEDICATION

This project is dedicated to

My son

Mokete Reitumetse Phelane



UNIVERSITY *of the*
WESTERN CAPE

TABLE OF CONTENTS

<i>Title page</i>	i
<i>Abstract</i>	ii
<i>Keywords</i>	iv
<i>Declaration</i>	v
<i>Acknowledgements</i>	vi
<i>Dedication</i>	vii
<i>Table of content</i>	viii
<i>List of figures</i>	xiv
<i>List of tables</i>	xix
<i>Abbreviation</i>	xxi
<i>Academic Output</i>	xxiv
Chapter 1	1
1.1 Background	1
1.2 Scope of this study	6
1.3 Aims and Objectives of this study	8
1.3.1 Aims of the study	8
1.3.2 Objectives of this study	8
1.4 Conceptual diagram	9
1.5 Overview of the thesis	10
References	11
	viii

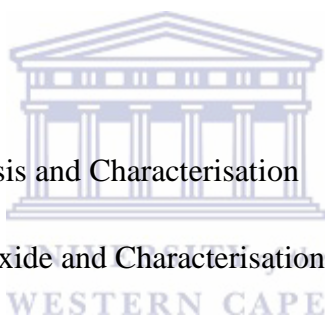


Chapter 2	14
2. Introduction	14
2.1 Classification of antibiotics	14
2.1.1 Aminoglycoside antibiotics	16
2.1.2 Sulfonamide antibiotics	18
2.1.3 β -Lactam antibiotics	20
2.1.4 Fluoroquinolone antibiotics	23
2.2 Methods used to detect antibiotics	26
2.2.1 High-Performance Liquid Chromatography	26
2.2.2 ELISA- Enzyme Linked Immunosorbent Assay	27
2.2.3 Spectrophotometer as a detection method	27
2.3. Limit of detection for fluoroquinolones	28
2.4 Limit of detection for β – Lactams	32
2.5. Limit of detection for Aminoglycoside	35
2.6. Conclusion	40
References	42
Chapter 3	56
3. Introduction	56
3.1. Electrochemical techniques	57
3.1.1 Voltammetric techniques	57
3.1.2 Impedimetric technique	59

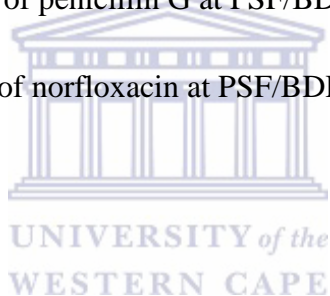
3.1.3 Amperometric technique	59
3.2. Electrochemical detection of Fluoroquinolone	59
3.3. Electrochemical detection of β -Lactam	65
3.4. Electrochemical detection of Aminoglycoside	68
3.5. Conclusion	70
References	72
Chapter 4	79
4.1. Spectroscopic Techniques	79
4.1.1 Fourier Transform Infra-Red Spectroscopy (FTIR)	79
4.1.2 UV-Vis Spectroscopy	80
4.1.3 Raman Spectroscopy	82
4.2. Scanning Electron Microscopy	83
4.3. Contact Angle	84
4.4. Electrochemical techniques	86
4.4.1 Cyclic Voltammetry	86
4.4.2 Square Wave Voltammetry	87
4.4.3 Electrochemical Impedance Spectroscopy	88
4.5. Reagents	91
4.5.1 Reagents or Chemicals used in this study	91
4.6. Instrumentation	91
4.6.1 Electrochemical measurements	91



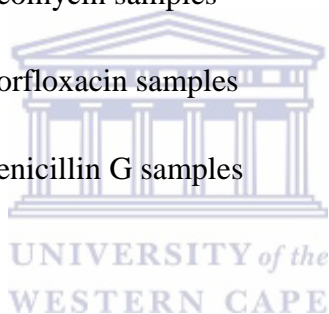
4.6.2 Scanning Electron Microscopy (SEM)	91
4.6.3 Contact Angle Instrument	91
4.6.4 Raman Spectroscopy	92
4.6.5 UV-Vis Spectroscopy	92
4.6.6 Fourier Transform Infrared Spectroscopy	92
4.6.7 Atomic Force Microscopy	92
References	93
Chapter 5	94
5.1. Graphene Oxide	95
5.2 Polysulfone	96
5.3 Materials Preparation, Synthesis and Characterisation	97
5.3.1 Synthesis of Graphene oxide and Characterisation	97
5.3.2 Characterisation of Graphene oxide	97
5.4. Preparation of polysulfone, composite of polysulfone with graphene oxide and Characterisation	102
5.4.1 Preparation of polysulfone	102
5.4.2 Modification of polysulfone with graphene oxide	104
5.4.3 Characterisation of polysulfone and polysulfone with graphene oxide composite	104
5.5. Contact angle studies	107
5.6. Conclusion	108
References	110



Chapter 6	113
6.1. Boron Doped Diamond electrode	113
6.2. Electrochemical Evaluation of polysulfone, polysulfone with graphene oxide and boron doped diamond	115
6.2.1 Cyclic voltammetry	115
6.2.2 Electrochemical impedance spectroscopy	120
6.3. Electrochemical response of three antibiotic residues at PSF/BDDE, PSF-GO/BDDE and BDDE	125
6.3.1 Cyclic voltammetry of neomycin at PSF/BDD, PSF-GO/BDD and BDDE	125
6.3.2 Cyclic Voltammetry of penicillin G at PSF/BDD, PSF-GO/BDD and BDDE	127
6.3.3 Cyclic voltammetry of norfloxacin at PSF/BDD, PSF-GO/BDD and BDDE	130
6.4. Conclusion	133
References	135
Chapter 7	137
7.1. Detection studies of neomycin	139
7.1.1 SWV detection of neomycin	139
7.1.2 EIS detection of neomycin	140
7.2. UV/Vis Analysis of neomycin	144
7.3 Detection studies of penicillin G	146
7.3.1 SWV detection of penicillin G	146
7.3.2 EIS detection of penicillin G	148
7.4. UV/ Vis analysis of penicillin G	152



7.5 Detection of norfloxacin	153
7.5.1 SWV detection of norfloxacin	153
7.5.2 EIS detection of norfloxacin	155
7.6. UV/Vis analysis of norfloxacin	159
7.7. Conclusion	163
References	165
Chapter 8	168
8.1. Recovery studies	168
8.1.1 Analysis of spiked neomycin samples	168
8.1.2 Analysis of spiked norfloxacin samples	171
8.1.3 Analysis of spiked penicillin G samples	174
8.2. Interference Studies	177
8.3. Conclusion	180
References	181
Chapter 9	182
9.1. Conclusion	182
9.2. Future Recommendations	185
Appendix	186



LIST OF FIGURES

FIGURE	TITLE	PAGE
1.1	Mechanisms of horizontal gene transfer (HGT) in bacteria and various antibiotic resistance strategies	4
2.1	Classes of antibiotics and their modes of action on bacteria	15
2.2	Chemical structure of Streptomycin (isolated from <i>Pseudomonas spp</i>) and Azithromycin (isolated from <i>Saccharopolyspora erythraea</i>)	17
2.3	Chemical structure of sulphonamide antibiotic known as Furosemide and Sulfamethoxazole sulphonamide antibacterial	19
2.4	Examples of β -lactam backbones	21
2.5	Nalidixic acid	24
2.6	Examples of Fluoroquinolones; norfloxacin (1 st generation), levofloxacin (2 nd generation) and moxifloxacin (3 rd generation)	24
4.1	Schematic diagram of an FTIR spectrometer	80
4.2	UV/Vis transition levels	81
4.3	Raman's energy levels	83
4.4	Schematic representation of SEM	84
4.5	Contact angle water droplets	85
4.6	SWV potential wave form	88
4.7	EIS spectrum and the Randles-Sevcik circuit	90
5.1	Conceptual diagram	94
5.2	(a) FTIR spectra of graphite	98

5.2	(b) FTIR spectra of graphene oxide	98
5.3	(a) Raman spectra of graphite	100
5.3	(b) Raman spectra of graphene oxide	100
5.4	SEM image of graphene oxide	101
5.5	(a) FTIR spectra of polysulfone	103
5.5	(b) FTIR spectra of polysulfone-graphene oxide	103
5.6	(a) Raman spectra of polysulfone	104
5.6	(b) Raman spectra of polysulfone-graphene oxide	104
5.7	SEM image of polysulfone	105
5.8	SEM image of polysulfone-graphene oxide nanocomposite	106
6.1	(a) Characterisation of 5 mM $K_3[Fe(CN)_6]$ at BDDE by CV	116
6.1	(b) Current vs. \sqrt{v} plot at bare BDDE	116
6.2	(a) Characterisation of 5 mM $K_3[Fe(CN)_6]$ at PSF/BDDE by CV	117
6.2	(b) Current vs. \sqrt{v} plot at unmodified PSF/BDDE	117
6.3	(a) Characterisation of 5 mM $K_3[Fe(CN)_6]$ at PSF-GO/BDDE by CV	118
6.3	(b) Current vs. \sqrt{v} plot at PSF-GO/BDDE	118
6.4	(a) Nyquist plot of bare BDDE	121
6.4	(b) Bode plot of bare BDDE	121
6.5	(a) Nyquist plot of unmodified PSF/BDDE	122
6.5	(b) Bode plot of unmodified PSF/BDDE	122
6.6	(a) Nyquist plot of PSF-GO/BDDE	123

6.6	(b) Bode plot of PSF-GO/BDDE	123
6.7	(a) Characterisation of neomycin at bare BDDE by CV	125
6.7	(b) Characterisation of neomycin at unmodified PSF/BDDE by CV	126
6.7	(c) Characterisation of neomycin at PSF-GO/BDDE by CV	126
6.8	(a) Characterisation of penicillin G at bare BDDE by CV	128
6.8	(b) Characterisation of penicillin G at unmodified PSF/BDDE by CV	128
6.8	(c) Characterisation of penicillin G at PSF-GO/BDDE by CV	129
6.9	(a) Characterisation of norfloxacin at bare BDDE by CV	131
6.9	(b) Characterisation of norfloxacin at unmodified PSF/BDDE by CV	132
6.9	(c) Characterisation of norfloxacin at PSF-GO/BDDE by CV	132
7.1	Conceptual diagram	137
7.2	(a) Detection of neomycin by SWV	139
7.2	(b) Calibration curve of neomycin with standard error bars	140
7.3	(a) Detection of neomycin by EIS at PSF-GO/BDDE	141
7.3	(b) Bode plot of neomycin at PSF-GO/BDDE	141
7.4	Randles-Sevcik equivalent circuit	142
7.5	(a) Calibration curve of neomycin at PSF-GO/BDDE	142
7.5	(b) Calibration curve of neomycin with error bars (SN=3)	143
7.6	(a) Detection of neomycin by UV/Vis	145
7.6	(a) Calibration curve of neomycin	145
7.7	(a) Detection of penicillin G by SWV	146

7.7	(b) Calibration curve of penicillin G	147
7.8	(a) Detection of penicillin G by EIS at bare BDD electrode	149
7.8	(b) Bode plot of penicillin G at bare BDDE	149
7.9	(a) Calibration curve of penicillin G at bare BDDE	150
7.9	(b) Calibration curve of penicillin G with error bars (SN=3)	150
7.10	(a) Detection of penicillin G by UV/Vis	152
7.10	(b) Calibration curve of penicillin G	153
7.11	(a) Detection of norfloxacin by SWV	154
7.11	(b) Calibration curve of norfloxacin (SN=3)	154
7.12	(a) Detection of norfloxacin by EIS at unmodified PSF/BDDE	156
7.12	(b) Bode plot of norfloxacin at unmodified PSF/BDDE	156
7.13	(a) Calibration curve of norfloxacin at unmodified PSF/BDDE	157
7.13	(b) Calibration curve of norfloxacin with error bars (SN=3)	158
7.14	(a) Detection of norfloxacin by UV/Vis	159
7.14	(b) Calibration curve of norfloxacin	160
8.1	(a) Figure 8.1a: SWV response of tap water sample spiked in 0.1 M PBS pH 7.0	169
8.1	(b) SWV response of sample 1 (neomycin + tap water sample) spiked in 0.1 M PBS pH 7.0	169
8.1	(c) SWV response of sample 2 spiked in 0.1 M PBS pH 7.0.	170
8.2	Calibration curve of Neomycin	170
8.3	(a) SWV response of tap water sample spiked in 0.1 M HCl	172

8.3	(b) SWV response of sample 3 (norfloxacin + tap water) spiked in 0.1 M HCl	172
8.3	(c) SWV response of sample 2 spiked in 0.1 M HCl	173
8.4	Calibration curve of norfloxacin at unmodified PSF/BDDE	173
8.5	(a) SWV response of tap water sample in 0.1 M PBS pH 7.0	175
8.5	(b) SWV response of sample 4 (tap water + penicillin G) spiked in 0.1 M PBS pH 7.0	175
8.5	(c) SWV response of sample 2 spiked in 0.1 M PBS pH 7.0	176
8.6	Calibration curve of penicillin G	176
8.7	SWV response of urine sample spiked with penicillin G at bare BDD electrode	177
8.8	SWV response of urine sample spiked with norfloxacin at unmodified PSF/BDD electrode	178
8.9	SWV response of urine sample spiked with neomycin at PSF-GO/BDD electrode	179

LIST OF TABLES

TABLE	TITLE	PAGE
1.1	Different classes of antibiotics and their mechanism of action	2
1.2	Characteristics of different elements involved in the spread of resistance gene	5
2.1	Comparison of fluoroquinolones LODs from different analytical methods	29
2.2	Comparison of β -Lactams LODs from different analytical methods	33
2.3	Comparison of aminoglycoside LODs from different analytical methods	36
3.1	Biosensor performance for fluoroquinolones.	61
3.2	Biosensor performance for β -lactams	66
3.3	Biosensor performance for Aminoglycosides	69
5.1	Contact angle results of the prepared materials.	108
6.1	Diffusion coefficient, sensitivity and formal potential of $K_3[Fe(CN)_6]$ at BDD, PSF/BDD and PSF-GO/BDD	119
6.2	Impedance results of $K_3[Fe(CN)_6]$ dissolved in water only at BDD, PSF/BDD and PSF-GO/BDD	124
6.3	Diffusion coefficient of penicillin G at different electrode material	129
6.4	Diffusion coefficient of norfloxacin at different electrode material	133
7.1	LOD of all three selected antibiotics residues	160
7.2	Comparison of Sensor performance	162
7.3	Summary of Sensor Performance	163

8.1	Recovery % of neomycin at PSF-GO/BDDE	171
8.2	Recovery % of norfloxacin at PSF/BDDE	174



ABBREVIATIONS

FTIR	Fourier Transform Infrared
CV	Cyclic Voltammetry
SEM	Scanning Electron Microscopy
EIS	Electron Impedance Microscopy
SWV	Square Wave Voltammetry
PSF	Polysulfone
GO	Graphene Oxide
PSF-GO	Polysulfone with graphene oxide
BDDE	Boron Doped Diamond Electrode
NOR	Norfloxacin
CIP	Ciprofloxacin
MOX	Moxifloxacin
ENO	Enofloxacin
LOM	Lomefloxacin
FQ	Fluoroquinolone
AG	Aminoglycoside
HPLC	High Performance Liquid Chromatograph
ELISA	Enzyme-Linked Immunosorbent Assay
UV	Ultraviolet
Vis	Visible
LOD	Limit of Detection
PABA	p-Aminobenzoic acid
APA	6-Aminopenicillanic acid
MIC	Minimum Inhibitory Concentration

MRL	Maximum Residue Limits
GCE	Glassy Carbon Electrode
DPV	Differential Pulse Voltammetry
CA	Chrono Amperometry
ASV	Anodic Stripping Voltammetry
Ampero	Amperometry
HRP	Horseshoe Peroxidase
PPy	Polypyrrole
MWCNT	Multi-Walled Carbon Nanotube
LUMO	Lowest Unoccupied Molecular Orbital
HOMO	Highest Occupied Molecular Orbital
DNA	Deoxyribonucleic acid
ssDNA	single-stranded Deoxyribonucleic acid
STD	Sexually Transmitted Disease
NMR	Nuclear Magnetic Resonance
TLC	Thin Layer Chromatography
AAS	Atomic Absorption Spectroscopy
CL	Chemoluminescence
BRO	Bromanil
AP	Alkaline Phosphate
SDS	Sodium Dodecyl Sulfate
BLaR	Bacillus licheniformis beta-lactamase
CTD	Carboxy terminal
TFA	Trifluoroacetic acid
TGA	Thioglycolic acid
HFBA	Heptafluoro butyric acid

ESI	Electrospray ionization
MS	Mass Spectroscopy
EDC	1-Ethyl-3-[3-dimethylaminopropyl]carbodiimide hydrochloride
GDA	Glutaraldehyde
STRS	Streptomycin Sulphate
SLNS	Solid Lipid Nanoparticle
SNP	Sodium Nitroprusside
FLD	Fluorescence detection
SELEX	Systematic Evolution of Ligands by Exponential Enrichment
AuNP	Gold nanoparticle
FRET	Fluorescence Resonance Energy Transfer
SERS	Surface Enhance Raman Spectroscopy
LDI	Laser Desorption Ionization



ACADEMIC OUTPUT

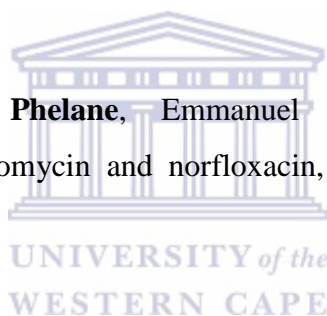
Publications

Lisebo Phelane, Francis N. Muya, Heidi L. Richards, Priscilla G.L. Baker, Emmanuel I Iwuoha, Polysulfone Nanocomposite Membranes with improved hydrophilicity. *Electrochimica Acta*, 128 326–335 (2014).

Francis N. Muya, **Lisebo Phelane**, Priscilla G. L. Baker, Emmanuel I. Iwuoha, Synthesis and Characterization of Polysulfone Hydrogels; *Journal of Surface Engineered Materials and Advanced Technology*, 4 227-236 (2014).

Lisebo Phelane, Siyabulela Hamnca, Priscilla Baker, Emmanuel Iwuoha, Electrochemical transduction at modified boron doped diamond Interfaces, *Journal of Nanoresearch*, 44, 51-62 (2016).

Siyabulela Hamnca, **Lisebo Phelane**, Emmanuel Iwuoha and Priscilla Baker, Electrochemical detection of neomycin and norfloxacin, *Analytical Letters* (accepted for publication) 2016



Conferences

Poster presentation, Materials, Analytical and Physical Electrochemistry Today, 3rd International Symposium on Electrochemistry, 26-28 May 2015, South Africa

Oral presentation, 67th Annual Meeting of the International Society of Electrochemistry, Electrochemistry: from Sense to Sustainability, 21 - 26 August 2016, Netherlands

CHAPTER I

INTRODUCTION

This Chapter gives the background and introduction of the study. Different classes of antibiotics are discussed and also discuss the mechanism of antibiotic resistant bacteria. Both the aims and objectives of the study are listed.

1.1 Background

Antibiotics are defined as chemical compounds used in the treatment and prevention of bacterial infection. They may either kill or inhibit the growth of bacteria. Sir Alexander Fleming in 1928 discovered the first antibiotic. The structure of penicillin was discovered and later published as a remedy for infections, inflammations and diseases [1-3]. The term antibiotic was first used by Waksman in 1945, when he defined it as a chemical substance of microbial origin that possesses antibiotic effect. Most antibiotics are natural drugs produced by several fungi or bacteria and the chemotherapeutic drugs are man-made substances. Nonetheless the differences were put an end after chemical synthesis of some antibiotics has been realized and new drugs have been developed from the natural products with various binding side chains to the basic structure [2-7]. The history of antibiotics begun in 1932 when the first sulfonamide was prepared and their expansion appeared to have developed 5000 substances during years 1932-1945. They are effective in treating and inhibiting urinary tract infections, pneumococcal pneumonia and even in purulent meningitis. The effect of sulfonamides was exceeded by that of penicillin and streptomycin. It was a great chance that these two antibiotics covered the whole spectrum of bacteria. Penicillin was highly effective against the most microbes of that time. Streptomycins are effective against the gram-negative aerobic bacteria and *Mycobacterium tuberculosis* [3-6].

Antibiotic compounds are mainly made-up of cyclic structures, represented by benzene rings, piperazine units, hexahydropyrimidines, as well as sulfonamides, quinolone and morpholine groups. These compounds have meta-stable properties and yield activated metabolites. Conjugates and hydroxylated forms of compounds after processing in humans and animals

lead to a range of diverse active chemical compounds being continuously released in the environment [1,8-10]. Antibiotics may be classified based on bacterial spectrum (broad versus narrow), route of administration, type of activity (bactericidal versus bacteriostatic), and origin (natural versus synthesized) [4-5]. They can also be classified based on their chemical structure. Table below (Table 1.1) consist of different classes of antibiotics, their mechanism of action and use. Antibiotics within a structural class generally have similar patterns of effectiveness, toxicity, and allergic potential.

Table 1.1: Different classes of antibiotics and their mechanism of action

Antibiotic class	Mechanism of action	Use
Aminoglycosides (Gentamycin, Neomycin, Amikacin)	Inhibition of bacterial protein synthesis	Growth promoter
Sulfonamides (Sulfadiazine, sulfamethoxazole, sulfapyridine)	Blocks bacterial cell metabolism by inhibiting enzymes	Therapeutic
β-lactam (penicillins, amoxicillin)	Inhibition of bacterial cell wall synthesis	Therapeutic
Fluoroquinolones (Norfloxacin, ofloxacin, enoxacin)	Inhibition of bacterial DNA synthesis	Growth promoter
Tetracyclines (chlortetracycline, oxytetracycline, doxycycline)	Inhibition of bacterial protein synthesis	Growth promoter
Macrolides (erythromycin, azithromycin, tylosin)	Inhibition of bacterial protein synthesis	Therapeutic

Antibiotics offered a solution to the problems faced against infectious diseases. They are useful in a wide variety of infections and their discovery improved the lives of humans for the better. The intensive use of antibiotics for human (domestic and hospital use), veterinary and agriculture purposes, these compounds are continuously released into the environment. Anthropogenic sources, such as wastewater treatment plants which are considered as one of the major source of evolution and spreading of antibiotic resistance into the environment. The presence of antibiotics in environmentally relevant concentration levels has been associated to chronic toxicity and the prevalence of resistance to antibiotics in bacterial species [12]. Most antibiotics are excreted from humans and animals as the parent compound. These compounds enter natural environments either through wastewater treatment plants and fertiliser [1,13,14].

The use of antibiotics may induce the development of antibiotic resistant bacteria (ARB) and antibiotic resistant genes (ARGs), which involves health risks to humans and animals [15]. Prolonged therapy with antibiotics can lead to the development of resistance in a microorganism that was initially sensitive to antibiotics, but later it can adapt gradually and develop resistance to antibiotics. Bacteria have developed and optimized their genetic arsenal to deal with the action of antibiotics. When an antibiotic attacks bacteria, bacterial cells susceptible to it will die, but those that have some insensitivity will survive [13-16]. Bacterial antibiotic resistance can be attained through intrinsic or acquired mechanisms; Figure 1.1 illustrates the different mechanisms of antibiotic resistance. Intrinsic mechanisms are those specified by naturally occurring genes found on the host's chromosome. Acquired mechanisms involve mutations in genes targeted by the antibiotic and the transfer of resistance determinants borne on plasmids, bacteriophages, transposons, and other mobile genetic material. This exchange is accomplished through the processes of transduction (via bacteriophages), conjugation (plasmids and, conjugative transposons), and transformation (via incorporation into the chromosome of chromosomal DNA plasmids, and other DNAs from dying organisms). Plasmids contain genes for resistance and many other traits; they replicate independently of the host chromosome and can be distinguished by their origins of replication. Transposons are mobile genetic elements that can exist on plasmids or integrate into other transposons or the host's chromosome [13,17]. Different characteristic elements involved in the spread of resistance gene are listed in Table 1.2.

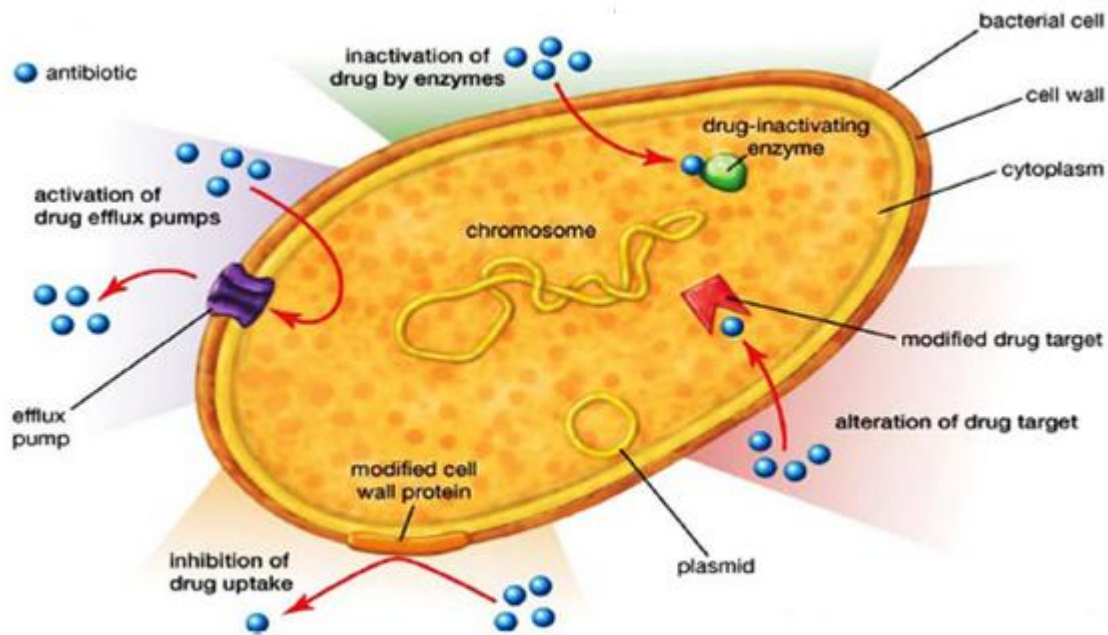


Figure 1.1: Mechanisms of horizontal gene transfer (HGT) in bacteria and various antibiotic resistance strategies [18]

The above figure shows the different mechanisms for antibiotic resistance against bacteria. The mechanism of bacteria resistance is focused mainly on four mechanisms which are: inactivation or modification of the antibiotic which render it inactive through physical removal from the cell, or modify target site so that it is not recognized by the antibiotic. The second mechanism is an alteration in the target site of the antibiotic that reduces its binding capacity; modification of metabolic pathways to circumvent the antibiotic effect; reduced intracellular antibiotic accumulation by decreasing permeability and/or increasing active efflux of the antibiotic.

Table 1.2: Characteristics of different elements involved in the spread of resistance gene

Element	Characteristic	Role in spread of resistance gene
Self-transmissible plasmid	Circular, autonomously replicating element; carries genes needed for conjugal DNA transfer	Transfer of resistance genes, mobilization of other elements that carry resistance genes
Conjugative transposon	Integrated elements that can excise to form a non-replicating circular transfer intermediate; carries genes needed for conjugal DNA transfer	Same as transmissible plasmid
Mobilizable plasmid	Circular, autonomously replicating element; carries genes that allows it to use conjugal apparatus provided by a self-transmissible plasmid	Transfer of resistance genes
Transposon	Can move from one DNA segment to another within the same cell	Can carry resistance genes from chromosome to plasmid or vice versa
Gene cassette	Circular, non-replicating DNA segments containing only open reading frames; integrates into integrons	Carry resistance genes
Integron	Integrated DNA segments that contains an integrase, a promoter, an integration site for gene cassette	Form clusters of resistance genes, all under the control of the integron promoter

The increasing concern about anti-bacterial resistance resulted in the development of many analytical methods to determine levels of antibiotic residues in the environment. Measurement of antibiotics is a necessity to remediate the overloading of antibiotics. Analytical methods for determining or detecting antibiotics can be classified into two groups, which are confirmatory and screening method [17-19]. Confirmatory methods are based on chromatographic techniques coupled with UV detector for the determination of the concentrations of analyte. However the drawback of this method limits their use because they are time-consuming, expensive, and require intricate laboratory equipment and trained personnel. The second method namely screening method enables the detection of an analyte or a family at the level of interest, and usually provides semi-quantitative results [19-20]. The use of this method offers ease of use, short analysis time, good selectivity and low cost. The drawbacks of these techniques limit their use, therefore biosensors address the problems faced when the confirmatory and screening methods are used. Biosensors use a semi-quantitative approach, which makes them a very practical solution in the large-scale detection of antibiotic residues.



1.2 Scope of this study

The importance of antibiotics is increasingly slowed down by incredibly and globally spread occurrence of bacterial resistance against these treatments, a phenomenon that arose with the discovery of antibiotics and remains an increasing problem. The further development of bacterial resistance has to be stopped, by reducing the contamination of the environment with antibiotics. The overuse and the misuse of antibiotics have led to microbial resistance. As a result, common infections are more difficult to treat, extending hospitalization and increasing the cost to the health system. Currently, resistance affects virtually all major bacterial pathogens and all types of epidemiological settings. During continuous exposure to antibacterials, sequential chromosomal mutations can occur, leading to the appearance of resistance mechanisms step by step [1,13]. Several factors contribute to the occurrence of bacterial resistance: (i) the inappropriate use/misuse of antibacterials in humans; (ii) the veterinary use of antibacterials in pets, farm animals and animals raised in aquaculture; and (iii) the increased occurrence of antibacterials or their metabolites contaminating the environment, mainly resulting from the latter applications [14]. To ensure the efficiency of

antibacterial treatments in the near future, the further development of bacterial resistance has to be stopped, by reducing the contamination of the environment with antibiotics [23].

Pharmaceutical residues have traditionally been detected using qualitative or semi-quantitative screening methods, with only suspected samples being subsequently analyzed for confirmation by chromatographic techniques gas chromatography (GC) or high performance liquid chromatography (HPLC) coupled to mass spectrometry (MS). Since most classes of pharmaceuticals have to be derivatized due to their lack of volatility before GC analysis, HPLC-MS is more universally applicable. Capillary electrophoresis (CE) has also been employed, but, since CE is less sensitive than HPLC, its application to analysis of pharmaceuticals is less attractive. Recent developments in detectors, sample-preparation units and other components have improved the limits of detection (LODs) of these techniques [11-24]. However, chromatographic methods are time consuming and laborious when a large number of samples must be screened for several pharmaceuticals, they require expensive equipment, trained personnel, and complex sample preparation steps. As an alternative, the high-sample throughput capability of immunochemical methods could respond to the demands of pharmaceutical analysis [13]. Compared to chromatographic techniques, immunoassays are easy to use and have a low cost per analysis or sample. Moreover, immunoassays have demonstrated their reliability, selectivity and detectability in analyzing small organic molecules [14]. Biomolecular analytical devices constitute a different approach, which has evolved rapidly in recent years, since they allow real-time, automated analysis with relatively high capacity. Biosensors are useful tools in the antibacterial research field, their usefulness to fight against the spread of bacterial resistance, and the development of new antibacterial compounds. The number of biosensor approaches in this area has increased during the last five years, dominated by studies for the detection of antibacterials in the environment [4]. Biosensors are among the potential applications of new materials and devices and novel approaches to nanobiotechnology [24]. Therefore, reliable and low-cost effective methods for detection of antibiotic residues will be developed in this study. A chemical sensor will be developed for detecting antibiotic residues.

The research hypothesis for this study was to develop PSF-GO modified BDD electrode to be used as transducer material for electrochemical sensor to detect antibiotic residues. PSF-GO/BDDE sensor will offer wide potential window due to use of BDD working electrode as

well as low detection limit due to the use of GO, which offers high electrochemical conductivity.

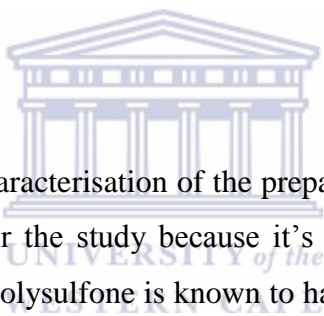
1.3 Aims and Objectives of this study

1.3.1 Aims of the study

The aim of this study is developing an electrochemical sensor for the screening of antibiotics residues in wastewater. Three different electrode materials are investigated as sensor material for each antibiotic residue. The sensor reactivity is modelled using electrochemical techniques such as square voltammetry and electrochemical impedance spectroscopy.

The following objectives highlighted will be achieved to fulfil the aim of this research work.

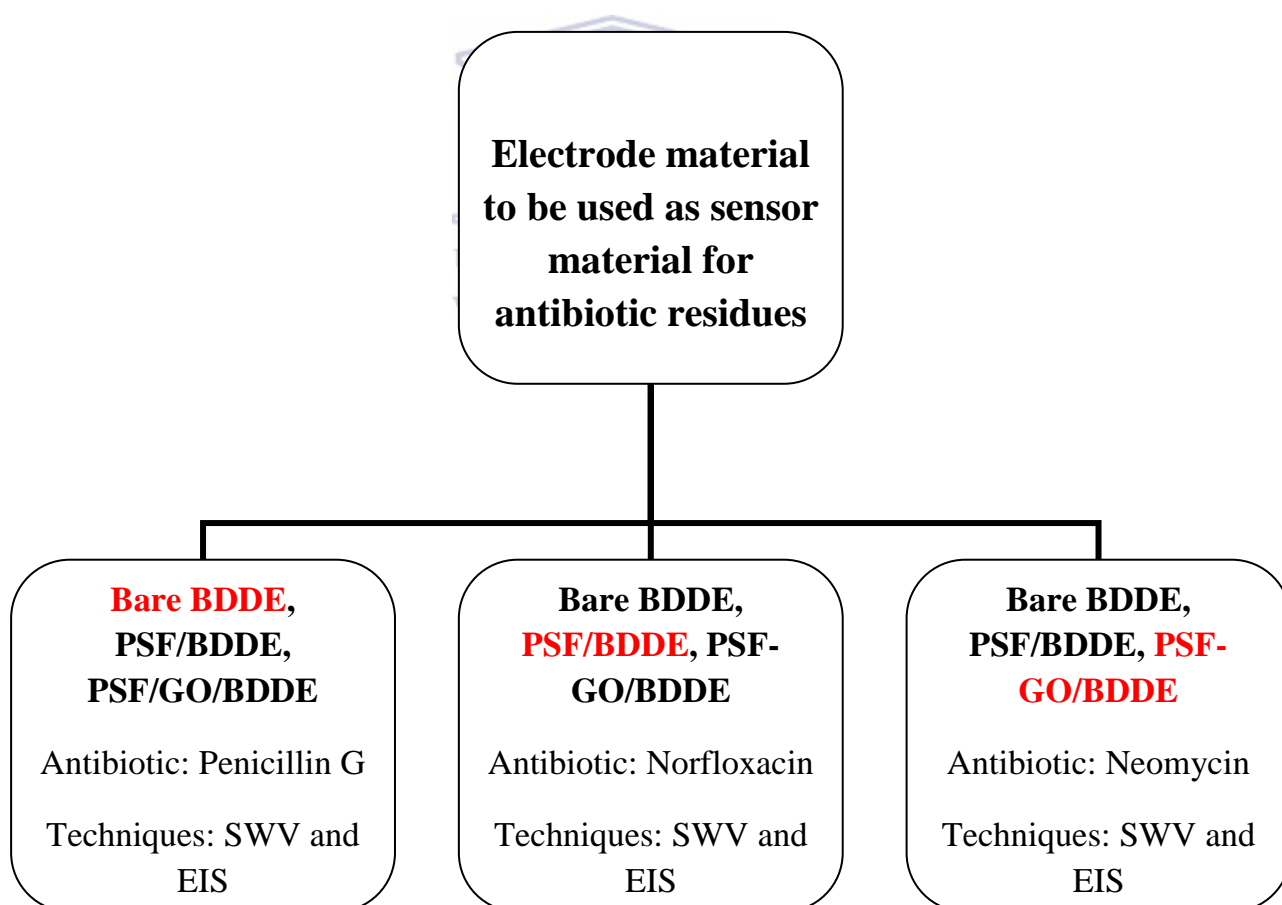
1.3.2 Objectives of this study

- 
- Preparation and characterisation of the prepared material. Polysulfone was the chosen polymer for the study because it's a polymer that I used during the masters research. Polysulfone is known to have two major drawbacks which is membrane fouling and that it is not a conductive polymer for electrochemical studies. Therefore the modification of polysulfone helps the polymer to improve its hydrophilicity and conductivity. Graphene oxide was used to modify the polysulfone. Graphene oxide (GO), is a derivative of graphene obtained by the use of strong oxidizing agents to obtain graphene oxide, a nonconductive hydrophilic carbon material. Its unique properties include high surface area, tunable band gap, and room temperature Hall effect, excellent electrical, thermal and conducting properties.
 - Studying the electrochemistry of the three selected antibiotics at the selected sensor platforms of choice. Chromatographic methods were used for the determination and quantification of the antibiotics but they are time consuming and laborious when a large number of samples must be screened

for several pharmaceuticals, they require expensive equipment, trained personnel, and complex sample preparation steps. Biosensors are among the potential applications of new materials and devices and novel approaches to nanobiotechnology. Therefore, reliable and low-cost methods for detection of antibiotic residues will be developed in this study.

- Sensor application for recovery of antibiotics from spiked tap water sample. The water was taken directly from the tap water from the City of Cape Town municipal reservoir.

1.4. Conceptual diagram



1.5. Overview of the thesis

The thesis is divided into 9 chapters:

- Chapter 1: Background introduction. A brief overview of antibiotic and antibiotic resistance in wastewater. Followed by a description of the project goals and aims
- Chapter 2: Literature review. Focuses on classification of different classes of antibiotics and also highlights on the detection of antibiotics using different techniques such as HPLC, ELISA and UV/Vis
- Chapter 3: Literature review. Is the second part of the literature review which reviews on the electrochemical detection techniques for antibiotics.
- Chapter 4: Discusses the techniques that are used for the characterisation of polysulfone, graphene oxide and the composite of polysulfone with graphene oxide
- Chapter 5: Synthesis, Preparation and Characterisation: Characterisation results of the prepared material will be presented and discussed. Characterisation techniques used are FTIR, Raman, SEM, Contact angle.
- Chapter 6: Electrochemical Characterisation. Electrochemical response of polysulfone, polysulfone with graphene oxide and bare BDD will be presented and discussed. Also the response of the above mention material in the presence of antibiotic residues will be discussed.
- Chapter 7: Detection of antibiotic residues. The electrochemical detection of antibiotic residues will be illustrated and discussed. The obtained results will be compared with other studies from the literature

- Chapter 8: Application and Interference studies. This chapter discusses the application of the transducer material to real water samples. Also discusses the selectivity of the transducer material in the synthetic urine
- Chapter 9: Conclusion and Recommendations. Draws the general conclusion in terms of performance of the chemical sensor in standard laboratory experiments and future recommendations.



References

1. Manzetti S and Ghisi R, The environmental release and fate of antibiotics, *Marine Pollution Bulletin* 79 (2014) 7–15
2. Davies J. and Davies D., Origins and Evolution of Antibiotic Resistance, *Microbiology And Molecular Biology Reviews*, 74 (2010) 417-433
3. Alexandre Augusto Borghi, Mauri Sergio Alves Palma, Tetracycline: production, waste treatment and environmental impact assessment, *Brazilian Journal of Pharmaceutical Sciences*, 50 (2014) 25-40
4. Mojica E-RE and Aga DS, Antibiotics Pollution in Soil and Water: Potential Ecological and Human Health Issues, Elsevier BV, 16 (2011) 97-110
5. Novo A., Andre S., Viana P., Nunes O. C., Manaia C. M., Antibiotic resistance, antimicrobial residues and bacterial community composition in urban wastewater, *water research* 47 (2013) 1875 -1887
6. Kümmerer K., Antibiotics in the aquatic environment – A review (Part II), *Chemosphere* 75 (2009) 435–441
7. Pruden A., Pei R., Storteboom H., Carlson K.H., Antibiotic resistance genes as emerging contaminants: studies in northern Colorado. *Environ. Sci. Technol.*, 40 (2006) 7445–7450.
8. Sapkota A.R., Curriero F.C., Gibson K.E., Schwabb K.J., Antibiotic-resistant Enterococci and fecal indicators in surface water and groundwater impacted by a concentrated Swine feeding operation, *Environ. Health Persp.*, 115 (2007) 1040–1045.
9. Kümmerer K., Resistance in the environment, *J. Antimicrob. Chemoth.*, 54 (2004) 311–320.
10. Neela F.A., Nonaka L., Suzuki S., The diversity of multi-drug resistance profiles in tetracycline-resistant *Vibrio* species isolated from coastal sediments and seawater, *J. Microbiol.*, 45 (2007) 64–68.
11. Córdova-Kreylos A.L., Scow K.M., Effects of ciprofloxacin on salt marsh sediment microbial communities, *ISME J*, 1 (2007) 585–595
12. Michael I., Rizzo L., McArdell C.S., Manaia C.M., Merlin C., Schwartz T., Dagot C. and Fatta-Kassinos D., Urban wastewater treatment plants as hotspots for the release of antibiotics in the environment: A review, *Water research*, 47 (2013) 957- 995

13. Barbosa T.M., Levy S.B., The impact of antibiotic use on resistance development and persistence, *Drug Resistance Updates*, 3 (2000) 303–311
14. Kümmerer K., Significance of antibiotics in the environment, *Journal of Antimicrobial Chemotherapy*, 52 (2003) 5–7
15. Bouki C, Venieri D., Diamadopoulos E., Detection and fate of antibiotic resistant bacteria in wastewater treatment plants: A review, *Ecotoxicology and Environmental Safety*, 91 (2013) 1–9
16. Giedraitienė A., Vitkauskienė A., Naginienė R., Pavilonis A., Antibiotic Resistance Mechanisms of Clinically Important Bacteria, *Medicina (Kaunas)*, 47 (2011) 137-146
17. Michael N. Alekshun, and Stuart B. Levy, Molecular Mechanisms of Antibacterial Multidrug Resistance, *Cell*, 128 (2007) 1037-1050
18. Nawfal Adam Mungroo and Suresh Neethirajan, Biosensors for the Detection of Antibiotics in Poultry Industry—A Review, *Biosensors*, 4 (2014) 472-493
19. Cháfer-Pericás C., Maquieira Á., Puchades R., Fast screening methods to detect antibiotic residues in food samples., *Trends Anal. Chem.*, 29 (2010) 1038–1049.
20. Huet, A.; Fodey, T.; Haughey, S.A.; Weigel, S.; Elliott, C.; Delahaut, P. Advances in biosensorbased analysis for antimicrobial residues in foods, *Trends Anal. Chem.*, 29 (2010) 1281–1294.
21. Koyun, A.; Ahlatcolu, E.; Koca, Y. Biosensors and their principles. In *A Roadmap of Biomedical Engineers and Milestones*; Kara, S., Ed.; InTech: Rijeka, Croatia, 2012
22. Bbosa G. S, Mwebaza N, Odda J, Kyegombe D. B., Ntale., Antibiotics/antibacterial drug use, their marketing and promotion during the post-antibiotic golden age and their role in emergence of bacterial resistance, *Health*, 6 (2014) 410-425
23. Reder-Christ K and Bendas G, Biosensor Applications in the Field of Antibiotic Research—A Review of Recent Developments, *Sensors*, 11 (2011) 9450-9466
24. Nuria Sanvicens, Ilaria Mannelli, J.-Pablo Salvador, Enrique Valera, M.-Pilar Marco, Biosensors for pharmaceuticals based on novel technology, *Trends in Analytical Chemistry*, 30 (2011) 541-553

CHAPTER II

Literature Review

This chapter focuses on different analytical techniques used to determine and quantify antibiotic residues; the techniques are HPLC, ELISA and UV-Vis spectroscopy. It also describes how each technique is used also gives examples of the studies performed for detecting the three classes of antibiotics. The limit of detection for the above mentioned techniques are compared.

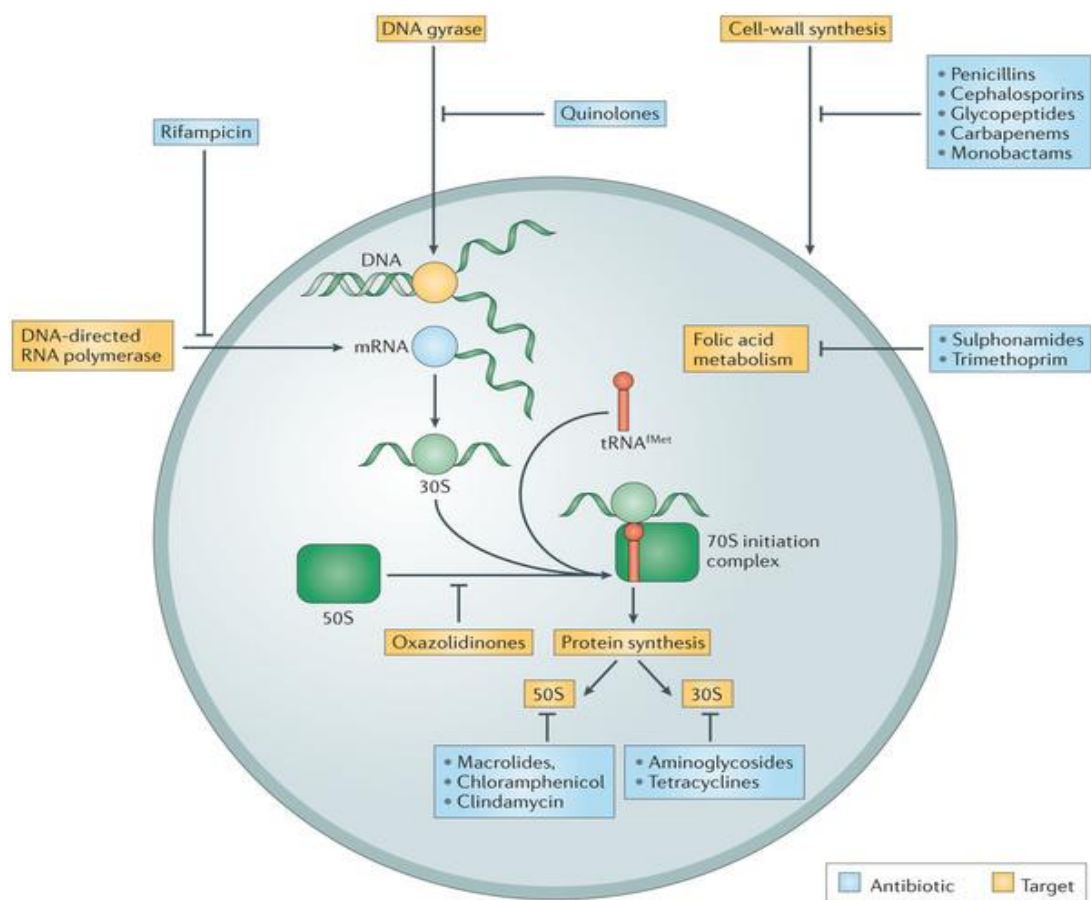
2. Introduction

Antibiotics are a set of compounds used in large quantities to kill or inhibit bacterial diseases in humans and prevent disease in animals. They are also used as growth promoters in animals. Often, these compounds are only partially metabolized by the user and can later be excreted into wastewater, manure, or directly into water systems during fish farming [1-3]. Unused therapeutic drugs are sometimes disposed of into the sewage system. If the drugs are not degraded or eliminated during sewage treatment, in soil or in other environmental compartments, they will reach surface water and ground water, and might end up in drinking water [3]. This chapter will highlight the different classes of antibiotics and also reviews the different detection methods as useful tools in the antibacterial research field, their usefulness to fight against the spread of bacterial resistance, and the development of new antibacterial compounds.

2.1 Classification of antibiotics

The classification of antibiotics depends mainly on their bacterial spectrum, how they are administered, type of activity and their origin. The grouping can depend on their chemical structure as well as mechanism or spectrum of action [1-2]. Antibiotics that target the bacterial cell wall (penicillins and cephalosporins), or interfere with essential bacterial enzymes (quinolones and sulfonamides) have bactericidal activities. Antibiotics that target protein synthesis (aminoglycosides, macrolides and tetracyclines) are usually bacteriostatic [2-3]. Figure 2.1 shows the different classes of antibiotics and their mechanism of action.

Some antibiotics are specific and targets either gram-positive or gram-negative bacteria (narrow spectrum antibiotics), others target both (broad spectrum antibiotics) [3]. Antibiotics are not effective against all types of bacteria. Narrow-spectrum antibiotics are only effective against a narrow range of bacteria, whereas broad-spectrum antibiotics are effective against a broad range of bacteria. Penicillin G is very effective at killing gram-positive bacteria, but not very effective against gram-negative bacteria. Gram-positive bacteria have a relatively loose outer wall that many antibiotics can diffuse through. However, gram-negative bacteria have a complex outer layer that prevents the passage of many larger or fat-soluble molecules [4].

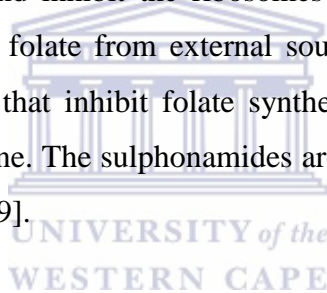


Nature Reviews | Drug Discovery

Figure 2.1: Classes of antibiotics and their modes of action on bacteria [5]

Both penicillins and cephalosporins are examples of β -lactam antibiotics; they function by interrupting peptidoglycan synthesis. These antibiotics enter the bacterial cell and bind to

enzymes known as penicillin-binding proteins. This results in the formation of a weak or deformed cell wall, which swells and then bursts [6]. The reproduction of the DNA and cell division leads to the formation of new bacterial cells, and some antibiotics operate by inhibiting the manufactured DNA. Therefore, these kinds of antibiotics are likely to be bactericidal in action and include quinolones as well as drugs like metronidazole, nitrofurantoin and rifampicin [7]. The fluoroquinolones and quinolones inhibit the action of two enzymes, DNA gyrase and topoisomerase IV, which are important for DNA replication. The consequences of damaging the DNA will mean that the cell cannot be preserved, resulting in cell death [6]. The aminoglycosides, tetracyclines and macrolides interferes with protein synthesis [7]. Gentamicin an aminoglycosides is bactericidal and cause misreading of the code on mRNA and end up in the bacteria creating proteins that are dysfunctional. Tetracyclines inhibit protein synthesis by blocking the transfer RNA. This is the molecule that transports the amino acids necessary for the production of proteins. Macrolides bind to one of the ribosomal subunits and inhibit the ribosomes from performance well [7-8]. In contrast to mammals that obtain folate from external sources (food), bacteria manufacture their own. Important antibiotics that inhibit folate synthesis include trimethoprim and the sulphonamides such as sulfadiazine. The sulphonamides are now rarely used as monotherapy because of growing resistance [7-9].



2.1.1 Aminoglycoside antibiotics

Aminoglycoside antibiotics are the most important agent in killing and fighting the bacteria. After the discovery on streptomycin around 1944, this class of antibiotics was recognized and become one of the most vital antibiotics [10]. The first aminoglycoside antibiotic to be discovered was the streptomycin and isolated from the soil bacteria called *Pseudomonas spp* species and *Micromonospora* (shown in Figure 2.2). Streptomycin was the first antibiotic used for the treatment of *Mycobacterium tuberculosis* successfully and was later introduced into the clinics in the mid 1940s [11]. Following the discovery of streptomycin, many other aminoglycosides antibiotics such as azithromycin were also isolated from the bacteria called *Saccharopolyspora erythraea* (shown in Figure 2.2). The overuse of aminoglycoside led to the development of antibiotic resistance which was overcome by the rapid discovery and introduction of new aminoglycosides [12]. Examples of the early discovered antibiotics include neomycin, gentamicin, tobramycin and sisomicin. They showed inherent

effectiveness against gram-positive and also a number of gram-positive bacterial infections. Based on their chemical structure and biosynthesis allows them to be divided into different classes. Its structure determines the accessibility to different aminoglycoside-modifying enzymes, thus has resulted in the development of antibiotic resistance [12-13].

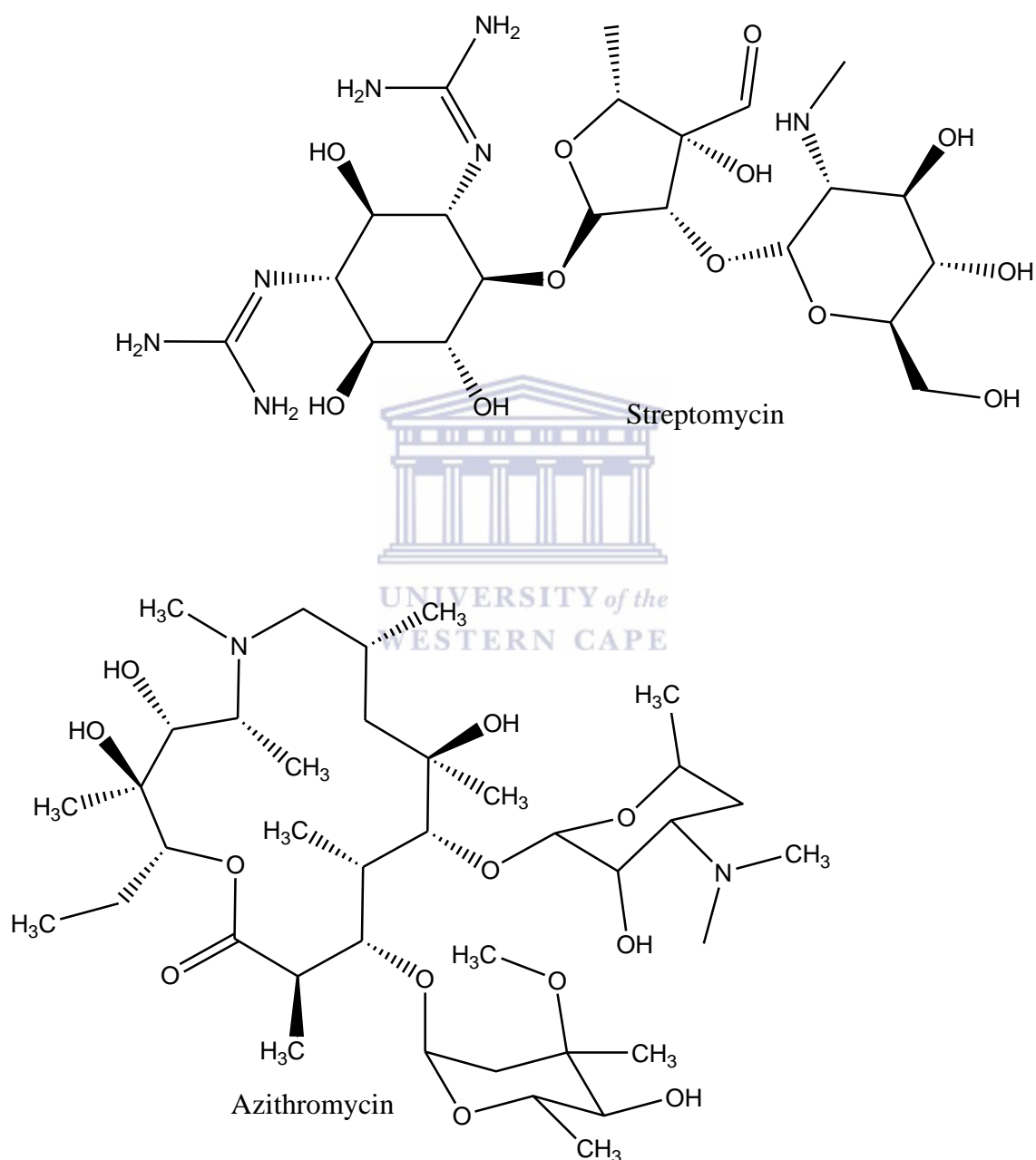


Figure 2.2: Chemical structure of Streptomycin (isolated from *Pseudomonas spp*) and Azithromycin (isolated from *Saccharopolyspora erythraea*)

Aminoglycosides are the most commonly used antibiotics for treating harsh infections caused by gram-negative bacteria, including bacilli such as *Escherichia coli*, *Enterobacter* [13], *Pseudomonas* and *Salmonella* species, and gram-positive pathogens such as *Staphylococcus* and some *Streptococci* as well as *Mycobacteria* [11,14]. Using aminoglycoside against broad-spectrum species is challenged by drug modifying enzymes and the decreased uptake in gram-positives resulting in membrane composition and prevents aminoglycoside permeation. Between aminoglycosides, differences in the spectrum activity are related to the presence of drug-modifying enzymes that inactivate antibiotics and efflux pumps [15].

The dosing of aminoglycosides favors once-a-day concentration depending on bacterial activity [11]. Killing the bacteria using aminoglycosides is determined by the ratio of the peak exposure to minimum inhibitory concentrations as suggested by the pharmacodynamic profiling. In a day, single doses that are high in concentration are used to maximize peak levels while shunning away from continued high levels of aminoglycoside. Temporary high levels of aminoglycosides do not result in toxicity but lead to improved bacterial killing. The after-effects of aminoglycoside continue to maintain their bactericidal activity at lower post-peak levels of the drugs [11-12]. The most important disadvantage of aminoglycoside is the unpleasant effects that are common and aggressive than those of other antibiotics [16].

UNIVERSITY of the
WESTERN CAPE

2.1.2 Sulfonamide antibiotics

The first introduction of sulphonamides was in the 1930s and even today they still continue being important due to their effectiveness, fairly safe and inexpensiveness [17-18]. Sulphonamides are a basic foundation of several group of drugs which consist of SO_2NH_2 moiety, they are known as sulfa drugs. The chemical class of sulphonamides shares a common moiety of p-aminobenzoyl ring with an aromatic group substituted at position N-4 and differ in the substitution at N-1 position [19-20]. Examples of sulfonamides are presented in the below figure (Figure 2.3). The aromatic and heteroaromatic sulphonamide are applied as antitumor agent that operate by inhibiting carbonic anhydrase. Sulphonamides and p-aminobenzoic acid (PABA) are quite similar to each other. PABA is a contributory factor required by the bacteria to synthesize folic acid and therefore compete for incorporation. [21]. Sulphonamides are commonly used to treat bacterial infectious cells because they are less effective against the antigenic properties of the infective organism or the growth of specific

antibodies. The antibiotic resistance against sulphonamides occurs when the bacteria changes its cell wall permeability enhancing important production of metabolites and also increased enzyme production [22-24].

Frequently, sulphonamides are used both in humans and in animals for the purpose of healing and prevent diseases and occasionally used as supplements in the animal feed and the extended ingestion of this drugs promotes growth in animals. If the medicated animals are slaughtered or milked before the withdrawal phase monitory, the meat and milk from these animals could be contaminated with sulphonamide residues [18,20]. Sulphonamides slow down the dihydropteroate (bacterial enzyme) which is responsible for the PABA integration into folic acid. The synthesis of dihydrofolic acid is prevented by the bacterial enzyme inhibition and lessens the amount of metabolically active tetrahydrofolic acid, a contributory factor in the synthesis of purines, thymidine and DNA. The enzyme dihydrofolate reductase in bacteria is prevented by trimethoprim which interferes with the conversion of dihydrofolinic acid [25-26].

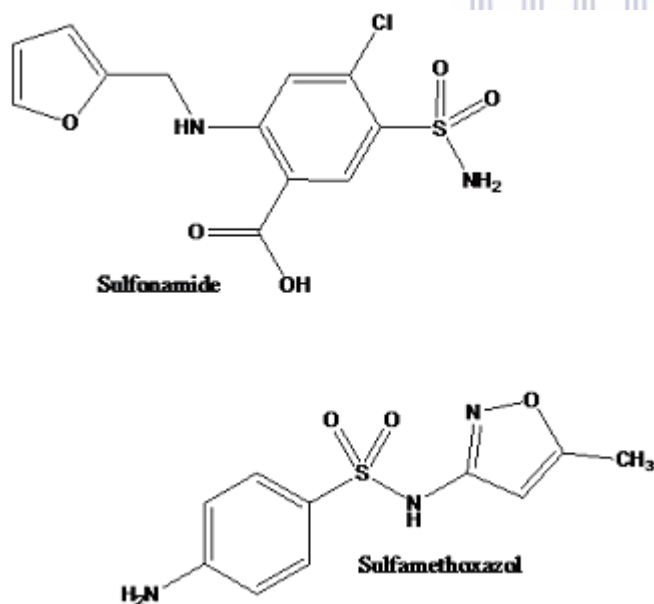


Figure 2.3: Chemical structure of sulphonamide antibiotic known as furosemide and Sulfamethoxazole sulphonamide antibacterial.

Sulfisoxazole a sulphonamide antibiotic requires 2.0 - 4.0 g/day prescribed amount in every 4 hours, and sulfamerazine also requires a 0.48 g/day dosage. A long acting sulphonamide known as sulfamethaxazole requires a prescribe amount of 1.6 – 2.4 g/day for only two times a day. Sulfamethaxazole are fairly soluble and when good fluid intake is maintained the crystalluria is prevented. The recommended prescribed amount for urinary tract infection is 2 g at first and followed by 1 g four times for a week to two weeks. The common dosage for adults with shigella diarrhea is 160 mg of trimethoprim with 800 mg of sulfamethoxazole every 12 hrs for a week. The required concentration of sulphonamides in plasma should be 80 – 160 g/mL [27].

2.1.3 β -Lactam antibiotics

β -lactam antibiotics are agents that have a β -lactam ring, they include penicillins, cephalosporins, monobactams and carbapenems (shown in Figure 2.4). Alexander Flemming was the first person to discover penicillins and it was the first antibiotic to be introduced for use in clinics. They are used as a remedy for infections, inflammations and diseases [28-29]. They are most frequently used antibiotics and function by inhibiting cell wall biosynthesis in bacteria [28]. The 6-aminopenicillanic acid (APA) is the β -lactam nucleus and an important factor in the synthesis of penicillin and modification. The formation of penicillin V was possible through the acylation of chemically synthesized APA [29]. The discovery of β -lactams led to many opportunities where novel agents could be largely produced by the addition various side chains to the APA. Semi-synthetic β -lactam compounds have been developed constantly and systematically. The early semi-synthetic penicillin introduced was the methicillin, able to resist penicillinase hydrolysis and was clinically approved in 1960. Carbenicillin is a chemical compound related to penicillins and consists of a carboxyl group instead of an amino group and was launched in 1967 [30]. It is a semi-synthetic β -lactam that is effective against *Pseudomonas aeruginosa*. β -lactam antibiotics which consist of 7 aminocelaphalosporanic acid nucleus are called cephalosporins. The difference between penicillins and cephalosporins is their basic structure. Cephalosporins consist of six-membered dihydrothiazine ring in place of a 5 membered thiazolidine ring fused to the β -lactam ring [28]. Their similarity is in their action as antibiotic and convulsant drug. The other family of β -lactam is the carbapenems which prevents the bacterial cell wall synthesis by binding to the penicillin binding protein (PBP). This antibiotic resembles broad spectrum

activity against most gram positive and gram negative bacteria. Nonetheless, ertapenem is less effective against *Pseudomonas aeruginosa* and *Acinetobacter sp* unlike imipene and ertapenem. β -lactams are used for the treatment of a wide range of severe infections such as intra-abdominal, urinary tract, lower respiratory tract or skin infections [31].

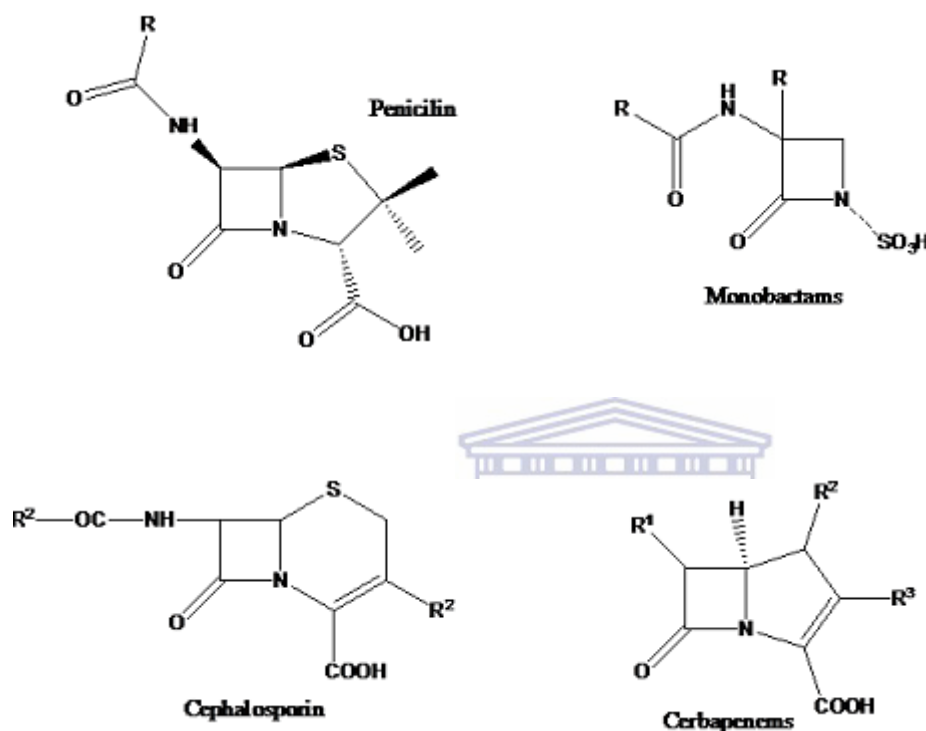


Figure 2.4: Examples of β -lactam backbones

β -lactams specifically targets bacteria that are gram-positive because of the high peptidoglycan found in the cell wall of these pathogens [32]. The protection of the cell shape and rigidity of the bacteria relies mainly on the cross-linked peptidoglycan layer or cell wall. The cell wall is made up of a basic repeating unit of an alternating disaccharide of N-acetyl glucosamine and N-acetyl muramic acid. Each peptidoglycan units are produced in the cell, but their cross-linking is catalyzed outside the cytoplasmic membrane by a membrane referred to as cell-wall transpeptidases [33]. A peptide bond is formed between the D-alanine on one chain and the free amino end of a gram-negative or gram-positive residue on the other chain. β -lactam antibiotics capably inhibit the bacterial transpeptidases, nonetheless

these enzymes are known as penicillin binding proteins. This is possible due to the stereochemical similarity of the β -lactam moiety with the D-alanine-Dalanine substrate. In the case where the antibiotic is present the transpeptidases form a lethal covalent penicilloyl-enzyme complex that provides the blockage of the normal transpeptidation reaction. Therefore, the above reaction produced a weakly cross-linked peptidoglycan which makes the bacteria vulnerable to cell lysis and death [33]. In growing bacteria cell walls are often synthesized, their inhibition during synthesis is useful at controlling the growth [31-33].

This class of antibiotics is categorized as time dependent or concentration-independent antibiotics as they have shown to be most valuable when the concentration is retained above the minimum inhibitory concentration (MIC) of the pathogen [34]. β -Lactams are time-dependent antibiotics, which mean that their activity is primarily linked to the time during which their serum concentration remains above the MIC for the offending organism. The major parameter determining efficacy of β -lactam antibiotics is the period above the MIC [35]. Many researchers suggest that the time the concentration of the antibiotic remains above the MIC should be long, from 40 to 70% of the interval-time between doses. Sometimes, a more long time, up to 100% of the dosing interval, may be needed in case of resistant organisms [35-36]. As stated from literature, the MIC for antibiotics are very different from one bacteria to the other, but are very often comprised between 0.5 and 4 g/mL for the most sensitive germs. Like other β -lactams the parameter that is linked with the effective treatment with carbapenems is the time that plasma concentration is retained above the MIC and according to researchers the most advantageous bactericidal activity is obtained when the time is greater or equal to 40% of the time interval between two dosages [37-40]. Many researchers witnessed that the current recommended doses of imipenem, meropenem and ertapenem do not guarantee the achievement of this pharmacodynamic endpoint. For instance, Moczygemba et al. [39], found that for infections with bacteria producing extended spectrum β -lactamases, the 1 g once-a-day ertapenem dose does not provide the optimal exposure in 22% of the patients [39]. Burgess and Frei [41], also witnessed that around 30% of the patients suffering from pulmonary infections with *Pseudomonas aeruginosa* or *Acinetobacter baumannii* cannot achieve a satisfying imipenem exposure with a 0.5 g every 6hr dose [41]. This results were consistent with the study of DeRyke et al. [42], who found that, for the same bacteria and equivalent doses, around 15–30% of the patients do not achieve the optimal efficacy with imipenem or meropenem [42]. Similarly, Kuti et al. [38],

showed that for MICs of 2 and 4 mg/L, only 60 and 15% of the patients, respectively attained the pharmacodynamic endpoint during skin infections with the recommended 0.5 g three times a day meropenem dose [32].

2.1.4 Fluoroquinolone antibiotics

Quinolones and fluoroquinolones are a novel class of synthetic antibiotics with potent bactericidal, broad spectrum activity against many important clinical pathogens which are responsible for different infection including urinary tract infection, gastro intestinal infections, respiratory infections, sexually transmitted diseases (STD) and skin infections [43]. Nalidixic acid (shown in Figure 2.5) is the parental compound for quinolones class. The use of nalidixic acid was limited due to its narrow spectrum, low serum levels and toxicity issues, and later has regained attention in the 1980s, have been used for treating infections caused by gram positive and gram negative, aerobic and anaerobic organisms [44]. Fluorination of quinolone compounds resulted in the birth of norfloxacin and ciprofloxacin which were followed by other generation of fluoroquinolones. Second and third generation of fluoroquinolones resulted after the additional modification of quinolones, examples of different fluoroquinolones generation is presented in Figure 2.6. Fluoroquinolones first-generation antibiotics are primarily active against gram-negative and a number of gram-positive organisms. Second-generation fluoroquinolones, i.e levofloxacin which is the L-isomer of ofloxacin and demonstrates improved gram-positive activity. However, studies show that levofloxacin is less effective than ciprofloxacin against gram-negative pathogens such as *Pseudomonas aeruginosa* and other enterobacteriaceae [45]. Third generation fluoroquinolones such as moxifloxacin and gatifloxacin have improved gram-positive efficacy and improved anaerobic coverage compared with first and second-generation fluoroquinolones. Particularly, this new antibiotic representative of fluoroquinolones manifests greater activity against streptococcus pneumonia and important respiratory pathogen [46-47].

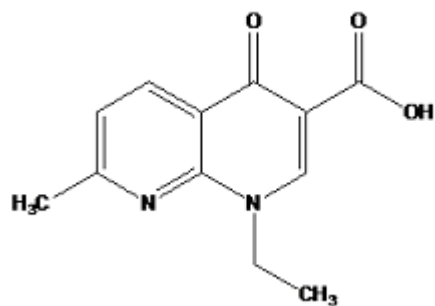


Figure 2.5: Nalidixic acid

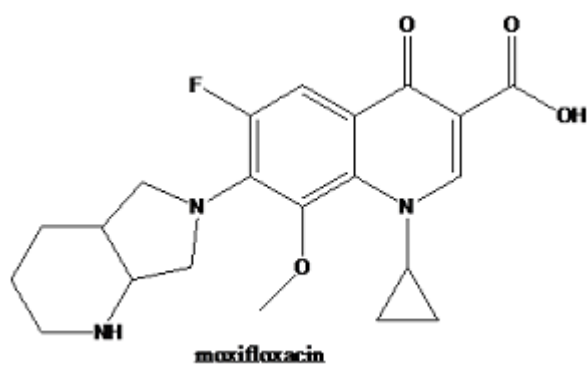
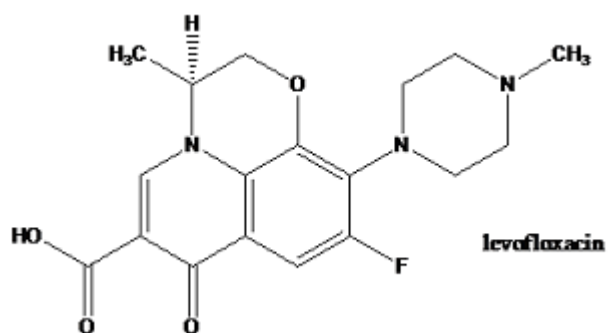
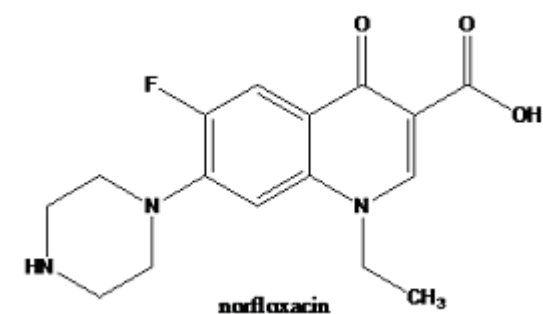


Figure 2.6: Examples of Fluoroquinolones; norfloxacin (1st generation), levofloxacin (2nd generation) and moxifloxacin (3rd generation)

Quinolones operate by inhibiting DNA synthesis by promoting cleavage of bacterial DNA in the DNA-enzyme complexes of DNA gyrase and type IV topoisomerase, therefore results in killing the bacteria fast. Generally, the activity of the gram-negative bacteria correlates with the DNA gyrase inhibition whereas the activity of gram-positive bacteria corresponds with DNA type IV topoisomerase inhibition [48]. Fluoroquinolones binds with the DNA in a stacking manner; this is possible because of the coplanar aromatic ring and the binding interactions also taking place between the substituent at the first position [43,48]. The DNA bind with the carbonyl and carboxyl of the fluoroquinolones by hydrogen bonding, while the fluoro substituent at carbon-7 and carboxylate ion are involved in binding interactions with the enzyme. The complex formed from the DNA binding is stable and raised the activity and pharmacology of fluoroquinolones. Improving the activity and pharmacology of fluoroquinolones are mainly focused over the stacking domain and the binding sites to enzymes and DNA [43].

The excellent bioavailability of most quinolones makes them ideal for ambulatory patients and intravenous-to-oral antibiotic switches in hospitalised patients. Higher drug concentrations paradoxically inhibit RNA and protein synthesis, thereby reducing bactericidal activity [49]. The quinolone shows dependency in concentration for bacterial killing. At lower values, the AUC_{24h}/MIC (minimum inhibitory concentration) ratio became more predictive, perhaps because of the decreased rate of bacterial killing [50-51]. Early studies show that quinolones and aminoglycosides are similar but different to β -lactams, they function in a concentration-dependent manner and exert a marked post-antibiotics effect although this is not consistent for all species [44].

Most of the time antibiotics compounds are only partially metabolized by the user and can be later excreted into wastewater, manure, or directly into water systems during fish farming [52]. Unused therapeutic drugs are sometimes disposed of into the sewage system. If the drugs are not degraded or eliminated during sewage treatment, in soil or in other environmental compartments, they will reach surface water and ground water, and might end up in drinking water [52-53]. Until the early 1980s different antibacterial classes were identified. Then, until the end of the 20th century, there was no further development of real novel antibiotics, which strengthens the present efforts to find novel modes of action or to attack hitherto unknown target structures. This section will highlight on different detection

methods as useful tools in the antibacterial research field, their usefulness to fight against the spread of bacterial resistance, and the development of new antibacterial compounds [53].

2.2 Methods used to detect antibiotics

To detect antibiotic residues, different kinds of methods were developed. Screening methods and chromatographic techniques were developed to detect antibiotics. The screening method is generally performed by microbiological, enzymatic and immunological methods. Current available methods and test microorganisms use different antibiotic residue detection assays. For the detection of antibiotic residues, microbiological assays use bacteria such as *Bacillus stearothermophilus* because of its high sensitivity to the majority of antibiotics. Microbiological assay techniques have been recommended as official and conventional methods because of their simplicity, the bioassay methods lack specificity and provide only semi-quantitative measurements of residues detected and sometimes produce false positives [54]. Therefore, chromatographic techniques, such as high performance liquid chromatography (HPLC) as well as enzyme linked immunosorbent assay (ELISA) have been developed to measure and quantify antibiotic residues [55].

UNIVERSITY of the
WESTERN CAPE

2.2.1 High-Performance Liquid Chromatography (HPLC)

The properties of HPLC such as versatility, resolving capability and quantitative accuracy make it a method of choice for most analyses of antibiotics. HPLC is coupled with other techniques like mass spectrometry, UV and NMR to be able further resolve mixtures of related compound and to provide insight into chemical structures [56-57]. Different things must be considered when optimizing or developing a chromatographic system such as column selection, mobile phase, elution profile and the detector to be used. The most relevant characteristics of aminoglycosides to HPLC analysis is the lack of chromophore and its high hydrophilicity. They are usually derivatized before and after chromatographic separation to improve detectability and separation [56]. Usually aminoglycosides are not partitioned on reverse-phase columns, when they are portioned to C18 columns the use of acetate buffer in the mobile phase improves the partition. The acetate ions from the acetate buffer acts as a counterion that forms ion pairs with aminoglycosides. The commonly used reagents for

derivatization are o-phthalaldehyde and 1-fluoro-2,4-dinitrobenzene. The separation columns usually contain C8 and C18 samples, mobile phase consist of acidic buffers with methanol and acetonitrile. This technique is widely used for the determination of sulphonamide residues and their separation is usually performed with silica-based reverse phase columns, mainly C18, C8 or C4, but in some cases ion-pair column is also used [56-58].

2.2.2 Enzyme Linked Immunosorbent Assay (ELISA)

ELISA has become the basic immunoassay on which many of the modern assay formats are based. This method involves the direct competitive assay in which the antigen is bound to the solid surface [59]. The sandwich format is the most preferred assay format because the analyte to be measured is bound between two primary antibodies being the capture antibody and the detection antibody. The following are examples of commonly used enzyme labels; horseradish peroxidase (HRP), alkaline phosphatase (AP), and β -d-galactosidase. The enzyme label can attach to either the antigen or the antibody in a way that the binding reaction is not impaired. [59-61]. It is important when designing a sandwich ELISA to consider the capture and detection antibodies that recognize two non-overlapping structural regions on the target molecule. The region that is recognized by the detection antibody can't be disturbed or disrupted in any way when the antigen binds to the capture antibody. The ELISA experiment is divided into a sequence of four basic steps: dispensing, incubation, washing and reading. ELISA has become the most popular method for chemical residue detection due to its high sensitivity, simplicity and ability to screen large number of samples [59-61].

2.2.3 Ultraviolet/Visible spectroscopy (UV/Vis)

Different analytical methods have been developed for the analysis of chemical drugs; the commonly used methods are HPLC, TLC, AAS and spectrofluorimetry. UV-Vis spectroscopy is one of the methods that is less expensive, available and effective for the analysis of chemical drugs [56-57]. Literature explains that this method has been applied in assaying and identification of sample in different research fields. This principle is also

applied in drug metabolites, where samples are taken from various sites of the body and analyzed to determine the amount of metabolites at those sites [57].

2.3. Limit of detection for fluoroquinolones

For HPLC, in order to optimize the working conditions it is important to test the effects of different variables such as solubility, polarity and UV absorption. Quinolones have different physical properties and they can be grouped into acidic quinolones and piperazinyl quinolones [62]. Fluoroquinolones solution contains no colour and cannot absorb in the visible range, their absorbance lies in the ultraviolet range [60]. When selecting a proper wavelength for the method, it depends on the nature of the sample and its solubility. The best solvent for chemoluminescence (CL) method is acetonitrile other solvents like methanol and ethanol were unsuitable because of the solubility of norfloxacin being limited [73]. The method used for quinolones is developed mostly on C8 or C18 columns [69]. It is also vital to test different pHs of the mobile phase because it is a major factor influencing the chromatographic behaviour of quinolones. In ELISA, when preparing an immuno assay the most important step is the design and synthesis of the best possible hapten. The interaction of the hapten or antigen-antibody is dependent on the molecular shape, defined by the geometry, and on interactions such as hydrogen bonding (low-energy), hydrophobic interactions, and electrostatic and dipole-dipole forces together with σ - σ complementary ring-bonding [56].

Table 2.1: LOD comparison for Fluoroquinolones by HPLC, ELISA and UV/Vis

Method	Analyte	LOD	Ref
HPLC	Ciprofloxacin	2.5 mg/mL	[63]
	Norfloxacin	0.08 µm/mL	[67]
		3 ng/mL	[66]
	Ciprofloxacin	0.0147 µm/mL	[82]
		6.2 mg/L	[76]
UV/Vis	Norfloxacin	0.67 µg/mL	[79]
	Orbifloxacin	0.04 µg/mL	[84]
	Levofloxacin	2.1 µg/mL	[85]
	Norfloxacin	6 ng/mL	[80]
ELISA	Enrofloxacin	0.2 ng/mL	[69]
	Ciprofloxacin	0.019 ng/mL	[74]
	Sarafloxacin	0.002 ng/mL	[73]
	Norfloxacin	0.06 ng/mL	[72]

Conditions for chromatographic analysis can be influenced by different properties of antibiotics such as solubility, polarity and UV absorption. A variety of mobile phase were investigated and different organic solvents such as acetonitrile, methanol and/or in combination with different aqueous buffers were tested during chromatographic method development [62-63]. Khattab and co-workers [63], studied the separation of ciprofloxacin (CIP) and moxifloxacin (MOX). Different ratios of buffer solution and acetonitrile were tested. Increasing the ratio of acetonitrile resulted in peak broadening and that the use of methanol instead of acetonitrile for separating CIP and MOX was unsuccessful. Different pHs of the mobile phase were also studied because it plays a major role influencing

chromatographic behaviour of fluoroquinolones. Results obtained in their showed that the best peak separation and satisfactory separation of the two antibiotics were obtained when the pH of sodium dihydrogen phosphate buffer was 2.5 with orthophosphoric acid and acetonitrile with the ratio of 80:20 v/v [63-67]. Canada-Canada et.al [68], in their study found that the best separation performance was achieved they used a mobile phase consisting of methanol, acetonitrile and acetic acid 10 mmol/L at pH 4.5. The simultaneous detection of selected analytes the conditions were specifically optimised for each analyte. The selected fluoroquinolone analytes showed varied fluorescence response, excitation or emission wavelength were 280/450 nm for norfloxacin (NOR), 280/495 nm for marfloxacin and 280/405 nm for enofloxacin (ENO), respectively [68-69]. A new method for analysis of nalidixic acid and CIP was developed. The optimised conditions for nalidixic acid were; UV detector wavelength was 266 nm, mobile phase was acetonitrile and 0.05 M phosphate buffer pH 5.1 (30:70 v/v). For CIP the conditions were: UV detector wavelength 282 nm, C18 reversed phase column, mobile phase methanol and 0.25 M H₃PO₄ pH 4.6 (80:20 v/v). The results for both methods showed that the recovery for nalidixic acid was 99.5% and CIP was 99.6% [70-71].

The development of a generic ELISA for fluoroquinolones, the specific class antibody recognition site must involve the piperazine ring which is common to all fluoroquinolones and the specificity is determined by targeting areas of the molecule distal or space structure. Fan and co-workers used NOR to produce polyclonal antiserum for following immunoassay of various fluoroquinolones. Norfloxacin was chosen due to its structure which imitates the common part in the fluoroquinolone. A carrier protein was conjugated to NOR to stimulate the immune response of rabbits and resulted in anti-norfloxacin pAb [72]. The bovine serum albumin (BSA) and ovalbumin (OVA) are the commonly used carrier proteins because of their outcome when used. Specific standard curves for the ELISA were developed for NOR, CIP, perfloxacin and enofloxacin. The standard curves for the respective icELISA were constructed and the recoveries obtained were; for intra-assay 84-104% and for inter-assay 91-106%. Therefore it was concluded that this method that was developed is capable of detecting fluoroquinolones simultaneously [72-73]. Jinqing and colleagues [73], did a study which aimed at preparing an artificial antigen of CIP and produce anti-ciprofloxacin pAb. The molecular weight of CIP is too small to be immunogenic, hence it needs to be conjugated to a carrier protein prior to immunization to draw an immune response. A comparative detection

of the prepared CIP at different concentrations was done to study the accuracy of the analysis method developed. The obtained results showed a correlation coefficient of 0.984, this means that an admirable correlation was obtained and suggest the veracity of the icELISA for the detection of CIP residues [73-74]. An immunoassay against CIP using antibody fragments, known as the single-chain variable fragment (scFvs) was developed. The source of antibody fragment is a phage library which articulates human scFvs as fusion protein with the phage coat protein III. Antibodies or antibody fragment specific for haptens that are small and selected from libraries, a challenge arises of adsorbing the molecules onto a solid surface. The possible solution to this challenge is that a preliminary step of conjugation of small haptens to a carrier protein is required [75-76]. Gomes and colleagues [76], used paramagnetic beads with CIP covalently bound to their surface and carried out the elutions with soluble CIP. The results obtained suggested the limits of detection and quantification of the competitive ELISA was lower than the threshold limits of CIP [76].

A method was proposed for developing a validating the ultraviolet (UV) and visible (Vis) spectrophotometric methods applied for determining the NOR in pharmaceutical formulations. The use of UV method for norfloxacin in 0.1 M HCl medium showed no absorption maximum at 277 nm whereas for the Vis method NOR reacted with the chloranilic acid reagent forming a purple colour solution with an absorption maximum at 520 nm. The obtained calibration curves were linear over the working range of 2.0 – 7.0 µg/mL for the UV method and 90 – 120 µg/mL for the Vis method [77-79]. For the analysis of fluoroquinolone in the pharmaceutical dosage or in biological fluids was developed through charge transfer complex formation with bromanil using a spectrofluorometric technique. Bromanil (BRO) was found to react with the FQs drugs and resulted in stable complexes and the fluorescence intensity for the complexes was enhanced. The formed complexes showed excitation maxima ranging from 275 – 290 nm and emission maxima ranging from 450 – 470 nm. The obtained linear calibration curves were in the concentration range of 0.02 -3.0 µg/mL for the studied FQ drugs [80]. Spectrometric based UV method was developed focusing on water:acetonitrile:methanol (90:5:5) solvent to determine the levofloxacin content in bulk and pharmaceutical dosages. The pre-determined maximum wavelength of 292 nm was proven to be linear in the concentration range of 1.0 – 12.0 µg/mL and showed good correlation coefficient and great recoveries. Hence, this method was considered the best method to be successfully applied for the determination of levofloxacin content in market brands [81].

2.4. Limit of detection for β – Lactams

Many chromatographic methods that are based on UV detection for the analysis of penicillins require a derivatization reaction using reagents that are toxic like mercury. Some researchers have managed to develop separation methods that do not require derivatization [86-88]. When developing a method for separation of polar compounds like amoxicillin using C18 column the aqueous mobile phase often collapses because of the alkyl chain this results in poor retention, selectivity and reproducibility. The possible solution to this challenge is using amino columns, the amine groups are bonded to the silica polar stationary phases. Stationary phases bonded amine groups will be protonated at neutral and acidic mobile phase. This amino column will retain polar compounds longer than non-polar compounds when the mobile phase is polar [56-58]. In the case of phenyl columns their behaviour is described by hydrophobic and π - π interactions. This column has a high retention property which is due to their natural high aromaticity and also the molecule is planar in shape, therefore it enables stronger retention through π - π interactions [57-58].



Table 2.2: LOD comparison of β -Lactams by HPLC, ELISA, UV/Vis

Method	Analyte	LOD	Ref
HPLC	Amoxicillin	0.06 ug/mL	[57]
	Amoxicillin	0.1 ug/mL	[96]
	Penicillin G	0.1 ug/mL	[97]
	Amoxicillin	4.0 mg/L	[86]
	Ampicillin	0.12 ug/L	[95]
ELISA	Amoxicillin	1.3 ng/mL	[101]
	Amoxicillin	0.1 ug/L	[93]
	Chloramphenicol	1.2 ng/mL	[102]
UV/Vis	Flucloxacillin	0.15 ug/mL	[98]
	Ampicillin	0.162 ug/mL	[99]
	Cefoxitin	1.391 ug/mL	[87]
	Amoxicillin	0.4 mg/mL	[88]
	Ceftriaxone	0.0646 ug/mL	[100]

Analysis of penicillins by chromatographic methods coupled with UV detector requires a derivatization reaction. Due to toxicity and how complex the derivatization reagents are, some researchers have come up with methods which do not require the derivatization step. A method that does not require derivatization but facilitates the separation of the selected antibiotic residues was developed. Two chromatographic columns were selected for the study; the first column was the most commonly used C18 particle-packed column and the other was the monolithic silica column. Monoliths offer better performance for fast separation with low pressure at high flow rates. The monolithic column was the preferred

column over the conventional C18 column, because it allowed faster analytes more than two times with separable efficiency [56-57]. The retention of amoxicillin was investigated using three different columns; phenyl, amino and C18 columns using pure micellar mobile phases containing SDS. For the analysis, all three columns showed an appropriate retention factor, good efficiency and asymmetry. Looking at the performance of the three tested columns; C18 presented a lower retention factor whereas the phenyl column presented high efficiency. The amoxicillin peak overlapped with the protein band and also with the compounds of the urine mixture in the amino column. Therefore, the phenyl column was the column of choice for further analysis of amoxicillin [57-58].

Cephalosporins are antibiotics that belong to the β -lactam class. Cefoxitin sodium is a secondary generation antibacterial which belongs to cephalosporins. A simple, selective, less time consuming and less expensive method for the analysis of cefoxitin was developed. The prepared standard solution of cefoxitin was studied using UV-Vis spectrophotometer in the wavelength range of 200-400 nm. The drug absorbed light at 231 nm. Cefoxitin showed a linear relationship and obeyed the Beer's law in the concentration range 10-50 $\mu\text{m}/\text{mL}$ and a correlation coefficient of 0.999 [87]. The determination of amoxicillin using an indirect spectrophometric method was developed for both forms of amoxicillins; pure and pharmaceutical preparation. The study focused on reacting potassium permanganate a known oxidizing agent with amoxicillin, the disappearing violet colour from permanganate was observed to be proportional to the amount of amoxicillin in the prepared pharmaceutical. Beer's law was obeyed from 0.1-0.6 mg/dL and the limit of detection was 0.04 mg/dL with recovery of 98% [88]. Two methods were developed for the detection of ampicillin. The first method was based on the kinetic investigation of the oxidation reaction of the drug with alkaline KMNO_4 at room temperature. The λ_{max} was observed at 610 nm for the coloured manganate ions. The other method focused on reacting ampicillin with 1-chloro-2,4-dinitrobenzene in 0.1 M sodium bicarbonate. The measured absorbance was achieved by recording the absorbance at 490 nm. The concentration against absorbance plots was linear over the range of 5-30 and 50-260 $\mu\text{g}/\text{mL}$ with recoveries of 99.80 and 99.91% for both procedures [89].

A study was presented to develop a receptor based ELISA for the detection of β -lactam antibiotics in various tissues from the meat. A trans-membrane protein called BlaR of *Bacillus licheniformis* which plays a role in the regulation for the production of β -lactamase. The carboxy-terminal of BlaR (BlaR-CTD) is located on the outer face of the membrane and serves as penicillin receptor [90]. BlaR-CTD from *B. licheniformis* 749/I would complex most members of β -lactam antibiotics in just a short time [90-93]. β -lactam antibiotics with absolutely intact β -lactams can be detected by BlaR-CTD [90,92]. Using the receptors of BlaR-CTD for detecting β -lactam antibiotics showed significant advantages. Many β -lactam antibiotics can be recognized by BlaR-CTD, β -lactams antibiotics from penicillin group and cephalosporins [91], which is more than PBP2x* can recognize. The second advantage is that the BlaR-CTD is able of complexing a huge number of β -lactam antibiotics in a short time with high affinity [91-92]. Lastly, the used protein can be produced in commercially useful amounts due to its recombinant origin, and the small size of BlaR-CTD favors its solubility in the recombinant expression. An immunoassay which is able to detect low concentration of penicillins was developed. Many attempts have been made over the last decade, but only the antibodies obtained recently that are good enough to be applied for detection in milk samples, with limits of quantification close to the require MRL. The proposed method enabled the analysis of the samples with simple and fast treatment of the matrix with biohybrid magnetic particles to hydrolyze the β -lactam ring. A novel immunizing hapten has been produced and the polyclonal antibodies obtained showed high specificity for open ring penicillins and no cross reactivity with other antibiotic classes [90-94].

2.5 Limit of detection for Aminoglycoside

For aminoglycoside chromatographic separation many challenges take place due to the sorption properties and the polarity of the compounds. HPLC separation of aminoglycoside is achieved by ion-pair to chromatography because they are not retained by the reverse phase column [103-104]. The appropriate MS detection is the perfluorinated ion pair agent because of their elevated volatility. The two other ion pair agents are the trifluoro-acetic (TFA) acid which causes a dramatic ion suppression in the electrospray ionization (ESI) and heptafluorobutyric acid (HFBA) which has a limited ion suppression, retention times and limited peak shapes and analyte response [104-107]. Fluorescence technique is more specific

than the UV-Visible because not all UV absorbing compounds can fluoresce. Due to the extra high selectivity of the spectrofluorometric detector has been receiving favour for aminoglycosides monitoring and its very high sensitivity and the appropriate selection of excitation and emission wavelengths, the filter fluorometer is preferred in pharmacokinetic studies of this group of drugs [105].

Table 2.3: LOD comparison of aminoglycoside by HPLC, ELISA and UV/Vis

Method	Analyte	LOD	Ref.
HPLC	Streptomycin	0.03 µg/mL	[116]
	Kanamycin A	38 mg/L	[105]
	Amikacin	5.5µg/mL	[117]
UV/Vis	Kanamycin A	0.3 nM	[113]
	Amikacin	0.068 ug/mL	[119]
	Gentamicin	6.16 ug/mL	[121]
	Amikacin	0.015 mg/mL	[114]
	Gentamicin	7.4 nM	[120]
ELISA	Gentamicin	2 mg/kg	[109]
	Kanamycin	1.1 ng/ml	[108]
	Kanamycin	59 nM	[118]

Many challenges arise when developing chromatographic method for analysis and determination of aminoglycosides [103]. Kanamycin is a polar polyamine compound and belongs to the aminoglycosides class. A study focusing on the optimization of the mobile phases was performed to provide best conditions for the detection of kanamycin. The separation method using mobile phases based methanol was unsuccessful because kanamycin residues were not separated efficiently. The acetonitrile-water solvent system and ion-pairing agents (TFA, TGA (thioglycolic acid) and HFBA) were all tested and optimized. Both the acetonitrile and methanol are known to be volatile organic solvents that are used as organic phase. The use of ion-pair reversed phase retention mechanism for aminoglycoside was found to be suitable for use on the non-polar C18 column [104]. The performance of three different HPLC columns based on their separation and peak shape of aminoglycosides was investigated. The 1st column investigated was the Zorbax Extend column which showed good results with regards to peak shape and selectivity, however, before the method could be validated the column performance falling significantly, peak shoulders, excessive peak tailing and poor repeatability were observed. Therefore the Zorbax column was rejected due to being unstable and not suitable for the application. The second column tested was the apHera, a polymeric column coated with C18 particles and can resist high pH. The use of this column resulted in poor peak shapes when compared to silica based reverse phase columns. The column resisted temperatures up to 60 °C which was insufficient to improve peak shape. These types of columns are expensive and are not readily available in labs. Therefore, their use was also declined for the study. The last column was Xbridge column which proved to be more stable than the Zorbax column, and its performance was better than the performance obtained with the apHera [105]. Gentamicin has a weak chromophore therefore it does not absorb light in its native form. A method was developed focusing on the pre-column derivatization of gentamicin and the obtained fluorescent product was detected at much higher sensitivity using HPLC coupled with fluorescence detector. Gentamicin reacted with non-fluorescent o-phthalaldehyde (OPA) in the presence of an excess N-acetylcysteine as a thiol compound resulting in a fluorescent isoindole. The data obtained proved that a significant excess of OPA reagent was needed for performing the derivatization process [106-107].

Jang and colleagues [107], developed a study which looked at producing monoclonal antibody that was highly specific for kanamycin. The specificity of the antibody can be

described by the differences in the molecular structure of the aminoglycoside. All aminoglycosides consist of two or more amino sugars joined by a glycosidic linkage to a hexose nucleus which is either a streptose or 2-deoxystreptamin [108-109]. The amino groups are distinguished by the amino sugars attached to the nucleus, in either, kanamycin and gentamicin because they have two amino sugars attached to 2-deoxystreptamin, or in neomycin due to its three amino sugars attached. ELISA method developed resulted in the detection limits of 1.1 ng/mL in PBS, 1.4 ng/mL in plasma and 1.0 ng/mL in milk [108]. An ELISA method was developed using a polyclonal antibody with high affinity and specificity for detecting gentamicin. Both the immunogen-I and the coating antigen-I were prepared according to the active ester method using EDC (1-ethyl-3-(3-dimethylaminopropyl) carbodiimide hydrochloride) as the crosslinker. The immunogen-II and coating antigen-II were both prepared according to the GDA method using glutaraldehyde (GDA) as a crosslinker. The IC₅₀ which is the half-maximum inhibition concentration and detection limit were calculated as IC₁₅ of the gentamicin in phosphate buffer to be 0.3 and 0.03 ng/mL. The assay showed low cross-reactivity with other aminoglycoside antibiotics except for sisomicin [109]. A colorimetric competitive direct ELISA method was developed using polyclonal antibody to determine neomycin residues. No cross-reactivity of the antibody with other aminoglycosides was observed. The method was validated by HPLC and the results showed a good correlation which was greater than 0.9 [110].

Streptomycin is an antitubercular drug which belongs to the class of aminoglycosides. They appear to lack a chromophore or fluorophore moiety which is vital for spectrophometric analysis. A study was performed reporting on a simple method and reproducible colorimetric analysis of streptomycin and its application to evaluate the streptomycin sulphate loaded solid lipid nanoparticles (STRS-SLNS). This method was based on the nucleophilic substitution reaction between STR and sodium nitroprusside (SNP), resulting in the formation of a red-coloured product in an alkaline medium. The obtained adduct was measure at a maximum wavelength absorption at 495 nm in visible light. The method was found to be linear in the range of 4.0 – 256.0 µg/mL for streptomycin [111]. A novel colorimetric method for kanamycin a commonly used aminoglycoside was developed using unmodified silver nanoparticles as sensing probe. It was found that the analyte used for this study can protect Ag nanoparticles against salt-induced aggregation and nucleic acid aptamers can decrease the risk of false positives through an aptamer-selective sensing mechanism. The use of the

proposed method for the selective quantification of kanamycin can be achieved over the concentration range from 0.05 – 0.6 $\mu\text{g/mL}$ [112]. A simple and sensitive aptamer-based fluorescence method for the detection of kanamycin residue using gold nanoparticles was investigated. Gold nanoparticles (AuNPs) were used as a DNA nanocarrier as well as the quencher. In the case of kanamycin A being absent, a dye-labelled aptamer could be adsorbed onto the surface of the nanoparticles and the fluorescence signal was quenched. When the kanamycin A is present, the specific binding between dye-labelled aptamer and its target induced the formation of rigid structure which led to dye-labelled aptamer released from the surface of nanoparticles and fluorescence intensity was recovered eventually. Under favourable conditions, calibration modelling showed that the analytical linear range covered from 0.8 – 350 nM and the detection limit of 0.3 nM were obtained successfully [113]. Amikacin sulphate also lacks a chromophore and a conjugated system is a prerequisite for UV and fluorescent light detection. Hence, there is a need of simple and reliable methods for introducing a chromophore in the structure of amikacin sulphate for its determination by UV and fluorescence detection (FLD) [112]. Shehzadi and colleagues [114], described the development and validation of a simple, cost effective and fast colorimetric method for amikacin in their study. The amikacin and aqueous ninhydrin solution were heated for 2-5 min and produced a Ruhemann purple coloured derivative which was detected at two wavelengths at 400 nm and 567 nm. The obtained results obeyed the Beer's law over the concentration ranges from 0.417 mg/mL to 2.5 mg/mL. The obtained results suggest that the method is easy to perform, specific, sensitive and suitable to be applied for the determination of amikacin sulphate [114]. A study was done focusing on single-stranded deoxyribonucleic acid (ssDNA) aptamer showing high specificity for kanamycin that was obtained by SELEX using affinity chromatography. The binding affinity and interacting region of the ssDNA aptamer for kanamycin were confirmed by AuNPs based colorimetric method [113,115]. AuNP based colorimetric methods are known to be a powerful tool for detecting DNA interacting with small molecules because of their large surface area, easy conjugation with biomaterial and visibility. A colorimetric method without any labelling was developed for this study. The detection limit for the colorimetric method using a label-free was low as 25 nM which was much lower than the acceptable level of kanamycin residue in animals and plants used as food [115].

2.6 Conclusion

Many efforts in the past have been made to develop different analytical methods to determine antibiotics both qualitatively and quantitatively. Chromatography was found to offer better performance for the conventional detection of antibiotics, the methods includes thin-layer chromatography , gas chromatography combined with mass spectrometric , gas chromatography coupled with electron capture, and high-performance liquid chromatography [122-125]. Nonetheless, the major drawback of chromatographic methods is the expensive apparatus and time-consuming have limited their use. The enzyme-linked immunosorbent assay is widely used for the detection of antibiotic residues with accuracy and precision, but still has some limits such as difficult sample pretreatment process and requires highly trained technical personnel [123-124].

The analysis of antibiotics such as aminoglycoside is important for different purposes, like residue analysis in food of animal origin and, given its frequent use in veterinary applications, in environmental samples such as different water compartments and soil. The analysis or screening of AGs and their allied products is important in drug formulations and in therapeutic drug monitoring in body fluids and tissues. The prolonged use or exposure to antibiotics can lead to a serious health hazard and result in the development of bacterial resistance to different antibiotics [122-123]. Aminoglycosides lack a chromophore and also exhibit poor chromatic properties because their high polarity. Different studies have been done to solve the problem of the absent UV chromophore or fluorophore by using derivatizing agents to detect these antibiotics. However, the derivatizing step makes the method more time consuming and may introduce contaminants or impurities. In addition, is the possibility of degradation of the used derivatizing agents within hours after their formation [122-125].

Another preferred technique for screening antibiotics is ELISA, because it provides a high-throughput and low-cost method than chromatographic analysis. Both the specific and sensitive antibodies for β -lactam antibiotics are not easy to grow because of the reactivity of the β -lactam ring. . It is evident all ELISA method for determining β -lactams had to modify the structure to produce antibodies with appropriate specificity. Therefore, an ELISA method with high sensitivity for detecting penicillins has not been developed, particularly the aminopenicillins which are the frequently used worldwide. From literature it is evident that

penicillin immunogens are unstable, probably due to the β -lactam ring opening, this result in difficulty to develop immunoassays against penicillins [61].

A method is required which will offer the following properties such as sensitivity, selectivity, convenient, robust, and rapid detection method for antibiotic residues for human health and safety is highly desirable. Biosensors emerge as the suitable alternative or complementary analytical tools for the detection of antibiotics due to their advantages of high selectivity, rapid detection, and in-situ applications. Recently, there is a growing rise in the fabrication of antibiotic biosensors [123]



References

1. Mojica E-RE and DS Aga, Antibiotics Pollution in Soil and Water: Potential Ecological and Human Health Issues, Elsevier BV, 16 (2011) 97-110
2. Calderon CB and Sabundayo BP (2007). Antimicrobial classifications: Drugs for bugs. In Schwalbe R, Steele-Moore L and Goodwin AC (eds). Antimicrobial susceptibility testing protocols. CRC Press, Taylor and Frances group. ISBN 978-0-8247-4100-6
3. Frederick Adzitey, Antibiotic Classes and Antibiotic Susceptibility of Bacterial Isolates from Selected Poultry; A Mini Review, World Vet J, 5(2015) 36-41
4. Sarah M. Drawz and Robert A. Bonomo, Three Decades of β -Lactamase Inhibitors, Clinical Microbiology Reviews, 23 (2010) 160–201
5. Kim Lewis, Platforms for antibiotic discovery, Nature Reviews Drug Discovery, 12 (2013) 371–387
6. Karch AM, Focus on Nursing Pharmacology. Fourth Edition. (2008) Lippincott Williams & Wilkins, Philadelphia PA
7. Hills T, Antibacterial chemotherapy. In Lynn J, Bowskill D, Bath-Hextall F, Knaggs R (Eds), The New Prescriber: An Integrated Approach to Medical and Non-Medical Prescribing. John Wiley & Sons, Chichester, (2010) 444-460.
8. Frost KJ, An overview of antibiotic therapy. Nursing Standard. 22 (2007) 51-57
9. Kaufman G, Antibiotics: mode of action and mechanisms of resistance. Nursing Standard. 25 (2011) 49-55.
10. Schiffelers R, G Storm, I Bakker-Woudenberg, Liposome-encapsulated aminoglycosides in pre-clinical and clinical studies, Journal of Antimicrobial Chemotherapy 48 (2001), 333-344
11. Hermann T., Aminoglycoside antibiotics: old drugs and new therapeutic approaches, Cell. Mol. Life Sci. 64 (2007) 1841 – 1852

12. Cunha, B. A. New uses for older antibiotics: Nitrofurantoin, amikacin, colistin, polymyxin B, doxycycline, and minocycline revisited. *Med. Clin. N. Am.*, 90 (2006) 1089–1107.
13. Bernd Becker and Matthew A. Cooper, Aminoglycoside Antibiotics in the 21st Century, *ACS Chem. Biol.*, 8 (2013)105–115
14. Gad GF, Mohamed HA, Ashour HM, Aminoglycoside Resistance Rates, Phenotypes, and Mechanisms of Gram-Negative Bacteria from Infected Patients in Upper Egypt. *PLoS ONE*, 6 (2011). e17224. doi:10.1371/journal.pone.0017224
15. Geisla Mary Silva Soares , Luciene Cristina Figueiredo , Marcelo Faveri , Sheila Cavalca Cortelli , Poliana Mendes Duarte , Magda Feres, Mechanisms of action of systemic antibiotics used in periodontal treatment and mechanisms of bacterial resistance to these drugs, *J Appl Oral Sc*, 20 (2012) 295-309
16. Liat Vidal, Anat Gafter-Gvili, Sara Borok, Abigail Fraser, Leonard Leibovici^{1,2} and Mical Paul, Efficacy and safety of aminoglycoside monotherapy: systematic review and meta-analysis of randomized controlled trials, *Journal of Antimicrobial Chemotherapy*, 60 (2007) 247–257
17. William B Smith, Sulfonamide antibiotic allergy. *Australasian Society of Clinical Immunology and Allergy*, 2007
18. Schwarz S, Chaslus-Dancla E., Use of antimicrobials in veterinary medicine and mechanisms of resistance. *Veterinary Research* 32 (2001) 201–225
19. Owa T. and T. Nagasu, Novel sulphonamide derivatives for the treatment of cancer, *Expert Opinion on Therapeutic Patents*, 1 (2000) 1725–1740,
20. Wang S., H. Y. Zhang, L. Wang, Z. J. Duan, & I. Kennedy, Analysis of sulphonamide residues in edible animal products: A review, *Food Additives and Contaminants*, April 23 (2006) 362–384
21. Christiana Nonye Igwe and Uchechukwu Chris Okoro, Synthesis, Characterization, and Evaluation for Antibacterial and Antifungal Activities of *N*-Heteroaryl Substituted Benzene Sulphonamides, *Organic Chemistry International*, Volume 2014, Article ID 419518, 5 pages

22. Supuran C. T., A. Scozzafava, and A. Casini, Carbonic anhydrase inhibitors, *Medicinal Research Reviews*, 23(2003) 146–189,
23. Muhammad Abdul Qadir, Mahmood Ahmed, Hina Aslam, Sadia Waseem, and Muhammad Imtiaz Shafiq, Amidine Sulfonamides and Benzene Sulfonamides: Synthesis and Their Biological Evaluation, *Journal of Chemistry*, Volume 2015
24. . Supuran C. T and A. Scozzafava, Applications of carbonic anhydrase inhibitors and activators in therapy, *Expert Opinion on Therapeutic Patents*, 12 (2002) 217–242.
25. Pentti Huovinen, Resistance to Trimethoprim-Sulfamethoxazole, *CID* 32 (2001) 1604-1614
26. Skold O. Sulfonamide resistance: mechanisms and trends. *Drug Resistance Updates* 3 (2000)155–60
27. Silke Marie Fuchs And Peter Elsner, Sulfonamides in Dermatology, *Clinics in Dermatology* Y 21 (2003) 7-11
28. Lakshmi R, Nusrin K.S., Georgy Sharon Ann, Sreelakshmi K.S., Role of beta lactamases in antibiotic resistance: A review. *Int.Res.J.Pharm.* 5 (2014)
29. Ana Maria Vélez, Adilson José da Silva, Antonio Carlos Luperni Horta, Cintia Regina Sargo1, Gilson Campani, Gabriel Gonçalves Silva, Raquel de Lima Camargo Giordano and Teresa Cristina Zangirolami, High-throughput strategies for penicillin G acylase production in rE. coli fed-batch cultivations, *BMC Biotechnology* 2014, 14:6
30. Kok-Fai Kong, Lisa Schneper, and Kalai Mathee, Beta-lactam Antibiotics: From Antibiosis to Resistance and Bacteriology, *APMIS*. 18 (2010) 1–36
31. Tiphaine Legrand, Stéphanie Chhun, Elisabeth Rey, Benoît Blanchet, Jean-Ralph Zahar, Fanny Lanternier, Gérard Pons, Vincent Jullien, Simultaneous determination of three carbapenem antibiotics in plasma by HPLC with ultraviolet detection, *Journal of Chromatography B*, 875 (2008) 551–556
32. Sharma S.K, Lalit Singh, Suruchi Singh, Comparative Study between Penicillin and Ampicillin, *Sch. J. App. Med. Sci.*, 1 (2013) 291-294

33. Mark S Wilke , Andrew L Lovering and Natalie CJ Strynadka, β -Lactam antibiotic resistance: a current structural perspective, *Current Opinion in Microbiology*, 8 (2005) 525–533
34. Jason A. Roberts, Jennifer Paratz, Elizabeth Paratz, Wolfgang A. Krueger, Jeffrey Lipman, Continuous infusion of β -lactam antibiotics in severe infections: a review of its role, *Continuous infusion of β -lactam antibiotics in severe infections: a review of its role*, *International Journal of Antimicrobial Agents* 30 (2007) 11–18
35. Gustafsson, E. Lowdin, I. Odenholt, O. Cars, Pharmacokinetic and pharmacodynamic parameters for antimicrobial effects of cefotaxime and amoxicillin in an in vitro kinetic model. *Antimicrob. Agents Chemother.* 45 (2001) 2436-2440.
36. Raphael Denooz, Corinne Charlier, Simultaneous determination of five β -lactam antibiotics (cefepim, ceftazidim, cefuroxim, meropenem and piperacillin) in human plasma by high-performance liquid chromatography with ultraviolet detection, *Journal of Chromatography B*, 864 (2008) 161–167
37. Livermore D.M., A.M. Sefton, G.M. Scott, Properties and potential of ertapenem. *J. Antimicrob. Chemother.* 52 (2003) 331-344
38. Kuti J.L., P.K. Dandekar, C.H. Nightingale, D.P. Nicolau, Use of Monte Carlo simulation to design an optimized pharmacodynamic dosing strategy for meropenem., *J. Clin. Pharmacol.* 43 (2003) 1116-1123.
39. Moczygemba L.R., C.R. Frei, D.S. Burgess, Pharmacodynamic modeling of carbapenems and fluoroquinolones against bacteria that produce extended-spectrum beta-lactamases, *Clin. Ther.* 26 (2004) 1800-1807
40. Krueger W.A., J. Bulitta, M. Kinzig-Schippers, C. Landersdorfer, U. Holzgrabe, K.G. Naber, G.L. Drusano, F. Sorgel, Evaluation by monte carlo simulation of the pharmacokinetics of two doses of meropenem administered intermittently or as a continuous infusion in healthy volunteers. *Antimicrob. Agents Chemother.* 49 (2005) 1881-1889.

41. Burgess D.S. and C.R. Frei, Comparison of b-lactam regimens for the treatment of Gram-negative pulmonary infections in the intensive care unit based on pharmacokinetics/pharmacodynamics, *J. Antimicrob. Chemother.* 56 (2005) 893-898
42. DeRyke C.A, J.L. Kuti and D.P. Nicolau, Pharmacodynamic target attainment of six beta-lactams and two fluoroquinolones against *Pseudomonas aeruginosa*, *Acinetobacter baumannii*, *Escherichia coli*, and *Klebsiella* species collected from United States intensive care units in 2004 *Pharmacotherapy* 27 (2007) 333.
43. Prabodh Chander Sharma, Ankit Jain And Sandeep Jain, Fluoroquinolone Antibacterials: A Review On Chemistry, Microbiology And Therapeutic Prospects, *Acta Poloniae Pharmaceutica ñ Drug Research*, 66 (2009) 587- 604,
44. Van Bambeke F., J.-M. Michot, J. Van Eldere and P. M. Tulkens, Quinolones in 2005: an update, *CMI*, 11 (2005) 256–280
45. Kriti Soni, Fluoroquinolones: Chemistry & Action – A Review, *Indo Global Journal of Pharmaceutical Sciences*, 2 (2012) 43-53
46. Phillips I, King A., Shannon K. Comparative in-vitro properties of the quinolones. In: Andriole VT, editor. *The quinolones*. 3rd ed. San Diego: Academic Press; (2000) 99–137
47. Scheld Michael W., Maintaining Fluoroquinolone Class Efficacy: Review of Influencing Factors, *Emerging Infectious Diseases*, Vol. 9 (2003)
48. Catherine M. Oliphant And Gary M. Green, Quinolones: A Comprehensive Review, *American Family Physician*, 65 (2002) 455 – 464
49. Patrick G.L.: Antibacterial agents, in *An Introduction to Medicinal Chemistry*, p. 379-435, Oxford University Press, Oxford, New York 2003.
50. Hooper D. Quinolones. In: Mandell GL, Bennett JE, Dolin R. *Mandell, Douglas, and Bennett's Principles and practice of infectious diseases*. 5th ed. Philadelphia: Churchill Livingstone, (2000) 404-23.

51. Amisha D. Shah, Antibiotics in Water Treatment: The Role of Water Quality Conditions on their Fate and Removal during Chlorination and Nanofiltration, (2008) Thesis
52. Pei-Ying Hong, Nada Al-Jassim, Mohd Ikram Ansari and Roderick I. Mackie, Environmental and Public Health Implications of Water Reuse: Antibiotics, Antibiotic Resistant Bacteria, and Antibiotic Resistance Genes, *Antibiotics* 2 (2013) 367-399
53. Katrin Reder-Christ and Gerd Bendas, Biosensor Applications in the Field of Antibiotic Research—A Review of Recent Developments, *Sensors* 11 (2011) 9450-9466
54. Jussi Kurittu, Stefan Lönnberg, Marko Virta, and Matti Karp Qualitative Detection of Tetracycline Residues in Milk with a Luminescence-Based Microbial Method: The Effect of Milk Composition and Assay Performance in Relation to an Immunoassay and a Microbial Inhibition Assay. *Journal of Food Protection*, 63 (2000) 953-957.
55. Desalegne Abebew Syit, Detection And Determination Of Oxytetracycline And Penicillin G Antibiotic Residue Levels In Bovine Bulk Milk From Debrezeit And Nazareth Dairy Farms, Proceedings of the 1st International Technology, Education and Environment Conference
56. Nina Isoherranen and Stefan Soback, Chromatographic Methods for Analysis of Aminoglycoside Antibiotics, *Journal Of Aoac International*, 82 (1999) 1017 -1045
57. Maria Rambla-Alegre, Micellar Liquid Chromatography in the Determination of Antibiotics: An Overview, *J. Chem. Chem. Eng.* 5 (2011) 1059-1068
58. Olsen B.A., Hydrophilic interaction chromatography using amino and silica columns for the determination of polar pharmaceuticals and impurities. *J. Chromatogr. A*, 913 (2001) 113.
59. Furusawa N., Rapid liquid chromatographic determination of residual penicillin G in milk, *Fresenius J Anal Chem*, 368 (2000) 624–626
60. Ruth Babington & Sonia Matas & M.-Pilar Marco & Roger Galve, Current bioanalytical methods for detection of penicillins, *Anal Bioanal Chem*, 403 (2012) 1549–1566

61. Cliquet P, Cox E, Van Dorpe C, Schacht E, Goddeeris BM, Generation of class-selective monoclonal antibodies against the penicillin group. *J Agric Food Chem* 49 (2001) 3349–3355
62. Samsonova Z, Shchelokova O, Ivanova N, Rubtsova M, Egorov A Enzyme-linked immunosorbent assay of ampicillin in milk. *Appl Biochem Microbiol* 41(2005) 589–595
63. Fatma I. Khattab, Hesham Salem, Safaa M. Riad, and Heba T. Elbalkiny Determination of Fluoroquinolone Antibiotics in Industrial Wastewater by High-Pressure Liquid Chromatography and Thin-Layer Chromatography–Densitometric Methods, *Journal of Planar Chromatography* 27 (2014) 4287–293
64. Sara Abdulgader Mohammed Ebraheem , Abdalla Ahmed Elbashir, Spectrophotometric Method For The Determination Of Ofloxacin And Levofloxacin In Pharmaceutical Formulations, *American Academic & Scholarly Research Journal*, 4 (2012)
65. Ramamohana Rao, Development Of New HPLC Method And Identification And Quantification Of Nalidixic Acid, Ciprofloxacin In Fish Tissue, *The Experiment*, November, 4 (2012) 243-252
66. Huan Yu , Yanfei Tao , Dongmei Chen , Yuanhu Pan , Zhenli Liu , Yulian Wang , Lingli Huang , Menghong Dai, Dapeng Peng, Xu Wang, Zonghui Yuan, Simultaneous determination of fluoroquinolones in foods of animal origin by a high performance liquid chromatography and a liquid chromatography tandem mass spectrometry with accelerated solvent extraction, *Journal of Chromatography B*, 885– 886 (2012) 150–159
67. Ashok Kumar Bera, Amit Kumar De and Biswajit Pal, Validated and Precise Reverse Phase-HPLC Method for the Quantitative Estimation of Norfloxacin from Marketed Formulation, *International Journal of PharmTech Research*, 6 (2014) 1189-1194
68. Florentina Cañada-Cañada, Anunciacion Espinosa-Mansilla, Ana Jiménez z Girón and Arsenio Muñoz de la Peña, Simultaneous Determination of the Residues of Fourteen Quinolones and Fluoroquinolones in Fish Samples using Liquid Chromatography with Photometric and Fluorescence Detection, *Czech J. Food Sci*, (2012) 74–82

69. Hong Zhang, Si Chen, Yanbin Lu, Zhiyuan Dai, Simultaneous determination of quinolones in fish by liquid chromatography coupled with fluorescence detection: comparison of sub-2 μm particles and conventional C18 columns, *Journal of Separation Science*, 33 (2010) 1959-1967
70. Amit Kumar De , Ashok Kumar Bera And Biswajit Pal, Quantification Of Fluoroquinolones From Bulk, Pharmaceutical Formulations And Biological Matrices Using Chromatographic Techniques, *IJPSR*, 7(2016) 531-542
71. Stoilova N., M. Petkova, Developing And Validation Of Method For Detection Of Quinolone Residues In Poultry Meat, *Trakia Journal Of Sciences*, 8 (2010) 64-69,
72. Guo-Ying Fan, Ruo-Song Yang, Jin-Qing Jiang, Xin-Yao Chang, Development Of A Class-Specific Polyclonal Antibody-Based Indirect Competitive ELISA For Detecting Fluoroquinolone Residues In Milk, *J Zhejiang Univ-Sci B (Biomed & Biotechnol)* 13 (2012) 545-554
73. Jiang Jinqing, Zhang Haitang Zhao Kun, Huang Huaguo and Wang Ziliang, Comparison between Direct Competitive ELISA and LC-MS/MS Method for Detecting Sarafloxacin Residue in Poultry, *IPCBE*, 5 (2011) 156-160
74. Jiang Jinqing, Zhang Haitang, An Zhixing, Xu Zhiyong, Yang Xuefeng, Huang Huaguo and Wang Ziliang, Development of an Heterologous Immunoassay for Ciprofloxacin Residue in Milk, *Physics Procedia* 25 (2012) 1829 – 1836
75. Zhanhui Wang, Yan Zhu, Shuangyang Ding, Fangyang He, Ross C. Beier, Jiancheng Li, Haiyang Jiang, Caiwei Feng, Yuping Wan, Suxia Zhang, Zhenpeng Kai, Xinling Yang, and Jianzhong Shen, Development of a Monoclonal Antibody-Based Broad-Specificity ELISA for Fluoroquinolone Antibiotics in Foods and Molecular Modeling Studies of Cross-Reactive Compounds, *Anal. Chem.* 79 (2007) 4471-4483
76. Francisco Bruno Moreira Brás Gomes , Symon Riedstra, João Paulo Medeiros Ferreira, Development of an immunoassay for ciprofloxacin based on phage-displayed antibody fragments, *Journal of Immunological Methods* 358 (2010) 17–22
77. Carey, F. A., *Organic chemistry*, 4th Ed., the McGraw-Hill Companies Inc. New York, (2000) 522-534

78. Affo, W., Mensah-Brown, H., Awuku, J. F., Markwo, A, Quantitative Analysis of Ciprofloxacin Sodium Chloride Pharmaceutical Infusions Using Ultraviolet-visible Spectroscopy, *ARPN Journal of Science and Technology*, 3 (2013) 296-300
79. Chierentin L. and H. R. N. Salgado, Performance Characteristics of UV and Visible Spectrophotometry Methods for Quantitative Determination of Norfloxacin in Tablets, *J. Sci. Res.* 6 (2014) 531-541
80. Salem H., L. Fada and W. Khater, Spectrofluorimetric Determination of Certain Fluoroquinolones Through Charge Transfer Complex Formation, *American Journal of Pharmacology and Toxicology* 2 (2007) 18-25
81. Mahfuza Maleque, Md. Raquib Hasan, Farhad Hossen, Sanjana Safi, Development and validation of a simple UV spectrophotometric method for the determination of levofloxacin both in bulk and marketed dosage formulations, *Journal of Pharmaceutical Analysis*, 2 (2012) 454-457
82. Najma Sultana, M. Saeed Arayne, Nighat Shafi, Asia Naz, Shabana Naz, Hina Shamshad, A Rp-Hplc Method For The Simultaneous Determination Of Diltiazem And Quinolones In Bulk, Formulations And Human Serum, *J. Chil. Chem. Soc.*, 54 (2009) 358-362
83. Patyra E., E. Kowalczyk, A. Grelik, M. Przeniosło-Siwczyńska, K. Kwiatek, Screening method for the determination of tetracyclines and fluoroquinolones in animal drinking water by liquid chromatography with diode array detector, *Polish Journal of Veterinary Sciences*, 18 (2015) 283-289
84. Edith Cristina Laignier Cazedey, Hérica Regina Nunes Salgado, Development and validation of UV spectrophotometric method for orbifloxacin assay and dissolution studies, *Brazilian Journal of Pharmaceutical Sciences* vol. 50 (2014) 457-467
85. Krupa M. Kothekar, Balasundaram Jayakar, Amit P. Khandhar, Rajnish K. Mishra, Quantitative Determination of Levofloxacin and Ambroxol hydrochloride in Pharmaceutical Dosage Form by Reversed-Phase High Performance Liquid Chromatography, *Eurasian Journal of Analytical Chemistry* 2 (2007) 21-32
86. Rade Injac, Nina Kočevár, Borut Štrukelj, Optimized Method for Determination of Amoxicillin, Ampicillin, Sulfamethoxazole, and Sulfacetamide in Animal Feed by

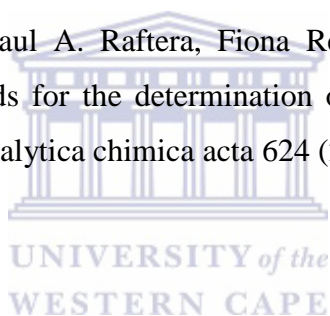
- Micellar Electrokinetic Capillary Chromatography and Comparison with High-Performance Liquid Chromatography, *Croat. Chem. Acta*, 82 (2009) 685–694
87. Revathi Ramadoss, N. Reddiyar Lisha, Bipin Chandra, Development & validation of stability indicating UV spectroscopic method for quantitation of cefoxitin sodium in pharmaceutical dosage form, *Indian Journal of Chemical Technology* 20 (2013) 327-330
88. Omed I. Haidar Omed I. Haidar, Simple Indirect Spectrophotometric Determination of Amoxicillin in Pharmaceutical Preparations, *Journal of Natural Sciences Research*, 5 (2015) 142 – 146
89. Aftab Aslam Parwaz Khan, Ayaz Mohd , Shaista Bano, K.S. Siddiqi, Abdullah Mohammed Asiri, Spectrophotometric methods for the determination of ampicillin by potassium permanganate and 1-chloro-2,4-dinitrobenzene in pharmaceutical preparations, *Arabian Journal of Chemistry*, 8 (2015) 255–263
90. Duval V, Swinnen M, Lepage S, Brans A, Granier B, Franssen C, Frere JM, Joris B The kinetic properties of the carboxy terminal domain of the *Bacillus licheniformis* 749/I BlaR penicillin-receptor shed a new light on the derepression of beta-lactamase synthesis. *Mol Microbiol* 48 (2003) 1553–1564
91. Kerff F, Charlier P, Colombo ML, Sauvage E, Brans A, Frere JM, Joris B, Fonce E Crystal structure of the sensor domain of the BlaR penicillin receptor from *Bacillus licheniformis*. *Biochemistry* 42 (2003) 12835–12843
92. Juan Peng & Guyue Cheng & Lingli Huang & Yulian Wang & Haihong Hao & Dapeng Peng & Zhenli Liu & Zonghui Yuan, Development of a direct ELISA based on carboxy-terminal of penicillin-binding protein BlaR for the detection of β -lactam antibiotics in foods, *Anal Bioanal Chem* 405 (2013) 8925–8933
93. Marta Broto , Sonia Matas , Ruth Babington, M.-Pilar Marco, Roger Galve, Immunochemical detection of penicillins by using biohybrid magnetic particles, *Food Control* 51 (2015) 381-389

94. Posyniak, A., Zmudzki, J., Niedzielska, J., Evaluation of sample preparation for control of chloramphenicol residues in porcine tissues by enzyme-linked immunosorbent assay and liquid chromatography, *Anal. Chim. Acta* 483 (2003) 307-311.
95. Fawzia A. Ibrahim and Jenny Jeehan M. Nasr, Direct determination of ampicillin and amoxicillin residues in food samples after aqueous SDS extraction by micellar liquid chromatography with UV detection, *Anal. Methods*, 6 (2014) 1523- 1529
96. Luis Renato Pires de Abreu, Rodrigo Agustin Mas Ortiz, Silvana Calafatti de Castro, José Pedrazzoli Jr., HPLC determination of amoxicillin comparative bioavailability in healthy volunteers after a single dose administration, *J Pharm Pharmaceut Sci* 6 (2003) 223-230,
97. Neagu Maria, Soceanu Georgiana, Bucur Ana Caterina, Simple and rapid method on High Performance Liquid Chromatography for simultaneous determination of benzylpenicillin potassium, streptomycin sulphate and related substances in Ascomycin – a veterinary use ointment, *Veterinary Drug*, 9 (2015) 75-83
98. Suddhasattya Dey, Ratnakar Ch. , S. Vaithiyanathan, Himansu Bhusan Samal, Y.Vikram Reddy, Bala Krishna, Y. Anil Reddy, G. Navin Kumar And Subhasis Mohapatra, Spectrophotometric Method Developed For The Estimation Of Flucloxacilin In Bulk And Dosage Form Using Uv-Vis Spectrophotometric Method, *International Journal of Pharma and Bio Sciences*, 1 (2010), 35-43
99. Shazia Khan, Ulysses W Sallum, Xiang Zheng, Gerard J Nau and Tayyaba Hasan, Rapid optical determination of β -lactamase and antibiotic activity, *BMC Microbiology* 14 (2014) 84
100. Reddy Bhaskar C.M, G.V. Subbareddy, Development And Validation Of UV–Spectrophotometric Methods For Estimation Of Ceftriaxone In Bulk And Tablet Dosage Form, *International Journal of ChemTech Research*, 5 (2013)472-477
101. Yeh L.-C., W.-M. Lee, B.-W. Koh, J. P. Chan, C.-H. Liu, J.-P. Kao, and C.-C. Chou, Development of Amoxicillin Enzyme-Linked Immunosorbent Assay and Measurements of Tissue Amoxicillin Concentrations in a Pigeon Microdialysis Model, *Poultry Science* 87 (200) 8577–587
102. Murilla G. A., J.O. Wesongah, T. Foddey, S. Crooks, A. N. Guantai, W. M. Karanja And T. E. Maitho, Validation Of A Competitive Chloramphenicol Enzyme Linked

- Immunosorbent Assay For Determination Of Residues In Ovine Tissues, East And Central African Journal Of Pharmaceutical Sciences Vol. 13 (2010) 12-18
103. Dirk Löffler, Thomas A. Ternes, A nalytical method for the determination of the aminoglycoside gentamicin in hospital wastewater via liquid chromatography–electrospray-tandem mass spectrometry, *Journal of Chromatography A*, 1000 (2003) 583–588
104. Yong Zhang, Hui-Min He, Jin Zhang, Feng-Jiao Liu, Chao Li, Bing-Wu Wang and Ren-Zhong Qiao, HPLC-ELSD determination of kanamycin B in the presence of kanamycin A in fermentation broth, *Biomed. Chromatogr.* 29 (2015) 396–401
105. Blanchaert B., Jorge, E.P., Jankovics, P., Adams, E., Van Schepdael, A., Assay of Kanamycin A by HPLC with Direct UV Detection. *Chromatographia* 76, (2013) 1505–1512.
106. Dorota Kowalczyk, Rafał Pietraś, Beata Paw, Agnieszka Czerkies, Applying Liquid Chromatography with Fluorescence Detection to Determine Gentamicin, *Polish J. of Environ. Stud.*, 19 (2010) 587-591
107. Ladislav Šoltés, Aminoglycoside antibiotics Ð Two decades of their HPLC bioanalysis, *Biomed. Chromatogr.* 13 (1999) 3–10
108. Yong Jin, Jin-Wook Jang, Chang-Hoon Han, Mun-Han Lee, Development of immunoassays for the detection of kanamycin in veterinary fields, *J. Vet. Sci.*, 7 (2006) 111–117
109. Wei Sheng, Li Yang , Junping Wang, Yan Zhang, Shuo Wang, Development of an enzyme-linked immunosorbent assay for the detection of gentamicin residues in animal-derived foods, *LWT - Food Science and Technology* 50 (2013) 204-209
110. Wang S., B. Xu, Y. Zhang, J.X. He, Development of enzyme-linked immunosorbent assay (ELISA) for the detection of neomycin residues in pig muscle, chicken muscle, egg, fish, milk and kidney, *Meat Science* 82 (2009) 53–58
111. Manoj Kumar Verma, Mandeep Singh, Vandita Kakkar, Indu Pal Kaur, Applicability Of A Colorimetric Method For Evaluating Streptomycin Sulphate Loaded Solid Lipid

- Nanoparticles, *International Journal of Pharmacy and Pharmaceutical Sciences*, 4 (2012) 50-53
112. Yuanyuan Xu, Tian Han, Xiaqing Li, Linghao Sun, Yujuan Zhang, Yuanshu Zhang, Colorimetric detection of kanamycin based on analyte-protected silver nanoparticles and aptamer-selective sensing mechanism, *Analytica Chimica Acta* 891 (2015) 298-303
113. Jing Chen , Zhao H Li , Jia Ge , RanYang, LinZhang , Ling-boQu , Hong-qi Wang, Ling Zhang, An aptamer-based signal-on bio-assay for sensitive and selective detection of Kanamycin A by using gold nanoparticles, *Talanta* 139 (2015) 226–232
114. Naureen Shehzadi, Khalid Hussain, Muhammad Tanveer Khan, Muhammad Salman, Muhammad Islam and Humaira Majeed Khan, Development of a Validated Colorimetric Assay Method for Estimation of Amikacin Sulphate in Bulk and Injectable Dosage Form, *J.Chem.Soc.Pak.*, 38 (2016) 63 -67
115. Kyung-Mi Song, Minseon Cho, Hunho Jo, Kyoungin Min, Sung Ho Jeon, Taisun Kim, Min Su Han ,Ja Kang Ku , Changill Ban, Gold nanoparticle-based colorimetric detection of kanamycin using a DNA aptamer, *Analytical Biochemistry* 415 (2011) 175–181
116. Shafqat ullah, Arshad Hussain, Asad ullah, Waseem, Hussain and Khaliq-ur-Rehman, Simple and Rapid Method on High Performance Liquid Chromatography (HPLC) for Estimation of Streptomycin Sulphate, *World Applied Sciences Journal* 19 (2012) 645-649
117. Dave Vimal M., Development and Validation of Rp-Hplc Method for Simultaneous Estimation of Cefepime Hydrochloride and Amikacin Sulphate in Injection Dosage Form, *JPSBR*, 2 (2012) 138-143
118. Yun-Peng Xing, Chun Liu, Xiao-Hong Zhou & Han-Chang Shi, Label-free detection of kanamycin based on a G-quadruplex DNA aptamer-based fluorescent intercalator displacement assay, *Sci. Rep.* 5 (2015). 8125
119. Jose F. Ovalles, Maria del Rosario Brunetto, M´aximo Gallignani, A new method for the analysis of amikacin using 6-aminoquinolyl-*N*-hydroxysuccinimidyl carbamate (AQC) derivatization and high-performance liquid chromatography with UV-detection, *Journal of Pharmaceutical and Biomedical Analysis* 39 (2005) 294–298

120. Qianjin Liu Haibo Mu, Chunli Sunc and Jinyou Duan, Highly specific determination of gentamicin by induced collapse of Au–lipid capsules, *RSC Adv.*, 2016, 6, 14483
121. Szaniszló B, Iuga Cristina, Bojiță M, Indirect Determination of Gentamicin by Derivative Spectrophotometry, *Acta Medica Marisiensis*; 57 (2011) 516-518.
122. Chauhan, R., Singh, J., Sachdev, T., Basu, T., Malhotra, B.D., Recent advances in mycotoxins detection. *Biosens. Bioelectron.* 81 (2016) 532–545.
123. Lingyi Lan, Yao Yao, Jianfeng Ping, Yibin Ying, Recent advances in nanomaterial-based biosensors for antibiotics detection, *Biosensors and Bioelectronics* 91 (2017) 504–514
124. Faten Farouk a, Hassan M.E. Azzazy, Wilfried M.A. Niessen, Challenges in the determination of aminoglycoside antibiotics, a review, *Analytica Chimica Acta* 890 (2015) 21-43
125. Tara A. McGlinchey, Paul A. Raftera, Fiona Reganb, Gillian P. McMahanb, A review of analytical methods for the determination of aminoglycoside and macrolide residues in food matrices, *analytica chimica acta* 624 (2008) 1–15



CHAPTER III

Literature on Biosensors for Antibiotic Residues

This chapter defines a biosensor and also describes the different electrochemical techniques that are used in studying the electrochemical behaviour of the transducer with or of the analyte of interest. Different LOD values from literature were compared based on the three selected antibiotic residues that are used for this study.

3. Introduction

A biosensor is an analytical device that is used for the detection of a specific analyte which merges a biological element with a physicochemical detector. The biological element used can be an enzyme and its substrate, antibody/antigen pair, nucleic acids and proteins, they are biologically derived material or biomimetic component that interacts or recognizes the analyte of interest [1]. When detecting the interface of the pairing a biosensor would use a sensing device or a transducer that will convert the biological reaction into an electrical signal that is amplified, stored, and quantified by a processor. Biosensors consist of different types and can be classified based on the transducer system that is used for a particular study. The antibody/antigen recognition pair is commonly used to detect veterinary drug residues, this kind of biosensor is referred to as immunosensor [2]. For detecting antibiotic residues the immunosensor is the preferred method because of the antibody-antigen pairing interface. Immunosensors make use of either electrochemical or optical transducer method which can be based on potentiometric, amperometric or conductometric technique [3]. Potentiometric device investigates changes in pH and ion concentration when an antigen in a sample interacts with an antibody immobilized on an electrode. The potential difference between the electrode bearing the antibody and a reference electrode is a function of the concentration of analyte in the sample. An amperometric biosensor measures the current produced when an electroactive species is oxidized or reduced at an antibody-coated electrode to which an analyte binds specifically. Conductimetric and capacitive biosensors measure the alteration of the electrical conductivity in a solution at constant voltage, caused by biochemical reactions that specifically generate or consume ions. As these transducers are usually non-specific and have a poor signal/noise ratio, they have been little used. Indeed, they have not been used for the detection of antibiotics [1-3].

Electrochemical methods are both influential and flexible techniques that have advantages such as high sensitivity, accuracy, and precision as well as large linear dynamic range, with quite low-cost instrumentation. After the development of more sensitive pulse methods, the electroanalytical studies are frequently used on industrial, environmental applications and on the drug analysis in their dosage forms and particularly in biological samples [4]. Electroanalytical techniques offer a solution to many problems or challenges of pharmaceutical interest with a high level of accuracy, precision, sensitivity, and selectivity when this approach is employed. Some of the most useful electroanalytical techniques are based on the concept of continuously changing the applied potentials to the electrode-solution interface and the resulting measured current [4-6].

3.1. Electrochemical techniques

3.1.1 Voltammetric techniques

Voltammetry is known as a class of electroanalytical techniques, and it is used to assign the current-voltage measurement obtained at a given electrode. Voltammetric technique is based on voltage-current-time relationship taking place in a three cell electrodes: working electrode, reference electrode and counter electrode. Explaining this relationship the potential (unit E) is applied to the working electrode and the resulting current which flows to the electrochemical cell will be recorded. In some instances either the applied potential could be changed or the current that results from it can be recorded over a period of time. The potential applied to the working electrode serves as driving force for the reaction; it controls the parameter that causes the chemical species present in solution to be electrolyzed (reduced or oxidized) at the electrode surface [5,7].

Polarography is one of the voltammetric techniques which is based to current-voltage measurement resulted from using dropping mercury electrode with a constant flow of mercury drop. Polarography was firstly introduced by a chemist called Jaroslav-Heyrovsky in 1922 and later won a Nobel Prize [5]. Using mercury drop as an electrode offers a uniform area and clean electrode surface to be used over a series of applied potential. The resulting plot is called the voltamogram where the current is presented in the vertical axis and the potential in the horizontal axis [5-8].

Stripping analysis is another voltammetric technique which involves the concentrated analyte into or onto the surface of the working electrode. The step prior the concentration is followed by electrochemical measurement of the preconcentrated analyte or stripped from the electrode surface by the application of a potential scan [7-8]. The arrangement of the preconcentration step and the stripping step creates an extremely favourable signal to background ratio. The characterization property of stripping analysis is the presence of built in preconcentration step [8]. The presence of preconcentration step results in high sensitivity and more direct polarographic techniques for stripping analysis. The advantages of this technique are wide linear range and direct study of trace concentrations of the analyte.

Cyclic voltammetry has become the technique of choice for many areas of electro analytical chemistry. It is commonly used to study the redox behaviour to get the information about a particular chemical reactions taking place [5,8]. Cyclic voltammetry is a fast voltage scan technique in which the voltage scan is reversed. When the potential is applied at the working electrode the resulting current will record both the forward and reverse scan. Both the forward and reverse scan uses the same scan rate. The measured parameters in cyclic voltammetry are anodic and cathodic peak potential (E_{pa} and E_{pc}), anodic and cathodic peak current (I_{pa} and I_{pc}) [8]

Differential Pulse Voltammetry is a mixture form of linear sweep and pulsed voltammetry. It is a very sensitive technique which allows a detection limit in ppb or lower. DPV has been used excellently in analytical determination of trace level of organic species. However, multiple pulses in the waveform make it a relatively slower technique with each scans taking time to complete [9]

Square Wave Voltammetry is a fresh and popular pulse technique for electroanalytical work. It is an additional development of pulse technique based on a rapid step scanning of potential applied to the electrode and moreover on each step is superimposed a high frequency square wave. The frequently used form is the Osteryoung square wave and based on the current response to the potential excitation is sampled once on each forward pulse and once on each reverse pulse. The two currents are then summed up thereby extremely increasing sensitivity. As SWV effectively removes the background current from the measurement, it has advantage over CV because of its speed, sensitivity and dynamic range of detection. It can respond to both high and low concentrations of electroactive species. It can detect micromolar

concentration of analyte in contrast to CV which can detect only millimolar concentration [5,9]

3.1.2 Impedimetric technique

Electrochemical impedance spectroscopy merges the investigation of both the resistance and capacitance properties of materials, based on the perturbation of a system at equilibrium by a small amplitude sinusoidal excitation signal. In EIS, the potential of the impedance system can be scanned over a wide range of alternative current (AC) frequencies. The use equivalent circuit models offers useful information for the interpretation of impedance spectra and it is an important technique for characterization [10-12]. Impedance spectroscopy presents a useful method to explore the electric characteristics of surface modified electrodes. Recording the full impedance spectrum within a wide region of frequencies is time-consuming. Thus, impedimetric techniques are only used as a characterization method for most of the enzyme-based impedimetric biosensors, and indirect monitoring strategies are generally adopted [10].

3.1.3 Amperometric technique

Amperometric measurements are based on recording the current flow in the cell at a single applied potential. However, a voltammetric measurement is made when the potential difference across an electrochemical cell is scanned from one preset value to another and the cell current is recorded as a function of the applied potential. In both cases, the essential operational feature of voltammetric or amperometric devices is the transfer of electrons to or from the analyte [13].

3.2. Electrochemical detection of Fluoroquinolone

Fluoroquinolones are one of the most vital antimicrobial agents that have established activity against a wide range of gram-positive and gram-negative organisms. Fluoroquinolones examples include ofloxacin, ciprofloxacin, perfloxacin, levofloxacin and norfloxacin with newer ones introduced almost after every five years. This class of antibiotics have been analyzed by different methods which have been discussed in different literatures [14]. Fluoroquinolones have been widely used in different areas one being in the veterinary medicine to treat or prevent bacterial infections in food-producing animals, aquaculture, and also pets. Rising concerns about drug residues in the food chain and contaminating

environment, and as a result contributing to the development of bacterial resistance [15-19]. The European Commission has established the maximum residue levels of the FQs detected in a number of matrices and the required analytical method that can use by both the public health control and the veterinary laboratories were also established [15]. For determination of fluoroquinolones antibiotics HPLC coupled to fluorescence, mass spectrometric and ultraviolet detection is the most commonly used method [16-19]. Properties such as requirement of expensive equipment and sample treatment limit the use of this method. Even though they offer useful information for confirmation but their use for screening purposes of large numbers of test samples become expensive. As a result the development of rapid, inexpensive and sensitive high sample throughput or on-site analytical strategies would attract attention from researchers [19]. The table below (Table 3.1) show examples of the bio/sensor reported for fluoroquinolones.



Table 3.1: Biosensor performance of Fluoroquinolones.

Method	Electrode Material	LOD	Linear Dynamic Range	Fluoro Antibiotic	Reference
DPV	GO/ GCE	5.0 nM	0.1 nM – 7.0 μ M	Norfloxacin	[28]
SWV	MWCNT / MPG	40.6 nM	1.2 - 1000 mM	Norfloxacin	[27]
SW/ASV	GCE	5.0 nM	6.0 nM - 0.5 μ M	levofloxacin	[42]
LSV	MWCNTs/Nafion film-coated GCE	5 nM	0.1–100 μ M	Norfloxacin	[25]
LSV	poly(methyl red) film-modified GCE	0.1 nM	1 μ M – 0.1mM	Norfloxacin	[26]
DPV	salmon sperm DNA/ GCE	24 μ M	40–80 μ M	Ciproflaxacin	[43]
LSV	CuO/MWCNTs/GCe	0.32 nM	1 μ M to 47.7 μ M.	norfloxacin	[45]
CV	HRP/ GCE	0.4 nM	0.02–65 μ M	ciprofloxacin	[40]
DPV	CNT/graphite pencil	0.3 μ M	1–10 μ M	Norfloxacin	[44]

DPV (differential pulse voltammetry), LSV (linear stripping voltammetry, CV (cyclic voltammetry)

SWV (square wave voltammetry), ASV (anodic stripping voltammetry)

Materials that are smaller in size ($\times 10^{-9}$) have attracted attention in recent electrochemical sensor research due to their properties such as; electrical conductivity, unique structural and catalytic properties, high loading of biocatalysts, good stability and excellent penetrability. Carbon nanotubes are also considered as nanomaterial and used as electrode materials with useful properties for various potential applications including small biological devices [9]. Carbon nanotubes can be used to advance electron transfer reactions when used as electrode material in electrochemical devices, electrocatalysis and electroanalysis processes due to their significant mechanical strength, high electrical conductivity, high surface area, good chemical stability, as well as relative chemical inertness in most electrolyte solutions and a wide operation potential window [20–22]. Properties of nanomaterials have been explored in promoting the electron transfer reaction for a wide range of molecules and biological species including insulin, carbohydrates, hydrogen peroxide, trinitrotoluene, nucleic acids, dopamine, ascorbic and uric acids [23-24]. Huang and colleagues [25], developed a determination method for norfloxacin based on modified electrode with multi-walled carbon nanotubes. They investigated the voltammetric response of the modified electrode and the resulted sensor showed high sensitivity, fast response time, highly selective against potentially interfering species, good reproducibility and stability [25,26]. Agrawal and co-workers [27], also developed a label free method for determining NOR using carbon nanotubes. Their study focused on using MWCNT modified pyrolytic graphite (MPG) electrode and followed by investigating the effect of NOR on the caffeine catabolism through its electrochemical determination in urine samples. The results showed good stability and successful detection of NOR and caffeine in clinical samples [27]. Graphene oxide is a carbon material which commonly used as nanomaterial in modified electrodes because of the excellent characteristic in sensitive sensing of many analytes. A study by Ye and colleagues [28], reported on the performance of graphene oxide with nafion film composite modified electrode, the results showed highly sensitive voltammetric response for detection of NOR. Based on the results obtained by Ye and co-workers [28], a new voltammetric method for determination of NOR was proposed with high sensitivity and wider detection linear range. During the course of the study, the long-time stability of GO/Nafion/GCE was due to good film-forming property of Nafion, which firmly fixed the GO on surface of GC electrode. The high sensitivity of detection was from both the good electrochemical response of GO and accumulating action of Nafion for NOR. The determination of NOR was done in capsules containing NOR as the pharmaceutical active ingredient and the obtained results were acceptable [28].

Conducting polymers such as polyacetylene, polypyrrole, polyaniline or polythiophene are easily prepared by electrochemically oxidizing the substrate on the electrode surface. Different polymeric modification of electrodes initiated application in analysis of different analytes such as acetaminophen, chlorprothixene, isoniazid, chemotherapeutic agents like amoxicillin, tinidazole in biological fluids and drug formulations [9]. An electrochemical method for detecting norfloxacin at poly(methyl red) film GCE was developed by Huang and colleagues. Methyl red monomer consists of a dimethyl amine group, azo group and a carboxyl group which offers a promising adsorption of norfloxacin. Electrochemical response of NOR on the prepared electrode material shows electrochemical oxidation of NOR is a possibility. This proposed method has resulted in low detection limit, fast response, inexpensive and simple preparation method [25-26].

Molecularly imprinted polymers (MIPs) are synthetic polymer materials with synthetically generated recognition sites capable of specifically binding a target molecule in preference to other closely related compounds [29-30]. MIPs imitate the natural receptor systems as well as antibodies, hormones and enzymes and they offer characteristics such as ease of preparation, low cost, high chemical and mechanical stability. The production of MIP-based sensors uses the approach of synthesis of an imprinted polymeric film on the electrodes surface by electropolymerization. This approach results in controlling the thickness of the polymer by modifying the electrochemical setting. Polypyrrole has been widely used as the polymer of choice for preparing molecularly imprinted sensors because they offer excellent biocompatibility and the feasibility of immobilising different compounds [29-31]. Some studies result in reduced MIP sensitivity, therefore materials such as MWCNT, metallic nanomaterials and graphene have been used to improve the sensitivity of the MIP [32-34]. A method based on voltammetric detection of NOR using MIP/MWCNT/GCE was developed. NOR molecules were imprinted in a PPy film to create specific recognition for binding sites. Modification of imprinted PPy with MWCNTs resulted in better sensitivity of analysis by increasing electrochemical conductivity and the surface area. The developed sensor was applied in the analysis of human urine spikes samples and the sensor resulted in good selectivity, simplicity in fabrication, easy to use and successful application in real samples [34]. Another MIP sensor was developed based on the preparation of molecularly imprinted photopolymerization of acrylamide and trimethylolpropane trimethacrylate on the surface of a gold electrode for determining NOR. The receptor layer was prepared by molecularly

imprinted and NOR is linked to the cavities constructed by binding sites of molecularly imprinted film. The proposed method is sensitive, simple, and cheap, and is applied to detect NOR in human urine successfully and the detection limit of the sensor was $1.0 \times 10^{-10} \text{ mol L}^{-1}$ [35].

The recognition of antibacterials by biosensor systems consist two major principles. The first principle looks at the widespread use of immobilized aptamers as recognition elements (aptasensors). Aptamers of RNA and DNA are referred to as oligonucleic acid that attaches a particular analyte by their 3D structure by means of van-der Waals forces, hydrogen bonding or ionic interaction creating a detectable signal. The resulting sensitivity is similar to that of antibodies. The second principle is based on antibody-mediated binding processes. Immunosensor are commonly used for detecting antibacterials [36-39]. They function by immobilizing specific antibodies for antibiotics at the transducer to detect the antibiotic binding or capsized the assay and detect the binding of spiked antibody samples onto immobilized antibiotics in a competitive assay form [39]. For determination of fluoroquinolones an amperometric magneto-immunosensor was developed based on specific antibody biomodified magnetic beads. The production of electrochemical species an enzymes tracer was used and showed a wide selectivity profile for fluoroquinolones. HRP was covalently coupled to Ab171 and fluoroquinolone hapten 11 through a two steps procedure. The simplicity of the electrochemical magneto immunosensor presented makes it acceptable for rapid and cheap semi-quantitative and quantitative on-site analysis of fluoroquinolones [19]. Torriero and colleagues [40], presented a sensitive device based on the use of horseradish peroxidase – rotating biosensor for electrochemical determination of CIP and NOR. HRP catalyses the oxidation of catechol when H_2O_2 is present, electrochemical reduction back was obtained at peak potential of 70 mV. However, when piperazine-containing compound is added to the solution, it readily reacts with quinone derivative, through the Michael addition, decreasing the peak current obtained in proportion with the increase in concentration of the compound containing piperazine. The resulting biosensor offers a fast and cost effective solution to the recognition of quantitative information at extremely low levels of CIP concentrations [40-41]. Giroud and co-workers [38], reported on the formation of an electrogenerated polymer functionalized by the model that mimics the ciprofloxacin structure and its use for immobilizing the immunoreaction and the anticiprofloxacin antibody. When the target is present the immobilized antibody was

displaced owing to the stronger association constant of antibody-ciprofloxacin, resulting in an accepted strong impedimetric signal. The analytical response of the impedimetric immunosensor was investigated. These phenomena were detected and characterized by electrochemical impedance spectroscopy allowing the selective detection of extremely low ciprofloxacin concentration. Sensors exposed to ciprofloxacin showed a decrease in the sum of the interfacial resistances with the increase in ciprofloxacin concentration from 1×10^{-12} to 1×10^{-6} g mL⁻¹ [39].

3.3. Electrochemical detection of β -Lactam

β -Lactam antibiotics are classified as a broad class of antibiotics which consist of agents with a β -lactam ring in their molecular structure. Examples of β -lactams are penicillins, cephalosporins, monobactams and carbapenems [46]. Benzylpenicillin or commonly known as penicillin G is a parenterally administered form of penicillin, a pioneer in β -lactam antibiotics. The effectiveness of β -lactam is limited by naturally occurring bacterial β -lactamases enzymes that destroy β -lactam stopping them from destroying the bacteria's cell wall [47]. Literature based on analytical techniques for determination of penicillins in different mediums such as biological samples or pharmaceutical formulations have been reported. An analytical technique like the high-performance liquid chromatography is linked to different detection method; ultraviolet detection, mass spectrometry as well as fluorescence are among the frequently used analytical methods for detection and quantification of penicillins [47-49]. The use of this method is limited due to their disadvantages which includes high cost of instrumentation and regularly too laborious, in the case where derivatization, extraction and purification process are required. The electrochemical methods have acquired many advantages such as simplicity, low-cost and possibility of miniaturization that eliminate limitations of other analytical methods [50-53]. Below table (table 3.2) compares LODs measured by different electrochemical techniques.

Table 3.2: Biosensor performance for β -lactams

Method	Electrode Material	LOD	Linear Dynamic Range	β -lactam Antibiotic	Reference
DPASV	Thioglycolic acid/Penicillinase/AuE	1.26 nM	50.0 nM - 5.0 mM	Penicillin G	[57]
Ampero	MWCNTs/hematein/ β -lactamase/ GCE	50 nM	200–1000 μ M	Penicillin V	[55]
CA	CIMSGD-CC electrode	0.53 μ M	100 - 1000 μ M	Amoxicillin	[56]
EIS	Penicillinase immobilised onto Ta ₂ O ₅	50 μ M	5 -10 μ M	Penicillin G	[58]
CA	β -Lactamases / AuE	4.5 nM	10–50 nM	Penicillin G	[47]
DPASV	MME in HMDE	0.717 nM	0.007–2.13 μ M	Penicillin G	[59]
SWV	BDD electrode	0.32 μ M	0.4 - 100 μ M	Penicillin V	[48]
DPV	BDD electrode	0.25 μ M	0.5 to 40 μ M	Penicillin V	[53]

Ampero (amperometry), CA (chronoamperometry), EIS (electrochemical impedance spectroscopy)

β -lactam antibiotics are the most frequently used antibiotics and have long been widely used for treating different bacterial infections in human, livestock, poultry, and aquaculture. Therefore, detection of the residues of these antibiotics in food and environment is vital for protecting the public health. Pharmaceutical products of penicillin G have pure sodium or potassium salt and small additives. Determination of penicillin G in pharmaceutical products is vital because it is quite an unstable drug. Various methods have been used for penicillin G determination in pharmaceuticals, such as HPLC with spectrophotometric detection, potentiometry and amperometry biosensors [54]. An amperometric biosensor based on the co-immobilization of MWCNT, hematein and β -lactamase on GC electrode using a layer-by-layer assembly was created for determining penicillin. The detection limit of the biosensor was lower than the conventional biosensor based on change in pH and a minimum of 50 nM LOD [55]. Another amperometric biosensor was developed for penicillin G by immobilizing penicillinase to a gold electrode by means of a cysteine self-assembled monolayer. The biosensor amperometrically monitored the catalytic hydrolysis of penicillin in a very sensible manner. Furthermore, it was successfully used to measure the Michaelis–Menten enzymatic constant and a low limit of detection of 4.5 nM was obtained [47].

The catalytic oxidation of amoxicillin was presented by cyclic voltammetry, chronoamperometry and amperometry methods at the surface of the modified carbon ceramic electrode. The copper iodide was used for preparing a new carbon ceramic electrode because it offers high catalytic capability for electro-oxidation of amoxicillin. The proposed electrode showed significant characteristics such as high stability, good reproducibility, high sensitivity and easy surface regeneration and fabrication [56]. A DPV method was developed for determining penicillin V on a bare BDD electrode. A highly reproducible and a sharp irreversible oxidation peak at +1.6 V (vs. Ag/AgCl) was obtained as a result of the penicillin V oxidation. The use of BDD electrode is highly suggested as a transducer in clinical investigations of different biological active compounds due to rapidity, simplicity and accuracy. Good linear concentration range and low detection limit were obtained without electrochemical pretreatment or chemical modification of BDD electrode [48,53].

3.4. Electrochemical detection of Aminoglycoside

Aminoglycosides antibiotics are classified by two or more amino sugars linked by glycosidic bonds to an aminocyclitol component. They have two major subclasses which 4,5-disubstituted deoxystreptamine, e.g., neomycin, and 4,6-disubstituted deoxystreptamine, for example gentamicin, kanamycin. Aminoglycosides function by inhibiting the bacterial protein synthesis by binding to ribosomes irreversible, and injures the cell membranes. They are usually dispersed in the body after they have been taken and little is absorbed from the gastro-intestinal tract and they are excreted in their native form in the urine [60]. Their major disadvantage in clinical use is the side effects of nephrotoxicity and ototoxicity. Kanamycin is one of the aminoglycoside that has been broadly used in human therapy and as an additive to promote growth and prevent disease in forage. Its use in veterinary medicine may generate residues in milk, and consequently induce allergic reactions in humans. Kanamycin like other aminoglycosides demonstrates reasonably narrow safety margin and may cause many side effects, such as loss of hearing, toxicity to kidneys, and allergic reactions to the drug [61-62]. The remaining amount of kanamycin found in foodstuff may lead to antibiotic resistance from the pathogenic bacterial strains and threatening the life of a consumer. Therefore it is important to efficiently control and analyze kanamycin residues [62]. Table 3.3 compares the LODs from literature.

Table 3.3: Biosensor performance for Aminoglycosides

Method	Electrode Material	LOD	Linear Dynamic Range	Aminoglycoside Antibiotic	Reference
DPV	BSA/Apt1/GNPs/Gr-PANI/TH/GE	8.60 nM	0.01 - 200.0 ng/mL	kanamycin	[61]
Ampero	Hyd/MWCNT(Au NP)-Ab2	6.76 nM	10-250 ng/mL	neomycin	[62]
SWS	dsDNA/DCNT	0.37 μ M	1.0-14.0 ng/L	Neomycin	[66]
Ampero	SWNTs/pAnt Neo	24.60 nM	0.2 - 125 ng/mL	neomycin	[67]
DPV	DNA/Au	0.20 nM	0.15 - 57.5 μ M	Neomycin	[64]
Ampero	MIPs/GR-MWCNTs/CS-SNP/ Au	7.63 nM	9.0 nM - 7 μ M	Noemycin	[65]

An amperometric immunosensor for determining neomycin was developed based on the preparation of covalently immobilized monoclonal neomycin antibody onto a conductive polymer (pDPB). The sensor was used to detect neomycin in a sandwich-type form and the secondary antibody was binded to gold nanoparticle (AuNp) decorated MWCNTs label with hydrazine the resulted sensor probe was as follow Hyd-MWCNT(AuNP)-Ab2. Factors limiting the immunosensor response were the dilution ratio of the antibody, pH, applied potential and temperature and were optimized based on the required condition for the immunosensor. A linear dynamic range for neomycin analysis was obtained between 10 ng/mL and 250 ng/mL with a detection limit of 4.11 μ M. The proposed immunosensor was

successfully applied to detect neomycin content in real meat samples [63]. An electrochemical behaviour of neomycin based on the DNA modified gold electrode was investigated using CV, DPV and chronocoulometry. It was found that in 0.01M PBS pH 7.3 at DNA/Au electrode neomycin demonstrated an irreversible cathodic peak which is more positive and less sensitive compared with that at bare gold electrode [64]. A sensor based on MIP for neomycin recognition was developed using chitosan-silver nanoparticles (CS-SNP)/graphene-multiwalled carbon nanotubes (GR-MWCNTs) composites decorated gold electrode. The imprinted polymer was synthesized by electropolymerization of pyrrole as the monomer and neomycin as the template. Cyclic voltammetry and amperometry were used to investigate the sensor performance. The sensor performance under the optimized conditions, the linear range of the sensor was from 9.0 nM to 7.0 μ M and the limit of detection of 7.63 nM (SN = 3). The film displayed high binding affinity and selectivity towards the template neomycin, as well as good reproducibility and stability [63]. Li and co-workers [61], developed an aptasensor based on thionine, praphene-polyaniline composite and AuNps were produced for determining kanamycin. The aptasensor performance was investigated by cyclic voltammetry and electrochemical differential pulse voltammetry. The optimized conditions such as concentration of aptamer, incubation temperature, time, and pH were suitable of the experiment. Based on the response of the developed aptasensor, showed a favorable analytical performance for kanamycin detection with a detection limit of 8.6 nM [61].

3.5. Conclusion

The monitoring of antibiotic levels in the environment and also in animals produced for human consumption, it is crucial to have quick, accurate, low-cost tests. ELISAs and other conventional analytical techniques have been used to detect food contaminants for over 3 decades. They offer a simple and inexpensive determination technique but their use is limited long operation time, because of the multiple washing and incubation steps required. Development of biosensors offers solutions to some of the challenges faced by these techniques. Therefore, biosensors can provide real-time measurements, a high degree of automation, and improved throughput and sensitivity. They are less expensive than sophisticated physico-chemical instrumentation, require less time for analysis, and are more user friendly. The use of biomolecules in the development of biosensors is the most

commonly used systems for analysis of samples containing antibiotic residues. The number of relevant electrochemical sensors which mimics the biomolecule role in biosensors may be on the rise. For future studies, they should pay attention on developing electrochemical sensors and producing portable devices for use in the field



References

1. Huet Anne-Catherine, Terry Fodey, Simon A. Haughey, Stefan Weigel, Christopher Elliott, Philippe Delahaut, Advances in biosensor-based analysis for antimicrobial residues in foods, Trends in Analytical Chemistry, 29 (2010) 1281-1294
2. Patel P.D., (Bio)sensors for measurement of analytes implicated in food safety: a review, Trends Anal. Chem., 21 (2002) 96-115
3. Mello L.D. and L.T. Kubota, Review of the use of biosensors as analytical tools in the food and drink industries, Food Chem., 77 (2002) 237–256.
4. Bengi Uslu and Sibel A. Ozkan, Electroanalytical Methods for the Determination of Pharmaceuticals: A Review of Recent Trends and Developments, Analytical Letters, 44 (2011) 2644- 2702.
5. Joseph Wang, Analytical Electrochemistry, 3rd ed, 2006 by John Wiley & Sons, Inc
6. Farghaly O. A., Mohamed N. A. Gahlan., A. A and M.A. El-Mottaleb Stability Constants and Voltammetric Determination of Some Selected drugs”, Indian Journal of Analytical Chemistry, 7 (2008) 294-300.
7. Farghaly O. A, Abdel Hameed R. S., Abd-Alhakeem H. Abu-Nawwas, Electrochemical Analysis Techniques: A Review on Recent Pharmaceutical Applications, Int. J. Pharm. Sci. Rev. Res., 25 (2014) 37-45
8. Farghaly O.A., Abdel Hameed R. S, Abd-Alhakeem H. Abu-Nawwas, Analytical Application Using Modern Electrochemical Techniques, Int. J. Electrochem. Sci., 9 (2014) 3287 – 3318
9. Alpana K. Gupta, Rama S. Dubey and Jitendra K. Malik, Application of Modern Electroanalytical Techniques: Recent Trend in Pharmaceutical and Drug Analysis, Ijpsr, 4 (2013) 2450-2458.
10. Jian-Guo Guan, Yu-Qing Miao and Qing-Jie Zhang, Review: Impedimetric Biosensors, Journal Of Bioscience And Bioengineering, 97 (2004) 219–226.
11. Bott A.W.: Electrochemical techniques for the characterization of redox polymers. Curr. Separat., 19 (2001) 71–75.
12. Katz E. and Willner, I.: Probing biomolecular interactions at conductive and semiconductive surfaces by impedance spectroscopy: routes to impedimetric immunosensors, DNAsensors and enzyme biosensors. Electroanalysis, 15 (2003) 913–947

13. Nelson R. Stradiotto, Hideko Yamanaka and Maria Valnice B. Zanoni, Electrochemical Sensors: A Powerful Tool in Analytical Chemistry, *J. Braz. Chem. Soc.*, 14 (2003)159-173,
14. Henry A. Okeri and Ikhuoria M. Arhewoh, Analytical profile of the fluoroquinolone antibacterials. I. Ofloxacin, *African Journal of Biotechnology*, 7 (2008) 670-680
15. Commission 2002/657/EC. Commission decision of 12 August 2002 implementing council directive 96/23/EC concerning the performance of analytical methods and the interpretation of results. *Off. J. Eur. Communities* 2002, L221, 8–36.
16. Andreu, V.; Blasco, C.; Picó, Y., Analytical strategies to determine quinolone residues in food and the environment, *TrAC Trends Anal. Chem.*, 26 (2007) 534–556.
17. Hernandez-Arteseros, J.A.; Barbosa, J.; Compano, R.; Prat, M.D., Analysis of quinolone residues in edible animal products. *J. Chromatogr. A*, 945 (2002) 1–24.
18. Saleh, G.A.; Askal, H.F.; Refaat, I.H.; Abdel-aal, F.A.M. Review on recent separation methods for determination of some fluoroquinolones. *J. Liq. Chromatogr. Related Technol.*, 36 (2013) 1401–1420.
19. Daniel G. Pinacho, Francisco Sánchez-Baeza, María-Isabel Pividori and María-Pilar Marco, Electrochemical Detection of Fluoroquinolone Antibiotics in Milk Using a Magneto Immunosensor, *Sensors*, 14 (2014) 15965-15980
20. Ghoneim M.M., A. Radi, A.M. Beltagi, Determination of Norfloxacin by square-wave adsorptive voltammetry on a glassy carbon electrode, *J. Pharm. Biomed. Anal.* 25 (2001) 205-210.
21. Ni Y.N, Y.R. Wang, S. Kokot, Simultaneous determination of three fluoroquinolones by linear sweep stripping voltammetry with the aid of chemometrics *Talanta* 69 (2006) 216-225.
22. Sun D., X.F. Xie, Y.P. Cai, H.J. Zhang, K.B. Wu, Voltammetric determination of Cd²⁺ based on the bi functionality of single-walled carbon nanotubes-Nafion film, *Anal. Chim. Acta*, 581 (2007) 27-31.
23. Wang J. and M. Musameh, Electrochemical detection of trace insulin at carbon nanotubemodified electrode, *Anal. Chim. Acta*, 511 (2004) 33-36.
24. Rabianes M.D., G.A. Rivas, Carbon nanotubes paste electrode, *Electrochem. Commun.* 5 (2003) 689-694.

25. Ke-Jing Huang, Xue Liu, Wan-Zhen Xie, Hong-Xia Yuan, Electrochemical behavior and voltammetric determination of norfloxacin at glassy carbon electrode modified with multi walled carbon nanotubes/Nafion, *Colloids and Surfaces B: Biointerfaces* 64 (2008) 269–274
26. Ke-Jing Huang, Chun-Xuan Xu, and Wan-Zhen Xie, Electrochemical Behavior of Norfloxacin and Its Determination at Poly(methyl red) Film Coated Glassy Carbon Electrode, *Bull. Korean Chem. Soc.*, 29 (2008) 988-993
27. BharatiAgrawal, PranjaliChandra, Rajendra N.Goyal, Yoon-BoShim, Detection of norfloxacin and monitoring its effect on caffeine catabolism in urine samples, *Biosensors and Bioelectronics* 47(2013) 307–312
28. Zhuo Ye, Le Wang, Jianguo Wen, A simple and sensitive method for determination of Norfloxacin in pharmaceutical preparations, *Brazilian Journal of Pharmaceutical Sciences*, 51 (2015) 249-259
29. Suryanarayanan V, C.T. Wu, K.C. Ho, Molecularly imprinted electrochemical sensors, *Electroanalysis*, 22 (2010) 1795–1811
30. Turiel E., A. Martin-Esteban, Molecularly imprinted polymers for sample preparation: a review, *Anal. Chim. Acta* 668 (2010) 87–99
31. Mazzotta E, C. Malitesta, M. Díaz-Álvarez, A. Martin-Esteban, Electrosynthesis of molecularly imprinted polypyrrole for the antibiotic levofloxacin, *Thin Solid Films* 520 (2012) 1938–1943.
32. Gao Chao, Zheng Guo, Jin-Huai Liu and Xing-Jiu Huang, The new age of carbon nanotubes: an updated review of function-alized carbon nanotubes in electrochemical sensors, *Nanoscale*, 4 (2012) 1948–1963.
33. Shao Y., Wang, J., Wu, H., Liu, J., Aksay, I. A., & Lin, Y. Graphene based electrochemical sensors and biosensors: a review, *Electroanalysis*, 22 (10) (2010) 1027–1036.
34. Hélder da Silva, João Pacheco, Joana Silva, Subramanian Viswanathan, Cristina Delerue-Matos, Molecularly imprinted sensor for voltammetric detection of norfloxacin, *Sensors and Actuators B*, 219 (2015) 301–307
35. Wang Zhihua and Jinshu Li, Xiaole Liu & Jianming Yang and Xiaoquan Lu, Preparation of an amperometric sensor for norfloxacin based on molecularly imprinted grafting photopolymerization, *Anal Bioanal Chem*, 405 (2013) 2525–2533

36. Cha M.Y, Lee, H.Y. Ko, Y. Shim, H.; Park, S.B., Pharmacophore-based strategy for the development of general and specific scFv biosensors for abused antibiotics. *Bioconjug. Chem*, 22 (2011) 88-94.
37. Ionescu, R.E.; Jaffrezic-Renault, N.; Bouffier, L.; Gondran, C.; Cosnier, S.; Pinacho, D.G.; Marco, MP.; Sánchez-Baeza, F.J.; Healy, T.; Martelet, C. Impedimetric immunosensor for the specific label free detection of ciprofloxacin antibiotic. *Biosens. Bioelectron.*, 23 (2007) 549-555.
38. Giroud, F.; Gorgy, K.; Gondran, C.; Cosnier, S.; Pinacho, D.G.; Marco, M.-P.; Sánchez-Baeza, F.J. Impedimetric immunosensor based on a polypyrrole-antibiotic model film for the label-free picomolar detection of ciprofloxacin. *Anal. Chem.* 81 (2009) 8405-8409
39. Katrin Reder-Christ and Gerd Bendas, Biosensor Applications in the Field of Antibiotic Research—A Review of Recent Developments, *Sensors.*, 11 (2011) 9450-9466
40. Torriero Angel A.J., Juan J.J. Ruiz-D'íaz, Eloy Salinas, Eduardo J. Marchevsky, Maria I. Sanz, Julio Raba, Enzymatic rotating biosensor for ciprofloxacin determination, *Talanta*, 69 (2006) 691–699
41. Torriero Angel A.J., Eloy Salinas, Julio Rabaa, Juana J. Silber, Sensitive determination of ciprofloxacin and norfloxacin in biological fluids using an enzymatic rotating biosensor, *Biosensors and Bioelectronics*, 22 (2006) 109–115
42. Radi A.and Z. El-Sherif, Determination of levofloxacin in human urine by adsorptive square-wave anodic stripping voltammetry on a glassy carbon electrode, *Talanta*, 58 (2002) 319–324
43. Haq Nawaz, Sakandar Rauf, Kalsoom Akhtar, Ahmad M. Khalid, Electrochemical DNA biosensor for the study of ciprofloxacin–DNA interaction, *Analytical Biochemistry* 354 (2006) 28–34
44. Somjai Theanponkrang, Wipa Suginta, Helge Weingart, Mathias Winterhalter, Albert Schulte, Robotic voltammetry with carbon nanotube-based sensors: a superb blend for convenient high-quality antimicrobial trace analysis, *International Journal of Nanomedicine* 10 (2015) 859–868
45. Manoj Devaraj, Ranjith Kumar Deivasigamani, Santhanalakshmi Jeyadevan, Enhancement of the electrochemical behavior of CuO nanoleaves on MWCNTs/GC

- composite film modified electrode for determination of norfloxacin, *Colloids and Surfaces B: Biointerfaces*, 102 (2013) 554– 561
46. Lakshmi R, K.S Nursin, Georgy Sharon Ann, K.S Sreelakshmi, Review: Role of Beta Lactamases in Antibiotic Resistance, *Int. Res. J. Pharm*, 5 (2014) 37- 40
47. Gonçalves Luís Moreira, Welder F.A. Callera, Maria D.P.T. Sotomayor, Paulo R. Bueno, Penicillinase-based amperometric biosensor for penicillin G, *Electrochemistry Communications*, 38 (2014) 131–133
48. Švorc Lubomir, Jozef Sochra, Peter Tomcik , Miroslav Rievaj, Dusan Bustin, Simultaneous determination of paracetamol and penicillin V by square-wave voltammetry at a bare boron-doped diamond electrode, *Electrochimica Acta* 68 (2012) 227– 234
49. Medvedovici A., M. Ionescu, C. Mircioiu, V. David, Optimization of a liquid–liquid extraction method for HPLC-DAD determination of penicillin V in human plasm, *Microchem. J.* 72 (2002) 85–92.
50. Pasamontes A, M.P. Callao, Determination of amoxicillin in pharmaceuticals using sequential injection analysis (SIA) Evaluation of the presence of interferences using multivariate curve resolution, *Anal. Chim. Acta* 485 (2003) 195–204
51. El-Maali N.A., Voltammetric analysis of drugs, *Bioelectrochemistry* 64 (2004) 99–107.
52. Baranowska I, P.Markowski, A. Gerle, J. Baranowski, Determination of selected drugs in human urine by differential pulse voltammetry technique, *Bioelectrochemistry* 73 (2008) 5–10.
53. Švorc Lubomír, Jozef Sochr, Miroslav Rievaj, Peter Tomčík, Dušan Bustin, Voltammetric determination of penicillin V in pharmaceutical formulations and human urine using a boron-doped diamond electrode, *Bioelectrochemistry* 88 (2012) 36–41
54. Parviz Norouzi, Mohammad Reza Ganjali, Taher Alizadeh, Parandis Daneshgar, Fast Fourier Continuous Cyclic Voltammetry at Gold Ultramicroelectrode in Flowing Solution for Determination of Ultra Trace Amounts of Penicillin G, *Electroanalysis* 18 (2006) 947 – 954
55. Chen Bi, Ming Ma, Xiaoli Su, An amperometric penicillin biosensor with enhanced sensitivity based on co-immobilization of carbon nanotubes, hematein, and β -lactamase on glassy carbon electrode, *Analytica Chimica Acta* 674 (2010) 89–95

56. Ghasem Karim-Nezhad, Ali Pashazadeh, and Sara Pashazadeh, Electro-Catalytic Oxidation of Amoxicillin by Carbon Ceramic Electrode Modified with Copper Iodide, *Journal of the Korean Chemical Society*, 57 (2013) 322-328
57. Rahman Mohammed M. and Abdullah M. Asiri, Development of Penicillin G biosensor based on Penicillinase enzymes immobilized onto bio-chips, *Biomed Microdevices*, 17 (2015) 9-16
58. Poghosian A, A Simonis, H Ecken, H Luth and M. J Schoning, An ISFET-based penicillin sensor with high sensitivity low detection limit and long lifetime, *Sensors and Actuators B.*, 76 (2001) 519 – 526
59. Abbasi S., K. Khodarahmian and A. Farmany, Quantification of sub-nanomolar levels of Penicillin G by differential pulse adsorptive stripping voltammetry, *Drug Test. Analysis*, 4 (2012) 140–144
60. Ibrahim A. Darwish, Development of generic continuous-flow enzyme immunoassay system for analysis of aminoglycosides in serum, *Journal of Pharmaceutical and Biomedical Analysis*, 30 (2003) 1539 – 1548
61. Falan Li, Yemin Guo, Xia Sun, Xiangyou Wang, Aptasensor based on thionine, graphene–polyaniline composite film, and gold nanoparticles for kanamycin detection, *Eur Food Res Technol*, 239 (2014) 227–236
62. Oertel R, Neumeister V, Kirch W, Hydrophilic interaction chromatography combined with tandem-mass spectrometry to determine six aminoglycosides in serum. *J Chromatogr A*, 1058 (2004) 197–201
63. Ye Zhu, Jung Ik Son, Yoon-Bo Shim, Amplification strategy based on gold nanoparticle-decorated carbon nanotubes for neomycin immunosensors, *Biosensors and Bioelectronics* 26 (2010) 1002–1008
64. Xiuli Li, Yanling Chen, Xianyu Huang, Electrochemical behavior of neomycin at DNA-modified gold electrodes, *Journal of Inorganic Biochemistry*, 101 (2007) 918-924
65. Wenjing Lian, Su Liu, Jinghua Yu, Jie Li, Min Cui, Wei Xu , Jiadong Huang, Electrochemical sensor using neomycin-imprinted film as recognition element based on chitosan-silver nanoparticles/graphene- multiwalled carbon nanotubes composites modified electrode, *Biosensors and Bioelectronics*, 44 (2013) 70–76

66. Suw-Young Ly, Hai-Soo Yoo, Chang-Hyun Lee, Voltammetric Assay of Antibiotics for Modified Carbon Nanotube Sensor, *J. of Korean Oil Chemists' Soc.*, 29 (2012) 443-449
67. Xiaoling Wu, Hua Kuang, Changlong Hao, Changrui Xing, Libing Wang, Chuanlai Xu, Paper supported immunosensor for detection of antibiotics, *Biosensors and Bioelectronics*, 33 (2012) 309– 312



CHAPTER IV

Instrumentation and Reagents

This chapter focuses on the instrumentation and techniques that were used in this study. Giving a brief discussion on the principle of the instruments. All reagents were used are listed in this chapter.

4. Introduction

The methods that were used for this study were scanning electron microscopy (SEM) representing microscopic techniques. This allowed us to study the morphology and the elemental analyses of the prepared materials. Electrochemical techniques that were used were cyclic voltammetry (CV), square wave voltammetry (SWV) and electrochemical impedance spectroscopy (EIS). Raman spectroscopy was also used to evaluate the vibrational modes of polysulfone, graphene oxide and polysulfone with graphene oxide.

4.1 Spectroscopic Techniques

4.1.1 Fourier Transform Infra-Red Spectroscopy (FTIR)

Fourier transform infrared spectroscopy offers quantitative and qualitative analysis for organic and inorganic samples. FTIR classifies chemical bonds in a molecule by generating an infrared absorption spectrum. The produced spectra of the sample is profiled, a characteristic molecular fingerprint that can be used to screen and scan samples for many different components. FTIR instrument offers efficient detection of functional groups and characterizing covalent bonding information. This technique results in band of frequencies between 4000 and 200 cm^{-1} beyond the red end of the visible spectrum. The usually FTIR spectrometer is made up of a source, interferometer, sample compartment, detector, amplifier, analog-to-digital convertor, and a computer. The source produces radiation which passes through the sample via the interferometer and gets to the detector. The produced signal is amplified and transformed to digital signal by the amplifier and analog-to-digital converter. Finally, the signal is transferred to a computer in which Fourier transform is operated [1].

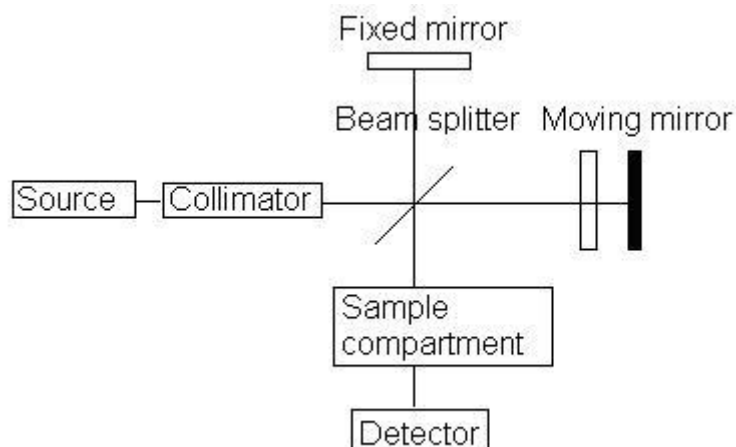
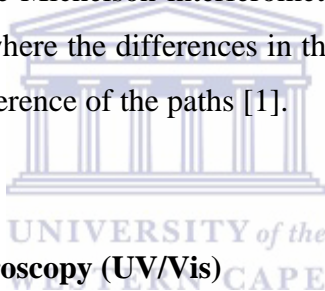


Figure 4.1: Schematic diagram of an FTIR spectrometer

The Michelson interferometer is the main difference between an FTIR spectrometer and a dispersive IR spectrometer and used to split one beam of light into two so that the paths of the two beams are different. Then the Michelson interferometer recombines the two beams and conducts them into the detector where the differences in the intensity of these two beams are measured as a function of the difference of the paths [1].



4.1.2 Ultra Violet-Visible Spectroscopy (UV/Vis)

UV/Vis spectroscopy refers to the measurement of the attenuation of a beam of light after it passes through a sample or after reflection from a sample surface. Electronic transition takes place when the electrons in the molecule move from a lower energy level to a high energy level in a few limited seconds. The absorption of the electromagnetic (EM) radiation excites an electron to the lowest unoccupied molecular orbital (LUMO) and creates an excited state. The more highly conjugated the system, the smaller the highest occupied molecular orbital (HOMO)-LUMO gap, and therefore the lower the frequency and longer the wavelength. The colours that are seen in inks, dyes and flowers are typically due to highly conjugated organic molecules. Chromophore is defined as a unit of the molecule that is responsible for absorption and the most common are C=C (π to π^*) and C=O (n to π^*) system. The following are the transitions levels $n \rightarrow \pi^*$, $\pi \rightarrow \pi^*$, $n \rightarrow \sigma^*$ and $\sigma \rightarrow \sigma^*$.

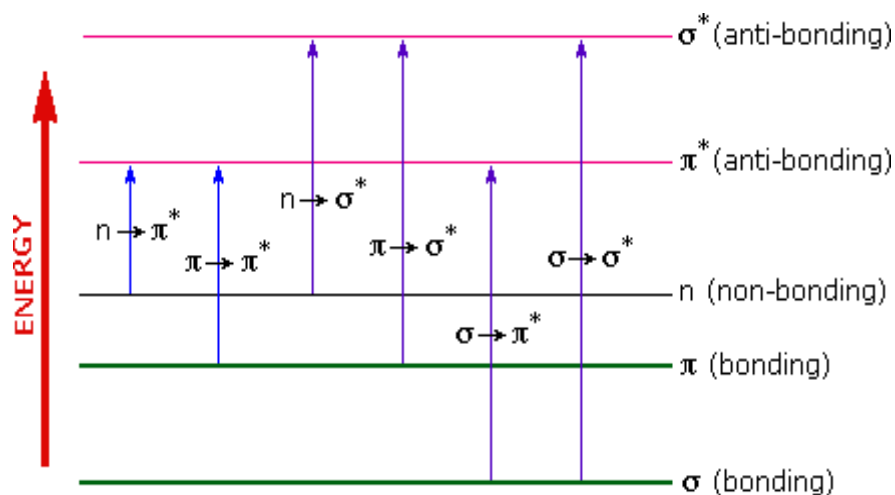


Figure 4.2: UV/Vis transition levels

UV spectroscopy is usually employed for the measurement of absorption, emission and transmission of the ultraviolet and the visible wavelengths by matter. UV-Vis technique is complementary to the fluorescence spectroscopy. Absorption of radiation by a sample is measured at various wavelengths and plotted by a recorder to give the spectrum which is a plot of the wavelength of the entire region versus the absorption (A) of light at each wavelength [2].

UV-Vis spectroscopy is routinely used in different ways. For detection of impurities this technique is the commonly used to determine the impurities in organic molecules. The spectral of the organic molecules shows additional peaks due to impurities in the sample and it can be compared with that of standard raw material. For quantitative analysis, the quantification of compounds that absorb UV radiation in analytical chemistry can also be done using UV absorption spectroscopy. Many other methods for quantitative analysis can be elucidated such as the calibration curve method; the simultaneous multi-component method; the difference spectrophotometric method; and the derivative spectrophotometric method. For qualitative analysis, UV absorption spectroscopy can be used to characterise those types of compounds which absorb UV radiation with the spectra applied on the characterisation of aromatic compounds and aromatic olefins [2].

4.1.3 Raman Spectroscopy

Raman spectroscopy gives the information based on the molecular vibrations of a sample that can be used for sample identification and quantitation. This technique operates by shining a monochromatic light source or laser on a sample of interest and detecting the scattered light. The bulk of the scattered light is of the same frequency as the excitation source; this is known as Rayleigh or elastic scattering. A small amount of the scattered light is shifted in energy from the laser frequency because of the interactions between the incident electromagnetic waves and the vibrational energy levels of the molecules in the sample. Raman spectrum of the sample results from plotting the intensity of this shifted light versus frequency. Normally, Raman spectra are plotted with respect to the laser frequency such that the Rayleigh band lies at 0 cm^{-1} . On this scale, the band positions will lie at frequencies that correspond to the energy levels of different functional group vibrations. The Raman spectrum can thus be interpreted similar to the infrared absorption spectrum [3-4].

In case where a monochromatic radiation is incident upon a sample then this light will interact with the sample in some fashion. It is the scattering of the radiation that occurs which can give the information about the sample's molecular structure. The incident photons will thus interact with the present molecule, the amount of energy change by a photon is characteristic of the nature of each bond present. The Stokes shift is whereby the final vibrational state of the molecule is more energetic than the initial state, and then the emitted photon will be shifted to a lower frequency in order for the total energy of the system to remain balanced. Whereas in the case of the final vibrational state is less energetic than the initial state, then the emitted photon will be shifted to a higher frequency, this is known as the Anti-Stokes shift [4].

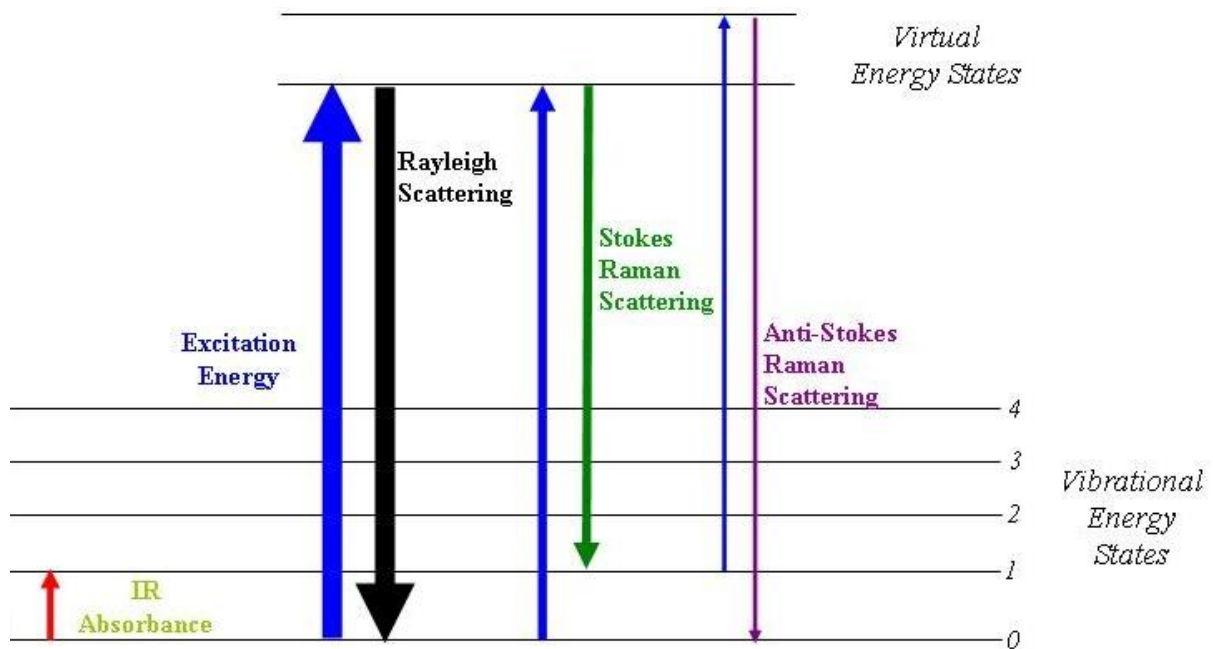


Figure 4.3: Raman's energy levels

4.2. Scanning Electron Microscopy

Scanning electron microscopy is a kind of electron microscope which uses electrons instead of light to produce an image of a sample by scanning it with a focused beam of electrons in a raster scan pattern. The electrons interact with electrons in the sample, signals are produced that can be detected and contain information about the sample's surface topography, composition, and other properties such as electrical conductivity. SEM produces various signals which are secondary electrons (SE), back-scattered electrons (BSE), X-rays, specimen current, cathodoluminescence (CL), and transmitted electrons. The signals result from interactions of the electron beam with atoms at or near the surface of the sample. The SEM can produce very high resolution images of a sample, revealing details less than 1nm in size [6].

SEM imaging involves specimens that are electrically conductive and electrically grounded to avoid the accumulation of electrostatic charge at the surface. Specimens that are non-conductive like polymers, coating with an electrically conductive material such as carbon and gold are used to enhance the imaging. The coating is done to prevent the accumulation of static electric charge on the specimen during electron irradiation and increases signals and surface resolution.

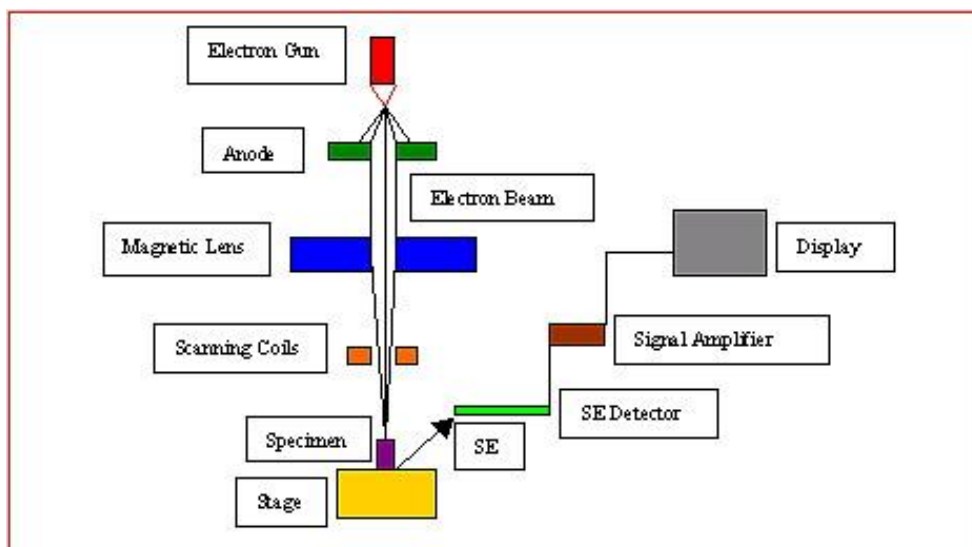


Figure 4.4: Schematic representation of SEM

Energy dispersive X-ray spectroscopy known as EDS/EDX is an analytical tool used for the elemental analysis or chemical composition of a sample. It relies on the investigation of a sample through interactions between electromagnetic radiation and matter, analyzing emitted X-rays by matter in response to being hit with charged particles. In stimulating the emission of characteristic X-rays from a specimen a high-energy beam of charged particles such as electrons, protons or beam of X-rays is focused into the sample.

4.3. Contact Angle

The contact angle is referred to as an angle at which a liquid/vapour interface meets a solid surface. Contact angle measurement is done by setting up the tangent or angle of a liquid drop with a solid surface at the base. The attractiveness of using contact angles θ to estimate the solid–vapor and solid–liquid interfacial tensions is due to the relative ease with which contact angles can be measured on suitably prepared solid surfaces. The method is illustrated with a small liquid droplet resting on a flat solid surface. The drop formed at the solid surface is quantified using the Young's Relation. A given system of solid, liquid, and vapour at a given temperature and pressure has a unique contact angle. The contact angle is commonly used in membrane material science to describe the relative hydrophobicity / hydrophilicity of a membrane surface [7]

There are different ways of measuring a drop. Contact angle can be measured on static drop, the drop formed before measurement and has a constant volume during the measurement. Dynamic drop is measured on increasing drops known as advancing angles and those measured on reducing drops as retreating angles. When a drop is deposited on a flat solid surface, the contact angle, θ , is the angle formed by a liquid at the three phase boundary where the liquid, vapour, and solid meet.

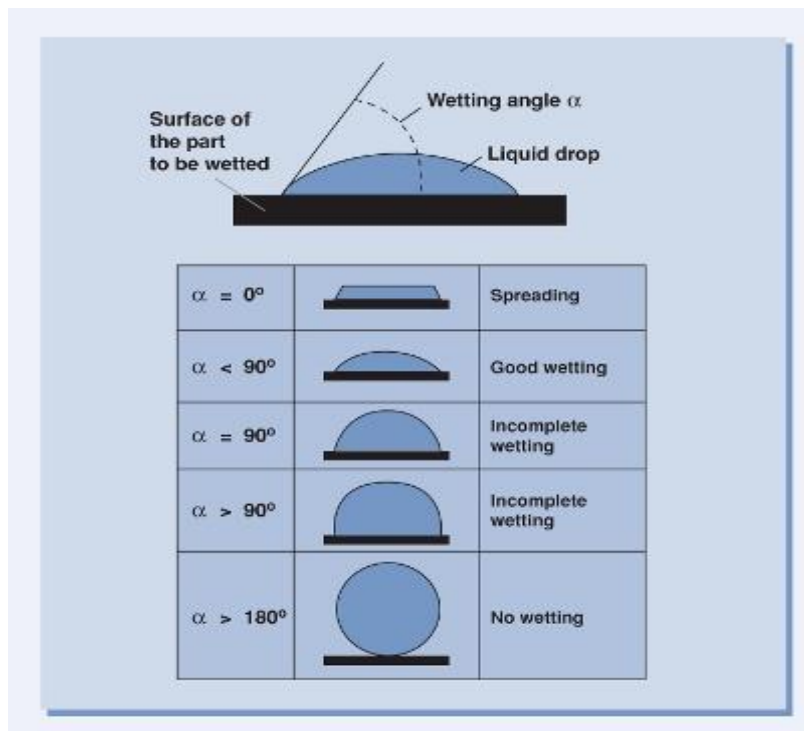


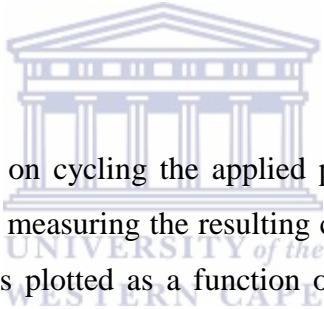
Figure 4.5: Contact angle water droplets

Another way of describing contact angle is to use cohesion and adhesion. Cohesion is the force between the liquid molecules which hold the liquid together, while the adhesion is the force between the liquid molecules and the solid molecules. Contact angle is a quantitative measure that demonstrates the ratio of cohesion vs. adhesion. If the contact angle is near zero, the liquid droplet spreads completely on the solid surface, adhesive forces are dominating. If the contact angle is very high, which means that the liquid droplet builds up on the solid surface, mean that cohesive forces are dominating [7].

4.4. Electrochemical techniques

4.4.1 Cyclic Voltammetry

Cyclic voltammetry is the most commonly used electrochemical technique for acquiring qualitative information about an electrochemical reaction. The method involves linearly varying an electrode potential between two limits at a specific rate while monitoring the current that develops in an electrochemical cell under conditions where voltage is in excess of that predicted by the Nernst equation. The influence of cyclic voltammetry results from its ability to rapidly provide considerable information on the thermodynamics of redox processes and the kinetics of heterogeneous electron transfer reactions and on coupled chemical reactions or adsorption processes. Cyclic voltammetry is often the first experiment performed in an electroanalytical study. Predominantly, it offers a rapid location of redox potentials of the electroactive species, and convenient evaluation of the effect of media on the redox process [8].



The cyclic voltammetry is based on cycling the applied potential to a stationary electrode immersed in an inert solution and measuring the resulting current. The output is exhibited as a voltammogram where current is plotted as a function of the applied potential. The time required to complete a particular scan depends upon the scan rate and the potential window to be traversed. The electrochemical cell used consists of three electrodes immersed in an electrolyte. An electrolyte is the solution at which dissolved substrates may pick up or lose electrons. For most cyclic voltammetry experiments an electrolyte is needed to provide electrical conductivity between the electrodes. The working electrode is the electrode at which the electrochemical redox (reduction or oxidation) phenomena being studied are taking place. The reference electrode provides a constant potential that can be taken as the reference standard for the potential applied at the working electrode. The commonly used reference electrodes are the silver-silver chloride (Ag/AgCl) and the Calomel electrode (Hg/HgCl/KCl). The third electrode is the counter electrode or auxiliary which serves as a collector in the cell, so that current can pass [8-9].

The potential of the working electrode is varied linearly with time, while the reference electrode maintains a constant potential. The auxiliary electrode conducts electricity from the signal source to the working electrode. The electrolytic solution normally contains ions, atoms or molecules that have lost or gained electrons and is electrically conductive. The key purpose of the electrolytic solution is to supply ions to the electrodes during the redox process. Cyclic voltammetry entails the application of a voltage to an electrode immersed in an electrolyte solution. A linear sweeping voltage is applied to an aqueous solution containing the compound of interest. During the potential sweep, the potentiostat measures the current resulting from the applied potential. The resulting current–potential plot is termed a cyclic voltammogram [8-9].

4.4.2 Square Wave Voltammetry

Square-wave voltammetry (SWV) is a large amplitude differential technique in which a waveform composed of an asymmetrical square wave superimposed on a base staircase potential applied to the working electrode. SWV is a small amplitude differential pulse technique in which a potential waveform composed of a symmetrical square wave is superimposed on a base-staircase potential. The difference in current between the forward and reverse pulses is plotted as a function of the potential applied to the working electrode resulting in a voltammogram [8].

A typical SWV involves a staircase potential ramp modified with square-shaped potential pulses. At each step of the staircase ramp, two equal in height and oppositely directed potential pulses are imposed. A single potential cycle in SWV is completed by two preceding potential pulses. For this technique a potential cycle is repeated at each step of the staircase ramp during the experiment. For the direction of the staircase ramp both the forward and backward potential pulses are recognized. Particularly, the potential pulses with odd serial number are forward pulses, while those with even serial numbers are set as reverse pulses. During the single potential cycle, the electrode reaction is determined in both anodic and cathodic directions, as a result giving a view into the electrode mechanism. The physical meaning of the frequency can be understood as a number of potential cycles in a unit of time. Characteristic frequency range offered by commercially available instrumentation is from 5

to 2000 Hz, which corresponds to the duration of a single potential pulse from 0.25 to 100 ms [8,10].

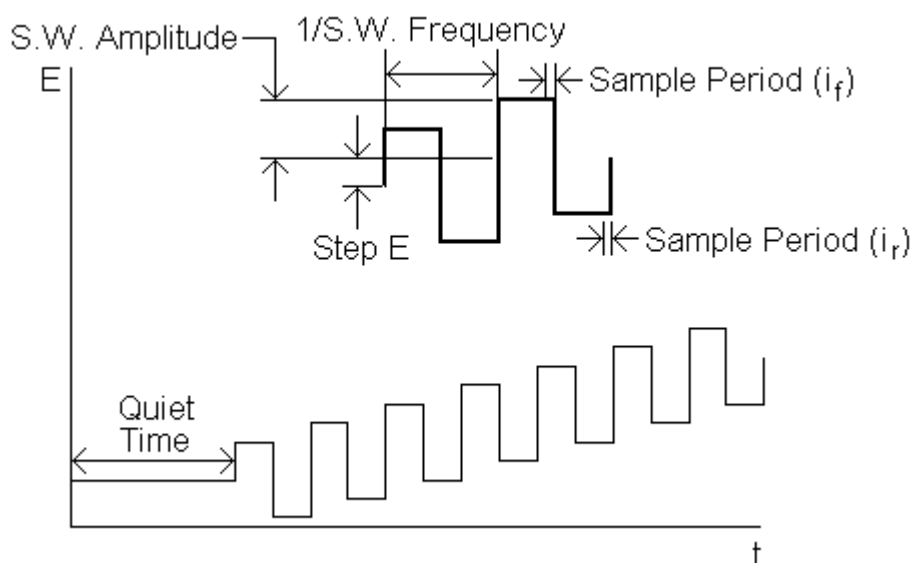


Figure 4.6: SWV potential wave form

The advantages of SWV includes fast scan rate, large frequency, large amplitude and short time required for measurements as well as the specific approach in the current sampling procedure make this technique one of the most applicable among the pulse voltammetric techniques. This unique advantage makes the SWV useful in analytical applications as well as in fundamental studies of electrode mechanisms [8].

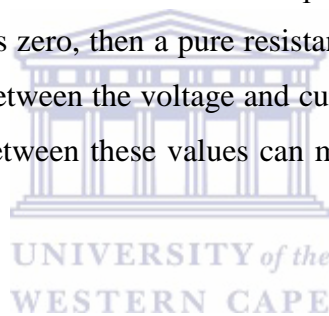
4.4.3 Electrochemical Impedance Spectroscopy

EIS involves measurements and analysis of materials in which ionic conduction strongly dominates. EIS investigates the system response to the application of a periodic small amplitude ac signal. These measurements are carried out at different ac frequencies. Analysis of the system response contains information about the interface, its structure and reactions taking place [8]

The main purpose of impedance spectroscopy is to play an important role in fundamental, applied electrochemistry and materials science in the future. EIS is divided into two applications which will demonstrate the power of the IS technique when it is applied to two

very diverse areas, aqueous electrochemistry and fast ion transport in solids. The following examples were selected because of their historical importance and because the analysis in each case is fairly simple. For the aqueous electrochemistry which is electrochemical impedance application, because it deals with real systems that do not necessarily behave ideally with processes that occur distributed in time and space, specialised circuit elements (CPE and ZW) is commonly used. The Warburg element (ZW) is used to represent the diffusion or mass transport impedances of the cell. The electrochemical impedance is the response of the electrode chemical system (cell) to an applied potential. The electrochemical impedance spectroscopy (EIS) is used for diagnostic purpose to characterise changes at a surface. The EIS is also used for application purpose to know the effect of the materials on an electrode surface [8,11].

From Ohms Law for AC conditions the impedance can be calculated by setting the input potential and measuring the induced current. When the phase angle, θ , between the voltage applied and the current induced is zero, then a pure resistance is present. In the case where a phase angle of 90° is measured between the voltage and current at the same frequency a pure capacitance is present. Angles between these values can mean a combination of a capacitor and resistance are present [8,11].



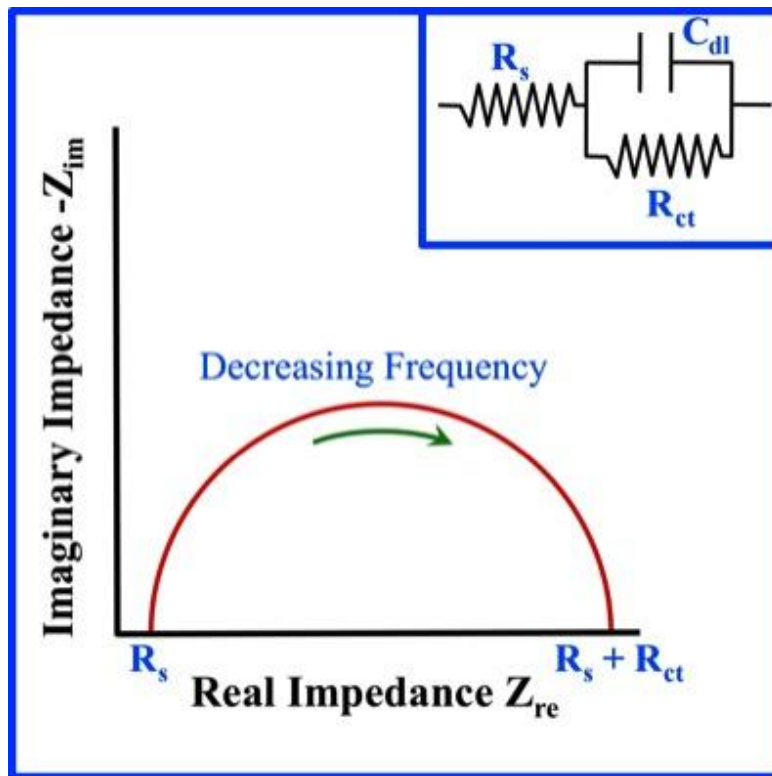


Figure 4.7: EIS spectrum and the Randles-Sevcik circuit

Impedance data is commonly analysed by fitting it to an equivalent circuit model. The circuit that is usually used in the Randles equivalent circuit which is composed of different elements such as resistors, and inductors joined in series or in parallel, to represent solution resistance, interfacial capacitance and charge transfer processes [12]

4.5. Reagents

4.5.1 Reagents or Chemicals used in this study

Graphite powder, H₂SO₄ (98%), NaNO₃, NaOH, H₂O₂ (30%), K₃Fe(CN)₆, HCl (37%) and KMnO₄ (>99%), Penicillin G sodium salt, Norfloxacin (≥98%) and Neomycin trisulfate salt hydrate, Sodium phosphate monobasic dehydrate and Sodium phosphate dibasic dihydrate were all purchased from Sigma-Aldrich. All the reagents used were of analytical grade and were used as they were. The aqueous solutions were prepared using Milli-Q water (18 MΩ cm⁻¹).

4.6. Instrumentation

4.6.1 Electrochemical measurements

Electrochemical measurements were carried out using a potentiostat Palm Instruments BV running with PS 4.4 software. Alumina micropolish and polishing pads (Buehler, IL, USA) were used for polishing the electrodes. The PSF and modified PSF was drop coated onto the BDD electrode and studied as the working electrode. Impedance studies were carried out on Voltalab PGZ 402 Universal Pulse dynamic EIS from Radiometer Analytical (Lyon, France).

4.6.2 Scanning Electron Microscopy (SEM)

The scanning electron measurements were carried out using Zeiss Auriga, High resolution (fegsem) field emission gun scanning electron microscope was used. Each sample was coated with carbon. Zeiss Auriga instrument with Gemini technology, employing a FEG Tip operated at an accelerating voltage

4.6.3 Contact Angle Instrument

The Contact Angle instrument was used in this study to measure the contact angle of water on the prepared polysulfone, graphene oxide and polysulfone with graphene oxide flat surface. Using the sessile drop method, a drop of dH₂O with a volume of 10 μl was drop coated onto the membrane surface. The angle that the droplet makes with the surface of the polysulfone was measured using KRUSS Drop Shape Angle software. Three measurements were done for each material and the mean contact angle and standard deviation results were reported.

4.6.4 Raman Spectroscopy

Horiba Xplora model Edge filter with gratings 600 – 2400 lines/mm Raman Spectrometer was used to study the stretching vibrations of polysulfone before modification and after modification with graphene oxide. Polysulfone and the nanocomposite of polysulfone with graphene oxide were dropped onto a microscopic glass slide and dried at room temperature

4.6.5 UV-Vis Spectroscopy

The Ultraviolet-visible (UV-Vis) spectroscopy was performed on the Nicolet evolution 100 spectrometer (Thermo Electron Corporation, UK). Measurements were recorded over a range of 190 - 900 nm using 3 cm³ quartz cuvettes.

4.6.6 Fourier Transform Infrared Spectroscopy

FTIR measurements were carried out on Perkin Elmer model Spectrum 100 series. The samples were prepared by making a pellet using KBr. Measurements were carried from 4000-400 cm⁻¹

4.6.7 Atomic Force Microscopy

AFM imaging was carried on Nanosurf easyScan 2 instrument, the samples were drop coated onto BDD working electrode and left to dry at room temperature. A non-contact tip was used since the polysulfone was rough and thick.



UNIVERSITY OF
WESTERN CAPE

References

1. Saptari V., Fourier-Transform Spectroscopy Instrumentation Engineering, SPIE Press, Bellingham, WA (2003).
2. Filip Monica Sanda, Macocian Eugen Victor, Toderas Adina Monica, Cărăban Alina, Base Theory For Uv-Vis Spectrophotometric Measurements, Internal Report, 2012
3. Gurvinder Singh Bumbrah, Rakesh Mohan Sharma, Raman spectroscopy – Basic principle, instrumentation and selected applications for the characterization of drugs of abuse, Egyptian Journal of Forensic Sciences, 6 (2016) 209–215
4. Derek A. Long. The Raman Effect. John Wiley & Sons, New York, 2002.
5. Skoog DA, Holler FJ, Crouch SR. Principles of instrumental analysis. 6th ed. Cengage Learning; 2006.
6. Ray F. Egerton, Physical Principles of Electron Microscopy An Introduction to TEM, SEM, and AEM, Springer Science + Business Media, Inc., 233 Spring St., New York, NY 10013, USA
7. Yuehua Yuan and T. Randall Lee, Contact Angle and Wetting Properties, Springer Series in Surface Sciences 51, (2013) 3-34
8. Joseph Wang, Analytical Electrochemistry, 3rd ed, 2006 by John Wiley & Sons, Inc
9. Özkan, S. A.; Uslu, B.; Aboul-Enein, H. Y., Analysis of pharmaceuticals and biological fluids using modern electroanalytical techniques. Critical Reviews in Analytical Chemistry, 33 (2003) 155-181
10. Milivoj Lovrić, Square-Wave Voltammetry, Chapter 3, Electroanalytical Methods, pp 121-145, 2009
11. Allen J. Bard, Larry R. Faulkner, 2002, Electrochemical Methods: Fundamentals and Applications, 2nd edition, John Wiley & Sons, New York, USA
12. Fernández-Sánchez C, CJ McNeil, K Rawson, Electrochemical impedance spectroscopy studies of polymer degradation: application to biosensor development, TrAC Trends in Analytical Chemistry, 24 (2005) 37-48

CHAPTER V

Materials Synthesis, Preparation and Characterisation

This chapter focuses on the synthesis, preparation and characterisation of Polysulfone, Graphene oxide and Polysulfone modified with Graphene oxide nanocomposite, to be used as transducer material to be applied for the detection of the three selected antibiotic residues, as presented by the conceptual diagram (Figure 5.1). This chapter studies the morphology of the prepared material measured by the SEM and AFM and also looking at the chemical composition of the material by spectroscopic techniques.

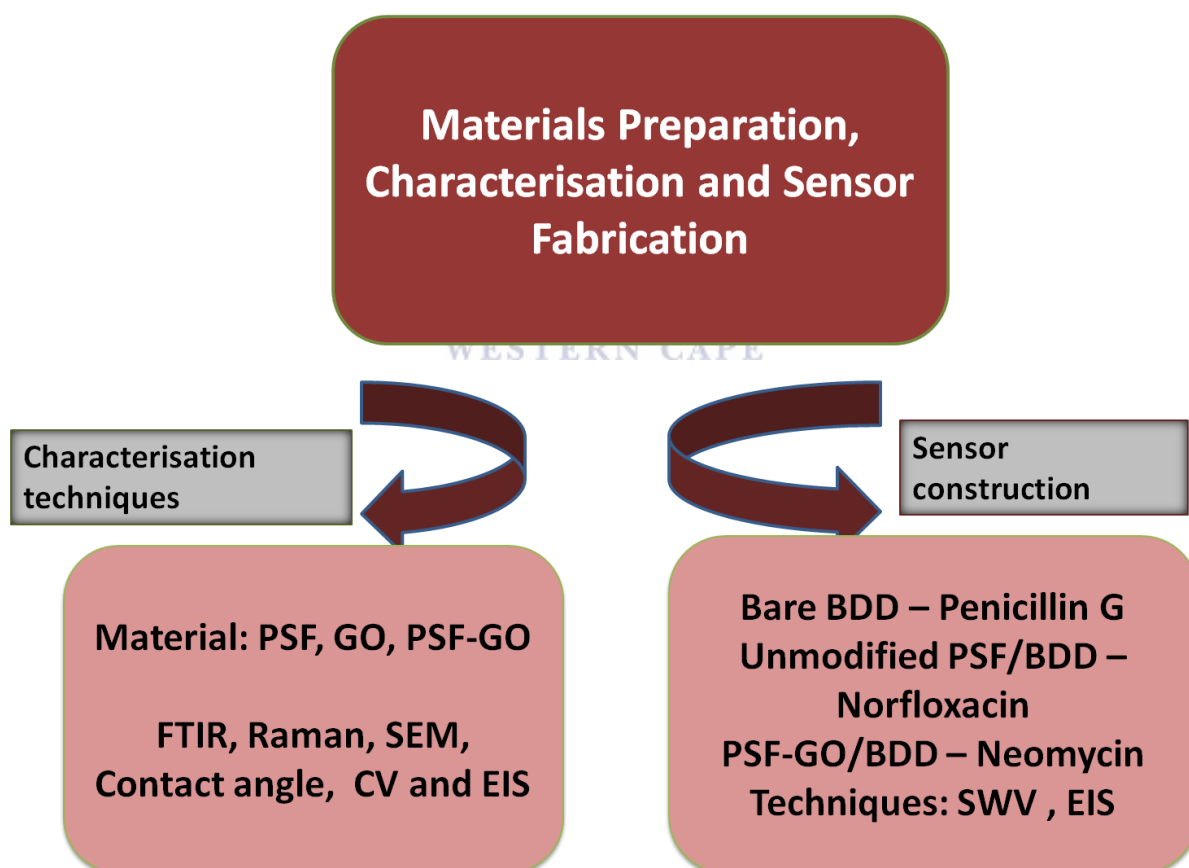


Figure 5.1: Conceptual diagram

5.1 Graphene Oxide

Graphene is a one atom layer thick carbon sheet, which has many interesting properties like electronic, optical and mechanical properties due to its two-dimensional (2D) crystal structure. The charge carriers of graphene move ballistic in the 2D crystal lattice of graphene; hence it possesses high conductivity despite it being an organic compound [1-2]. Graphene is a building block because it can be wrapped up to form fullerene, rolled-up to form carbon nanotube or stacked up to form graphite. All of the variation from graphene exhibit interesting electrical properties [1-3]. Graphene oxide (GO) is a branch of graphene, which consists of a single-layer of graphite oxide and is usually produced by the chemical treatment of graphite through oxidation, with successive dispersion and exfoliation in water or suitable organic solvents. It is insulating due to the large portion of sp³ hybridized carbon atoms bonded with the oxygen containing groups, which results in a sheet resistance of $> 10^{12} \Omega$ or higher [1-4].

Graphene oxide is one of the highly recognized materials for breaching new possibilities in the development of next generation biosensors. Owing to the coexistence of hydrophobic domain from pristine graphite structure and hydrophilic oxygen containing functional groups, GO exhibits good water dispersibility, biocompatibility, and high affinity for specific biomolecules as well as properties of graphene itself partly depending on preparation methods. These properties of GO offered a lot of opportunities for the development of new biological sensing platforms, including biosensors based on fluorescence resonance energy transfer (FRET), laser desorption/ ionization mass spectrometry (LDI-MS), surface-enhanced Raman spectroscopy (SERS), and electrochemical detection [4-5].

Singha and co-workers [7], studied for the first time the application of graphene oxide-chitosan (GO-CHI) nanocomposite for the fabrication of electrochemical DNA biosensor for rapid and sensitive detection of typhoid using specific 5-amine labelled probe from Vi capsular antigen gene region of *S. enteric serovars typhi*. The analytical performance of the designed electrochemical DNA biosensor have been evaluated for the complementary, non-complementary and one base mismatch sequence via monitoring the oxidation of redox indicator methylene blue (MB) using differential pulse voltammetry (DPV). The ssDNA/GO-CHI/ITO biosensor showed detection range of 10 fM to 50 nM and LOD 10 fM within 60 s hybridization times for complementary sequence. Further, ssDNA/GO-CHI/ITO bioelectrode

is able to detect complementary target present in serum samples with LOD of 100 fM at 25 °C. The excellent performance of biosensor is attributed to large surface-to-volume ratio and good electrochemical activity of graphene oxide, and good biocompatibility of chitosan, which enhances the DNA immobilization and facilitate electron transfer between DNA and indium tin oxide (ITO) electrode surface [6].

5.2. Polysulfone

The overwhelming interest on polysulfone (PSF) membrane is owed to its excellent characteristics such as: solubility in a large range of aprotic polar solvents, halogen derivatives, high thermal resistance (150–170° C), chemical resistance, high mechanical resistance of the films (fracture, flexure, torsion), moderate reactivity in aromatic electrophile substitutions reactions [7-8]. Good solubility allows all preparation methods for PSF membranes especially phase inversion by immersion precipitation, chemical resistance allows the sterilization (thermal and chemical), biocompatibility and moderate reactivity allows functionalization by aromatic electrophile substitution or other reactions [7]. However the polysulfones exhibit few main disadvantages, the hydrophobic character, the low resistance to UV radiation and less electrochemical conductivity [7,8]. Its porosity allows it to be used in micro, ultrafiltration and reverse osmosis processes as well as in the development of composite membranes to facilitate transport. It is also possible to modify the chemical nature of the polysulfone matrix in order to optimize membrane composition. Furthermore, it is easy and fast to prepare electrodes based on polysulfone membranes [8-9]. Non-conductive polymers like PSF are attractive in membrane technology due to its solubility properties and its high thermal, chemical and mechanical resistances. Making these polymers conductive is a challenge in polymer and membrane technologies [8].

Sanchez and co-workers [10], describe a simple and efficient method for preparing sensitive carbon nanotube/polysulfone/RIgG immunocomposite. Carbon nanotube/polysulfone membrane acts both as reservoir of immunological material and transducer while offering high surface area, high toughness and mechanical flexibility. The study was based on the competitive assay between free and labelled anti-RIgG for the available binding sites of immobilized rabbit IgG (RIgG). When comparing with graphite/polysulfone/RIgG

immunosensors shows a much higher sensitivity for those prepared with carbon nanotubes coupled with polysulfone [8,10,11].

5.3 Materials Preparation, Synthesis and Characterisation

5.3.1 Synthesis of Graphene oxide

The synthesis of graphene oxide was achieved by using the Hummers method [12]. Graphene oxide was prepared by dissolving 2 g of graphite powder (size range 1-2 micron) into 50 ml of concentrated sulphuric acid. About 3 g of KMnO_4 was added to the suspension kept in an ice bath. Distilled water (120 ml) was slowly added to the reaction mixture. The suspension was then further treated with 30 % H_2O_2 to reduce the residual permanganate [13-15]. The reaction flask was then removed from the ice bath and allowed to stir overnight at room temperature. The obtained suspension was centrifuged for 20 mins at 1400 rpm and washed with HCl and dH_2O (1:9) [12-15]. The product was dried overnight in a vacuum oven and the temperature 70 °C. The chemicals used for the synthesis of graphene oxide were all purchased from Sigma Aldrich and used without any pre-treatment.

UNIVERSITY of the
WESTERN CAPE

5.3.2 Characterisation of Graphene oxide

FTIR spectroscopy: Graphene oxide was synthesized using Hummers method which entails placing graphite in concentrated acid and an oxidizing agent. Oxidation of graphite resulted in a brown-colored viscous slurry, which included graphite oxide and exfoliated sheets along with non-oxidized graphitic particles and residue of the oxidizing agents in the reaction mixture [13]. The FTIR was performed using the Perkin Elmer spectrometer. The wavelength range was $4000 - 400 \text{ cm}^{-1}$ and scans used were 16. FTIR was used to monitor structural changes before and during the oxidation processes of the graphite to graphene oxide.

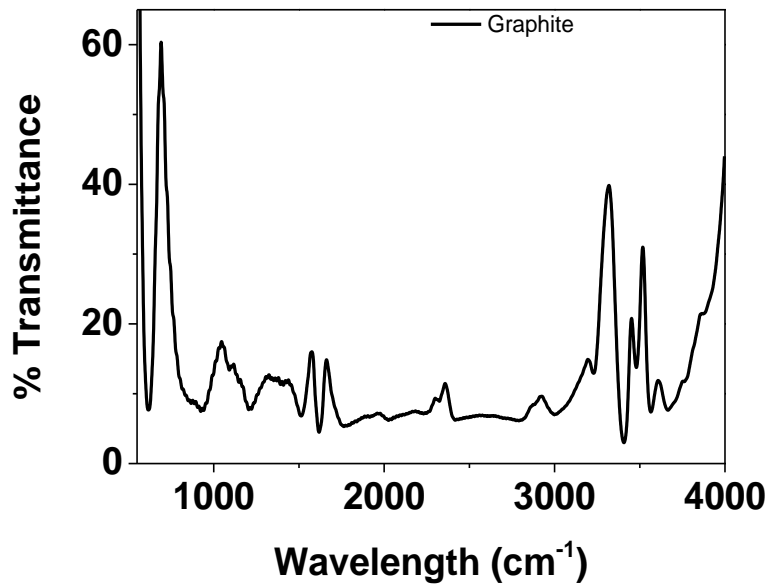


Figure 5.2a: FTIR spectra of graphite

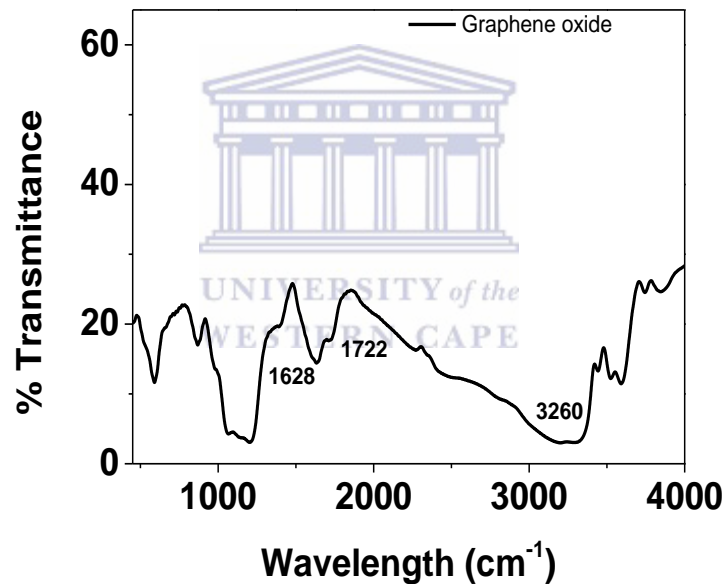


Figure 5.2b: FTIR spectra graphene oxide

Graphene oxide spectrum (Figure 5.2b) showed two bands at 1722 cm^{-1} and 1628 cm^{-1} assigned to C=O stretching vibration of the carboxylic group and C=C stretching mode of the sp^2 network [14]. The presence of different types of oxygen functionalities in graphene oxide was confirmed at 3260 cm^{-1} O-H stretching vibrations which is due to water molecules adsorbed on graphene oxide, at 1720 cm^{-1} stretching vibrations from C=O, and at 1220 cm^{-1} C-OH stretching vibrations [13-17]. Graphite spectrum (Figure 5.2a) didn't show the O-H peak at 3260 cm^{-1} . The existence of these oxygen-containing groups showed that the graphite was oxidized. The polar groups (hydroxyl groups) resulted in the formation of hydrogen

bonds between graphite and water molecules, this further explains the hydrophilic nature of graphene oxide. Therefore, it can be concluded that graphene oxide has hydrophilic properties, this is confirmed by the obtained contact value of 42 degree obtained for graphene oxide [15-18].

Raman spectroscopy: Raman spectroscopy was used for the characterization of the synthesized materials to study the vibrational changes of the prepared material. The most important characteristics of graphitic carbon-based materials in the Raman spectra are the D and G peaks and their overtones [19]. The Raman spectrum of a single-layer of graphene will be different to that of a multi-layer graphene. The increase of graphene layers will result in a splitting of the 2D peak into an increasing number of modes that can combine to give a wider and shorter peak intensity [20]. The first D and G peaks, both occurring from the vibrations of sp^2 carbon, appear respectively around 1350 cm^{-1} and 1580 cm^{-1} . The D peak represents in-plane vibrational mode of aromatic rings arising due to the defect in the sample [20-22]. The D-peak intensity is often used as a measure for the degree of disorder [21-23]. As the Raman intensity increases the degree of disorder also increases. The overtone of the D peak, is called a 2D peak around 2680 cm^{-1} , can be correlated to the number of graphene layers [22-24]. The number of graphene layers can be obtained from the ratio of peak intensities I_{2d}/I_g . The G peak corresponds to the carbon pairs optical E_{2g} phonons at the Brillouin zone center resulting from the bond stretching of sp^2 in both, rings and chains [21]. Two peaks were observed from the graphene oxide spectrum (Figure 5.3b) 1341 and 1578 cm^{-1} which are the D and G peaks. From the graphite spectrum (Figure 5.3a) only one was observed at 1570 cm^{-1} .

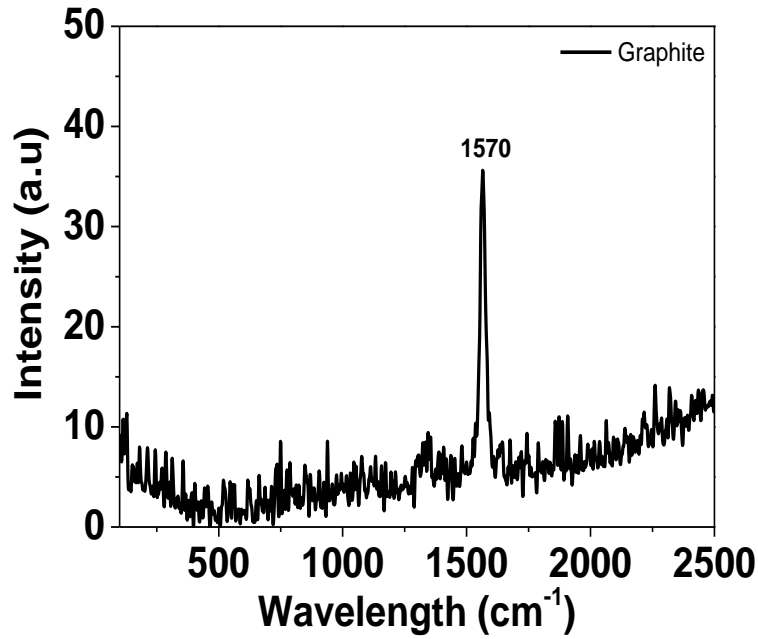


Figure 5.3a: Raman spectra of graphite

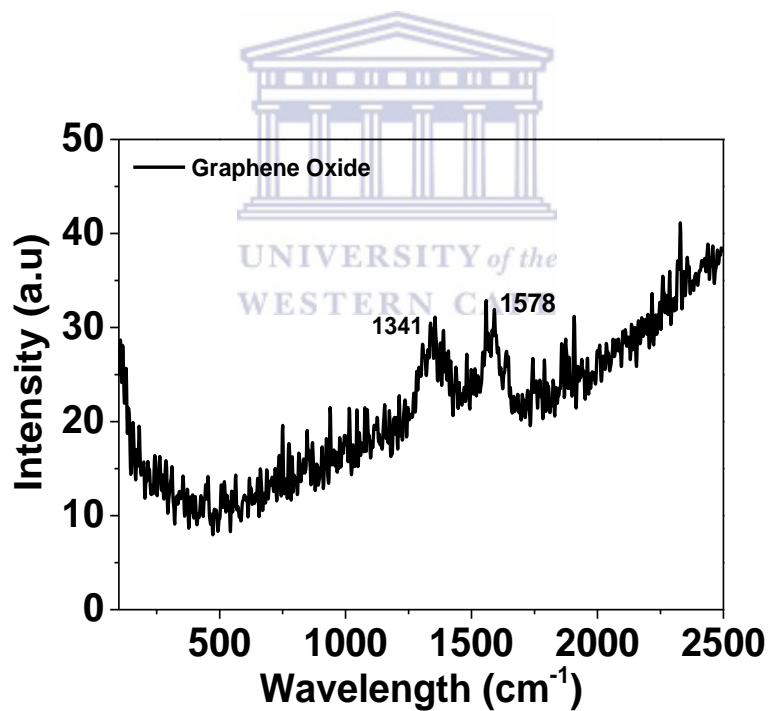


Figure 5.3b: Raman spectra of graphene oxide

Scanning electron microscopy: The scanning electron microscopy, Zeiss Auriga, High resolution (fegsem) field emission gun scanning electron microscope was used to study the morphology of graphene oxide. The graphene oxide was drop coated onto a copper grid and coated with carbon to improve the conductivity for imaging. Atomic force microscopy (AFM) imaging was carried out on NanoSurf EasyScan 2 instrument. The graphite and

graphene oxide were dispersed in distilled water and sonicated to form a homogenous suspension. The suspension of graphite and graphene oxide were drop coated onto BDD working electrode.

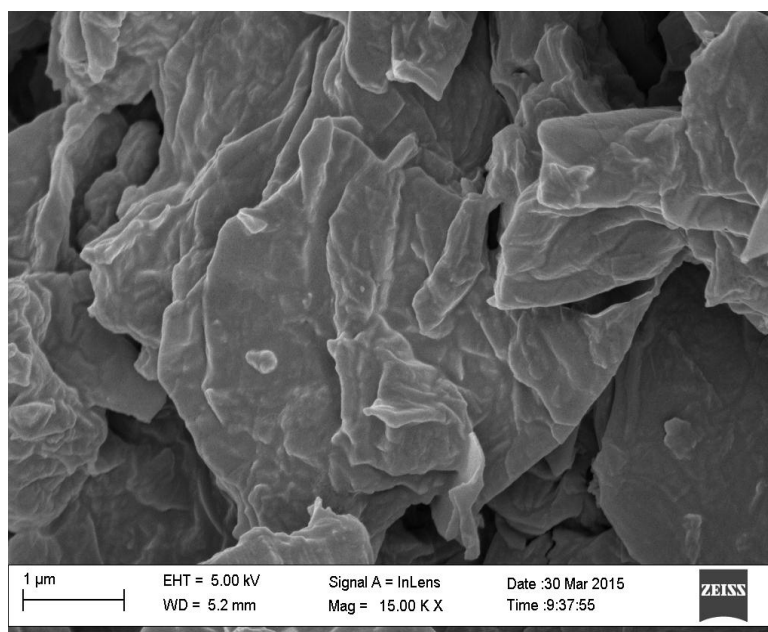


Figure 5.4: SEM image of graphene oxide

Morphological properties of graphene oxide were investigated with scanning electron microscopy. The SEM image of graphene oxide showed single flakes that are stacked together and laminar structures are formed. The data from EDS spectrum of graphene oxide confirms the oxidation of graphite to graphene oxide, this was evident by the presence of oxygen in the EDS spectra (Figure A4). The SEM image of the graphite showed flakes with an average size of 1 μm and the EDS of graphite shows only the carbon that is present in the graphite sample, the image and the EDS are presented in the appendix (Figure A1 and A2). AFM images of graphite and graphene oxide are presented in Figure A3 and A5 respectively. The deflection image and 3D topography image were presented because deflection image showed a better view of graphite and graphene oxide than the topographical image. Graphite image showed bulk particles of graphite not well dispersed during the sonication and the calculated average roughness was 1.65 mV with the average surface roughness of 4.15mV. The graphene oxide drop coated layer was thick and hence the imaging was not clearly visible, the average roughness was 84.54 mV with the average surface roughness of 94.768

mV. Therefore, it was concluded from the calculated roughness that the thick graphene oxide layer formed at BDD electrode was rougher than the graphite layer.

5.4. Preparation of polysulfone, composite of polysulfone with graphene oxide and Characterisation

5.4.1 Preparation of Polysulfone:

The preparation of 0.08 g.ml polysulfone polymer involves dissolving 4 g of polysulfone pellets in 50 ml N, N-dimethyl acetamide and the reaction mixture was sonicated in a water bath until a clear homogenous casting suspension was obtained [16]

5.4.2 Modification of polysulfone with graphene oxide:

Preparing a nanocomposite of polysulfone modified with graphene oxide. The nanocomposite was prepared by 50/50 wt% of polysulfone and graphene oxide dissolved in N,N-dimethyl acetamide, polysulfone polymer was used as it was without any dopant or prior treatment and the mixture was sonicated until a uniform homogenous casting suspension was formed [15]. From the homogenous suspension 10 μ l was drop coated onto the BDD working electrode and dried at room temperature for electrochemical evaluation.

5.4.3 Characterisation of polysulfone and polysulfone with graphene oxide composite

The FTIR measurements for polysulfone and polysulfone with graphene oxide were performed using the Perkin Elmer spectrometer. The wavelength range was between 4000 - 400 cm^{-1} . FTIR was used to study the structural properties of polysulfone and also monitor structural changes of polysulfone when modified with graphene oxide

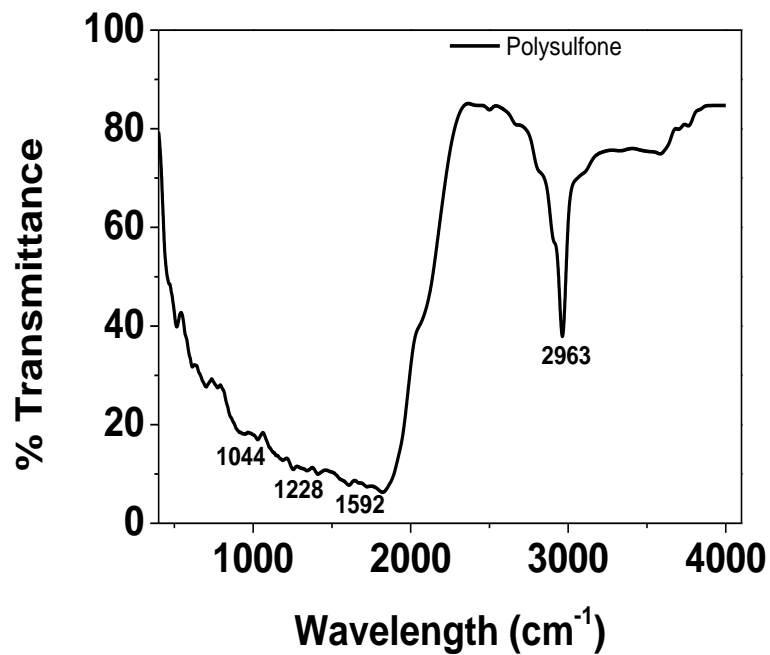


Figure 5.5a: FTIR spectra of polysulfone

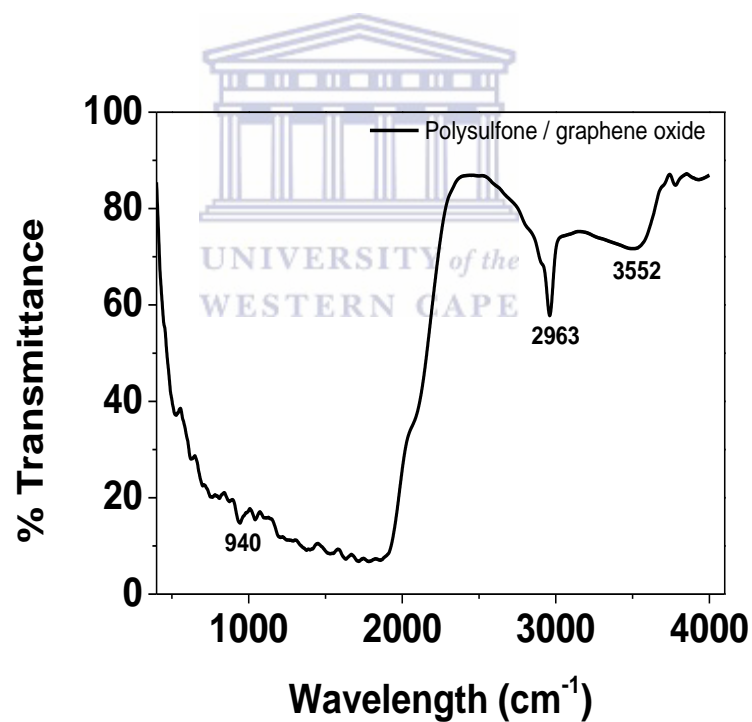


Figure 5.5b: FTIR spectra polysulfone-graphene oxide

FTIR spectroscopy: The figure above illustrates the FTIR spectra of polysulfone unmodified and polysulfone modified with graphene oxide. The obtained spectra for PSF (Figure 5.5a), the absorption bands present at 1044 cm^{-1} S=O group from polysulfone and 1228 cm^{-1} plane stretching symmetric vibration C=C from aromatic ring [25]. The C₆H₆ ring stretch has wavelength of 1592 cm^{-1} and the OH aliphatic group the wavelength is 2963 cm^{-1} [25-28].

The nanocomposite of PSF-GO (Figure 5.5b) exhibited a similar spectrum with the PSF, with a slight difference at 3552 cm^{-1} which was broader than the peak at Figure 5.5a and there's no occurrence of new bands. This was an indication that no chemical interaction between graphene oxide and polysulfone was taking place [27-31].

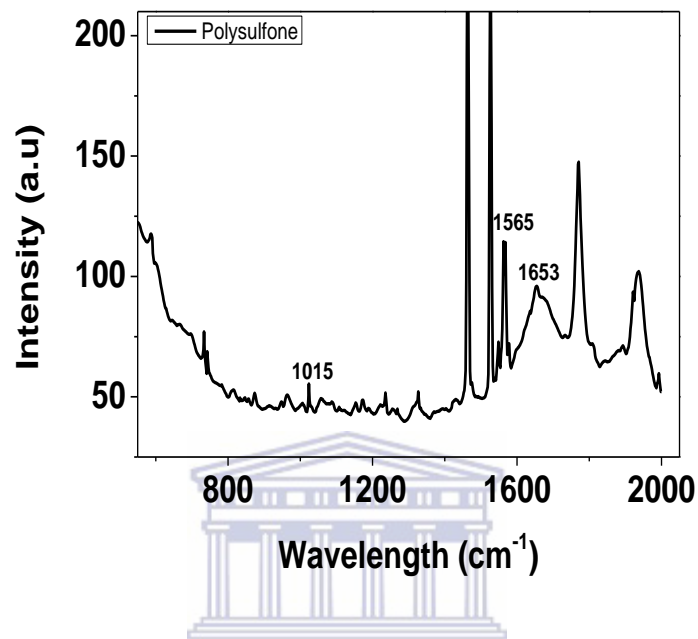


Figure 5.6a: Raman spectra polysulfone

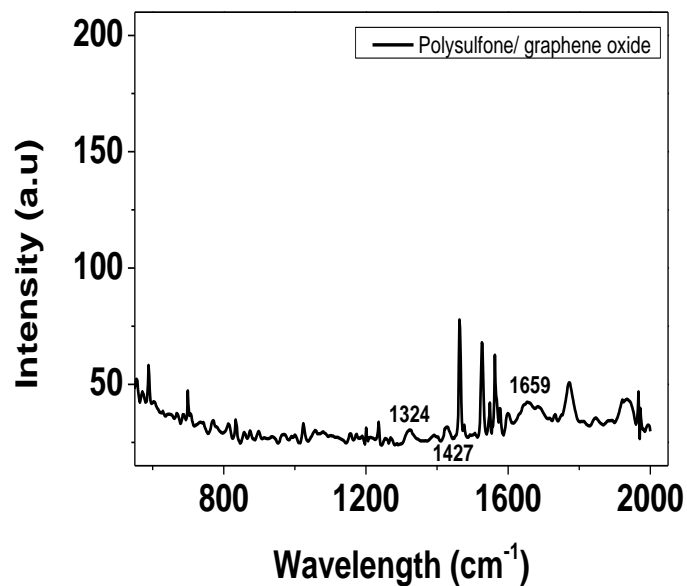


Figure 5.6b: Raman spectra of polysulfone-graphene oxide

Raman spectroscopy: The PSF spectra showed peaks at 1015 cm^{-1} - SO_2 symmetric stretching, 1565 and 1653 cm^{-1} in-plane benzene ring. The Raman spectra of nanocomposite showed low peak intensity when compared with the spectrum of polysulfone which was also observed for graphene oxide. This indicated that a graphene oxide/polysulfone nanocomposite with a PSF fingerprint and a high degree of disorder from GO.

Scanning electron microscope: Polysulfone and polysulfone-graphene oxide suspension was casted in $0.1\text{ M H}_2\text{SO}_4$ to obtain a thin film. The dried thin film was coated with carbon to enhance the conductivity for imaging.

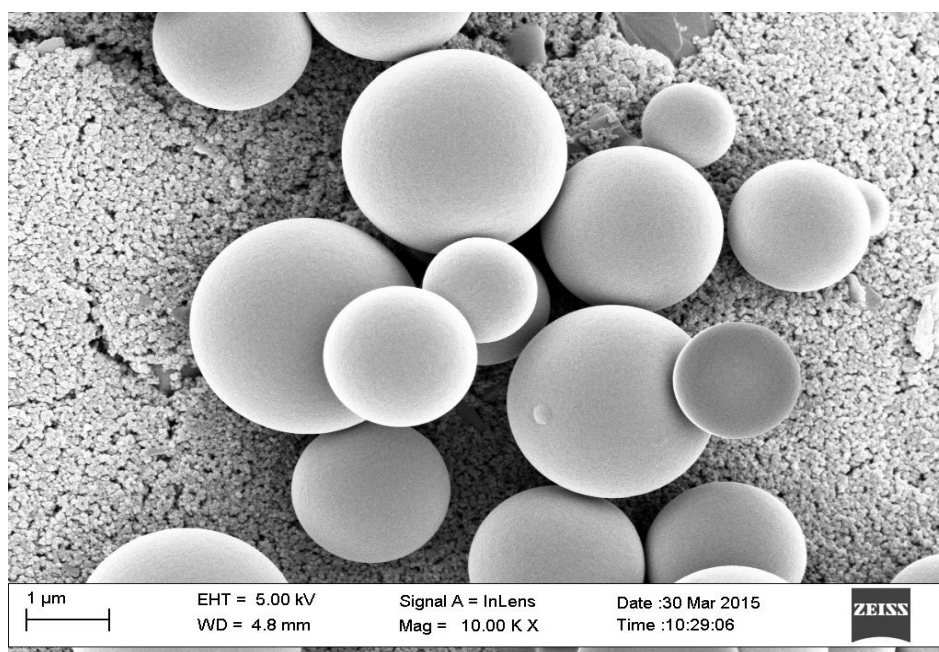


Figure 5.7: SEM image of polysulfone

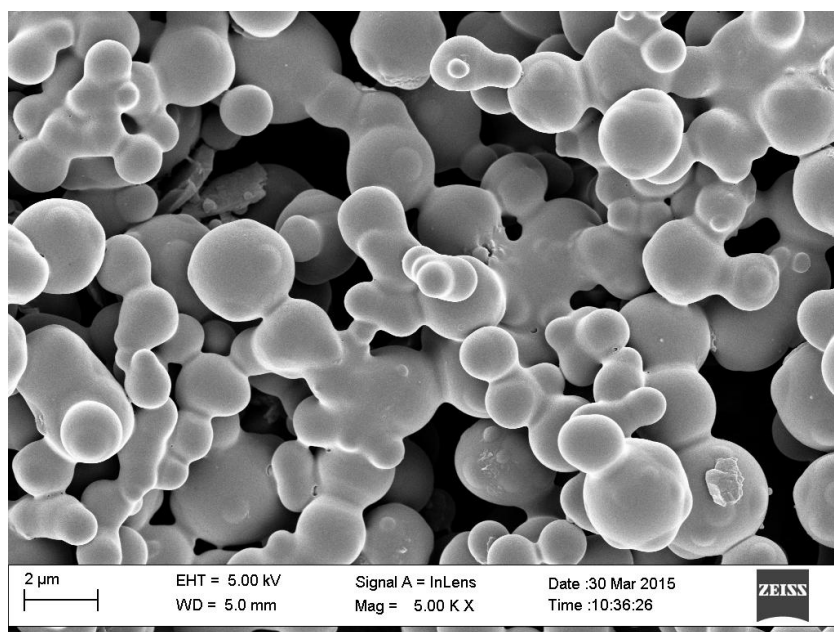


Figure 5.8: SEM image of polysulfone-graphene oxide nanocomposite

In pure polysulfone (Figure 5.7) the particle size diameter was observed to be average of 1 - 2 μm range and formed repeating spherical structures and the EDS spectra (Figure A6) showed carbon and sulphur. PSF spheres coated with graphene oxide (Figure 5.8) showed reduced particle size in the order of 0.5 μm with a high degree of clustering with the EDS spectra (Figure A8) showing the presence of the following elements oxygen, sulphur and carbon. The ionic channel transfer between graphene oxide and polysulfone are found due to strong hydrogen-bonding interactions between the oxygen containing groups on the graphene oxide surfaces and the SO_2 groups of the polysulfone chains [32]. Yasmin et. al. [32], suggested that PSF enhances the exfoliation of graphene sheets and increases the distance between the graphene sheets, which alter the chain network. Thereby, enhancing the overall surface area of polysulfone/graphene oxide.

Morphological characteristics of polysulfone are influenced based on parameters in polymer preparation such as casting solution (the type of polymer and solvent), preparation conditions (temperature, method), and additives used. The purpose of this comparison was learn how solvents can influence the morphology of polysulfone as well as electrochemical response. Two solvents were used to dissolve polysulfone pellets, the solvents used were DMAc and dichloromethane (DCM). The SEM images obtained for polysulfone dissolved in two different solvents showed different morphological characteristics. Polysulfone dissolved in DMAc (Figure 5.7) showed repeating spherical structures and the particle size diameter was

observed to be average of 2 μm range. The image of polysulfone dissolved in DCM (Figure A10) showed porous structure with an average size of 5 μm . The EDS spectrum (Figure A11) showed chlorine which is due to the solvent used and also sulphur which is from polysulfone. The incorporation of graphene oxide into the polymer matrix behaved the same. SEM image polysulfone dissolved in DMAc, showed reduced spherical structure with the average size of 0.5 μm . The image of polysulfone with graphene oxide dissolved in DCM showed highly organised pores with reduced average size of 2 μm (Figure A13 and A14). Solvent effects on the topography of the polysulfone dissolved in DMAc and DCM are shown in Figure A7 and A12 respectively. Image of PSF dissolved in DMAc (Figure A7) was not clearly visible and the 3D image showed the polysulfone layer formed was not smooth and flat on the electrode. The calculated average roughness and surface roughness were 22.804 mV and 37.74 mV. The image of PSF dissolved in DCM (Figure A12) showed similar morphological features as the SEM image. The AFM showed PSF to be porous with average roughness of 26.59 mV and surface roughness of 24.97 mV respectively. The surface roughness of PSF in both solvents was in the same range. AFM image of PSF modified with graphene oxide (Figure A8) in DMAc showed a flat surface with a bulk particle of graphene oxide. The calculated roughness and surface roughness for PSF/GO were 77.54 mV and 82.37 mV. AFM image of PSF/GO in DCM (Figure A15) showed reduced polysulfone pores with calculate roughness and surface roughness of 6.62 mV and 9.33 mV. The high surface roughness of PSF/GO in DMAc was due to the presence of graphene oxide in the PSF matrix.

5.5. Contact angle studies

Contact angle of the prepared material was measured by a water contact angle system (Drop shape analysis). Three different points of every sample were measured and the CA value was the average of the three measurements.

Table 5.1: Contact angle results of the prepared materials.

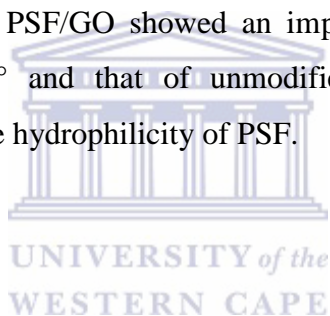
Prepared Material	Contact angle [degree]
Graphene Oxide	42
Polysulfone	87
Polysulfone / Graphene oxide	68

Hydrophilicity of the prepared material was evaluated by contact angle measurement. The contact angle was measured by the sessile drop method and distilled water was also used. Graphene oxide showed to have the least contact angle value when compared with polysulfone and polysulfone with graphene oxide which can be seen from Table 1. This suggests that graphene oxide is hydrophilic. Contact angle of polysulfone unmodified was high (87°) confirming the hydrophobic nature of polysulfone [9,33]. The addition of graphene oxide into polysulfone made it less hydrophobic compared with unmodified polysulfone.

5.6. Conclusion

The graphene oxide was synthesised successfully and also incorporated into the polysulfone matrix. Both the FTIR and Raman spectroscopy confirmed that graphene oxide was indeed the endproduct obtained after the synthesis using the Hummers method. FTIR spectrum of graphene oxide showed a peak at 3260 cm^{-1} which is due to the OH stretching vibration, this peak was not observed in the graphite spectrum. Raman spectrum of graphene oxide showed two bands one at 1341 cm^{-1} and the other at 1578 cm^{-1} , these two bands are known as the D and G bands. These two peaks are important characteristics of graphitic carbon based material. The two bands were not observed in the graphite spectrum. The OH peak observed for graphene oxide confirms the oxidation of graphene to graphene oxide, therefore this results obtained proves that graphene oxide was indeed synthesized successfully.

The modification of polysulfone with graphene oxide was studied and the characterisation techniques used confirmed that graphene oxide was incorporated into the polysulfone matrix. The FTIR spectra obtained for PSF showed a sharp peak at 2963 cm^{-1} which is due to the OH aliphatic group. While the FTIR spectra of the PSF with GO showed a peak at 2963 cm^{-1} but now the peak was smaller in size than the one obtained for PSF unmodified. Another peak was observed at 3552 cm^{-1} which is due to OH stretching vibration, this peak was also observed graphene oxide. Raman spectra of PSF/GO showed a decrease in intensity of the spectrum. The Raman spectra intensity for PSF was observed to be 200 a.u, whereas the intensity for PSF/GO was 50 a.u. The low Raman intensity for PSF/GO suggests that graphene oxide is incorporated into PSF because the Raman intensity for GO was also 50 a.u. SEM image of graphene oxide showed flakes that are stacked together. SEM image of polysulfone showed round spheres with the average size diameter of 1-2 μm , while the SEM image of PSF with GO showed spheres with decrease diameter in the order of 0.5 μm . The contact angle measurements for PSF/GO showed an improved contact angle because the contact angle for GO was 42° and that of unmodified PSF was 87° , therefore the incorporation of GO improved the hydrophilicity of PSF.



References

1. Fen Li, Xue Jiang, Jijun Zhao, Shengbai Zhang, Graphene oxide: A promising nanomaterial for energy and environmental applications, *Nano Energy*, 16 (2015) 488–515
2. Da Chen, Hongbin Feng, and Jinghong Li, Graphene Oxide: Preparation, Functionalization, and Electrochemical Applications, *Chem. Rev.* 112 (2012) 6027–6053
3. Martin Pumera, Graphene-based nanomaterials and their electrochemistry, *Chem. Soc. Rev.*, 39 (2010) 4146–4157
4. Martin Pumera, Electrochemistry of graphene, graphene oxide and other graphenoids: Review, *Electrochemistry Communications* 36 (2013) 14–18
5. Jieon Lee, Jungho Kim, Seongchan Kim, Dal-Hee Min, Biosensors based on graphene oxide and its biomedical application, *Advanced Drug Delivery Reviews* 105 (2016) 275–287
6. Allen M.J., V.C. Tung, R.B. Kaner, Honeycomb carbon: a review of graphene, *Chem. Rev.*, 110 (2010) 132–146
7. Anu Singh, Gaurav Sinsinbar, Meenakshi Choudhary, Veeresh Kumar, Renu Pasricha, H.N. Verma, Surinder P. Singh, Kavita Arora, Graphene oxide-chitosan nanocomposite based electrochemical DNA biosensor for detection of typhoid, *Sensors and Actuators B*, 185 (2013) 675–684
8. Stefan Ioan Voicu, Nicoleta Doriana Stanciu, Aurelia Cristina Nechifor, Danut Ionel Vaireanu, Gheorghe Nechifor, Synthesis and Characterisation of Ionic Conductive Polysulfone Composite Membranes, 12 (2009) 410 – 422
9. Phelane Lisebo, Francis N. Muya, Heidi L. Richards, Priscilla G.L. Baker, Emmanuel I. Iwuoha, Polysulfone Nanocomposite Membranes with improved hydrophilicity, *Electrochimica Acta*, 128 (2014) 326–335
10. Samuel Sánchez, Martin Pumera, Esteve Fabregas, Carbon nanotube/polysulfone screen-printed electrochemical immunosensor, *Biosensors and Bioelectronics*, 23 (2007) 332–340
11. Martos A.M., Sanchez J-Y., Várez A., Levenfeld B.. Electrochemical and structural characterization of sulfonated polysulfone. *Polymer Testing*, 45 (2015) 185–193

12. Syed Nasimul Alam, Nidhi Sharma, Lailesh Kumar, Synthesis of Graphene Oxide (GO) by Modified Hummers Method and Its Thermal Reduction to Obtain Reduced Graphene Oxide (rGO), *Graphene*, 6 (2017) 1-18.
13. Guo H., X. Wang, Q. Qian, F. Wang, X. Xia, A green approach to the synthesis of graphene nanosheets, *ACS Nano*, 3 (2009) 2653-59.
14. Du Q., M. Zheng, L. Zhang, Y. Wang, J. Chen, L. Xue, W. Dai, G. Ji, J. Cao, Preparation of functionalized graphene sheets by a low-temperature thermal exfoliation approach and their electrochemical supercapacitive behaviors. *Electrochim. Acta*, 55 (2010) 3897-3903.
15. Choi E, T. H. Han, J. Hong, J. E. Kim, S. H. Lee, H. W. Kim, and S. O. Kim, Noncovalent functionalization of graphene with end-functional polymers, supplementary material (ESI) for *J. Mater. Chem.*, 20 (2014) 1907-1912
16. Abdolhosseinzadeh S, H. Asgharzadeh and H. S. Kim, Fast and fully-scalable synthesis of reduced graphene oxide, *Sci. Rep.*, 5 (2015)
17. Fernandez-Merino M. J, Vitamin C is an ideal substitute for hydrazine in the reduction of graphene oxide suspensions. *J. Phys. Chem. C.*, 114 (2010) 6426–6432
18. Gao W., L.B. Alemany, L. Ci, and P. M. Ajayan, New insights into the structure and reduction of graphite oxide. *Nat. Chem.*, 1 (2009) 403–408
19. Tien H., Y. Huang, S. Yang, J. Wang, and C.M. Ma, The production of graphene nanosheets decorated with silver nanoparticles for use in transparent, conductive films, *Carbon*, 49 (2011) 1550–1560.
20. Ferrari A. C., J. C. Meyer, V. Scardaci, C. Casiraghi, M. Lazzeri, F. Mauri, S. Piscanec, D. Jiang, K. S. Novoselov, S. Roth, A. K. Geim, Raman Spectrum of Graphene and Graphene Layers, *Phys. Rev. Lett.*, 97 (2006) 1–4
21. Ferrari A. C., and J. Robertson, Interpretation of Raman spectra of disordered and amorphous carbon, *Phys. Rev. B*, 61 (2000) 14095–14107.
22. Guo Y., X. Sun, Y. Liu, W. Wang, H. Qiu, and J. Gao, One pot preparation of reduced graphene oxide (RGO) or Au (Ag) nanoparticle-RGO hybrids using chitosan as a reducing and stabilizing agent and their use in methanol electrooxidation, *Carbon* 50 (2012) 2513– 2523.
23. Jorio A, M. Dresselhaus, R. Saito, and G.F. Dresselhaus, *Raman Spectroscopy in Graphene Related Systems* (Wiley-VCH, 2011).

24. Shin H., K. Kim, A. Benayad, S. Yoon, H. Park, I. Jung, M. Jin, H. Jeong, J. Kim, J. Choi, and Y. Lee, Efficient Reduction of Graphite Oxide by Sodium Borohydride and Its Effect on Electrical Conductance, *Adv. Funct. Mater.*, 19 (2009) 1987–1992.
25. Liu Y., and X. Xie, High-concentration organic solutions of poly(styrene-cobutadiene-co-styrene)-modified graphene sheets exfoliated from graphite, *Carbon*, 49 (2012) 3529–3537.
26. Mushtaq A., H. B. Mukhtar and A. M. Shariff, FTIR study of enhanced polymeric blend membrane with amines, *Res. J. App. Sci. Eng. Technol.* 7 (2014) 1811-1820
27. Ahmed I., A. Idris, M.Y. Noordin and R. Rajput, High performance ultrafiltration membranes prepared by the application of modified microwave irradiation technique. *Ind. Eng Chem. Res.*, 50 (2011) 2272-2283.
28. Voicu S.I., M.A. Pandele, E. Vasile, R. Rughinis, L. Crica, L. Pilan, M. Ionita, The impact of sonication time through polysulfone graphene oxide composite films properties, *Dig. J. Nanomater. Biostruct.*, 8 (2013) 1389 – 1394
29. Zhang W., C. Zhou, W. Zhou, A. Lei, Q. Zhang, Q. Wan, B. Zou, Fast and considerable adsorption of methylene blue dye onto graphene oxide, *Bull. Environ. Contam. Toxicol.* 87 (2011) 86-90
30. Voicu S.I., A. Dobrica, S. Sava, A. Ivan, L. Naftanaila, J. Optoelectron. Cationic surfactants-controlled geometry and dimensions of polymeric membrane pores. *Adv. Mater.*, 14 (2014) 923–928.
31. Mark H.F., *Encyclopedia of Polymer Science and Technology*. Wiley Interscience, Hoboken, New York, Vol. 11 (2004).
32. Yasmin A., J.-J. Luo, I.M. Daniel Processing of expanded graphite reinforced polymer nanocomposites, *Compos. Sci. and Technol.*, 66 (2006) 1179-1186.
33. Muya F.N., L. Phelane, P.G. L. Baker, E.I. Iwuoha, Synthesis and Characterization of Polysulfone Hydrogels, *Journal of Surface Engineered Materials and Advanced Technology* 4 (2014) 227-236

CHAPTER VI

Electrochemical Characterisation of polysulfone, polysulfone with graphene oxide and boron doped diamond

This chapter investigates the electrochemical behaviour of the prepared polysulfone, polysulfone with graphene oxide and boron doped diamond electrode. The electrochemical response of the above mentioned materials will be investigated and discussed in this chapter.

6.1. Boron Doped Diamond electrode

Boron-doped diamond (BDD) electrodes have received attention as an easy-to-use and energy-efficient process for the generation of hydroxyl radicals directly from water [1-4]. This attractiveness is due to the unique properties of diamond, which are its high resistance to adsorption processes (presence of sp^3 hybridized diamond carbon atoms). The second important property of diamond is its inertness to most chemical reagents. Owing to the very strong sp^3 bonds in its lattice structure, this carbon allotrope is not only one of the hardest materials known, but it also possesses extremely high chemical stability [5-6]. The high electrochemical overpotential for oxygen evolution was created by the diamond surface. Oxygen evolution is suppressed at low potentials and sets in only at potentials higher than required for the evolution of hydroxyl radicals [2-3]. This non-toxic electrode material has several unique properties such as high thermal conductivity, good mechanical and electrochemical stability in both alkaline and acidic media, low background current, wide potential range (up to 3.5 V) and low sensitivity on dissolved oxygen in aqueous solutions [6]. BDD differs from other conventional carbon electrodes. Its properties can be influenced either by the structure (quantity of doping agents, presence of impurities) or by controllable (hydrogen or oxygen) surface termination. Consequently, BDD has been utilized as an effective alternative to traditional electrode materials in the determination of various biologically active compounds in the field of clinical and environmental trace analysis [6]

Diamond on its own is non-conductive because it has no free electrons. In order to be used as an electrode material, it is important to dope it [1,7]. Doping is done to replace other elements for carbon at certain positions of the diamond lattice. In the case of boron, a few electrons introduce a movable charge into the lattice by creating bond gaps. Doping with boron reduces

the total amount of electrons in the lattice and partially empties the valence band. Therefore, the positive charges can move along the material (i.e. the electrons flow to fill the holes) and electricity is conducted. The dopant (boron) concentration needs not be higher than 8000 ppm [8]. Doping with boron to produce a p-type semiconductor is more efficient than using for example nitrogen to create an n-type semiconductor [9].

There is a rising demand for sensors to give a stable response, in short time, but in the same time sensitive, selective, with high precision to use and inexpensive. This obligation led to the development of a new type of electrochemical electrodes, boron-doped diamond (BDD), which has been effectively used in various applications, from biomedical analysis, industrial process analysis to the environmental analysis, especially of heavy metals [9-10]. As boron, a trivalent atom, substitutionally incorporates into the diamond lattice, it leaves one uncompensated bond with the neighbouring tetravalent carbon atom, causing p-type conductivity in BDD [10]. Boron-doped diamond is an excellent electrode material introduced into electrochemistry few decades ago [11–13] as n-type semiconductor or as degenerate semiconductor material with properties depending on the boron doping level and surface functionalities [14-15]. Applications of boron-doped diamond electrodes have been proposed in anodic waste degradation, and decolouration, hydroxyl radical, analytical sensing, and n bio-sensors [16].

UNIVERSITY of the
WESTERN CAPE

Švorc et al [6], developed a simple, sensitive and selective differential pulse voltammetric method for determination of penicillin V on a bare boron-doped diamond. Penicillin V presented a well reproducible and well-defined irreversible oxidation peak at very positive potential of +1.6 V (vs. Ag/AgCl). Oxidation of penicillins usually occurs as not clearly defined waves at a very high positive potential and thus may be affected with electrochemical reactions limiting potential window from the anodic side [17]. Other reports dealing with determination of penicillins are based on pulsed amperometric technique [18], flow injection analysis or biosensors [17-18]. Boron-doped diamond (BDD) is a current electrode material which opens new possibilities of electrochemical investigations due to its excellent features, such as the low background current and wide potential window in aqueous solutions oxygen [6,17-18]. The best possible experimental conditions for oxidation of penicillin V were achieved in acetate buffer solution (pH 4.0). The modulation amplitude of 0.1 V, modulation time of 0.05 s and scan rate of 0.05 V s⁻¹ were selected as optimum instrumental parameters

for differential pulse voltammetry. Linear response of peak current on the concentration in the range from 0.5 to 40 μM with coefficient of determination of 0.999, good repeatability (RSD of 1.5%) and detection limit of 0.25 μM were observed without any chemical modifications and electrochemical surface pretreatment [6].

6.2. Electrochemical Evaluation of polysulfone, polysulfone with graphene oxide and boron doped diamond

6.2.1 Cyclic voltammetry

Unmodified polysulfone, polysulfone/graphene oxide nanocomposite and boron doped diamond performance of transducers as rapid response sensors was evaluated using electrochemical techniques. CV was performed for different sensor platforms (bare BDD, PSF/BDD and PSF-GO/BDD electrode) at different scan rates using $\text{K}_3[\text{Fe}(\text{CN})_6]$. The polymer solutions were drop coated onto a BDD working electrode and left to dry at room temperature. The drop coated BDD electrode formed the working electrode in a three electrode cell arrangement with 5 mL of 5 mM $\text{K}_3[\text{Fe}(\text{CN})_6]$ as the electrolyte. Voltammetric experiments were recorded with PalmSens conventional three-electrode system. A Pt wire (diameter 1.0 mm) and Ag/AgCl (3 M NaCl) electrode (Bioanalytical Systems Ltd., UK) were used as counter and reference electrodes, respectively, in the electrochemical evaluation. Alumina micro-polish (1.0, 0.3 and 0.05 mm alumina slurries) and polishing pads (Buehler, IL, USA) were used for cleaning the working electrode (BDDE) and sonicated first in ethanol then followed by sonicating in dH_2O . The same experiment was done for GO/BDD, PSF/BDD and PSF-GO/BDD electrode, with polysulfone dissolved in dichloromethane (DCM). The purpose of the experiments was to investigate the electrochemical influence of DCM as solvent in polysulfone reactivity. The obtained voltammograms are presented in the appendix from figure A16 to figure A21 and table A1 show the diffusion coefficient and the formal potential.

Cyclic voltammograms obtained for the sensor platforms are presented in figure 6.1. All three cyclic voltammetry graphs showed a reversible couple which is due to the oxidation and reduction of;



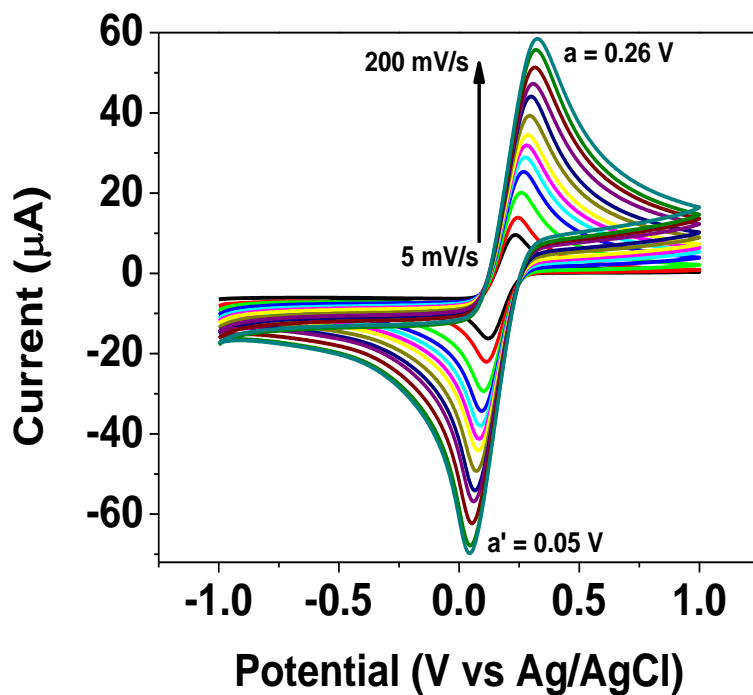


Figure 6.1a: Characterisation of 5 mM $K_3[Fe(CN)_6]$ at bare BDDE by CV from scan rate 5 mV/s – 200 mV/s

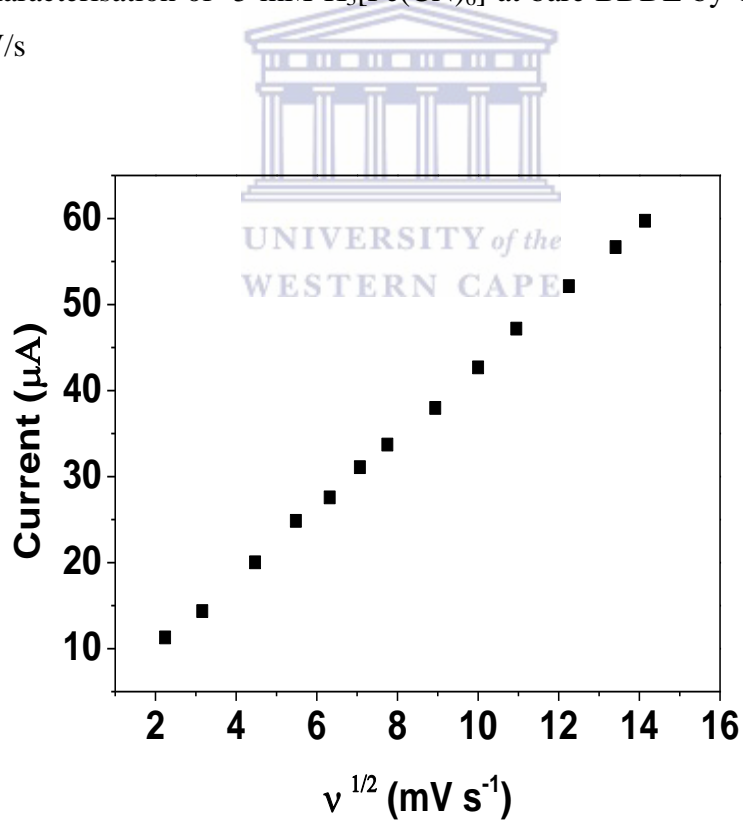


Figure 6.1b: Current vs. \sqrt{v} plot at bare BDD

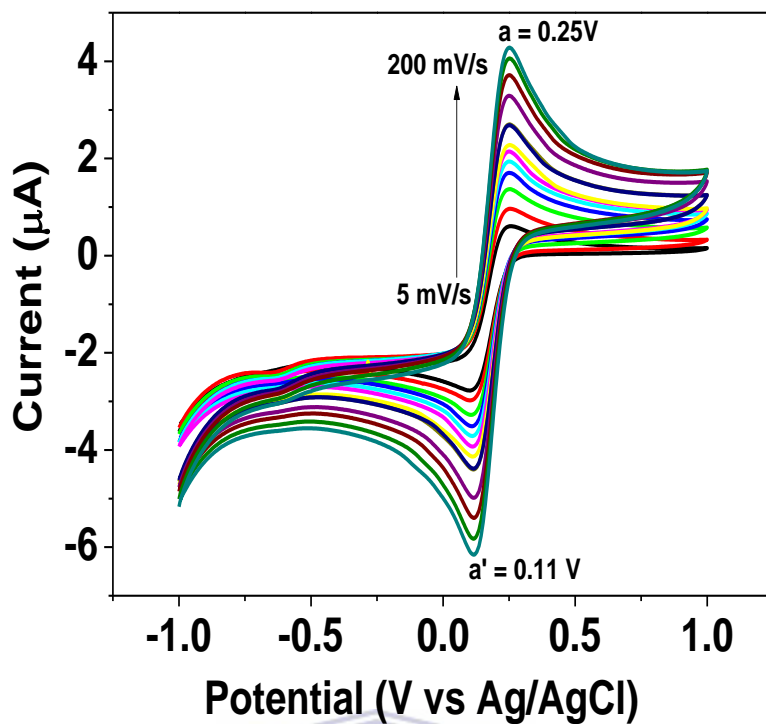


Figure 6.2a: Characterisation of 5 mM $K_3[Fe(CN)_6]$ at unmodified PSF/BDD electrode by CV from scan rate 5 mV/s – 200 mV/s

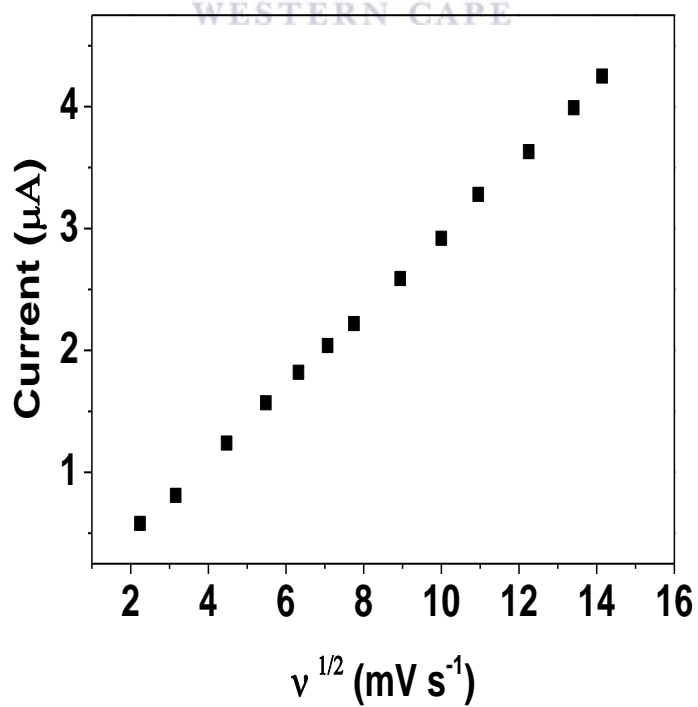


Figure 6.2b: Current vs. \sqrt{v} plot at unmodified PSF/BDD electrode

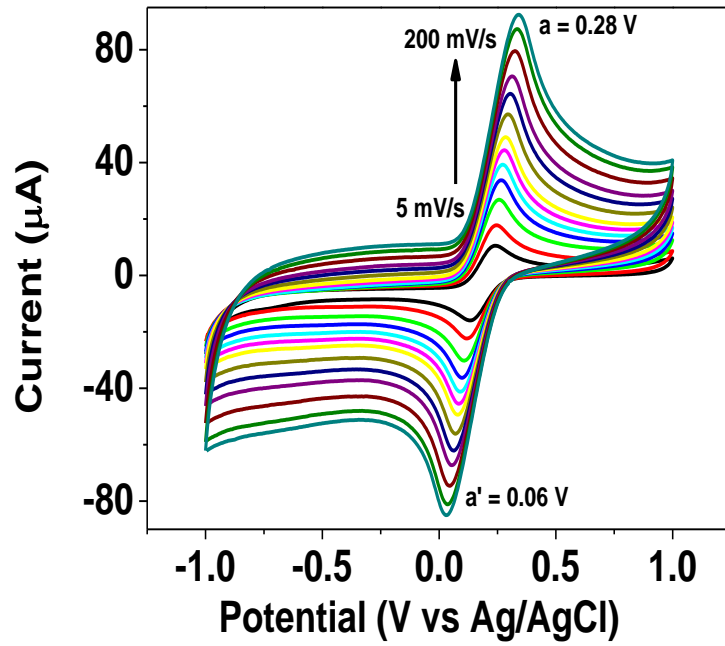


Figure 6.3a: Characterisation of 5 mM K₃[Fe(CN)₆] at PSF-GO/BDD electrode by CV from scan rate 5 mV/s – 200 mV/s.

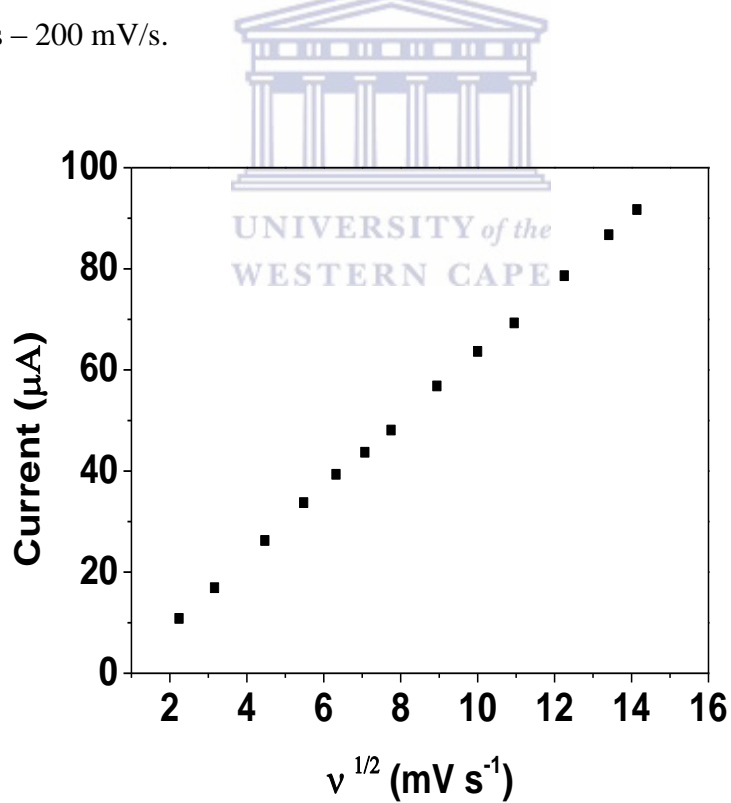


Figure 6.3b: Current vs. \sqrt{v} plot at PSF-GO/BDD electrode

Table 6.1: Diffusion coefficient and formal potential of $K_3[Fe(CN)_6]$ at bare BDD, unmodified PSF/BDD and PSF-GO/BDD electrode

Electrode Material	Diffusion Coefficient [$cm^2 s^{-1}$]	Formal Potential [mV]
Bare BDD	$I_{pa} = 2.071 \times 10^{-4}$ $I_{pc} = 2.136 \times 10^{-4}$	179.87
PSF/BDD	$I_{pa} = 5.6855 \times 10^{-5}$ $I_{pc} = 5.3467 \times 10^{-5}$	179.8
PSF-GO/BDD	$I_{pa} = 2.660 \times 10^{-4}$ $I_{pc} = 2.446 \times 10^{-4}$	183.75

All the voltammograms showed an increase in anodic peak current and cathodic peak current with increasing scan rate and are linearly related with the square root of the scan rates suggesting a diffusion controlled process of reactants at the electrode surface. The formal potential (E°) was determined from the anodic (E_{pa}) and cathodic (E_{pc}) peak potentials by using the Eq. 2:

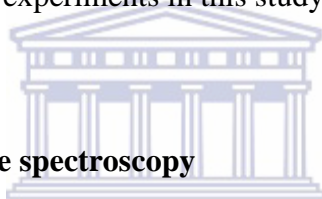
$$E_{pa} + E_{pc} / 2 = E^\circ \quad (2)$$

PSF modified with graphene oxide showed to have the highest formal potential when compared with bare BDD electrode and unmodified PSF/BDD electrode. For a reversible reaction the peak current, I_p , can be determined using the Randles–Sevcik equation [21]

$$I_p = 2.699 \times 10^5 AD^{1/2} n^{3/2} v^{1/2} C \quad (3)$$

where I_p is the peak current, A is the electroactive area, D is the diffusion coefficient of the analyte, n is the number of electrons involved in the redox reaction, v is the scan rate, and C is the concentration of the redox molecules in solution. Anodic peak current I_{pa} versus the

square root of the scan rate (\sqrt{v}) at $K_3[Fe(CN)_6]$ concentration of 5 mM was used to obtain the linear fit. Both the boron-doped diamond and the polysulfone-graphene oxide at BDD electrode showed to be better sensor materials because of the high slope of the current against $\sqrt{\text{scan rate}}$ plot and diffusion coefficient, PSF-GO/BDD electrode showed the highest diffusion coefficient followed by bare BDD electrode [19]. Graphene oxide at BDD electrode showed the highest diffusion coefficient in the order of magnitude ($\times 10^{-3}$) for both the anodic and cathodic diffusion and also the formal potential obtained was the lowest, shown in Table A1. In comparison, polysulfone dissolved in DCM performed better than polysulfone dissolved in DMAc, diffusion coefficient PSF dissolved in DCM was 1.058×10^{-4} and $1.060 \times 10^{-4} \text{ cm}^2 \text{ s}^{-1}$ and for PSF dissolved in DMAc diffusion coefficient calculated was 5.6855×10^{-5} and $5.3467 \times 10^{-5} \text{ cm}^2 \text{ s}^{-1}$. Nonetheless, even though PSF dissolved in DCM showed better electrochemical response than PSF dissolved in DMAc, because of the templating properties of PSF in DCM observed from figure A9. DMAc was selected as the solvent of choice to dissolve PSF for further experiments in this study.



6.2.2 Electrochemical impedance spectroscopy

Electrochemical impedance spectroscopy was used to characterise the properties of the prepared material at boron doped diamond electrode. The spectra were recorded at 0.25 V vs. Ag/AgCl in 5 mM $K_3[Fe(CN)_6]$ dissolved in distilled water only. All the EIS spectra, bare BDD, unmodified PSF/BDD and PSF-GO/BDD electrode were fitted using the same equivalent electrical circuit containing the solution resistance (R_s) in series with a parallel combination of capacitance (C) and charge transfer resistance (R_{ct}) with a constant phase element (CPE) representing a nonideal capacitance. The charge resistance describes the electron transfer kinetics of the redox at the electrode interface and the capacitance describes the charge separation

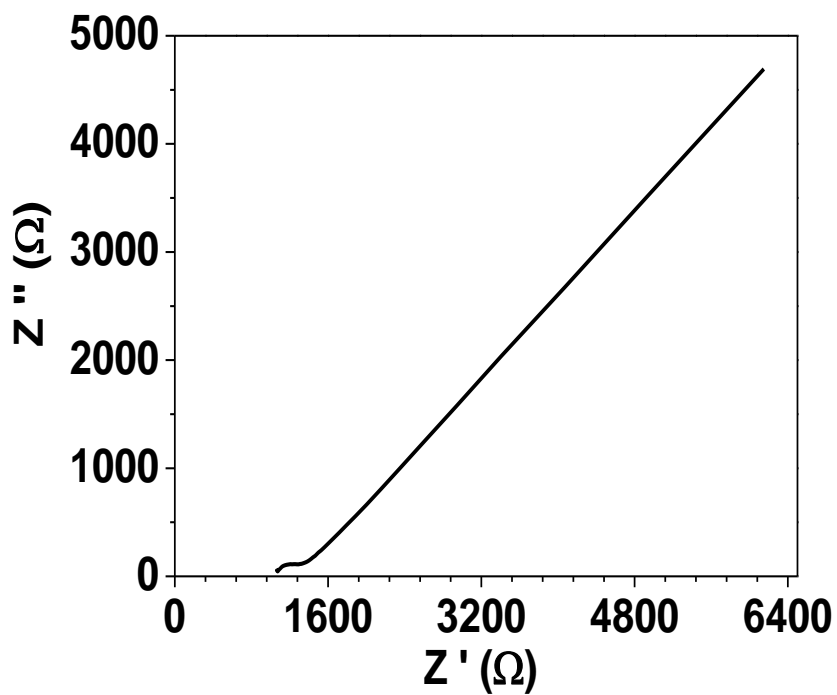


Figure 6.4a: Nyquist plot of bare BDD electrode in 5 mM $K_3[Fe(CN)_6]$, potential 0.25 V and frequency range 65 mHz – 100 kHz.

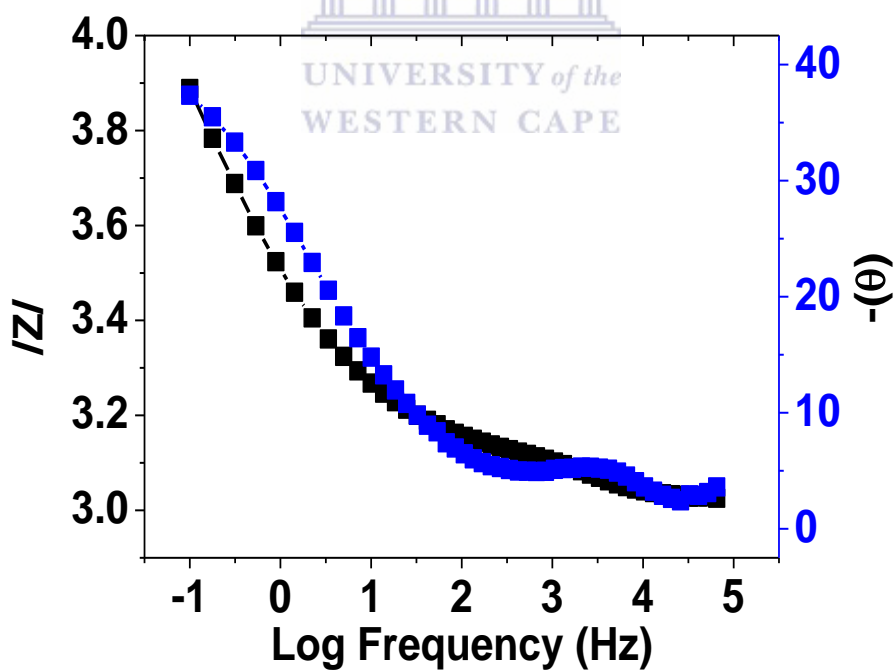


Figure 6.4b: Bode plot of bare BDD electrode

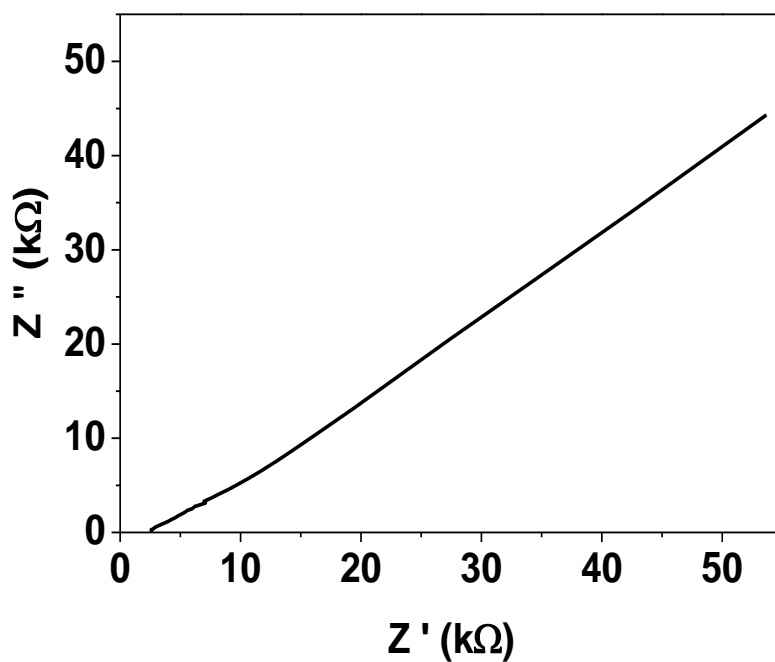


Figure 6.5a: Nyquist plot of unmodified PSF/BDD electrode in 5 mM $K_3[Fe(CN)_6]$, potential 0.25 V and frequency range 65 mHz – 100 kHz.

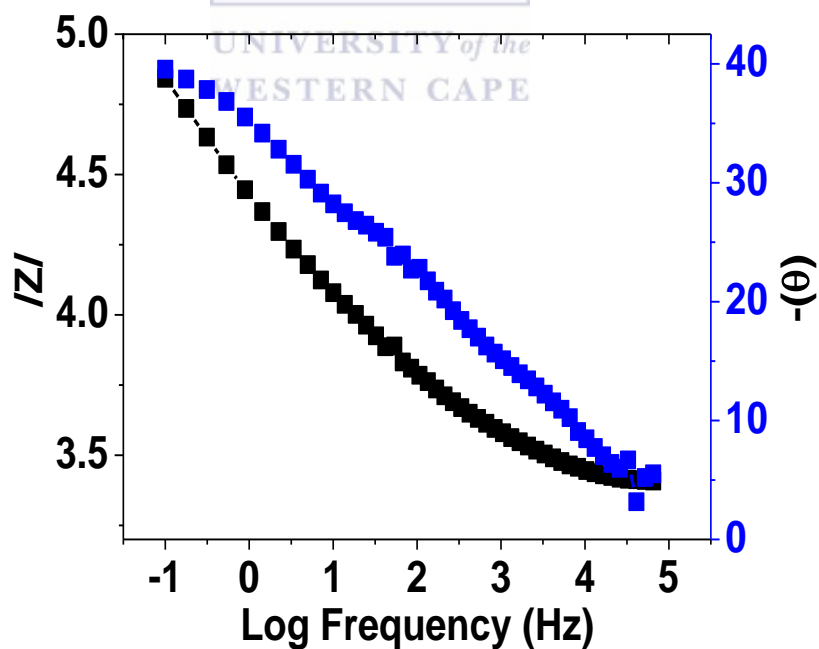


Figure 6.5b: Bode plot of unmodified PSF/BDD electrode

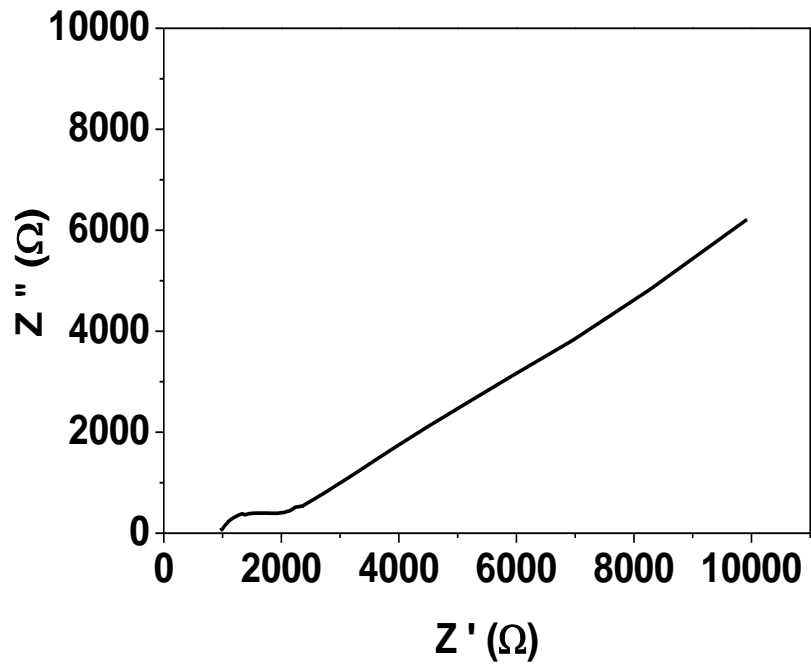


Figure 6.6a: Nyquist plot of PSF-GO/BDD electrode in 5 mM $K_3[Fe(CN)_6]$, potential 0.25 V and frequency range 65 mHz – 100 kHz.

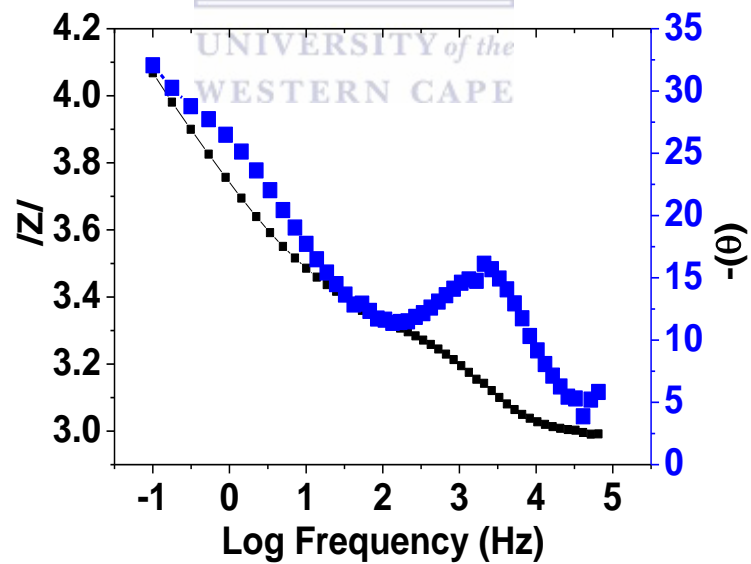


Figure 6.6b: Bode plot of PSF-GO/BDD electrode

Table 6.2: Impedance results of $K_3[Fe(CN)_6]$ dissolved in water only at bare BDD, unmodified PSF/BDD and PSF-GO/BDD electrode.

Electrode	Resistance (Rs)	Capacitance	Resistance (Rct)
	[Ω]	[F]	[Ω]
BDD	1062	3.4172×10^{-7}	170
PSF/BDD	2265	3.0508×10^{-7}	247
PSF-GO/BDD	847	2.3714×10^{-7}	433

The Rs values of the prepared material at BDD electrode were different for each platform. Polysulfone at BDD electrode (Figure 6.5a) showed the highest Rs value whereas the modified polysulfone with graphene oxide showed a decrease by more than a half to that value of PSF/BDD electrode. Looking at the charge transfer resistance values of the different platforms, bare BDD electrode (Figure 6.4a) showed the lowest Rct value, the Rct value increased as the working electrode was modified with PSF and PSF-GO. The capacitance values decreased systematically with every modification step. The Rct conclusion was difficult to resolve because of the dominant diffusion control which may be distinguished from Rct at BDD and PSF-GO/BDD electrode, but does not obey the Warburg diffusive mapping in circuit fitting of PSF/BDD electrode data. The reported Rct value has high error margins. The modification of BDD electrode with PSF and PSF-GO (Figure 6.6) respectively increases the surface of the electrode interface, making it more hydrophilic. The increased positive charge favours the $[Fe(CN)_6]^{3-}$ ions in solution, resulting in a decrease in interfacial charge double layer. This reflected as decrease in capacitance in the electrical equivalent circuit fitted data. Bode plot of bare BDD electrode (Figure 6.4b) showed a broad peak in phase angle at 5° and the same peak was observed from the bode plot of PSF-GO/BDD electrode (Figure 6.6b) but the peak was sharper and increased to 15° . The increase in phase angle of PSF-GO/BDD electrode could be due to the use of two less conductive materials

(PSF and GO), hence the insulating behaviour was observed. This behaviour was confirmed by the high charge transfer resistance determined after data fitting.

6.3. Electrochemical response of three antibiotic residues at unmodified PSF/BDD, PSF-GO/BDD and bare BDD electrode

The electrochemical behaviour of the three antibiotic residues (neomycin, penicillin G and norfloxacin) was investigated at polysulfone, polysulfone with graphene oxide and bare BDD electrode. Cyclic voltammetry was used to measure the current response of the antibiotic residues at the 3 transducer platforms.

6.3.1 Cyclic voltammetry of neomycin at unmodified PSF/BDD, PSF-GO/BDD and bare BDD electrode

The cyclic voltammetry was used to study the redox behaviour of the prepared electrode materials which are: bare BDD, unmodified PSF/BDD and PSF-GO/BDD electrode composite drop coated onto BDD working electrode in the presence of 0.1 M PBS pH 7.0 and 0.1 M Neomycin solution using different scan rates from 10 to 200 mV s⁻¹.

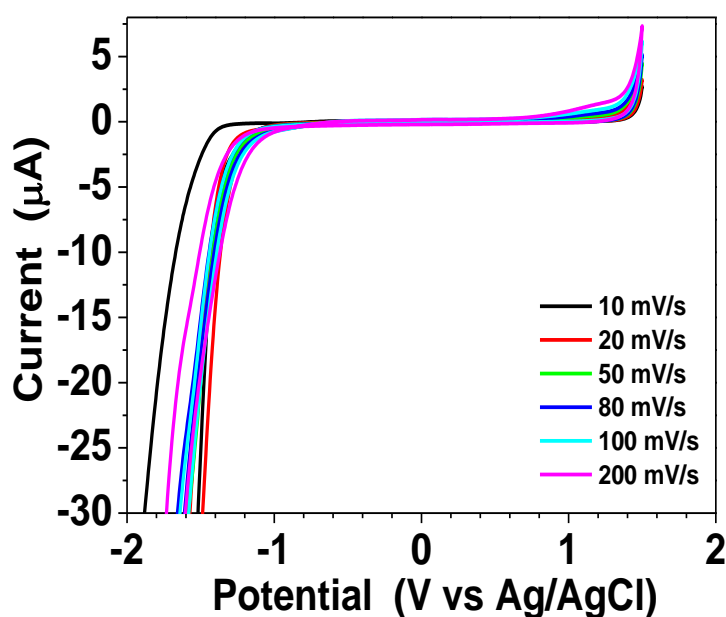


Figure 6.7a: Characterisation of neomycin by CV at bare BDD, scan rate 10 – 200 mV/s

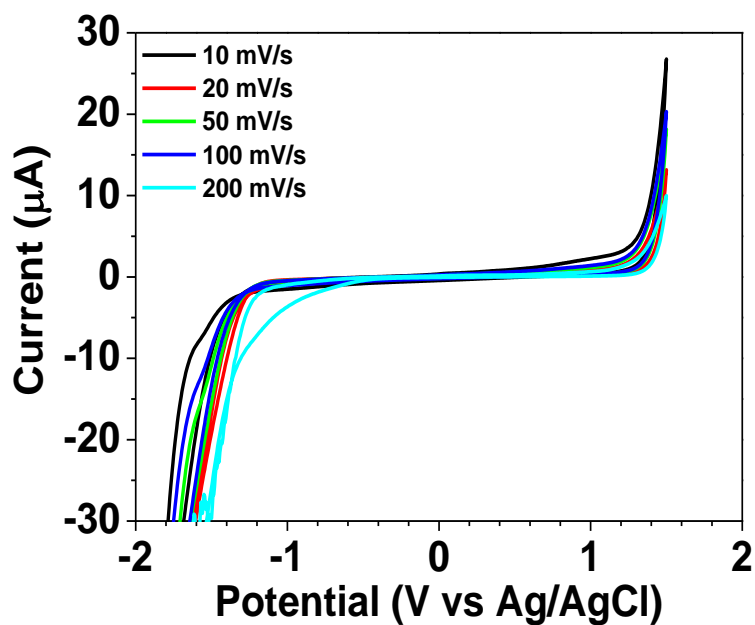


Figure 6.7b: Characterisation of neomycin by CV at unmodified PSF/BDD electrode, scan rate 10 – 200 mV/s

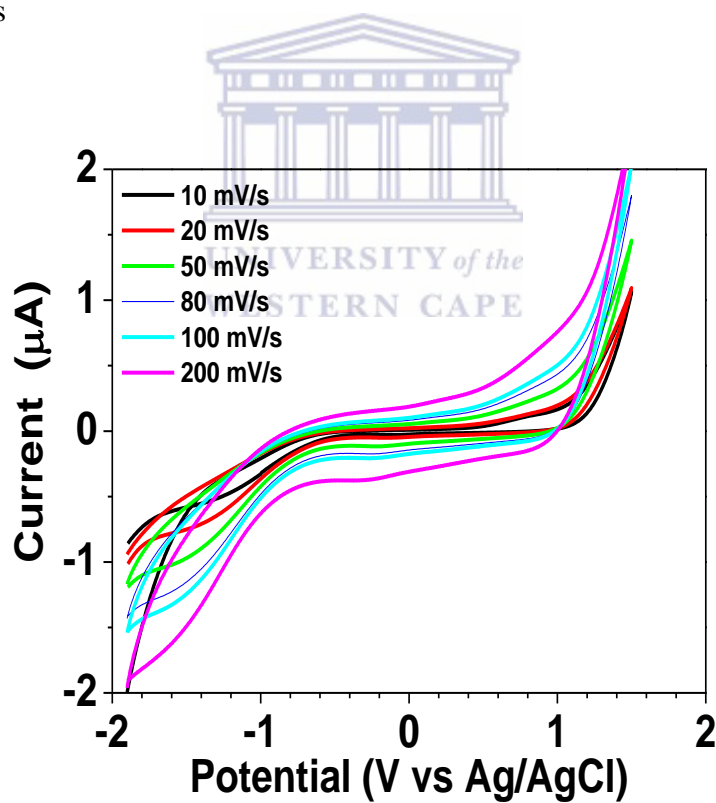


Figure 6.7c: Characterisation of neomycin by CV at PSF-GO/BDD electrode, scan rate 10 – 200 mV/s

The above cyclic voltammograms of neomycin (Figure 6.7a-c) at bare BDD, unmodified PSF/BDD electrode and the composite of polysulfone with graphene oxide respectively, all the voltammograms showed no analytical peak that can be used to calculate the diffusion coefficient. The PSF-GO/BDD electrode voltammogram showed high capacitive current when compared to bare BDD electrode and PSF/BDD electrode plots, hence the PSF-GO/BDD electrode was the electrode of choice for detecting Neomycin instead of the two other electrode materials.

6.3.2 Cyclic Voltammetry of penicillin G at unmodified PSF/BDD, PSF-GO/BDD and bare BDD electrode

The cyclic voltammetry was used to study the redox behaviour of the prepared electrode materials which are: bare BDD, unmodified PSF/BDD and PSF-GO/BDD electrode composite drop coated onto BDD working electrode using of 0.1 M PBS pH 7.0 as the electrolyte and the analyte was 0.1 M penicillin G solution. Cyclic voltametric studies were carried out scanning from 10 to 200 mV s⁻¹. About 5mL of 0.1 M PBS and 50 uL of 0.1 M penicillin were placed onto an electrochemical cell and purged for 10 mins. The final concentration of penicillin G was 9.1×10^{-4} M. The oxidation peak at 1.0 V (vs Ag/AgCl) was recorded without any cathodic peak on the reverse scan which clearly indicated that the charge transfer during electrode process is electrochemically irreversible on bare BDD electrode. The oxidation site of penicillin was within the β -lactam backbone. The effect of scan rate on the peak current was investigated in order to characterize the mass transport in of the three electrode material; bare BDD, PSF/BDD and PSF-GO/BDD electrode. Figure 6.7 demonstrated that the anodic peak current of penicillin G increased with increasing of scan rate this was observed for all three electrode materials. The mass transport is controlled by diffusion because the linear regression value for all three electrode material was close to 1[20].

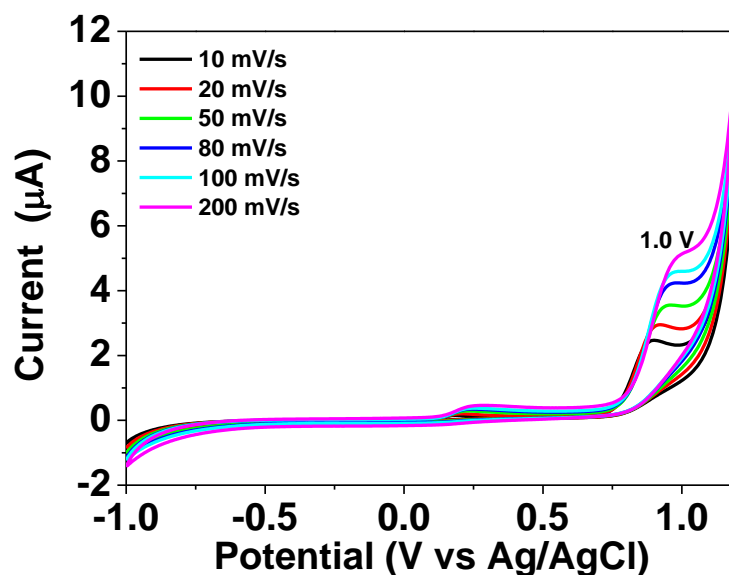


Figure 6.8a: Characterisation of penicillin G by CV at Bare BDD

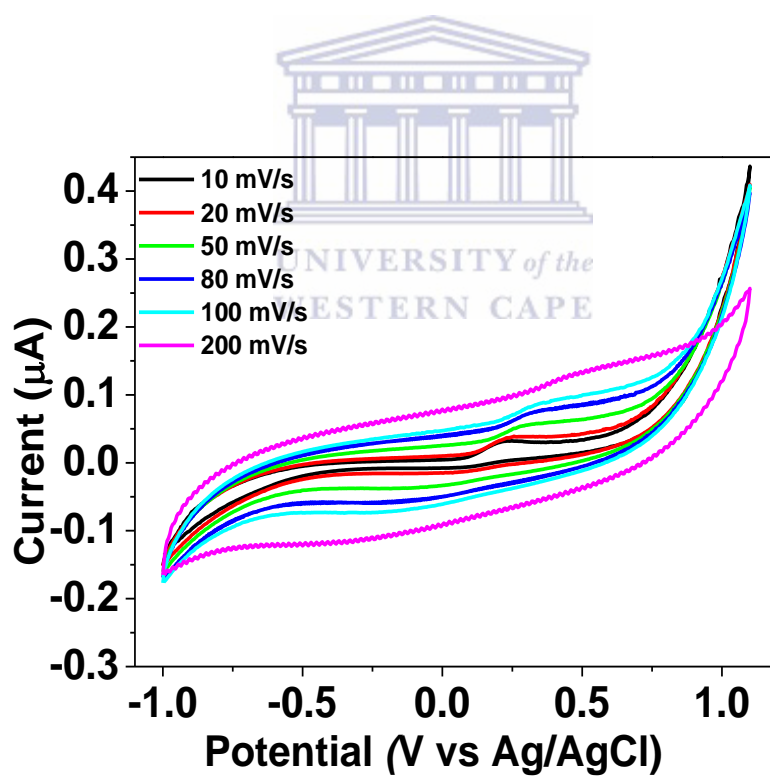


Figure 6.8b: Characterisation of penicillin G by CV at unmodified PSF/BDD electrode

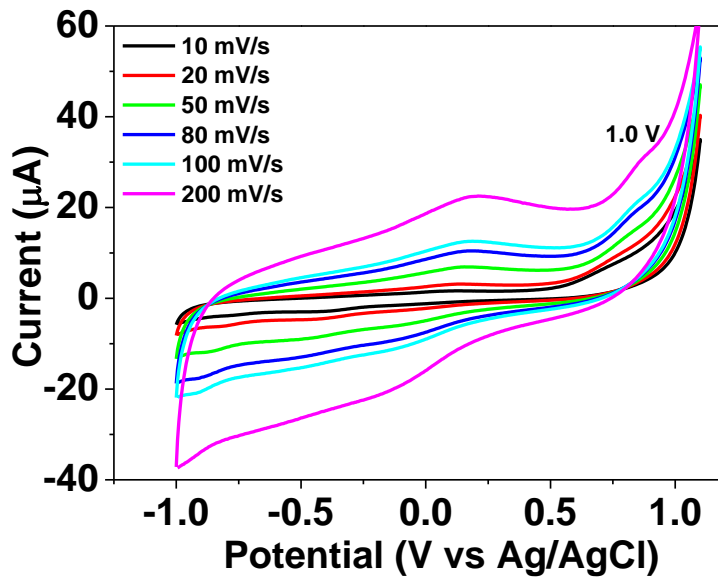


Figure 6.8c: Characterisation of penicillin G by CV at PSF-GO/BDD electrode

Table 6.3: Diffusion coefficient of Penicillin G at different electrode material

Electrode Material	Diffusion coefficient ($\text{cm}^2 \text{s}^{-1}$)
BDD	1.091×10^{-6}
PSF/BDD	1.317×10^{-7}
PSF-GO/BDD	2.119×10^{-6}

Cyclic voltammetry of PSF-GO/BDD electrode (Figure 6.8c), showed relatively high current values, which were significantly higher than those of the unmodified PSF/BDD (Figure 6.8b) and bare BDD electrode (Figure 6.8a), showing that the modification with graphene oxide led to an increase in current. The 1 V peak for pen G was not observed in figure 6.8b, the absence of the oxidation peak led to using the current at 1 V for calculating diffusion coefficient. The diffusion coefficient was calculated using the Randles–Sevcik equation for irreversible system

$$i_p = (2.99 \times 10^5) n(\alpha n_a)^{1/2} A C D^{1/2} \nu^{1/2} \quad \text{Eq.4}$$

where I_p is the peak current (A), A is the active area of the electrode (cm^2), D is the diffusion coefficient ($\text{cm}^2 \text{s}^{-1}$), n is the number of electrons transferred, ν is the potential scan rate (mV

s^{-1}) and C is the concentration of the bulk solution (mol cm^{-3}). In addition, α is the transfer coefficient and n_{α} is the number of electrons involved in the charge-transfer step. The diffusion coefficient of the composite was higher than that of unmodified PSF/BDD and bare BDD electrode. Table 6.1 compares the diffusion coefficient calculated from the cyclic voltammetry results which shows that PSF-GO/BDD electrode showed high diffusion coefficient value. Nonetheless, bare BDD electrode was selected as the electrode of choice for detecting penicillin G, this was decided upon evaluating the response of penicillin G at the three cyclic voltammograms (Figure 6.8a-c). CV response of bare BDD electrode showed a well defined and sharp penicillin G peak whereas in the other two voltammograms (unmodified PSF/BDD and PSF-GO/BDD electrode) the penicillin G peak was not well resolved which will be a challenge in developing a sensor, because a peak must be well resolved and defined so that it can be monitored for analytical quantification

6.3.3 Cyclic voltammetry of norfloxacin at unmodified PSF/BDD, PSF-GO/BDD and bare BDD electrode

The cyclic voltammetry was used to study the redox behaviour of the prepared electrode materials which are: bare BDD, unmodified PSF/BDD and PSF-GO/BDD composite drop coated onto BDD working electrode in the presence of 0.1 M PBS pH 7.0 and 0.1 M norfloxacin (NOR) solution different scan rates from 10 to 200 mV s^{-1} were used.

The voltammograms below (Figure 6.9a-c) show the cyclic voltammetric responses of norfloxacin (NOR) at bare BDD electrode (Figure 6.9a), PSF/BDD electrode (Figure 6.9b) and PSF-GO/BDD electrode (Figure 6.9c) in HCl medium. Under the same conditions, a relative weak anodic peak of NOR was observed at the PSF-GO/BDD electrode, and the peak currents increased at both PSF/BDD and bare BDD electrode. The electrochemical response of all three experiments showed that no reduction peak was observed in the reverse scan suggested that the electrochemical reaction was a totally irreversible process. At the PSF/BDD electrode, the peak current was higher and than that of bare BDD [21]. The observed oxidation peak of NOR at the PSF-GO/BDD electrode was weak and not well defined due to slow electron transfer, while the response was better at bare BDD electrode and PSF/BDD electrode. The peak current showed a linear relationship with respect to the scan rates, indicating the oxidation process of norfloxacin at the prepared electrode material

was diffusion-controlled. The Randles Sevcik equation (Eqn. 4) for irreversible systems was used to calculate the diffusion coefficient for all three electrodes. The calculated values are presented in a table form.

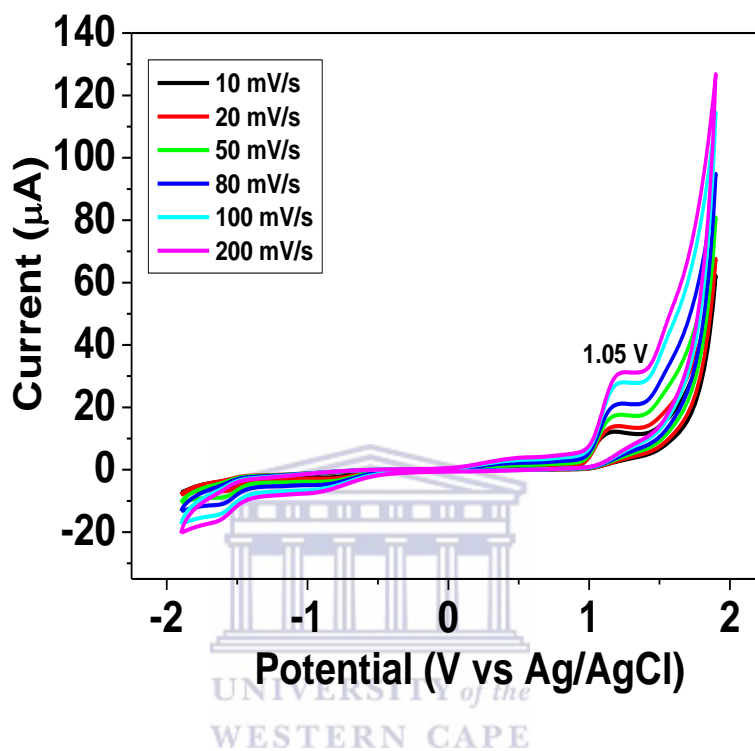


Figure 6.9a: Characterisation of norfloxacin by CV at bare BDD electrode

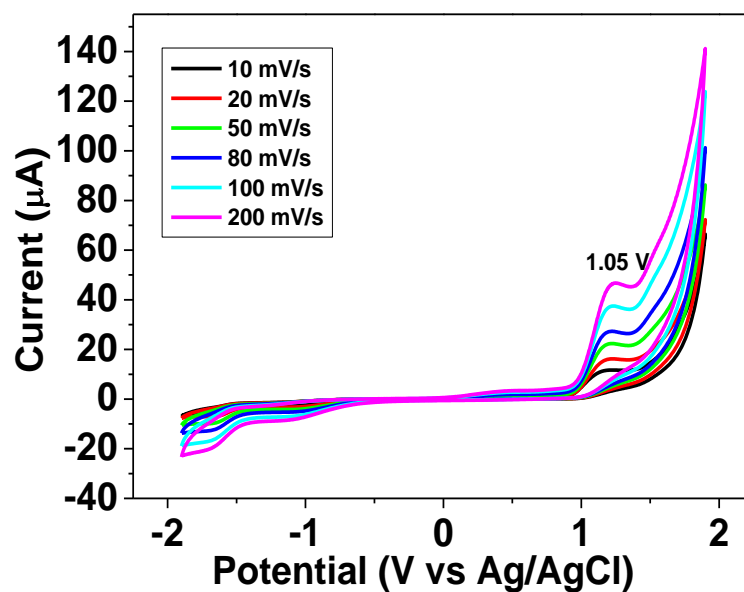


Figure 6.9b: Characterisation of norfloxacin by CV at unmodified PSF/BDD electrode

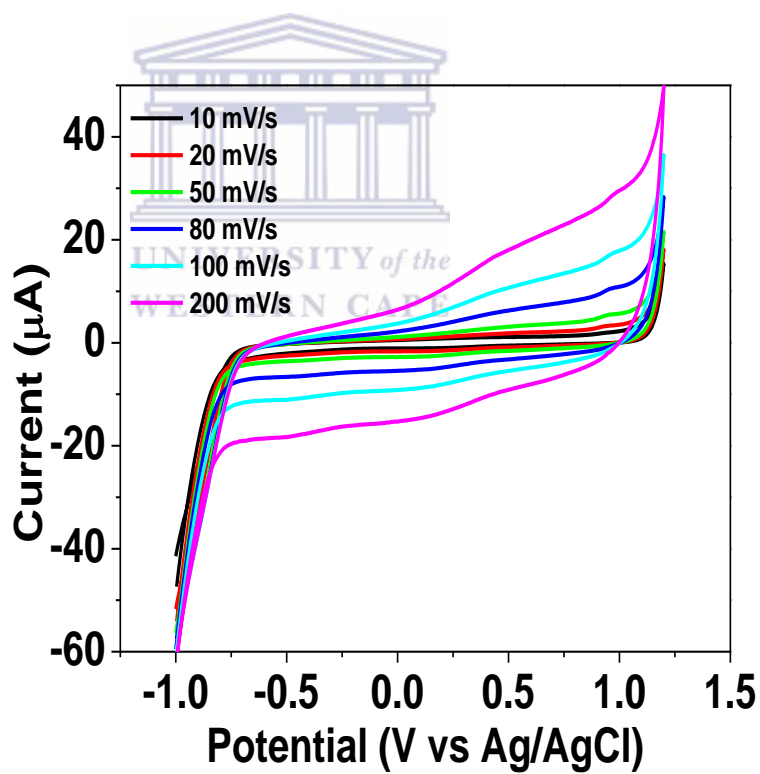


Figure 6.9c: Characterisation of norfloxacin by CV at PSF-GO/BDD electrode

Table 6.4: Diffusion coefficient of the prepared electrode materials

Electrode	Diffusion coefficient ($\text{cm}^2 \text{s}^{-1}$)
Bare BDD	3.074×10^{-6}
PSF/BDD	4.101×10^{-6}
PSF-GO/BDD	3.510×10^{-6}

The above table (Table 6.4) compares the diffusion coefficient calculated from the cyclic voltammetry. Electrochemical response of norfloxacin at the three electrode materials which shows unmodified PSF/BDD electrode will perform better than both the PSF-GO/BDD electrode and bare BDD electrode as a sensor, this was confirmed by the results in the table. Therefore, unmodified PSF/BDD electrode was chosen as the electrode of choice for monitoring norfloxacin concentrations during concentration dependant experiments. The decision was made after assesing the response of norfloxacin at the three cyclic voltammograms (Figure 6.9a-c). Electrochemical response of norfloxacin at unmodified PSF/BDD electrode showed a well defined and resolved peak for norfloxacin whereas in Figure 6.9a and 6.9c the peak was not resolved which poses a challenge in sensor development. Detection measurement by electrochemical techniques such as CV, SWV and DPV requires a resolved and defined peak so that it analytical performance and quantification can be possible

6.4. Conclusion

The deposition of polysulfone onto BDD serves to increase the nett positive charge at the interface. This is reflected in an increased charge transfer due to $[\text{Fe}(\text{CN})_6]^{3-}$ redox at 250 mV vs Ag/AgCl. The addition of graphene oxide onto the polysulfone matrix improved the reactivity of polysulfone polymer. Cyclic voltammetric response of the three selected antibiotic residues (neomycin, penicillin G and norfloxacin) at the electrode material (bare BDD, unmodified PSF/BDD and PSF-GO/BDD electrode) showed interesting responses for each antibiotic. Neomycin at the three modified electrodes showed higher capacitive currents

at PSF-GO/BDD electrode than bare BDD and unmodified PSF/BDD electrodes and this electrode material was selected as the electrode of choice for electrochemical detection of neomycin. Electrochemical response of penicillin G at bare BDD electrode produced a sharp and well defined peak. BDD electrode was selected for penicillin G electrochemical evaluation. The observed peak at 1.0 V (vs Ag/AgCl) was be used as the analytical peak to monitor the oxidation of penicillin G. Unmodified PSF/BDD electrode was selected as the electrode of choice for electrochemical evaluation of norfloxacin. Oxidation of norfloxacin was observed at 1.05 V and this peak was used to monitor the oxidation of norfloxacin.



References

1. Pleskov Y., Electrochemistry of diamond: A review. *Russian Journal of Electrochemistry*, 38 (2002) 1275-1291
2. Michaud, P., Panizza, M., Ouattara, L., Diaco, T., Foti, G., Comninellis, C., Electrochemical oxidation of water on synthetic boron-doped diamond thin film anodes. *Journal of Applied Electrochemistry* 33 (2003) 151-154.
3. Marselli, B., Garcia-Gomez, J., Michaud, P., Rodrigo, M., Comninellis, C., Electrogeneration of hydroxyl radicals on boron-doped diamond electrodes. *Journal of the Electrochemical Society*, 150 (2003) 79-83.
4. Kraft, A., Doped diamond: A compact review on a new, versatile electrode material. *International Journal of Electrochemical Science*, 2 (2007) 355-385.
5. Fujishima, A., Einaga, Y., Rao, T. N., Tryk, D. A., 2005. *Diamond Electrochemistry*. BKC, Elsevier; Tokyo
6. Lubomír Švorc, Jozef Sochr, Miroslav Rievaj, Peter Tomčík, Dušan Bustin, Voltammetric determination of penicillin V in pharmaceutical formulations and human urine using a boron-doped diamond electrode, *Bioelectrochemistry*, 88 (2012) 36–41
7. Comninellis, C., Chen, G., *Electrochemistry for the Environment*. Springer, New York, Dordrecht, Heidelberg, London (2009)
8. Fryda, M., Matthée, T., Mulcahy, S., Hampel, A., Schäfer, L., Tröster, I., Fabrication and application of Diachem R electrodes. *Diamond and Related Materials*, 12 (2003.) 1950-1956.
9. May, P. W., Materials science - the new diamond age? *Science*, 319 (2008)1490-1491
10. Kevin E. Bennet, Kendall H. Lee, James N. Kruchowski, Su-Youne Chang, Michael P. Marsh, Alexander A. Van Orsow, Aurelio Paez and Felicia S. Manciu, Development of Conductive Boron-Doped Diamond Electrode: A microscopic, Spectroscopic, and Voltammetric Study, *Materials* 6 (2013) 5726-5741
11. Fujishima A., Y. Einaga, T.N. Rao, D.A. Tryk (Eds.), *Diamond Electrochemistry*, Elsevier, Amsterdam, 2005.
12. Hupert M., A. Muck, R. Wang, J. Stotter, Z. Cvackova, S. Haymond, Y. Show, G.M. Swain, Conductive diamond thin-films in electrochemistry, *Diam. Relat. Mater.* 12 (2003)1940.

13. Angus J.C., Y.V. Pleskov, S.C. Eaton, Chapter 3 Electrochemistry of diamond,” *Semiconductors and Semimetals*, 77 (2004) 97-119.
14. Pastor-Moreno G., D.J. Riley, Electrochemical studies of moderately boron doped polycrystalline diamond in non-aqueous solvent, *Electrochim. Acta* 47 (2002) 2589-2595.
15. Latta M.N., G. Pastor-Moreno, D.J. Riley, The influence of doping levels and surface termination on the electrochemistry of polycrystalline diamond, *Electroanalysis* 16 (2004) 434-441.
16. Anbu Kulandainathan M., Clive Hall, Daniel Wolverson, John S. Foord, Stuart M. MacDonald, Frank Marken, Boron-doped diamond electrodes in organic media: Electrochemical activation and selectivity effects, *Journal of Electroanalytical Chemistry* 606 (2007) 150–158
17. Santos D.P., M.F. Bergamini, M.V.B. Zanoni, Voltammetric sensor for amoxicillin determination in human urine using polyglutamic acid/glutaraldehyde film, *Sens. Actuators B* 133 (2008) 398–403.
18. Bergamini M.F, M.F.S. Teixeira, E.R. Dockal, N. Bocchi, E.T.G. Cavalheiro, Evaluation of different voltammetric techniques in the determination of amoxicillin using a carbon paste electrode modified with [N, N-ethylene-bis(salicylideneaminato)] oxovanadium(IV), *J. Electrochem. Soc.*, 153 (2006) 94–98
19. Lisebo Phelane, Siyabulela Hamnca, Priscilla Gloria Lorraine Baker, Emmanuel Iheanyichukwu Iwuoha, Electrochemical Transduction at Modified Boron Doped Diamond Interfaces, *Journal of Nano Research* , 44 (2016) 51-62
20. Svorc Lubomir, Jozef Sochra, Peter Tomcik , Miroslav Rievaj, Dusan Bustin, Simultaneous determination of paracetamol and penicillin V by square-wave voltammetry at a bare boron-doped diamond electrode, *Electrochimica Acta* 68 (2012) 227– 234
21. Zhuo Ye, Le Wang, Jianguo Wen, A simple and sensitive method for determination of Norfloxacin in pharmaceutical preparations, *Brazilian Journal of Pharmaceutical Sciences* vol. 51 (2015) 249-259

CHAPTER VII

Detection of antibiotics residues by SWV, EIS and UV/Vis

This chapter investigates the electrochemical response of the selected antibiotic residues at each electrode material. For each antibiotic residue an appropriate electrode material was selected for a specific material, the selection was made based on the results that were obtained using cyclic voltammetry to measure the electrochemical response of each antibiotic at the 3 prepared electrode materials. The sensor performance was also investigated. The break down of this chapter is illustrated by Figure 7.1, which is the conceptual diagram. Showing the three electrode materials used to evaluate antibiotic residues and the measurement techniques that were used for the determination of the selected antibiotic residues.

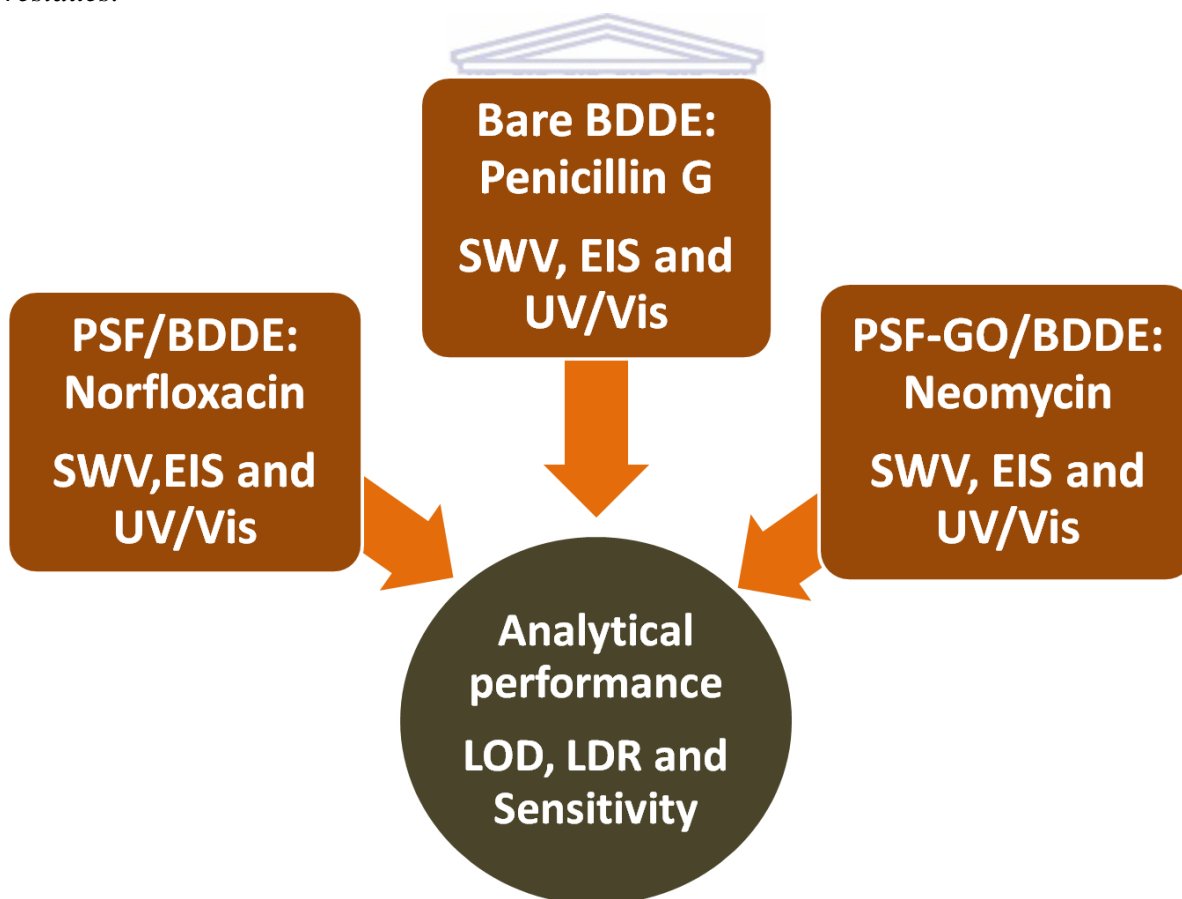
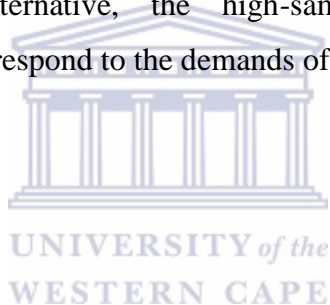


Figure 7.1: Conceptual diagram

Pharmaceutical residues have traditionally been detected using qualitative or semi-quantitative screening methods such as thin layer chromatography (TLC) and enzyme-linked immunosorbent assay (ELISA) with samples being subsequently analyzed for confirmation by chromatographic techniques gas chromatography (GC) or high performance liquid chromatography (HPLC) coupled to mass spectrometry (MS). Since most classes of pharmaceuticals have to be derivatized due to their lack of volatility before GC analysis, HPLC-MS is more universally applicable (antibiotics and estrogens). Capillary electrophoresis (CE) has also been employed, but since CE is less sensitive than HPLC, its application to analysis of pharmaceuticals is less attractive. Recent developments in detectors, sample-preparation units and other components have improved the limits of detection (LODs) of these techniques [1-2]. However, chromatographic methods are time consuming and laborious when a large number of samples must be screened for several pharmaceuticals, they require expensive equipment, trained personnel, and complex sample preparation steps. As an alternative, the high-sample throughput capability of immunochemical methods could respond to the demands of pharmaceutical analysis [3]



7.1. Detection of neomycin

7.1.1 Detection of neomycin by SWV

The SWV response of PSF-GO/BDD electrode to neomycin was investigated by successive additions of standard solution of neomycin to an electrochemical cell containing 0.1 M PBS pH 7.0.

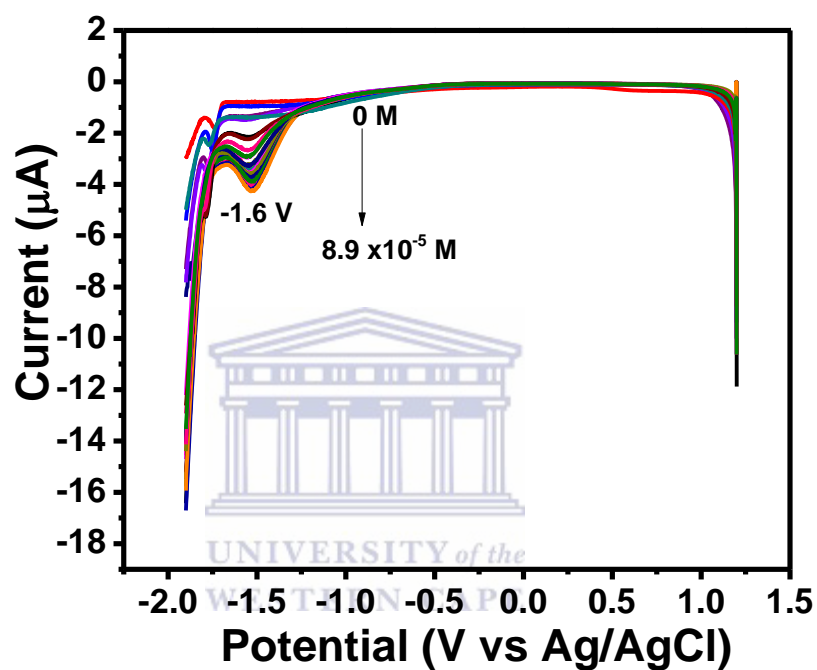


Figure 7.2a: Detection of neomycin at PSF-GO/BDD electrode measured by SWV

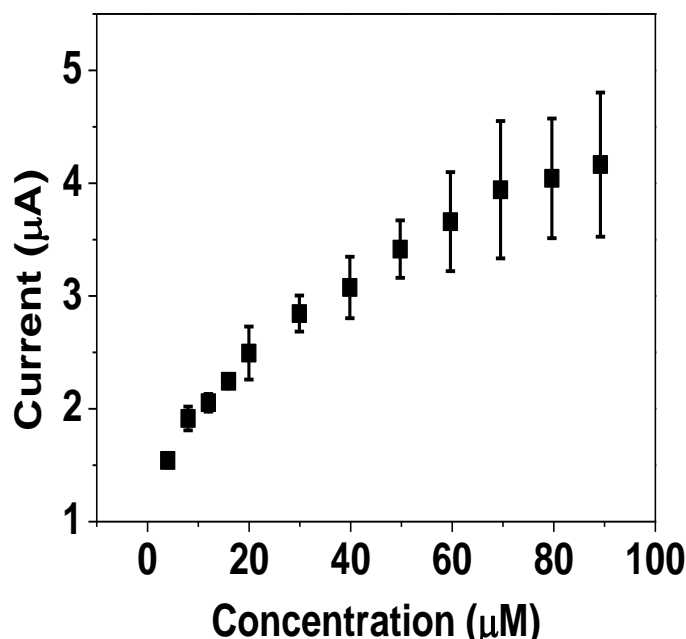


Figure 7.2b: Calibration curve of neomycin with standard error bars (S/N = 3)

The neomycin current response at the PSF-GO/BDD electrode is displayed from the above plot (Figure 7.2a), which showed a well defined reductive peak with the peak potential of -1.6 V vs Ag/AgCl. The reductive peak at -1.6 V increased with the increasing concentration of the neomycin at the PSF-GO/BDD electrode. The linear calibration plot at PSF-GO/BDD electrode along with error bars is presented in Figure 7.2b. The detection limit of the proposed sensor material has been calculated by using the formula $3\sigma/b$, where σ is the standard deviation of the blank and b is the slope of the calibration curve and was found to be 8.85×10^{-6} A / M with $R^2 = 0.992$

7.1.2 Detection of neomycin by EIS

The detection of neomycin using EIS as the measurement technique involved fixing the potential at -1.6 V for the wide frequency range (100 KHz – 65 mHz). Impedance data from Figure 7.3 was fitted using the electrical equivalent circuits. The circuit used for the chemical sensor at PSF-GO/BDD electrode, was a typical Randles circuit (Figure 7.4) consisting of a cell resistance, R_s (Ω), in series with a parallel combination of a constant phase element, CPE (F), as a non-ideal capacitance and a charge transfer resistance, R_{ct} (Ω). The low frequency range evaluation was performed fixing the potential at -0.2 V which was the reduction peak that was observed in figure A22. Stepwise potential EIS was performed for neomycin at PSF-GO/BDD electrode, obtained results presented in the appendix (Figure A22).

Low frequency EIS (Figure A25) was done to improve for the interfacial electrochemical separation of material effects at low frequency.

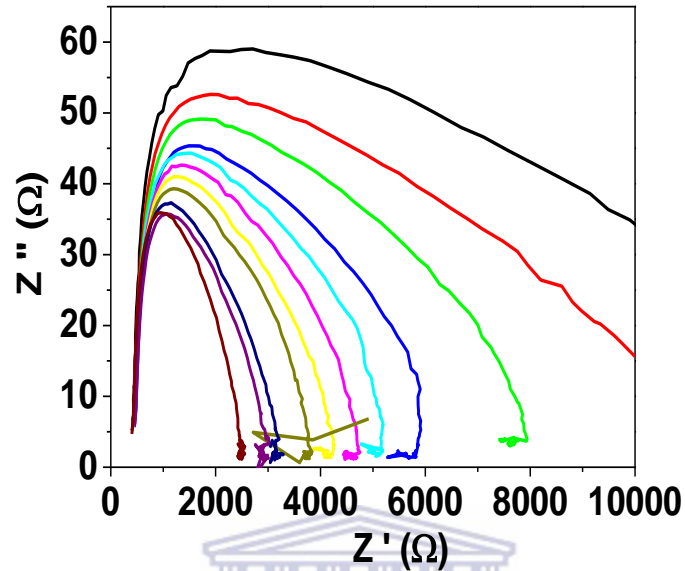


Figure 7.3a: Detection of neomycin at PSF-GO/BDD electrode by EIS (0 M – 8.9×10^{-5} M)

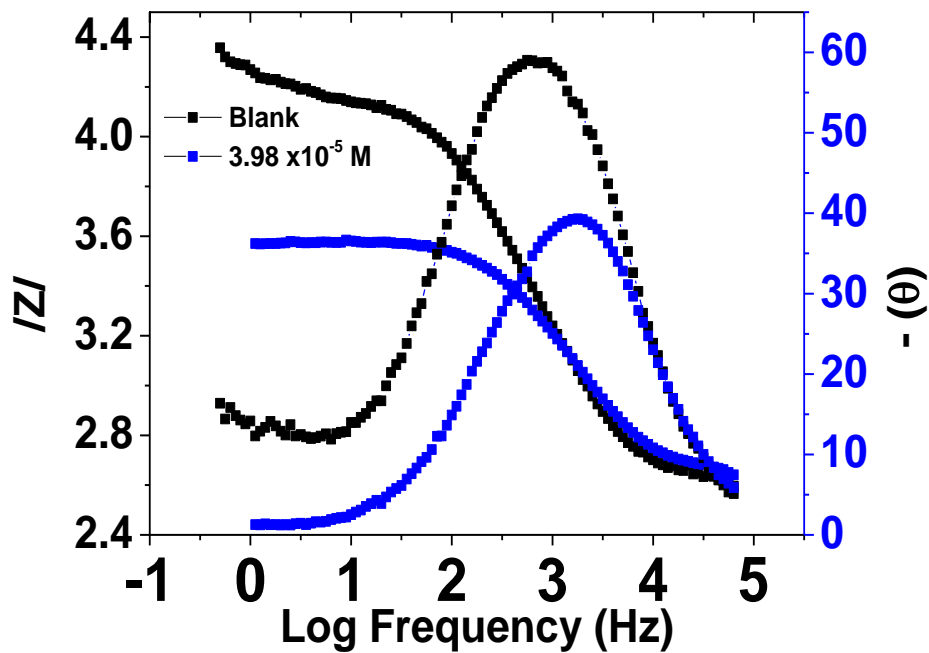
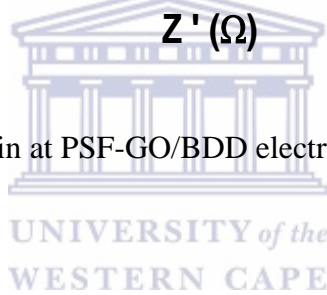


Figure 7.3b: Bode plot of neomycin at PSF-GO/BDD electrode

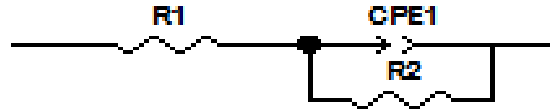


Figure 7.4: Randles-Sevcik equivalent circuit

The EIS results were recorded and fitted by the electrical equivalent circuit (Figure 7.4) to obtain the linear range and detection limit (LOD). Different concentrations of neomycin from the standard solutions were measured at PSF-GO/BDD sensor. The sensing potential was set at -1.6 V (vs Ag/AgCl). The above Randles-Sevcik circuit was used for both studies to fit the data. Figure 7.3b is the bode plot of neomycin which showed a decrease in phase angle and total impedance after the addition of neomycin to the electrolyte, illustrated by the blue line.

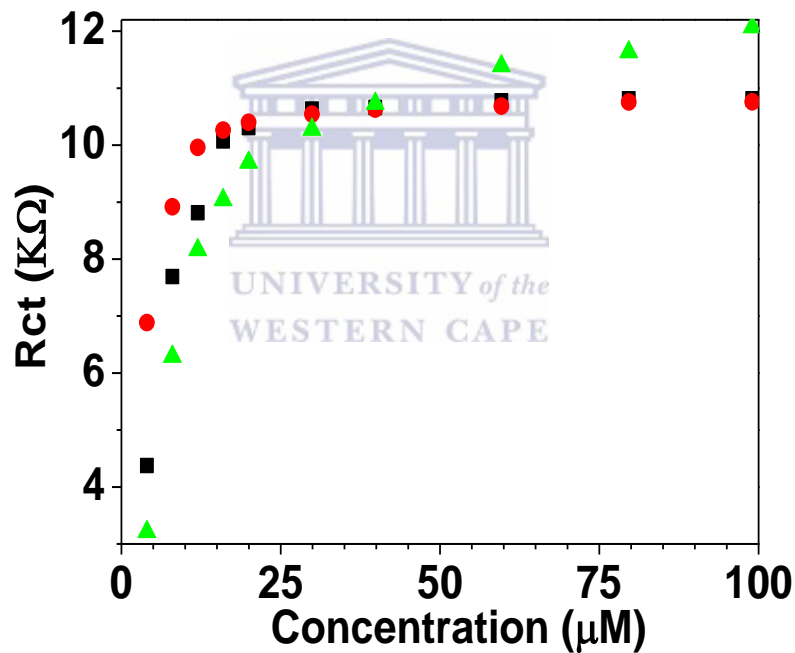


Figure 7.5a: Calibration curve of neomycin at PSF-GO/BDDE, showing 3 fitted data

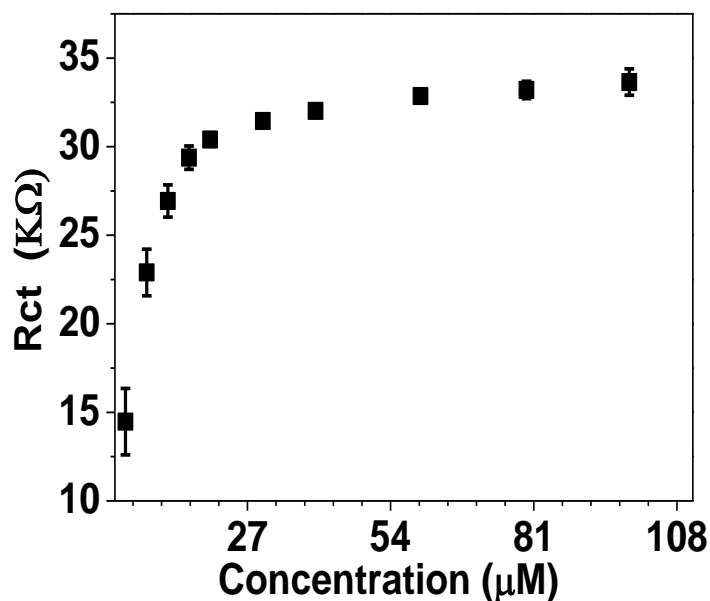


Figure 7.5b: Calibration curve of neomycin at PSF-GO/BDD with error bars (SN=3), showing the average Rct

The above figures show the nyquist plot representing the EIS response of neomycin at PSF-GO/BDD electrode (Figure 7.5a). The nyquist plot for high frequency EIS followed a pattern, the semi circle showed a decrease in size with increasing concentration of neomycin. The charge transfer resistance obtained after fitting also showed an increase in Rct values with increasing concentration of neomycin. The concentration vs. Rct plot (Figure 7.5b) showed a linear relationship with the correlation coefficient of 0.891 and the concentration range was between 3.99×10^{-6} – 1.99×10^{-5} M. The LOD calculated was 5.83×10^{-6} mol/L (SN=3).

The analytical peak observed at -1.6 V (vs Ag/AgCl) was used as the label peak to monitor the concentration dependant studies of neomycin. For EIS concentration dependant studies the potential was fixed at -1.6 V. The experiments were repeated three times and the same response was observed and shown in Figure 7.3b. From literature there is no study that confirms or supports this peak as the neomycin analytical peak. Electrochemical detection studies of neomycin focuses highly on biosensors based on the use of biomolecules such as DNA, aptamers as well as antibodies and chemical sensors uses ferricyanide as the electrolyte. Ferricyanide is known for its redox couple which is a standard in electrochemistry. It is easy to use the ferrocyanide peaks as labels when monitoring concentration of analytes with low electrochemical response. Zhu and colleagues [4],

developed a novel amperometric immunosensor with an enhanced sensitivity for the detection of neomycin. The immunosensor was prepared by covalently immobilizing a monoclonal Neo antibody onto a new conducting polymer, poly-[2,5-di-(2-thienyl)-1H-pyrrole-1-(p-benzoic acid)] (pDPB), as a sensor probe [4]. The probe was used to detect Neo in a sandwich-type approach, where the secondary antibody was attached to gold nanoparticle-decorated multi-wall carbon nanotubes labelled with hydrazine (Hyd-MWCNT/(AuNP)-Ab2. Another study based on the detection of neomycin was done focusing deoxyribonucleic acid (DNA) modified gold electrodes to detect neomycin using chronocoulometry and differential pulse voltammetry. A chemical sensor was developed which focused on the MIP of neomycin. The sensor material prepared was chitosan- silver nanoparticles (CS-SNP)/graphene-multiwalled carbon nanotubes (GR-MWCNTs) composites decorated gold electrode. Molecularly imprinted polymers (MIPs) were synthesized by electropolymerization using neomycin as the template, and pyrrole as the monomer. The CV was performed with a supporting electrolyte containing 5.0 mmol/L $K_3[Fe(CN)_6]$ solution containing 0.2 mol/L KCl [5].



7.2. UV/Vis Analysis of Neomycin

Ultraviolet-visible (UV/Vis) spectrophotometry represents a suitable method for the routine analysis of pharmaceutical active ingredients in raw materials, since it is fast, easy to perform and does not require expensive instruments. UV/Vis concentration analysis for neomycin was performed in an unrestricted environment free from any limitation imposed by transducer based analysis. Because aminoglycosidic antibiotics present low absorbance on the UV/Vis domain, direct determination by UV/Vis spectrophotometry would not assure adequate detection and quantitation limits, making direct quantification impossible [6].

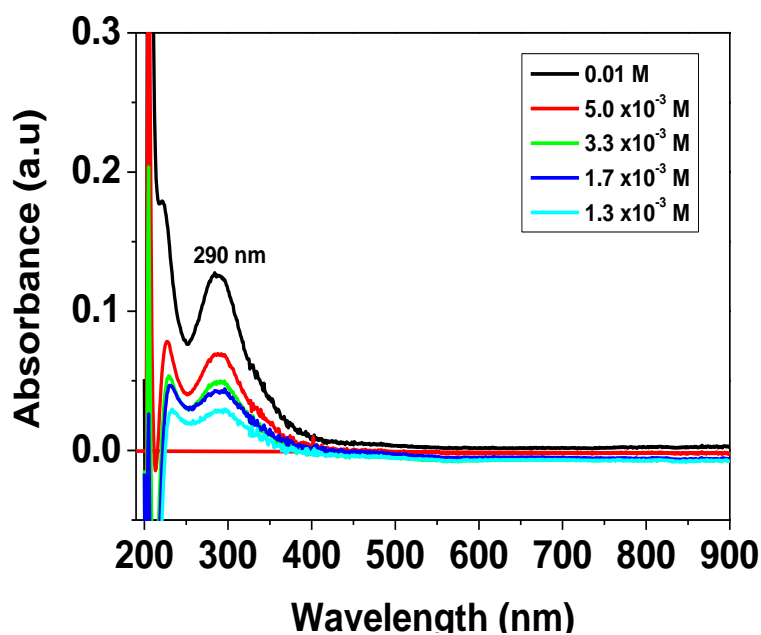


Figure 7.6a: Detection of neomycin by UV/Vis

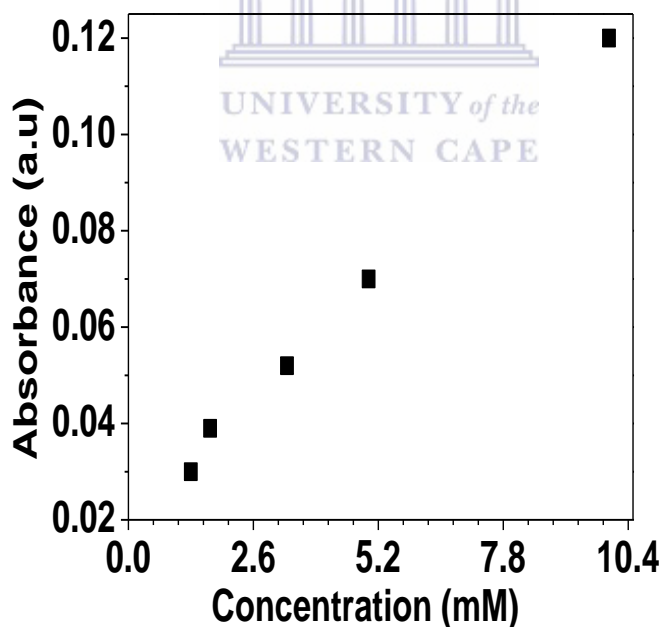


Figure 7.6b: Calibration curve of neomycin

Aminoglycoside antibiotics appear to lack a chromophore or fluorophore moiety which is vital for spectrophotometric analysis. The absorbance of neomycin was below 0.2 which is in agreement with the literature that neomycin does not absorb UV/Vis because they lack a

chromophore. The calibration curve (Figure 7.6b) of neomycin showing the concentration against the absorbance appeared to be linear with the $R^2 = 0.979$ and the concentration range was between 1.3 mM – 5.0 mM. The obtained sensitivity was 10.2 a.u./mM.

7.3 Detection of penicillin G

7.3.1 Detection of penicillin G by SWV

The SWV response of bare BDD electrode to penicillin G was investigated by successive additions of standard solution of penicillin G to an electrochemical cell containing 0.1 M PBS pH of 7.0

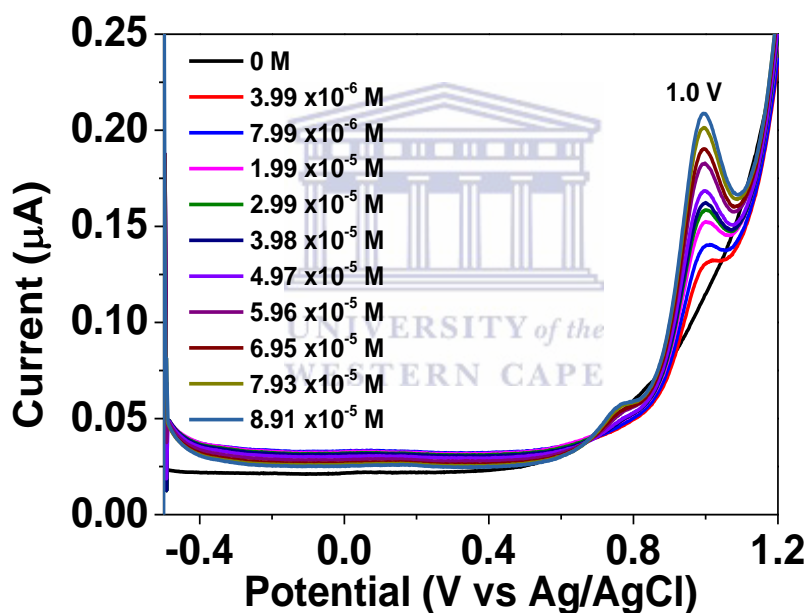


Figure 7.7a: Detection of penicillin G at bare BDD electrode by SWV.

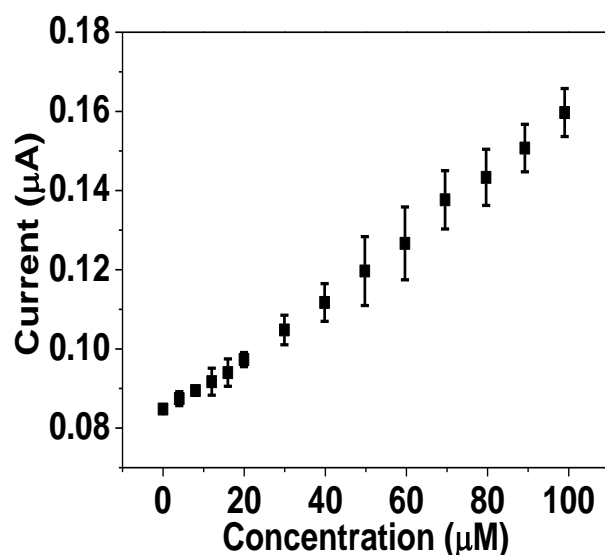
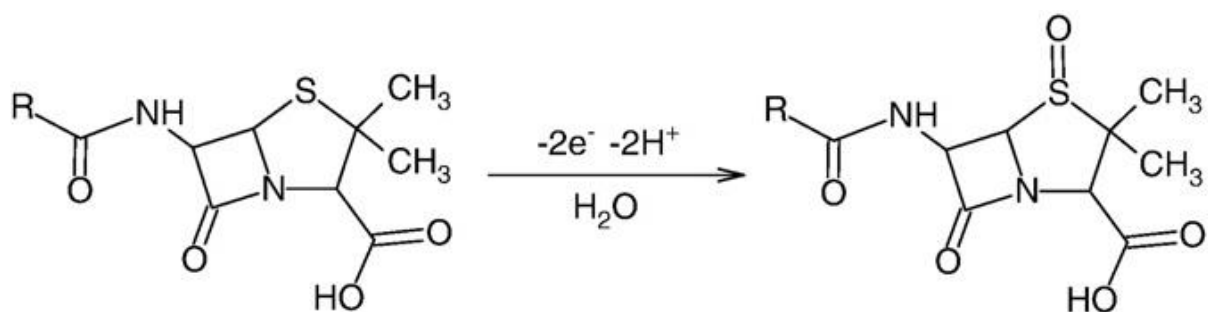
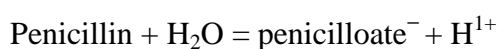


Figure 7.7b: Calibration curve of penicillin G (SN=3)

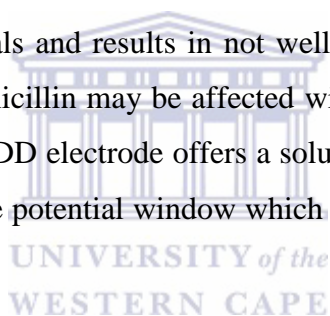
The electrochemical oxidation of penicillins has been studied many times and with different results from different studies. One possible electrochemical oxidation of penicillins could be due to the site of oxidation of penicillin the β -lactam backbone and not in the side chains whereas with amoxicillin a significantly different response would be expected because of the presence of a phenol group in the side chain. The sulfide moiety of the β -lactam ring might be oxidized into a sulfoxide derivative of penicillin in participation of water, two protons and transfer of two electrons as illustrated in Scheme 1. Another possibility could be when enzyme penicillinase is used it catalyzes the hydrolysis of penicillin to penicillinoic acid, this is shown in the equation below. The created hydrogen ions (H^{1+}) can be applied to detect the penicillin concentration [7].



Scheme 1: Electrochemical oxidation of penicillin G [8]

SWV response after the addition of penicillin G showed an oxidation peak at 1.0 V which is due to the oxidation of penicillin. The experiment were repeated 3 times (SN=3) so that the LOD can be determined. Figure 7.6 (a) is the SWV of different concentrations of penicillin G at bare BDD electrode and (b) the average plot of all 3 experiments. The Oxidation peak at 1.0 V (vs. Ag/AgCl) was used as the analytical peak to construct a calibration curve. The LOD calculated was 9.62×10^{-6} M with correlation coefficient of the regression line of 0.993.

When investigating sensor performance it is vital to assess different factors such as concentration detection range, selectivity, detection limit and reproducibility. The reproducibility is a prominent factor for the activity measurement of a sensor in order to see the consistency in the performance [7]. For this study three bare BDD electrode were used in this study to investigate the reproducibility and repeatability of the sensor material. The bare BDD electrode showed good reproducibility and repeatability this was confirmed by low error bars presented in Figure 7.6b. The electrochemical oxidation of penicillins usually occurs at high very high potentials and results in not well and clearly defined peaks. As a consequence the oxidation of penicillin may be affected with limited potential window from the anodic side [8]. The use of BDD electrode offers a solution to this challenge because one of the BDD properties is the wide potential window which makes the oxidation of penicillins possible.



7.3.2 Detection of penicillin G by EIS

The impedance response penicillin G at bare BDD electrode was investigated by successive additions of penicillin G standard solution to an electrochemical cell containing 0.1 M PBS pH of 7.0 at an applied potential of 1.0 V (vs. Ag/AgCl). The potential for low frequency EIS (500 Hz – 65 mHz) was fixed at 0.1 V (vs. Ag/AgCl) and the obtained spectra are presented in the appendix (Figure A26). The peak used in low frequency EIS was observed from stepwise potential EIS performed to characterise penicillin G at bare BDD electrode (Figure A23). All spectra for bare BDD (n=3), were fitted using the same electrical equivalent circuit as neomycin (Figure 7.4), containing the solution resistance (R_s) in series with a parallel charge transfer resistance (R_{ct}) with a constant phase element (CPE) representing a non-ideal capacitance. The charge resistance describes the electron transfer kinetics of the redox at the electrode interface and the capacitance describes the charge separation

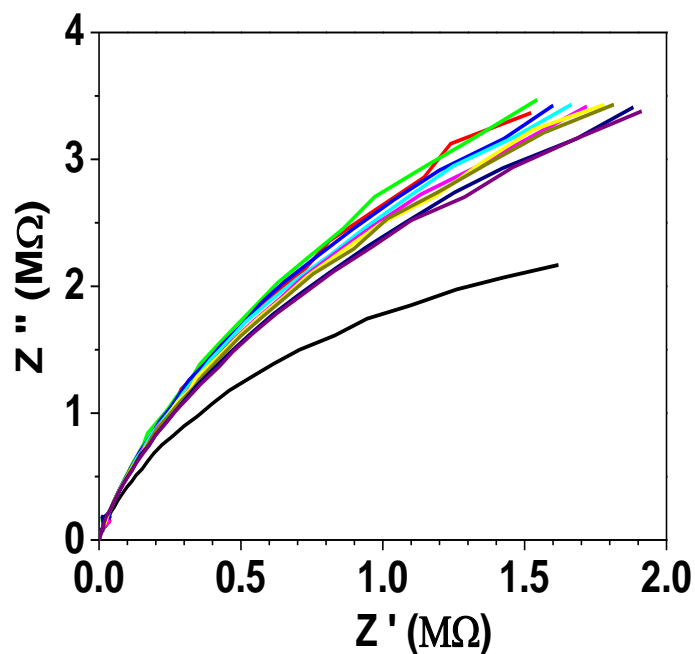


Figure 7.8a: Detection of penicillin G at bare BDD electrode by EIS

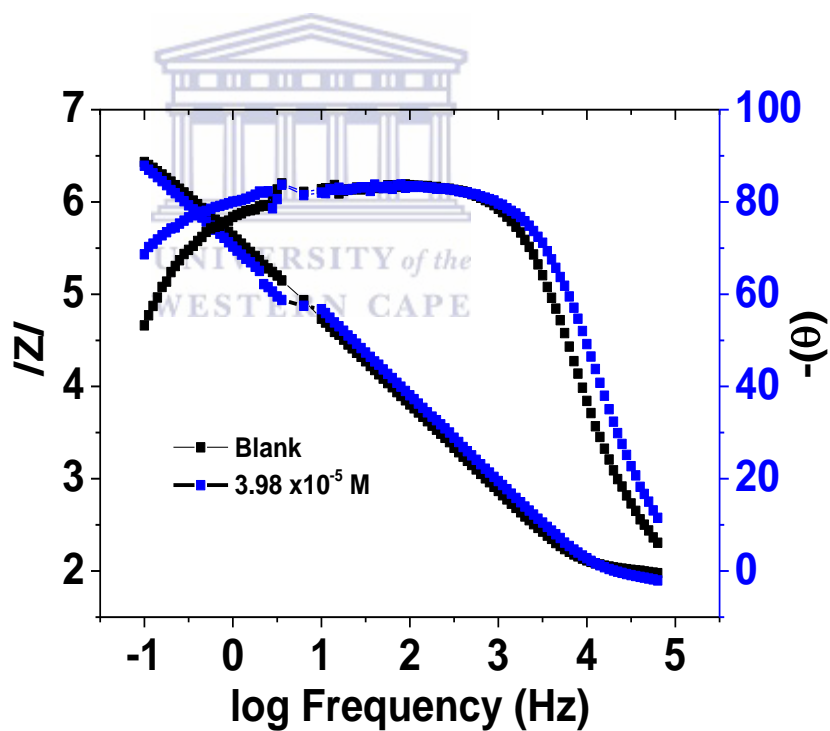


Figure 7.8b: Bode plot of penicillin G at bare BDD

Impedance spectra were fitted using the electrical equivalent circuits. The equivalent electrical circuit used for the chemical sensor of penicillin G at BDD electrode, was a typical Randles circuit (Figure 7.4) consisting of a cell resistance, R_s (Ω), in series with a parallel

combination of a constant phase element, CPE (F), as a non-ideal capacitance and a charge transfer resistance, R_{ct} (Ω). The charge transfer resistance values from the fitted data were not inconclusive, hence for the calibration curve the capacitance values were used to construct the calibration curve for the detection of penicillin at bare BDD electrode. The low frequency range EIS were performed to improve EIS results for the detection of penicillin G (Figure A26). The LOD and the linear dynamic range were determined for the sensor.

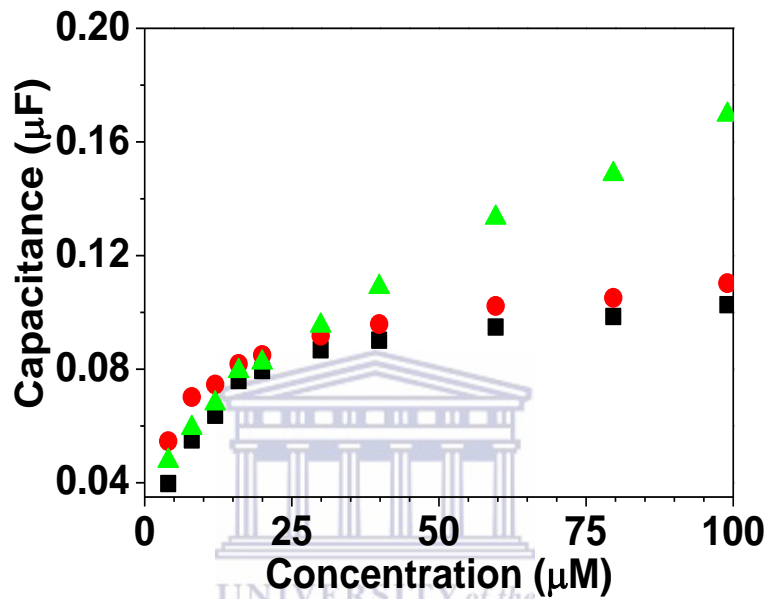


Figure 7.9a: Calibration curve of penicillin G (SN=3)

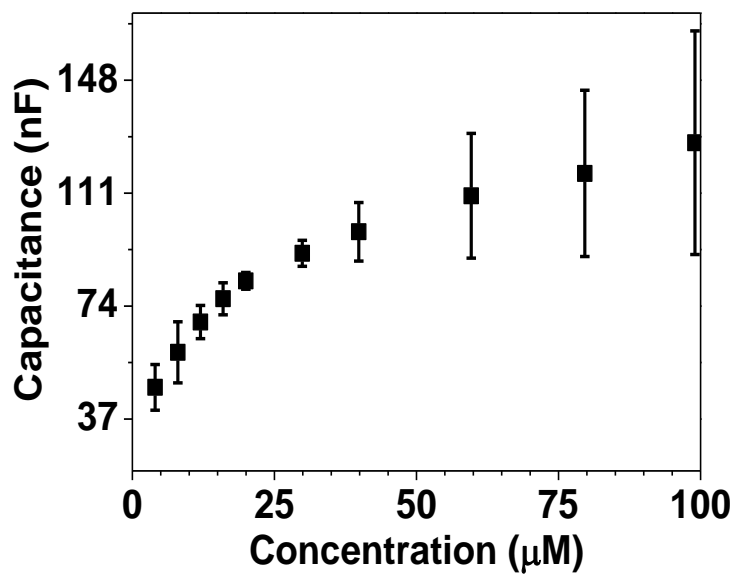


Figure 7.9b: Calibration curve of penicillin G with error bars (SN=3)

EIS after the addition of penicillin G showed a linear relationship where the value in capacitance increased with increasing concentration of penicillin G. The experiment was repeated 3 times (SN=3) so that the LOD and sensitivity can be determined. The response of bare BDD electrode based impedimetric detection was linear up to 1.99×10^{-5} M penicillin G concentration. The correlation coefficient of the regression line was 0.977. The sensitivity for this chemical sensor was 2.19×10^{-3} nF/mM, obtained from the calibration curve (Figure 7.9b). A detection limit ($LOD = 3.3 \times STEYx/slope$, where $STEYx$ is the standard error, $n = 3$, and the slope of the calibration curve) of 3.19×10^{-6} M was obtained. The low frequency EIS improved the behaviour of penicillin G when EIS was used as the analytical detection method. The charge transfer resistance data obtained from electrical equivalent circuit fitting was used to construct a calibration curve. Charge transfer resistance is an expected parameter in EIS because it results from the electron exchange under applied potential. The sensitivity evaluated for this slope of calibration curve (Figure A23) was found to be 3.420×10^{10} M Ω / μ M. The correlation coefficient of the regression line was 0.862.

Based of literature reports only few electrochemical studies focusing on penicillins are reported in comparison with other drugs. This is because the oxidation of penicillins usually takes place as not clearly defined waves at very high positive potentials and as a result this may affect the electrochemical reactions limiting potential window from the anodic side. The oxidation peak at 1.0 V (vs. Ag/AgCl) was confirmed as the penicillin oxidation peak by a study that was done by Svorc *et. al.* [8], who develop a chemical sensor for determination of penicillin V at bare BDD electrode. The oxidation peak at about 1.6 V (vs. Ag/AgCl) was observed and no cathodic was observed [8]. Several reports dealing with determination of penicillins are based on pulsed amperometric detection flow injection analysis and biosensors are reported in literature. Enzyme β -Lactamase is known to catalyze the hydrolysis of penicillin to penicillanic acid and results in a decrease of solution pH. This has led to many reported penicillin biosensors, in which the pH change is usually monitored by potentiometry, conductometry, colorimetry or fluorescence [19]. An amperometric penicillin biosensor was developed by co-immobilization of MWCNT, hematein, and β -lactamase on glassy carbon electrode using a layer-by-layer assembly technique [7]. Another study was developed based on amperometric detection of penicillin. This biosensor for penicillin G was constructed by immobilizing penicillinase to a gold electrode by means of a cysteine self-assembled monolayer. The biosensor amperometrically monitored the catalytic hydrolysis of penicillin

and the obtained limit of detection was 4.5 nM [7,19]. Surface acoustic wave (SAW) biosensors were introduced for rapid, label-free detection of penicillin G in milk and were reported for the first time by Gruhl *et.al.* The use of SAW biosensors offers a rapid detection of analyte concentrations with a minimum of experimental effort. Owing to the small mass of antibiotics, detection via binding inhibition assay was preferred for direct detection. The assay allowed the detection of 2 ng/ml penicillin G in buffer and 2.2 ng/ml in low-fat milk [20].

7.4. UV/ Vis analysis of Penicillin G

The absorbance of penicillin G was measured using the UV/Vis, this was achieved by preparing a 0.01 M penicillin G standard solution dissolved in 0.1 M PBS. From the prepared standard solution of penicillin dilutions were made to measure the absorbance at different concentrations of penicillin G. UV/Vis concentration analysis for penicillin G were performed in an environment free from any limitations imposed by the transducer based analysis

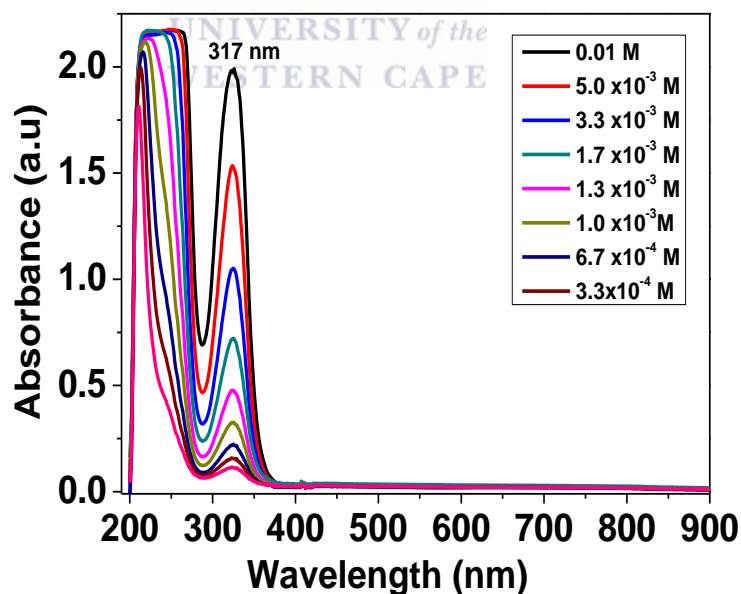


Figure 7.10a: Detection of penicillin G by UV/Vis

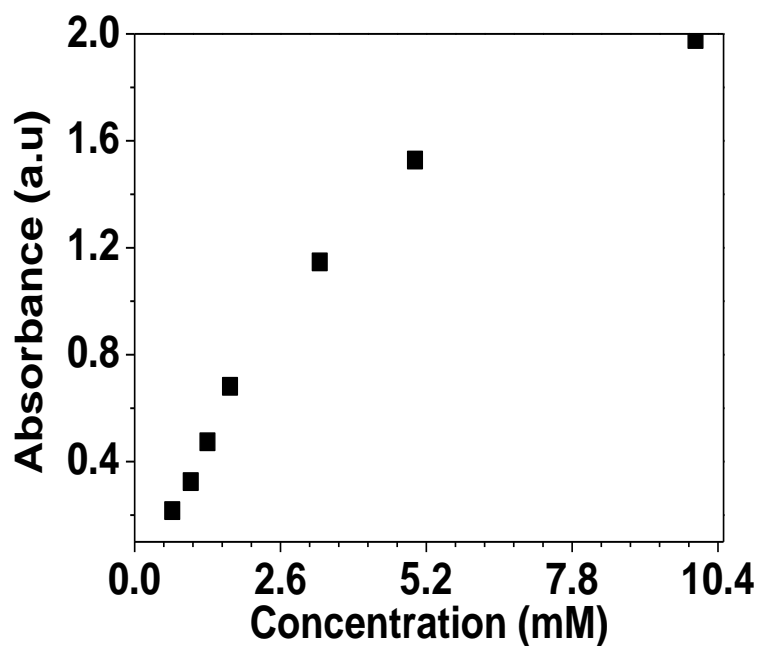


Figure 7.10b: Calibration curve of penicillin G

Absorption of penicillin G was observed at 317 nm (Figure 7.10a). The absorption of penicillin G was observed at the UV region may be due to the presence of unique ring structure which is the β -lactam ring present in penicillin. Penicillin G calibration curve (Figure 7.10b) showed linearity in the concentration range of 1.3 mM – 0.01 M and the slope obtained was 355 mM / a.u. The curve showed to be linear because of the correlation coefficient of the regression line was 0.9799 [9]

7.5 Detection of Norfloxacin

7.5.1 Detection of norfloxacin by SWV

The SWV response of bare BDD electrode to norfloxacin was investigated by successive additions of standard solution of norfloxacin to an electrochemical cell containing 0.1 M HCl.

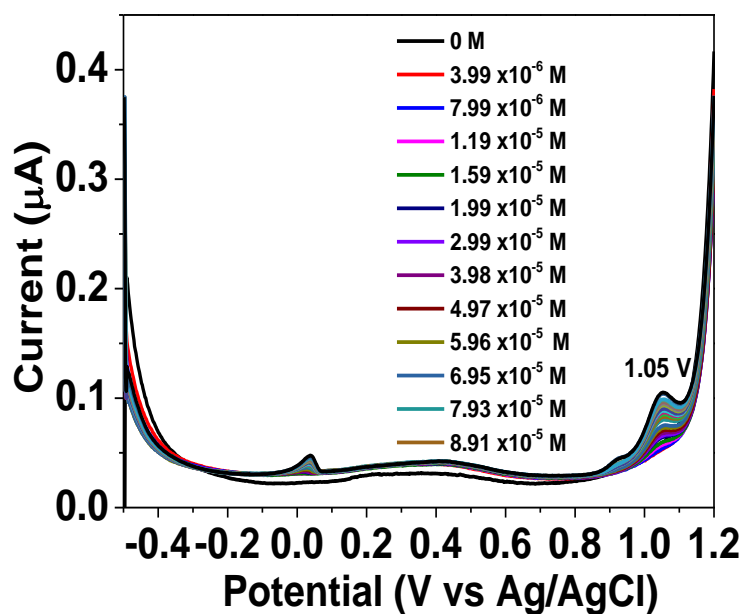


Figure 7.11a: Detection of norfloxacin at unmodified PSF/BDDE by SWV

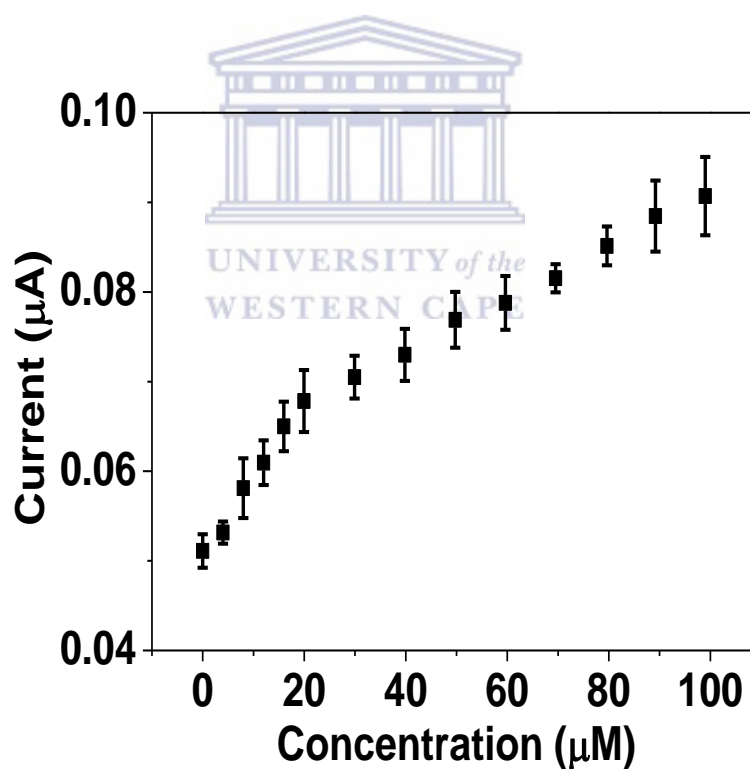
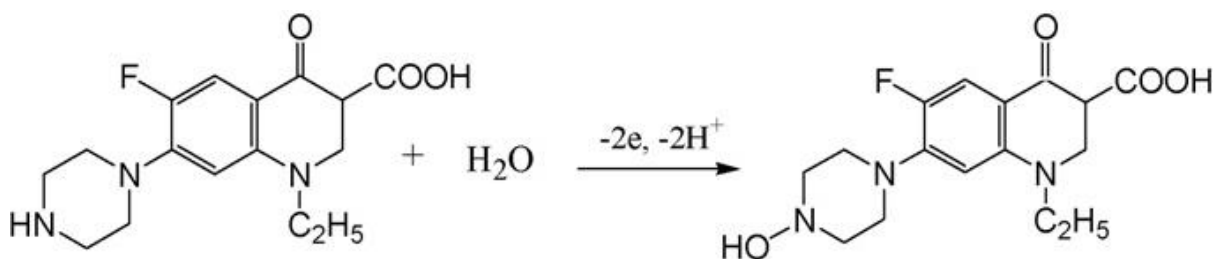


Figure 7.11b: Calibration curve of norfloxacin at unmodified PSF/BDD electrode (SN = 3).

The quantitative analysis of the antibiotic is based on the dependence of the peak current on the concentration of norfloxacin (NOR). The voltammogram illustrated the systematic increase in the peak current values with increasing concentration of NOR at unmodified

PSF/BDD electrode presented in Figure 7.11a. Calibration curve of NOR along with error bars presented in Figure 7.11b. The peak current was found to increase linearly with increasing concentrations of NOR. The detection limit of the proposed sensor material was calculated by using the formula $3\sigma/b$, where σ is the standard deviation of the blank and b is the slope of the calibration curve and the calculated LOD was 8.85×10^{-6} M with correlation coefficient of the regression line was 0.991. Although, the detection limit reported for NOR at unmodified PSF/BDD electrode, was not the greatest as the sensors from literature, on the other hand, the main advantage was that no complicated modification of the electrode surface was required. Electrochemical oxidation of NOR occurred by the transfer of the same number of electrons and protons, thus, two electrons and two protons transfer was involved in the electrode reaction. The electrochemical reaction process for NOR at PSF/BDD electrode can therefore be briefly shown by Scheme 2 as reported in the literature [10].



Scheme 2: Oxidation mechanism of norfloxacin

7.5.2 Detection of norfloxacin by EIS

The impedance response at the PSF/BDD modified electrode to norfloxacin was investigated by successive additions of standard solution of norfloxacin to an electrochemical cell containing 0.1 M HCl at an applied potential of 1.05 V (vs. Ag/AgCl). The potential for the low frequency range studies was fixed at 0.3 V (vs. Ag/AgCl), the peak used was observed from the stepwise potential EIS (Figure A24).

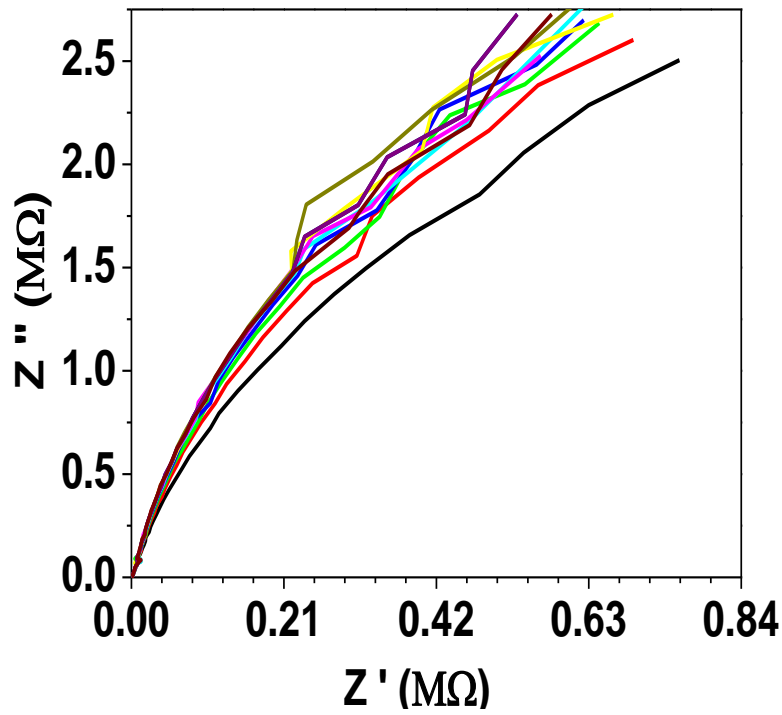


Figure 7.12a: Detection of norfloxacin at unmodified PSF/BDD electrode by EIS

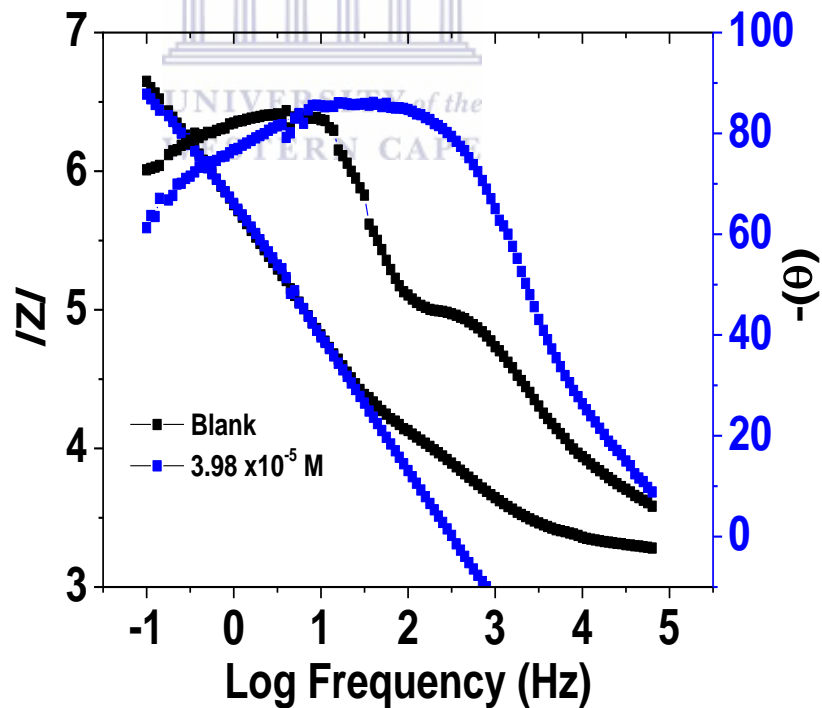


Figure 7.12b: Bode plot of norfloxacin at unmodified PSF/BDD electrode

EIS spectra (Figure 7.12a), were fitted using the electrical equivalent electrical circuits. The electrical equivalent circuit used for the chemical sensor at PSF/BDD electrode, was a typical

Randles-Sevcik circuit (Figure 7.4) consisting of a cell resistance, R_s (Ω), in series with a parallel combination of a constant phase element, CPE (F), as a non-ideal capacitance and a charge transfer resistance, R_{ct} (Ω). The CPE values increased with increasing concentrations of norfloxacin. A different electrical equivalent circuit was designed to fit the low frequency EIS spectra (Figure A27). The PSF/GO interface with norfloxacin was represented by a mass transport finite-diffusion Warburg element Z_w , in parallel with a constant phase element (CPE), representing the interfacial charge separation, is modelled as a non-ideal capacitor, owing to the polysulfone pore forming ability, and the obtained exponent α has a value around 0.77 and in series with the solution transfer resistance R_s [11-12].

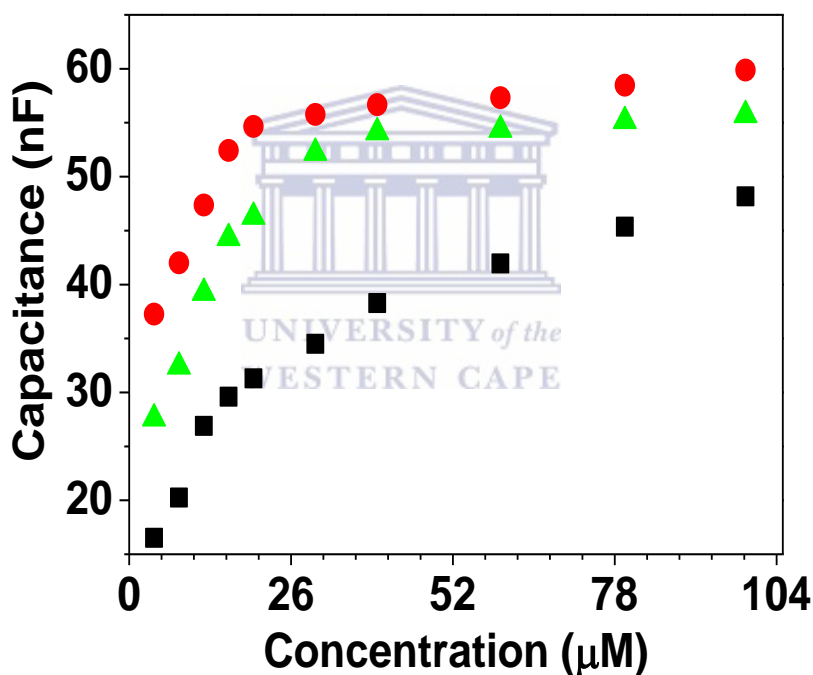


Figure 7.13a: Calibration curve of norfloxacin at unmodified PSF/BDD electrode

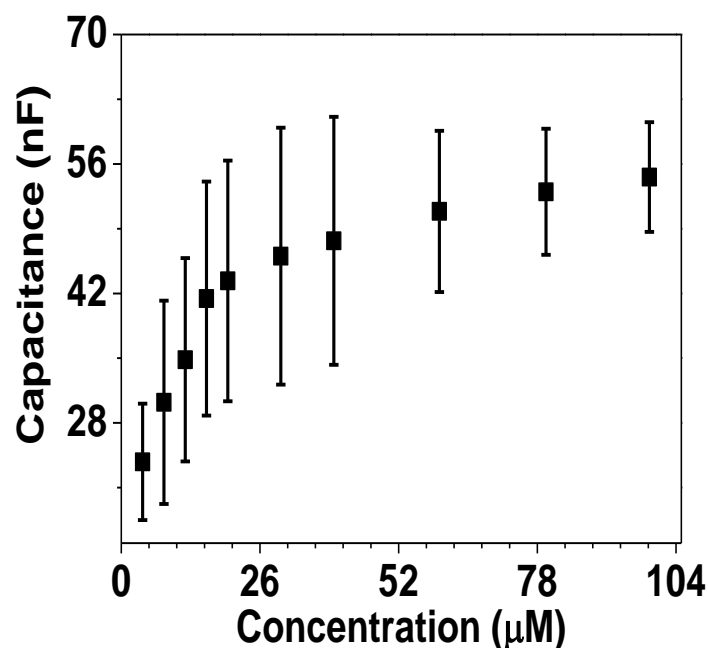


Figure 7.13b: Calibration curve of norfloxacin at unmodified PSF/BDD electrode with error bars (SN=3)

To complete the impedance analysis of the chemical sensor, an electrical equivalent circuit was designed in order to fit the impedance spectra obtained for unmodified PSF/BDD electrode based sensor (Figure 7.12a). The Randles-Sevcik electrical equivalent circuit was used to model AC impedance data of electrochemical cells. The resulted determined after fitting the EIS spectra was used to construct a calibration curve (Figure 7.13a) showing the capacitance against different concentrations of NOR. Under the optimum conditions there was a linear relationship, with a slope of the calibration curve (Figure 7.13b) of $1.2 \times 10^{-3} \mu\text{M/nF}$, between peak current and NOR concentration in the range $3.99 \times 10^{-6} - 1.99 \times 10^{-5} \text{ mol/L}$ ($R^2 = 0.969$); the detection limit was $3.69 \times 10^{-6} \text{ mol/L}$. The low frequency range calibration curves showed to be diffusionally controlled with the linear correlation value of > 0.9 for Zw plot (Figure A26b).

Polysulfone belongs to the family of sulfur-containing thermoplastics. Its porous nature allows it to be used in micro, ultrafiltration and reverse osmosis processes as well as in the development of composite membranes to facilitate transport. However, polysulfones exhibit few main disadvantages, the hydrophobic character, the low resistance to UV radiation and less electrochemical conductivity [13-14]. The use of polysulfone for detecting norfloxacin

was fraught with challenges such as the polysulfone layer detaching from the electrode surface and depending of the thickness of the polymer layer no reactivity or electrochemical response was observed due to the polymer blocking the movement of electrons from the electrolyte solution to the electrode surface. This was overcome by reducing the volume of the polymer drop coated onto the surface of working electrode. The variation in the EIS response observed for norfloxacin detection (Figure 7.13a) may be ascribed to the inconsistency in the thickness of the underlying PSF layer prepared by drop coating. Additionally, the PSF layer is inherently a non facile transducer, which may result in inconsistent catalysis of norfloxacin.

7.6. UV/Vis analysis of Norfloxacin

Fluoroquinolones drug solutions are colorless, they have no absorption in the visible range, and their absorption lies in the ultraviolet range. Because of the highly blue shifted λ_{max} of these drugs, their determination in the dosage forms based on the direct measurement of their absorption for ultraviolet is susceptible to potential interfering species from derivatization agents [15]. The absorbance of norfloxacin was measured using UV/Vis spectroscopy. The norfloxacin was dissolved in acetic acid to give a final concentration of 0.01 M. Different concentrations of norfloxacin were measured for absorbance.

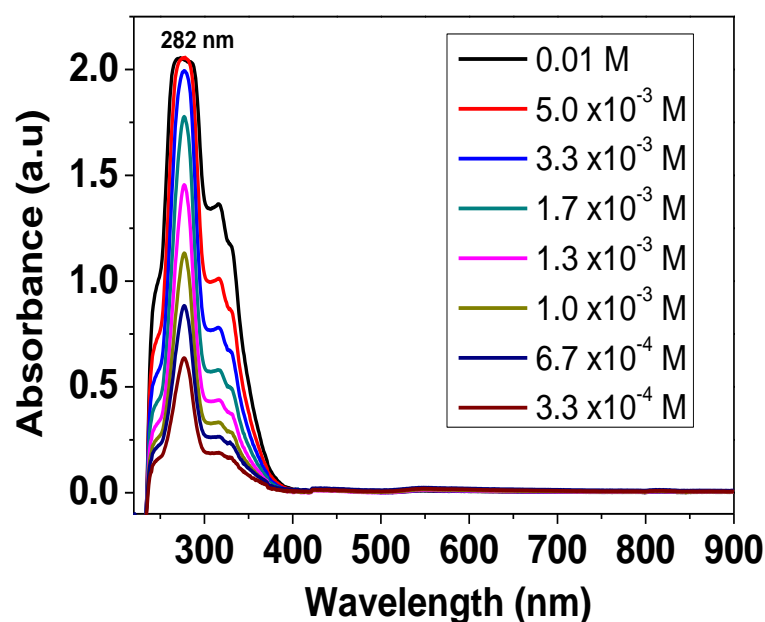


Figure 7.14a: Detection of norfloxacin by UV/Vis

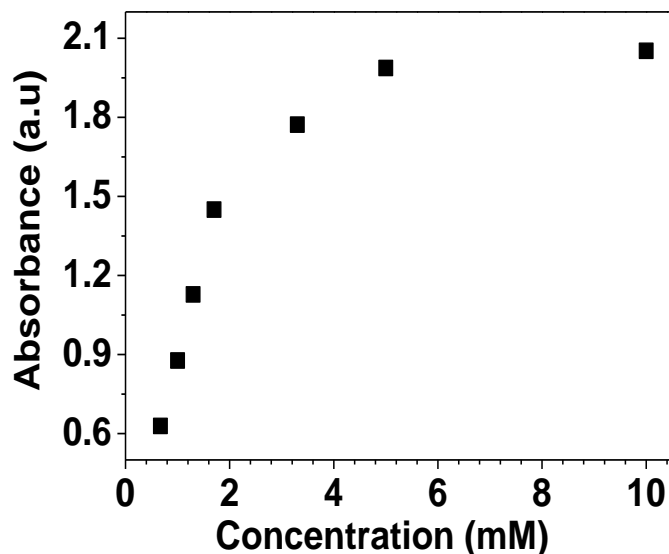


Figure 7.14b: Calibration curve of norfloxacin

The absorbance of different concentration of norfloxacin was measured by UV/Vis spectrometer and the absorption was at 282 nm (Figure 7.14a). Fluoroquinolones solution contains no colour and cannot absorb in the visible range, their absorbance lies in the ultraviolet range. The calibration curve (Figure 7.14b) norfloxacin showing the concentration against absorbance showed to be linear with the $R^2 = 0.999$ and the concentration range was between 1.3 mM – 5.0 mM.

Table 7.1: LOD of all three selected antibiotics residues

Antibiotic	LOD (SWV)	LOD (EIS)	LOD (UV/Vis)
Residue (Analyte)	(M)	(M)	(M)
Penicillin G	9.62×10^{-6}	3.13×10^{-6}	4.32×10^{-3}
Norfloxacin	4.92×10^{-6}	3.69×10^{-6}	1.13×10^{-3}
Neomycin	8.85×10^{-6}	5.83×10^{-6}	6.05×10^{-4}

The sensor performance for the quantitative detection of penicillin G, neomycin and norfloxacin were investigated. The above table compares the obtained LOD values for all three analytical performance measured by SWV, EIS and UV. Electrochemical techniques showed better sensor performance when compared with UV/Vis technique. This was due to the fact that there UV analysis was carried out by measuring the antibiotic residue directly and the environment was free from limitations such as transducers. Unmodified PSF/BDD electrode showed the lowest LOD value for the detection of norfloxacin measured by SWV, whilst bare BDD electrode showed the lowest LOD value for detecting penicillin G when measured by impedance. The EIS studies were done at low frequency range and also at wide frequency range to compare the performance of the fabricated sensor. The obtained results showed that EIS performed at wide frequency range were better than EIS at low frequency range because the electrochemical reporting of the material was an integral part of the analytical signal reporting for these analytical species with limited redox capability.



Table 7.2: Comparison of sensor performance

Electrode Material	LOD	Analyte	Peak Potential	Reference
Bare BDDE	0.32 μM	Penicillin V	1.6 V	[8]
Hyd/MWCNT/Ab2	6.76 nM	Neomycin	- 0.5 V	[4]
MWCNT/nafion	0.5 μM	Norfloxacin	+1.1 V	[18]
PSF-GO/BDDE	5.83 μM	Neomycin	-1.6 V	This work
PAA-GO/SPCE	33.7 μM	Norfloxacin	+0.89 V	S. Hamnca
PSF/BDD	3.69 μM	Norfloxacin	+1.05 V	This work
Bare BDDE	3.13 μM	Penicillin G	+ 1.0 V	This work

UNIVERSITY of the
WESTERN CAPE

The proposed method for determination of penicillin G, neomycin and norfloxacin were compared with other typical methods. The detection limit values were 3.69 μM , 3.13 μM , 5.83 μM and for norfloxacin, penicillin G and neomycin respectively, which compared well with the detection limit obtained from the chemical sensor based on bare BDD electrode developed for the detection penicillin V and also MWCNT based chemical sensor for detection of norfloxacin. Thus, the obtained results from this study clearly indicate that the proposed electrochemical method of analysis is appropriate for the determination of the three selected antibiotic residues (neomycin, norfloxacin and penicillin G) in aqueous solutions.

The reported concentrations of pharmaceuticals found in surface waters, groundwater and partially treated water are less than 0.1 $\mu\text{g/L}$, and concentrations in treated water are generally below 0.05 $\mu\text{g/L}$. European Union (EU) have established maximum residual limits (MRL) for neomycin in animal edible tissues, 500 $\mu\text{g/kg}$ (0.5 $\mu\text{g/mL}$) for meat and 1500 $\mu\text{g/kg}$ (1.5 $\mu\text{g/mL}$) for kidney. The concentration range of NOR in surface waters was

reported to be < 120 ng/L, while the MRL for fluoroquinolones in ppm are not yet reported on [21-22]. Converting WHO concentration values from g/mL to mol/mL resulted in the LOD results for this study showing low concentration limit and also the concentration are in the same concentration range as the WHO MRL results for antibiotic residues.

7.7. Conclusion

The results obtained for three chemical sensors are summarised in the table below.

Table 7.3: Summary of Sensor Performance

Electrode Material	BDD, PSF/BDD, PSF-GO/BDDE	BDD, PSF/BDD, GO/BDD	BDD, PSF/BDD, PSF-GO/BDD
Analyte	Neomycin	Penicillin G	Norfloxacin
LDR (M)	$3.998 \times 10^{-6} - 1.59 \times 10^{-5}$	$3.99 \times 10^{-6} - 1.99 \times 10^{-5}$	$3.99 \times 10^{-6} - 2.99 \times 10^{-5}$
SWV Sensitivity	1.87×10^{-5} A/M	1.04×10^{-3} A/M	4.11×10^{-4} A/M
SWV LOD (M)	8.85×10^{-6}	9.62×10^{-6}	4.92×10^{-6}
EIS Sensitivity	1.22×10^8 Ω /M	2.19×10^{-3} F/M	1.2×10^{-3} F/M
EIS LOD (M)	5.83×10^{-6}	3.19×10^{-6}	3.69×10^{-6}

LDR (linear dynamic range), LOD (limit of detection)

From the CV studies for the antibiotic residues at bare BDD, PSF/BDD and PSF-GO/BDD, the obtained results made it possible to select which electrode material is suitable for detecting the appropriate analyte of interest. CV results for neomycin showed that PSF-GO/BDD electrode is the appropriate transducer material for the chemical sensor neomycin because it was evident that the PSF-GO/BDD showed high capacitance that BDD and PSF/BDD. Bare BDD electrode was selected as the electrode of choice for the detection of penicillin G because the oxidation peak of penicillin G was well defined and clear whereas it

was not the case when compared with PSF/BDD and PSF-GO/BDD electrode. Lastly PSF/BDD was selected as the electrode of choice for detecting norfloxacin.

The table above gives a summary of the obtained results of the three selected antibiotic residues at the selected electrode material of choice. All three selected antibiotic residues (norfloxacin, neomycin and penicillin G) showed catalytic traits at the selected electrode material of choice in SWV and EIS, because an increase in antibiotic residue concentration with increase in current, capacitance or charge transfer resistance was observed. From the concentration dependant studies bare BDD electrode showed to be the most sensitive transducer material when compared with PSF/BDD and PSF-GO/BDD transducer material because of the highest slope of the calibration curve for SWV. The PSF/BDD transducer material showed better response for quantitative detection of norfloxacin because of the higher linear dynamic range.



References

1. Reder-Christ K and Bendas G, Biosensor Applications in the Field of Antibiotic Research—A Review of Recent Developments, *Sensors* 11 (2011) 9450-9466
2. Nuria Sanvicens, Ilaria Mannelli, J.-Pablo Salvador, Enrique Valera, M.-Pilar Marco, Biosensors for pharmaceuticals based on novel technology, *Trends in Analytical Chemistry*, 30 (2011) 541-553
3. Barbosa T.M., Levy S.B., The impact of antibiotic use on resistance development and persistence, *Drug Resistance Updates* 3 (2000) 303–311
4. Ye Zhu, Jung Ik Son, Yoon-Bo Shim, Amplification strategy based on gold nanoparticle-decorated carbon nanotubes for neomycin immunosensors, *Biosensors and Bioelectronics* 26 (2010) 1002–1008
5. Wenjing Lian, Su Liu, Jinghua Yu, Jie Li, MinCui, WeiXu , Jiadong Huang, Electrochemical sensor using neomycin-imprinted film as recognition element based on chitosan-silver nanoparticles/graphene- multiwalled carbon nanotubes composites modified electrode, *Biosensors and Bioelectronics* 44 (2013) 70–76
6. Szaniszló B, Iuga Cristina, Bojiță M, Indirect Determination of Gentamicin by Derivative Spectrophotometry, *Acta Medica Marisiensis (AMM)*, 57 (2011) 516-518
7. Gonçalves Luís Moreira, Welder F.A. Callera, Maria D.P.T. Sotomayor, Paulo R. Bueno, Penicillinase-based amperometric biosensor for penicillin G, *Electrochemistry Communications* 38 (2014) 131–133
8. Švorc Lubomír, Jozef Sochr, Miroslav Rievaj, Peter Tomčík, Dušan Bustin, Voltammetric determination of penicillin V in pharmaceutical formulations and human urine using a boron-doped diamond electrode, *Bioelectrochemistry* 88 (2012) 36–41
9. Vasim Ahmed, Jitendra Kumar, Manoj Kumar, Manu Bhambi Chauhan, Pushpa Dahiya & Nar Singh Chauhan, Functionalised iron nanoparticle–penicillin G conjugates: a novel strategy to combat the rapid emergence of β -lactamase resistance among infectious micro-organism, *Journal of Experimental Nanoscience*, 10 (2015) 718-728
10. Rajendra N. Goyal, Anoop Raj Singh Rana, Himanshu Chasta, Electrochemical sensor for the sensitive determination of norfloxacin in human urine and pharmaceuticals, *Bioelectrochemistry* 83 (2012) 46–51

11. Madalina M. Barsan, Edilson M. Pinto, Christopher M.A. Brett, Electrosynthesis and electrochemical characterisation of phenazine polymers for application in biosensors, *Electrochimica Acta* 53 (2008) 3973–3982
12. Ionescu R.E., Jaffrezic-Renault N., Bouffier L., Gondran C., Cosnier S., Pinacho D.G., Marco M.-P., Sánchez-Baeza F.J., Healy T., Martelet C., Impedimetric immunosensor for the specific label free detection of ciprofloxacin antibiotic. *Biosens. Bioelectron.*, 23 (2007) 549-555.
13. Samuel S´anchez , Martin Pumera , Esteve F`abregas, Carbon nanotube/polysulfone screen-printed electrochemical immunosensor, *Biosensors and Bioelectronics* 23 (2007) 332–340
14. Martos A.M., J-Y. Sanchez, A. V´arez, B. Levenfeld. Electrochemical and structural characterization of sulfonated polysulfone. *Polymer Testing*, 45 (2015) 185–193
15. Inamullaha, Sunil Singh, Surabhi Sharma, Ajit Ku. Yadav, Hemendar Gautam, Estimation of norfloxacin in tablet dosage form by using UV-Vis spectrophotometer, *Der Pharmacia Lettre*, , 4 (2012) 1837-1842
16. da Silva H´elder, Jo˜ao Pacheco, Joana Silva, Subramanian Viswanathan, Cristina Delerue-Matos, Molecularly imprinted sensor for voltammetric detection of norfloxacin, *Sensors and Actuators B*, 219 (2015) 301–307
17. Manoj Devaraj, Ranjith Kumar Deivasigamani, Santhanalakshmi Jeyadevan, Enhancement of the electrochemical behavior of CuO nanoleaves on MWCNTs/GC composite film modified electrode for determination of norfloxacin, *Colloids and Surfaces B: Biointerfaces* 102 (2013) 554– 561
18. Ke-Jing Huang, Xue Liu, Wan-Zhen Xie, Hong-Xia Yuan, Electrochemical behavior and voltammetric determination of norfloxacin at glassy carbon electrode modified with multi walled carbon nanotubes/Nafion, *Colloids and Surfaces B: Biointerfaces* 64 (2008) 269–274
19. Chen Bi, Ming Ma, Xiaoli Su, An amperometric penicillin biosensor with enhanced sensitivity based on co-immobilization of carbon nanotubes, hematein, and β -lactamase on glassy carbon electrode, *Analytica Chimica Acta*, 674 (2010) 89–95
20. Friederike J. Gruhl & Kerstin Lange, Surface Acoustic Wave (SAW) Biosensor for Rapid and Label-Free Detection of Penicillin G in Milk, *Food Anal. Methods* (2014) 7:430–437

21. WHO (World Health Organization). 2012. Pharmaceuticals in Drinking-Water. Geneva: WHO. Available: http://www.who.int/water_sanitation_health/publications/2012/pharmaceuticals/en/
22. World Health Organization. (2011). Pharmaceuticals in drinking water.
23. Siyabulela Hamnca, Lisebo Phelane, Emmanuel Iwuoha and Priscilla Baker, Electrochemical detection of neomycin and norfloxacin, Analytical Letters (accepted for publication) 2016



CHAPTER VIII

APPLICATION OF THE PREPARED SENSORS

This chapter investigates the application of the electrode material to real samples such as tap water sample and synthetic urine. The recovery and interference studies were done for all 3 antibiotic residues using tap water samples taken from the municipality tap and the synthetic urine was used for interference investigation. This was done to determine the selectivity of the BDD, PSF/BDD and PSF-GO/BDD electrode as well as the ability of the sensor material to detect antibiotic residues in water matrix

8.1. Recovery studies

The application of the prepared sensor for the detection of the three selected antibiotics in real samples was investigated. Tap water from the municipal supply was used as the real sample. The tap water (5 mL) was spiked with the antibiotic (1 mL), the same method developed for each antibiotic was used for all three antibiotics. The same volume of the tap samples was spiked with all three antibiotics and formed a mixed solution. The water samples were not pretreated but used directly from the tap water. The prepared water samples were stored in the refrigerator.

8.1.1 Analysis of spiked neomycin samples

The standard solution of neomycin was spiked into the tap water sample this was named as sample 1 and for sample 2 the tap water was spiked with 1 mL of each antibiotic (neomycin, penicillin G and norfloxacin) to produce a mixed sample. The final concentration sample 1 was 1.7 mM, from the stock solution of 0.01 M neomycin was diluted with municipal tap water matrix. Boron doped diamond electrode was modified with PSF-GO to be used as the sensor material for the real sample analysis. About 5 mL of 0.1 M PBS pH 7.0 was placed in an electrochemical cell and different concentration of sample 1 was added into the cell and SWV was measured.

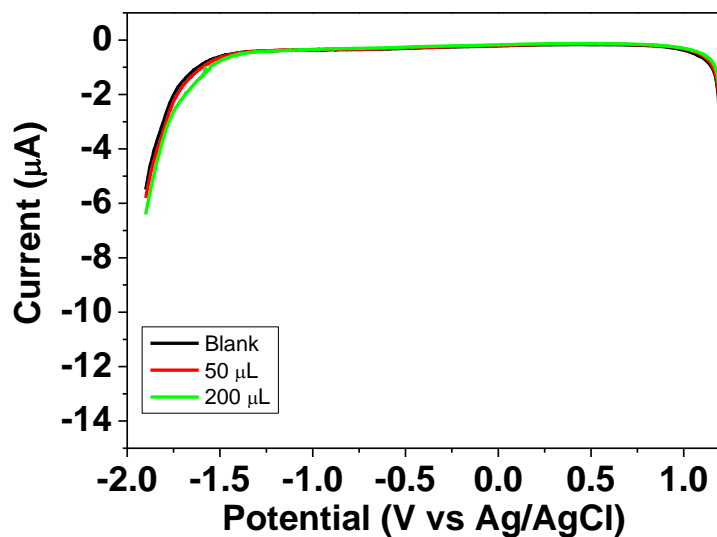


Figure 8.1a: SWV response of tap water sample spiked in 0.1 M PBS pH 7.0

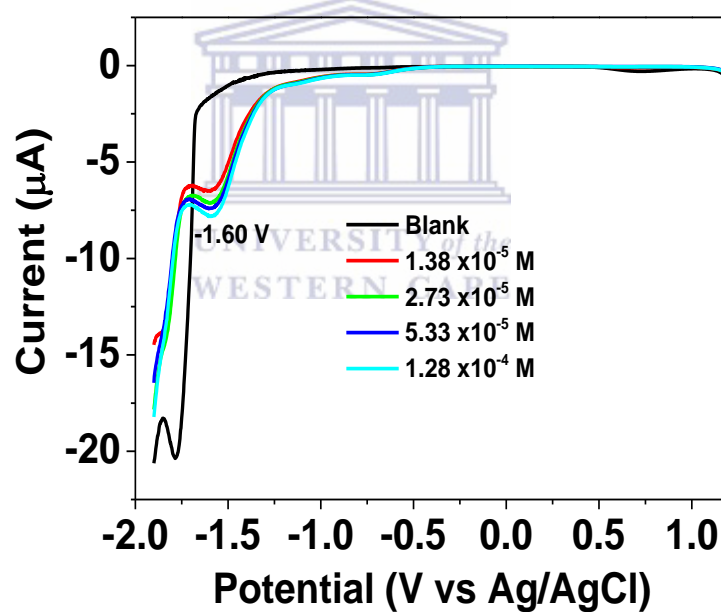


Figure 8.1b: SWV response of sample 1 (neomycin + tap water sample) spiked in 0.1 M PBS pH 7.0

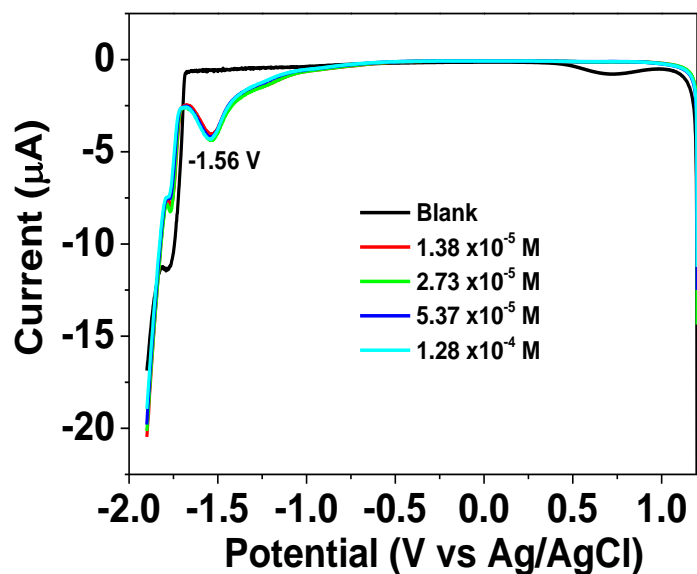


Figure 8.1c: SWV response of sample 2 spiked in 0.1 M PBS pH 7.0.

Figure 8.1a, is the SWV response of spiked tap samples at PSF-GO/BDD electrode which showed no electrochemical response towards the transducer. Sample 1 response showed the neomycin signature which is the reduction peak at -1.6 V. The presence of water in the sample did not show any interfere (Figure 8.1b). SWV response of the mixed sample (Figure 8.1c) also showed a reduction peak at a shifted potential as from figure 8.1b.

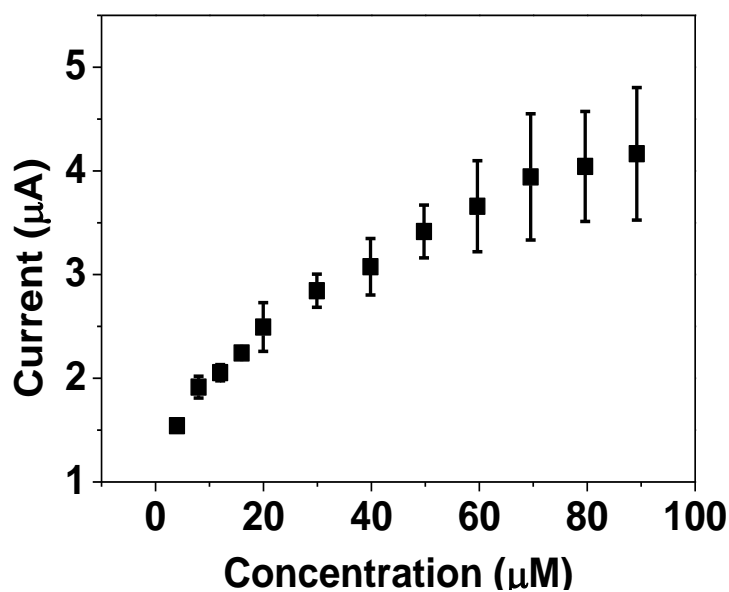


Figure 8.2: Calibration curve of neomycin

Table 8.1: Recovery % of neomycin at PSF-GO/BDDE

Sample	Recovery %
1 (Tap water + Neomycin)	92.5
2 (Tap water, Neomycin, Norfloxacin and Penicillin G)	104

In order to evaluate the validity of PSF-GO/BDDE sensor for the determination of neomycin real tap water samples were spiked with neomycin and measured by SWV. The analyses were carried out using SWV with optimised parameters same as those used for the determination of neomycin at PSF-GO/BDD electrode, and the obtained results were presented (Figure 8.1b) for tap water spiked with neomycin (Figure 8.1c) tap water spiked with three antibiotics (sample 2). The PSF-GO/BDD sensor presented recoveries between 92.5 for sample 1 and 104 % for sample of neomycin from the prepared samples. The voltammograms in Figure 8.1 clearly shows that the peak current increases with increasing concentrations of the prepared tap water sample for the peak at -1.6 V thereby confirming that it corresponds to the reduction of neomycin. Figure 8.2 is the calibration curve plot of neomycin at PSF-GO modified boron doped diamond electrode. The calibration was used to calculate the recovery percentages of the prepared tap water samples.

8.1.2 Analysis of spiked norfloxacin samples

The standard solution of norfloxacin was spiked into the tap water sample this was named as sample 3 and sample 2 is the mixed tap water sample with all three antibiotics (neomycin, penicillin G and norfloxacin). About 5 mL of 0.1 M HCl was used as the electrolyte and spiked with sample 3 and sample 2. Boron doped diamond electrode was modified with PSF to be used as the sensor material for the real sample analysis

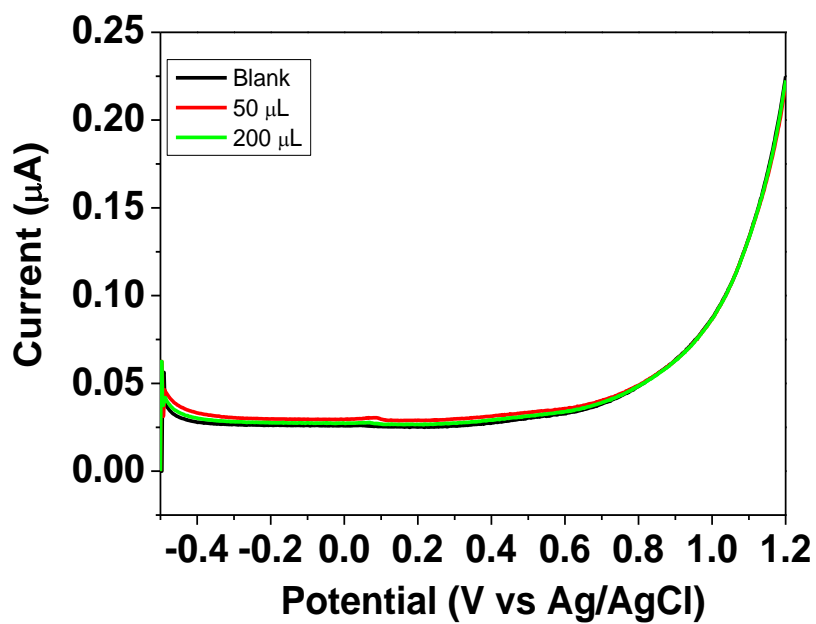


Figure 8.3a: SWV response of tap water sample spiked in 0.1 M HCl

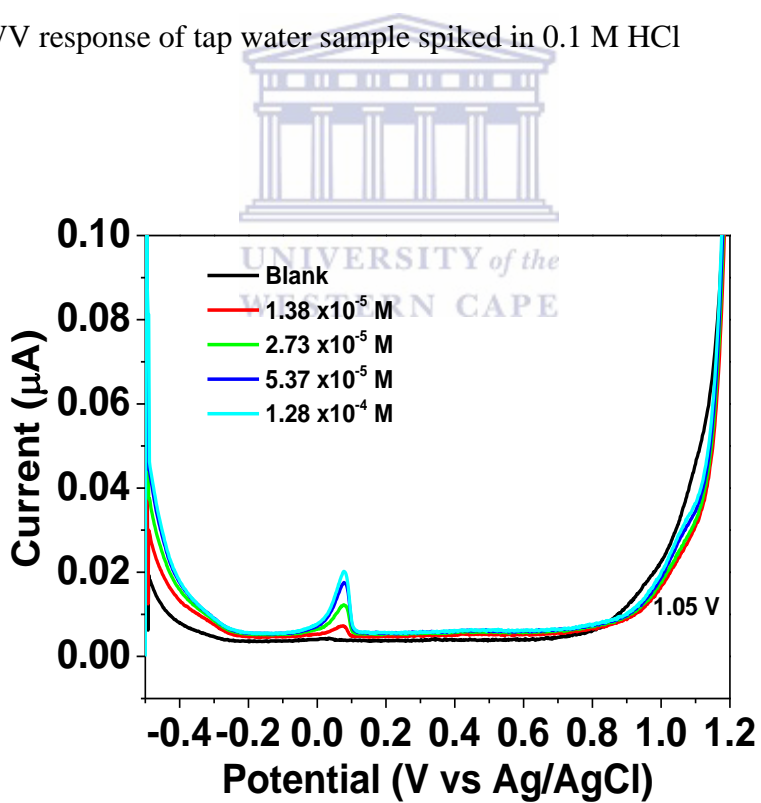


Figure 8.3b: SWV response of sample 3 (norfloxacin + tap water) spiked in 0.1 M HCl

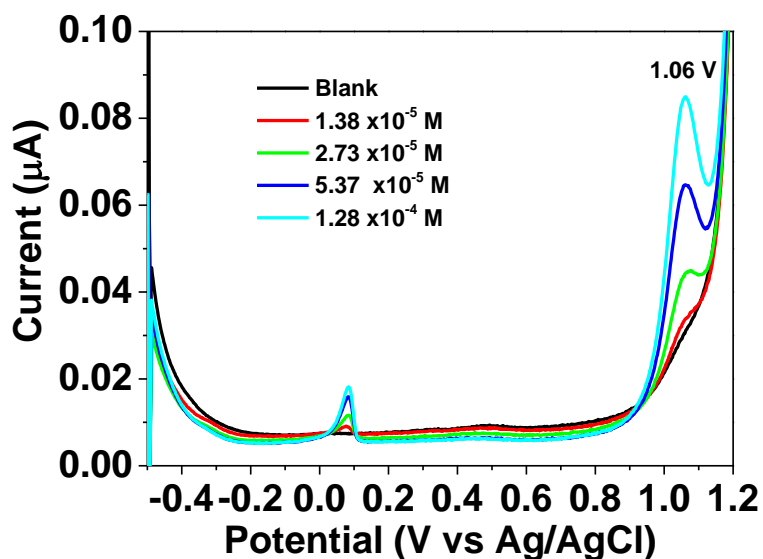


Figure 8.3c: SWV response of sample 2 spiked in 0.1 M HCl

The above voltammograms showed the SWV response of the prepared sensor when spiked with tap water sample (Figure 8.3a), sample 3 was also spiked at the unmodified PSF/BDD electrode and response presented (Figure 8.3b). The norfloxacin peak at 1.05 V is not well defined in Figure 8.3b where the mixture of all three antibiotics the peak is clear and well defined.

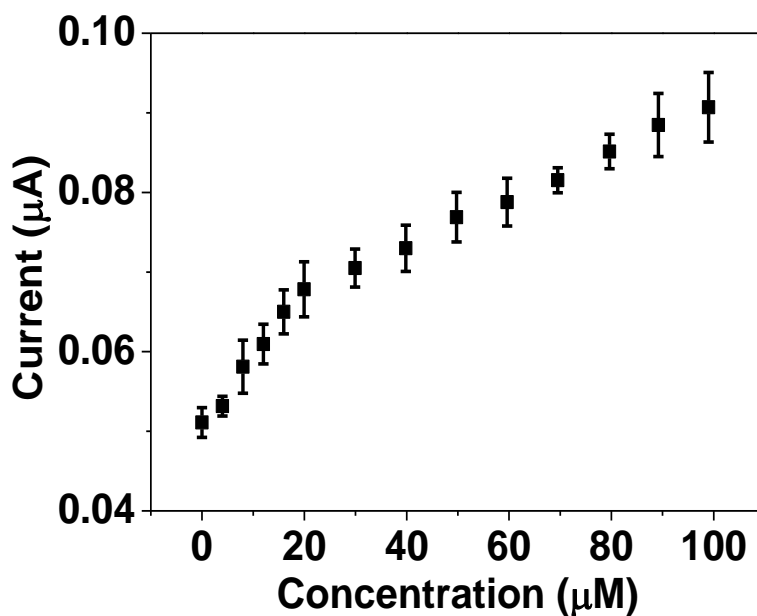
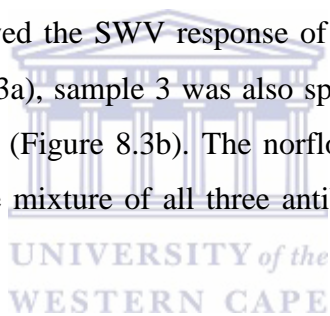


Figure 8.4: Calibration curve of norfloxacin at unmodified PSF/BDDE

Table 8.2: Recovery % of norfloxacin at PSF/BDDE

Sample	Recovery %
3 (Tap water + Norfloxacin)	75.59
2 (Tap water, Neomycin, Norfloxacin and Penicillin G)	72.58
	90.96

The application of the prepared sensor material for detecting norfloxacin in real samples was investigated. The analyses were carried out using SWV with optimised parameters same as those used for the determination of norfloxacin at unmodified PSF/BDD electrode, and the obtained results were presented in Figure 8.3b for tap water spiked with NOR and Figure 8.3c, tap water spiked with three antibiotics [1]. The PSF/BDD sensor presented recoveries between 75.59 for sample 3 and sample 2 both the peak one at 0.04 and 1.05 V vs. Ag/AgCl were used for recovery studies. The obtained percentage was 72.58 and 90.8% for sample 2. The voltammograms in Figure 8.4 clearly showed that the peak current increases with increasing concentrations of the prepared tap water sample for the peaks presented thereby confirming that it corresponds to the oxidation of NOR. Figure 8.4 is the calibration curve plot of norfloxacin at PSF modified boron doped diamond electrode. The calibration was used to calculate the recovery percentages of the prepared tap water samples

8.1.3 Analysis of spiked penicillin G samples

The standard solution of penicillin G was spiked into the tap water sample, this was referred to as sample 4. Sample 2 was the tap water spiked with 1 mL of each antibiotic (neomycin, penicillin G and norfloxacin). About 5 mL of 0.1 PBS was used as the electrolyte and spiked with sample 4 and sample 2. Bare boron doped diamond electrode was used as the sensor material for the real sample analysis

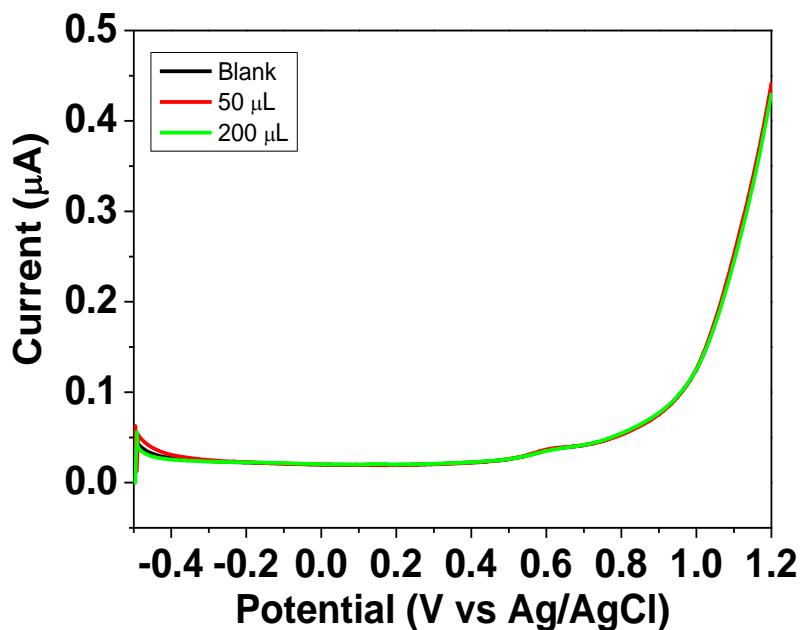


Figure 8.5a: SWV response of tap water sample in 0.1 M PBS pH 7.0

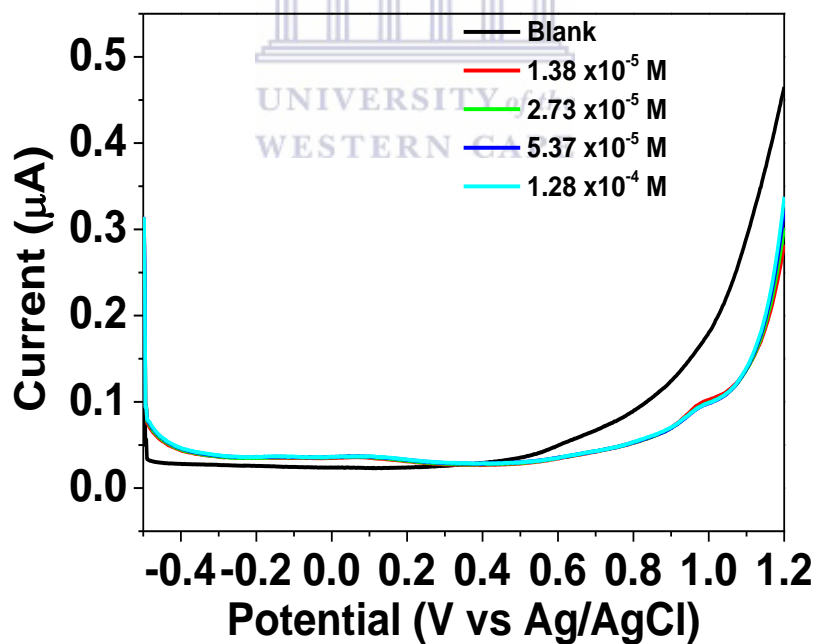


Figure 8.5b: SWV response of sample 4 (tap water + penicillin G) spiked in 0.1 M PBS pH 7.0

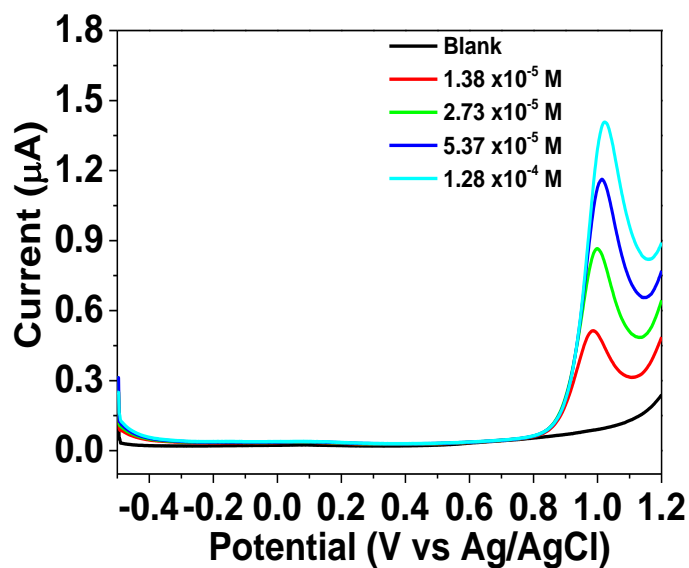


Figure 8.5c: SWV response of sample 2 spiked in 0.1 M PBS pH 7.0

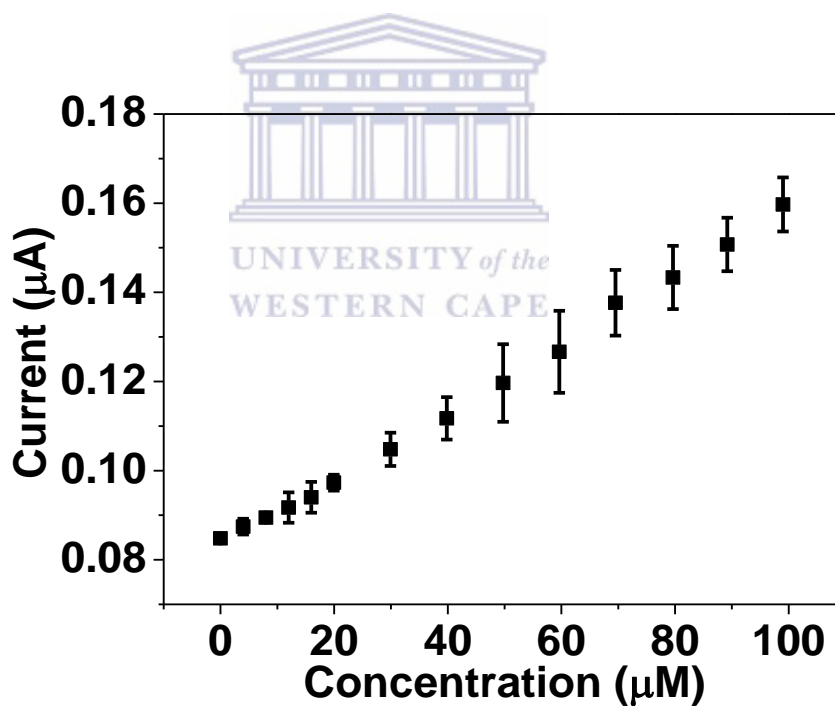


Figure 8.6: Calibration curve of penicillin G

The real sample analysis studies for penicillin G were inconclusive because the penicillin G was not recovered from the water sample. Penicillin G is susceptible to degradation because of the unstable β -lactam ring and thus it was not possible to recover it from the tap water samples. Literature reports that penicillin G and other β -lactam antibiotics have not been

detected in environmental samples, reason being the chemically unstable β -lactam ring due to its high sensitivity to pH, heat and β -lactamase enzymes [2].

8.2. INTERFERENCE STUDIES

The influence of some foreign species on the determination of the selected antibiotic residues was evaluated in detail. Expressly, some species possibly exist in biological sample. Synthetic urine was prepared according to Lee et.al [3], method. A fixed amount of the urine was used as the electrolyte and the antibiotic residue was spiked into the urine sample and SWV was used. The three different electrode materials were used for the appropriate antibiotic residue. For interference studies synthetic urine was prepared dissolving the following chemicals in dH₂O such as uric acid, ascorbic acid, citric acid, urea, KCl, NaOH and sulphuric acid. The synthetic urine was used as the electrolyte (5 mL) and the antibiotic residues were added and SWV measurements were carried out.

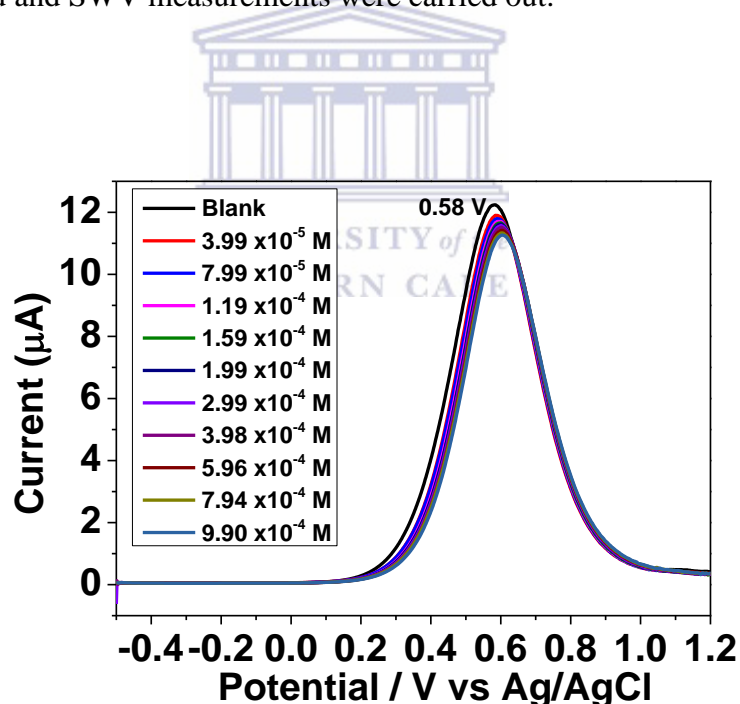


Figure 8.7: SWV response of urine sample spiked with penicillin G at bare BDD electrode

The influence of interfering compounds commonly existing in pharmaceutical formulations and human urine was also examined by SWV under the same experimental conditions. The urine sample was synthetic and stored in the refrigerator. The interference study was realized by addition of penicillin G into the urine sample, which was used as the electrolyte [4].

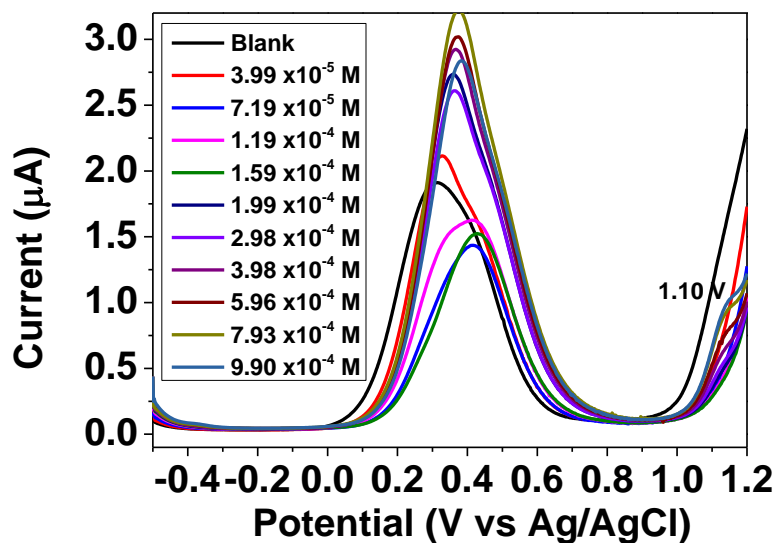


Figure 8.8: SWV response of urine sample spiked with norfloxacin at PSF/BDD electrode

Selectivity is an important parameter for the performance evaluation of a sensor or biosensors, as it gives the particular affinity for observing specific target ions in the presence of other interfering ions. The selectivity of any biosensor can be evaluated in the presence of interfering ions [5]. The selected interferents undergo oxidation below 1.0V, hence, they did not show any response in the NOR potential. The results showed that the presence uric acid, citric acid, urea, creatinine, K^+ , Na^+ , Cl^- had no interference on the current response of NOR. This suggested that the proposed method had good selectivity for the determination of NOR. From Figure 8.8, it can be seen that upon mixing all interfering components with the NOR solution, no changes on the current response was observed.

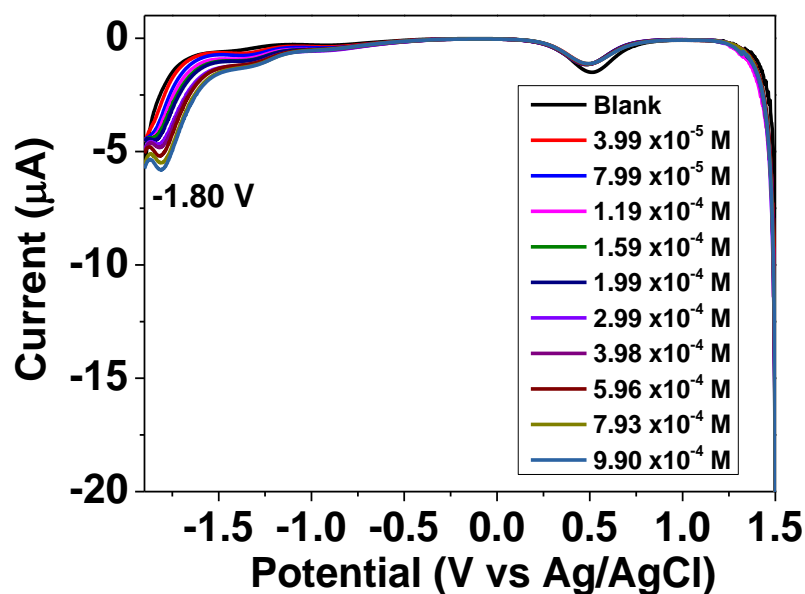


Figure 8.9: SWV response of urine sample spiked with Neomycin at PSF-GO/BDD electrode

The interference of urea, ascorbic acid, citric acid, urea, KCl, NaOH and other compounds that are used in preparing synthetic urine were used to examine the selectivity of the designed sensor. The current response of these substrates to neomycin sensor was shown in Figure 8.9. The results showed that these metabolites do not interfere with determination of Neo as they do not undergo reduction at -1.6 V vs. Ag/AgCl.

The analysis of antibiotics in tap water samples is challenging due to the high complexity of the water matrix. Analyzing analytes in municipality water requires optimal sampling, processing, and treatment which include digestion and filtration to remove all contaminants. In study water samples were taken directly from municipality tap water without any treatment, the samples were used as they were received. Tap water still contains some contaminants that are not removed during water treatment process. This explains the challenges fraught when evaluating the recovery evaluation in tap water sample. Hence, the inconsistency in the recovery results for penicillin G from tap water. Interferences can change or result in an unclear analytical signal by reacting with the analyte of interest or blocking the surface of working electrode. This action can lead to the analytical peak being suppressed when compared with the peak obtained in the absence of the interfering species. These challenges stated need some exploration and thorough investigation on the sensor application so that a clear understanding of how can these challenges can be overcome and solved in the

laboratory. Analytical techniques such as HPLC and UV-Vis can be used to investigate the elements or compounds that are present in the tap water sample matrix before and after performing any experiments with the analyte of interest. The same can be done investigating what happens to the antibiotic after being oxidized or reduced in the presence of the interfering species. Using these techniques we will be able to report whether the antibiotics forms complexes whether with the interfering species from the synthetic urine or from the tap water sample.

Studies focusing on pH dependence also need to be investigated for both synthetic urine and tap water sample matrix because no pre-treatment was performed before using them. The electrochemical response might be affected by supporting electrolyte and the solution pH. A study was performed looking at different electrolytes that can give an electrochemical response for norfloxacin, such as phosphate buffer, Britton-Robinson, acetate buffer, ammonium-hydrochloric buffer, H_2SO_4 and HCl were investigated and the best response was observed in H_2SO_4 solution. The pH of the electrolyte was also investigated in different pH of H_2SO_4 solution from 1.20 to 2.56. It was reported that the peak currents decreased and peak potentials shifted negatively by increasing of solution pH, meaning that the electrode reaction of norfloxacin oxidation was a losing proton process [6]. This study lacked pH dependence studies so that we can know which pH works better for which antibiotic residue.

8.3. Conclusion

The application of the three developed sensors in real samples was investigated by the detection of norfloxacin, neomycin and penicillin G in spiked water and synthetic urine samples. The results showed that the sensor was able to recognise norfloxacin and neomycin molecules respectively. The recovery% obtained for norfloxacin and neomycin were satisfactory (92.5% and 75.5%). The selectivity of the sensor was successfully demonstrated by matching the electrode material selected for a range of prepared materials were able to detect the selected antibiotic residue at the particular electrode material. The recovery and the interferences studies for penicillin G was inconsistent and results were inconclusive.

References

1. Ke-Jing Huang, Xue Liu, Wan-Zhen Xie, Hong-Xia Yuan, Electrochemical behavior and voltammetric determination of norfloxacin at glassy carbon electrode modified with multi walled carbon nanotubes/Nafion, *Colloids and Surfaces B: Biointerfaces* 64 (2008) 269–274
2. Dong Li, Min Yang, Jianying Hu, Yu Zhang, Hong Chang, Fen Jin, Determination of penicillin G and its degradation products in a penicillin production wastewater treatment plant and the receiving river, *Water Research*, 42 (2008) 307–317
3. Seung-Youl Lee, Eunjung Son, Jin-Young Kang, Hee-Seok Lee, Min-Ki Shin, Hye-Seon Nam, Sang-Yub Kim, Young-Mi Jang, and Gyu-Seek Rhee, Development of a Quantitative Analytical Method for Determining the Concentration of Human Urinary Paraben by LC-MS/MS, *Bull. Korean Chem. Soc.*, 34 (2013) 1131-1136
4. Švorc Lubomír, Jozef Sochr, Miroslav Rievaj, Peter Tomčík, Dušan Bustin, Voltammetric determination of penicillin V in pharmaceutical formulations and human urine using a boron-doped diamond electrode, *Bioelectrochemistry* 88 (2012) 36–41
5. Bharati Agrawal, Pranjal Chandra, Rajendra N.Goyal, Yoon-Bo Shim, Detection of norfloxacin and monitoring its effect on caffeine catabolism in urine samples, *Biosensors and Bioelectronics* 47(2013) 307–312
6. Zhuo Ye, Le Wang, Jianguo Wen, A simple and sensitive method for determination of Norfloxacin in pharmaceutical preparations, *Brazilian Journal of Pharmaceutical Sciences*, 51 (2015) 429-437

CHAPTER IX

CONCLUSION AND RECOMMENDATIONS

This chapter gives the overall conclusion of the study and recommendations of possible research in the future.

9.1. Conclusion

For the very first time here we report on polysulfone (PSF) and graphene oxide (GO) modified boron doped diamond (BDD) electrode based electrochemical sensor for detecting antibiotic residues in environmental water systems. Properties of PSF include high thermal, chemical and mechanical resistance. These properties make PSF attractive for application in membrane technology because they can withstand harsh environmental conditions. However, in electrochemical applications, the major drawback of this polymer is their hydrophilic and electrochemically non-conductive nature. The development of polysulfone based electrochemical sensor was motivated by the enhanced electrochemical performance observed for novel metal nanoparticle modified polysulfone, developed in our laboratory for the first time. Ground breaking research focusing on the use of polysulfone to detect antibiotics in water systems was developed in this dissertation. New technology is urgently needed for the detection and removal or degradation of antibiotics from environmental and municipal water systems. Increasingly we are faced with the threat of drug resistant bacterial strains which thrive in water systems with ever increasing antibiotic loading. The availability of antibiotics in the natural water systems allows the bacteria to mutate and develop resistant strains that subsequently return to infect humans and animals in an ever strengthening vicious cycle. We believe that early detection and quantification of classes and individual antibiotic species will provide the first line of defence by signalling the alarm for elevated antibiotic presence and providing baseline information to inform the development of genetic interventions.

The low electrochemical conductivity of polysulfone limits its use in electrochemistry, hence the modification of PSF with GO to improve the conductivity. Graphene oxide (GO) is considered a smart material because of its small size i.e. 10^{-9} m (nanometer range). Properties of graphene oxide include good water dispersibility, biocompatibility and high affinity for

specific biomolecules. Electrochemical sensors focusing on the use of GO have been reported in literature, but for the first time here we reported on polysulfone modified with graphene oxide at BDD electrode based chemical sensor for evaluating antibiotic residues. Modifying PSF with GO resulted in improved hydrophilicity of PSF which is confirmed by the decreased drop shape measurement for PSF, this is due to functional groups of GO containing hydrophilic oxygen. Additionally, electrochemical response of PSF was also improved based on the higher diffusion coefficient calculated for PSF-GO/BDD electrode.

Electrochemical sensors reported LOD of 3.19×10^{-6} , 3.69×10^{-6} and 5.83×10^{-6} M respectively for penicillin G, norfloxacin and neomycin. These values were comparable to other chemical sensors from literature. These LODs demonstrates that SWV and EIS are suitable techniques to measure and quantify antibiotic residues. Over several decades, chromatographic, colorimetric and immunoassay based methods for determining antibiotics in environmental systems and also in edible cattle have been used successfully. Their drawbacks involve long operation time and require skilled personnel for operation limit their use as detection methods. Biosensor and sensors offers real time measurement, requires less time for preparation and analysis, lastly they offer improved sensitivity. Chemical sensors developed in this study offered high reproducibility, selectivity, ease of materials preparation and lastly cost effective because no biomolecule was used. However, future work to produce polysulfone materials derivatized by polymers and other nanomaterials will offer even greater potential for detection of a wide range of antibiotic residues in water systems in support of the work started here. These developments could lead to greater sensitivity and wider detection of this broad range of pollutants, thereby reducing long term spread and cost of treatment for antibiotic resistant infections. Improved conductivity of PSF will result in antibiotic detection at much lower levels. Transducer materials (PSF/BDD, PSF-GO/BDD and bare BDD electrode) were highly selective for each antibiotic residue at the specific transducer electrode because no overlapping of peaks were observed when all three antibiotic residues were mixed together in tap water and also from interfering species in the synthetic urine matrix.

In conclusion, the novel transducers and electrochemical methods used for detecting these antibiotics constitutes a major contribution to new knowledge and creates the awareness that the use polysulfone cannot be limited to membrane technology only but can be applied as electrochemical sensor and biosensor transducers. Further development of polysulfone

derived nanomaterials can produce an arsenal of electrochemical weapons to be used in the war against antibiotic resistance, by identifying and quantifying antibiotic species in environmental and municipal water systems in future to improve the sensor performance of polysulfone so that very low concentrations of antibiotic residues can be detected with ease.



9.2. Future Recommendations

- It is known that penicillin G is not stable and susceptible to degradation. The electrochemical oxidation of β -lactam antibiotics occurs at highly positive potential which makes other working electrodes not suitable for sensor development of penicillin detection. However, BDD electrode proved to be a suitable electrode to be used to evaluate the electrochemical oxidation of penicillins. New electrodes are needed that will offer a wide potential window at high potentials that will be able to show the oxidation of penicillins.
- The other challenge was the use of polysulfone polymer, the polymer is mainly used in membrane filtration and also in energy but as a sensor material it is difficult to get good conductivity. We have demonstrated that GO (a highly conductive material) can be easily incorporated into PSF matrix to stabilise and improve electrochemical performance of the nanocomposite transducers. However the development of alternative nanocomposite based on incorporation of metal nanoparticle, MWCNT or a second hydrophilic polymer may yield the required nanocomposite transducers for effective antibiotic screening and quantification.
- There is a need for electrochemical sensors which will focus on the determination of antibiotic residues because the literature is limited and most of the literature studies are based on biosensors. There is very little literature on the electrochemical detection of aminoglycosides, more research studies are needed that will focus on the detection of aminoglycosides can be either biosensors or chemical sensors. Chemical sensors are more robust and do not require the special chemical pretreatment to stabilise the biomolecule in biosensors.

APPENDIX

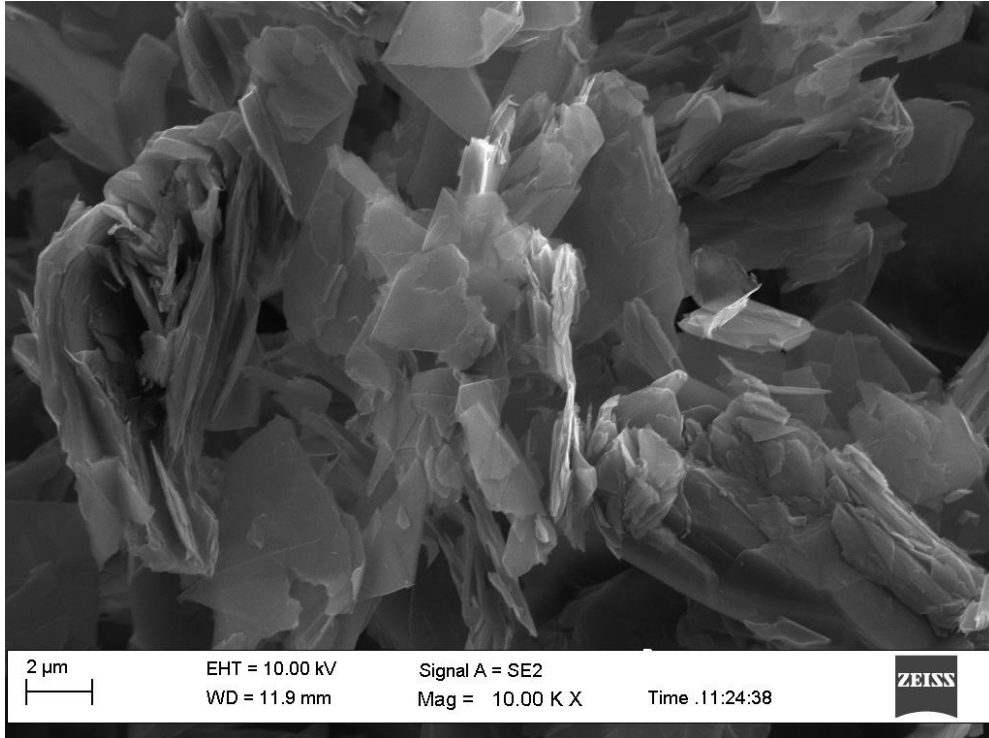


Figure A1: SEM image of graphite

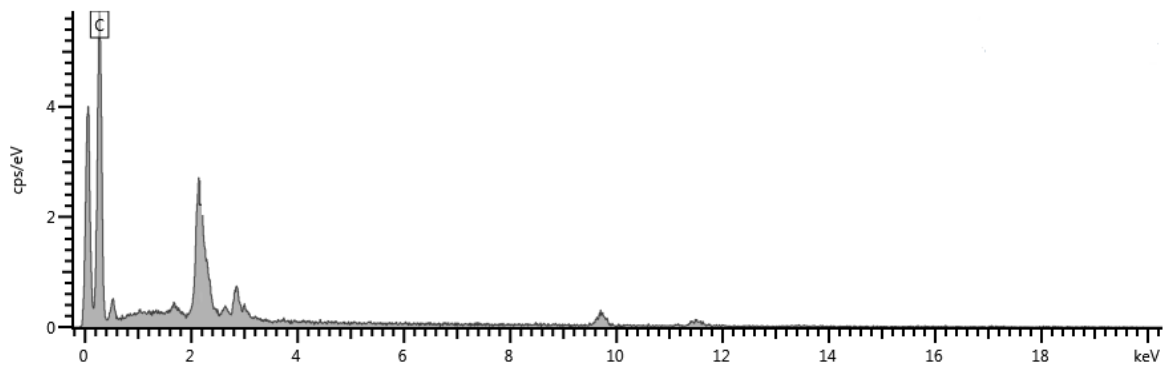


Figure A2: EDS spectra of graphite

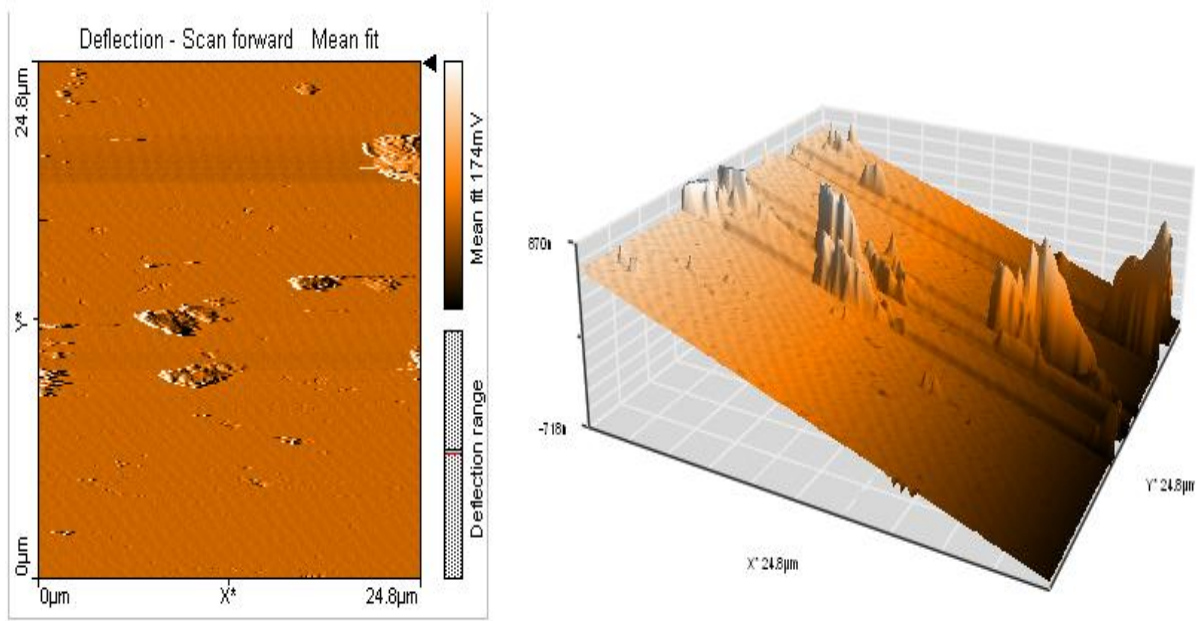


Figure A3: AFM image of graphite

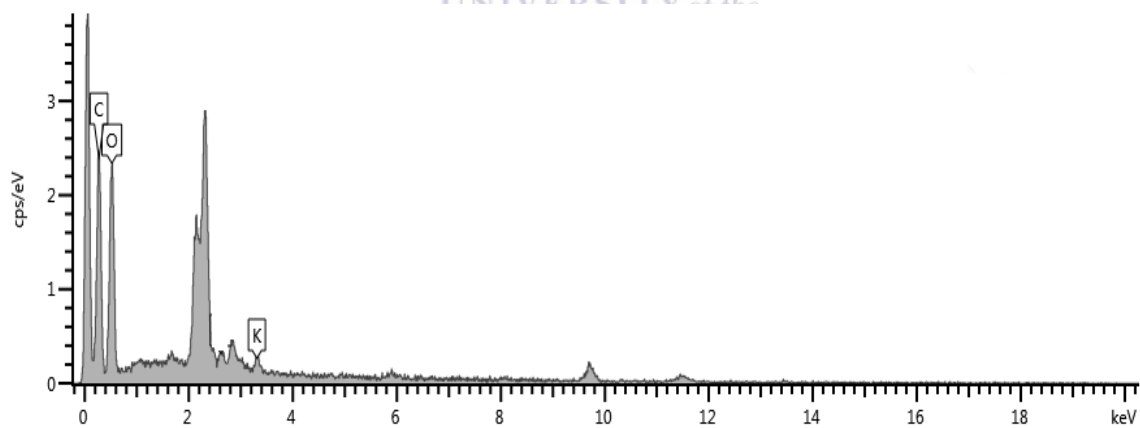


Figure A4: EDS spectrum of graphene oxide

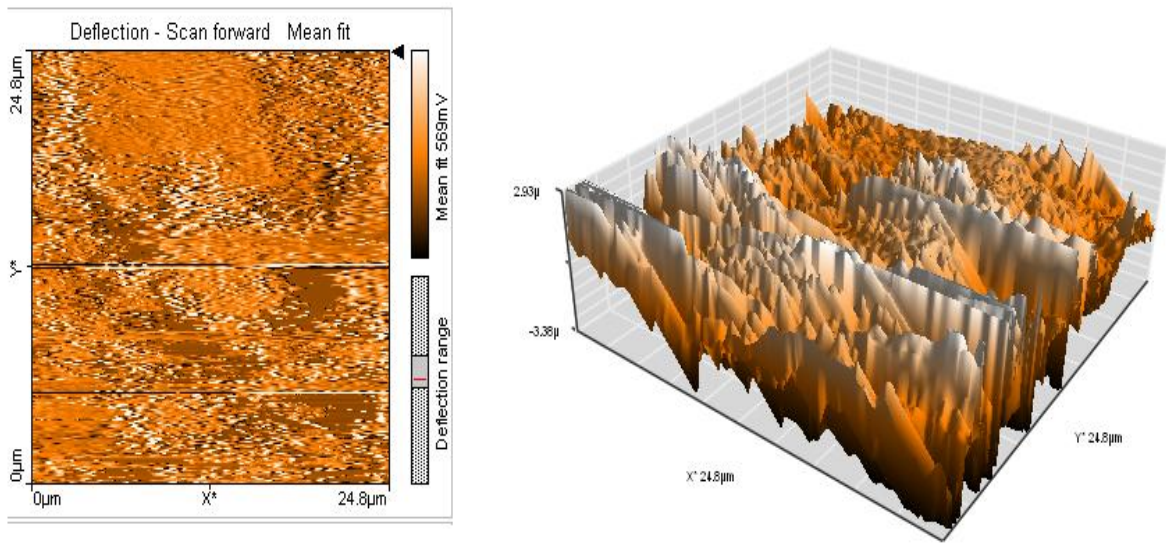


Figure A5: AFM image of graphene oxide

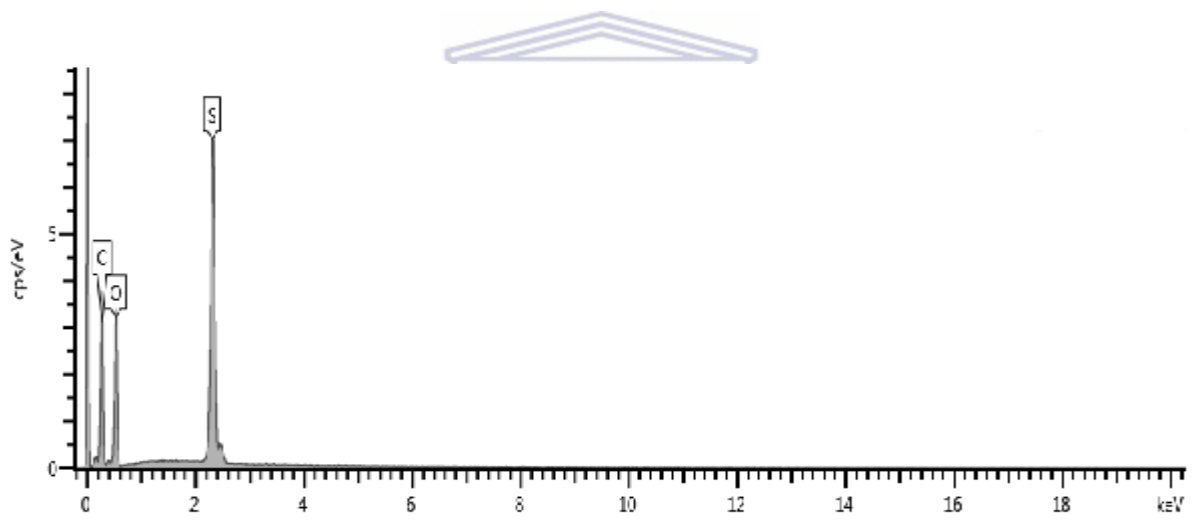


Figure A6: EDS spectrum of polysulfone

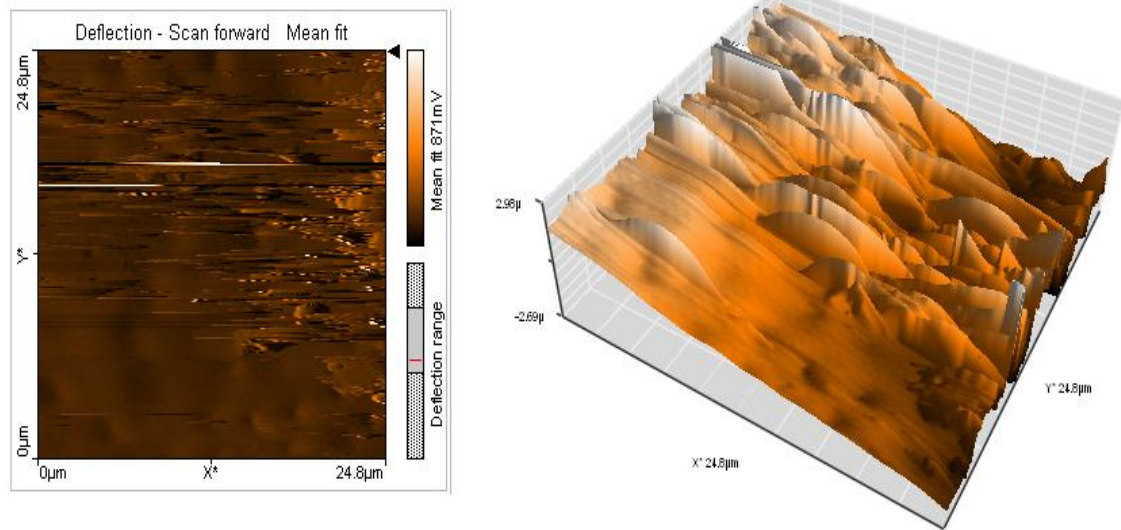


Figure A7: AFM image of polysulfone in DMAc

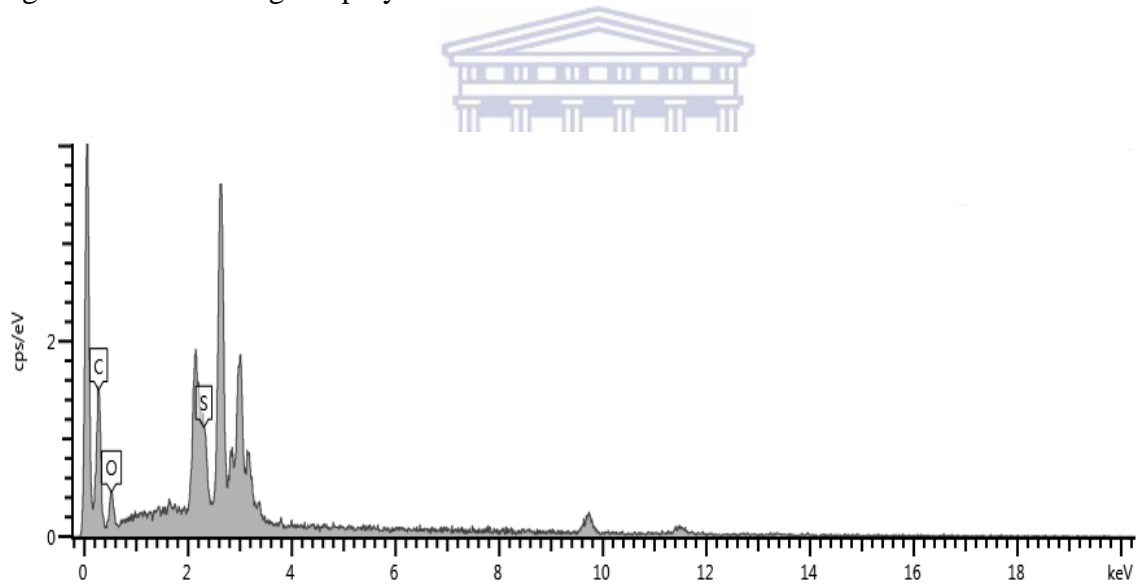


Figure A8: EDS spectrum of polysulfone with graphene oxide

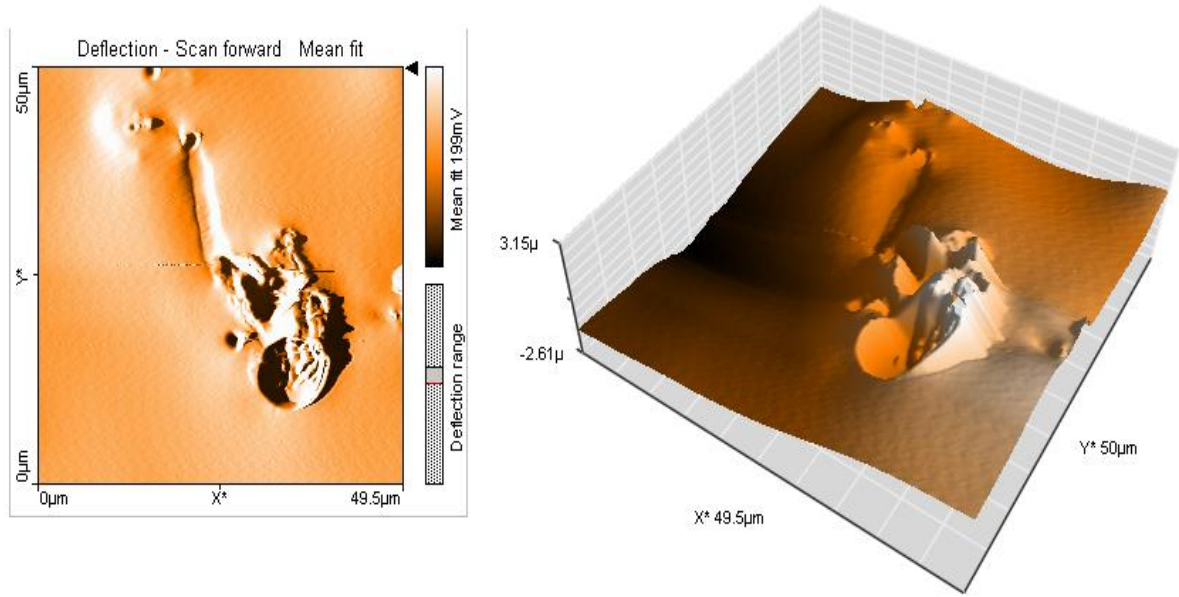


Figure A9: AFM image of polysulfone with graphene oxide in DMAc

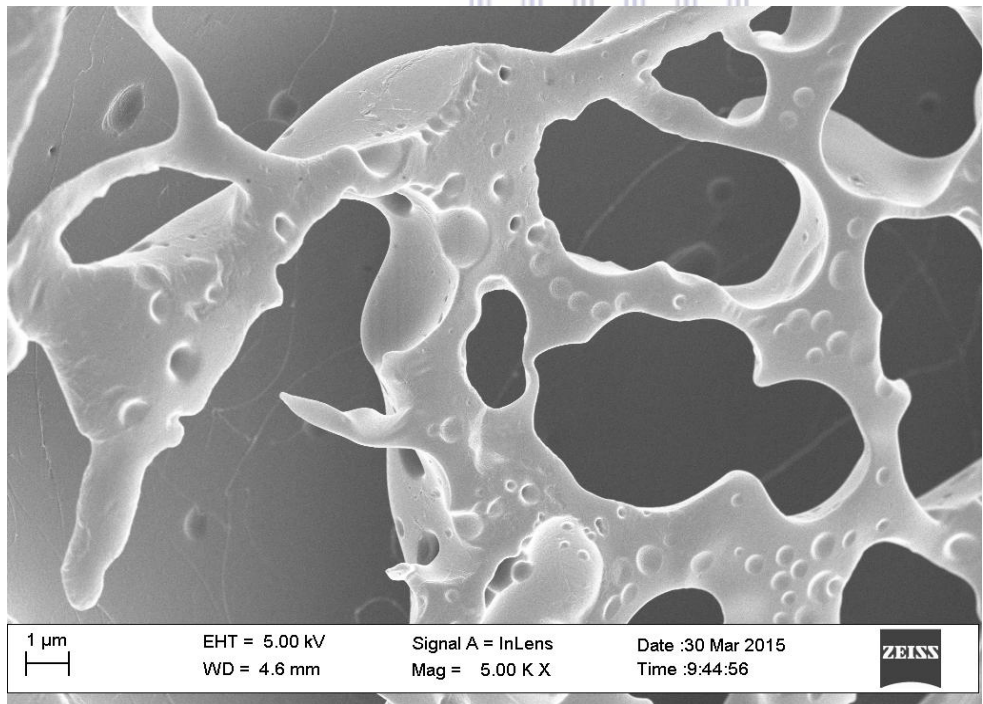


Figure A10: SEM image of polysulfone dissolved in DCM

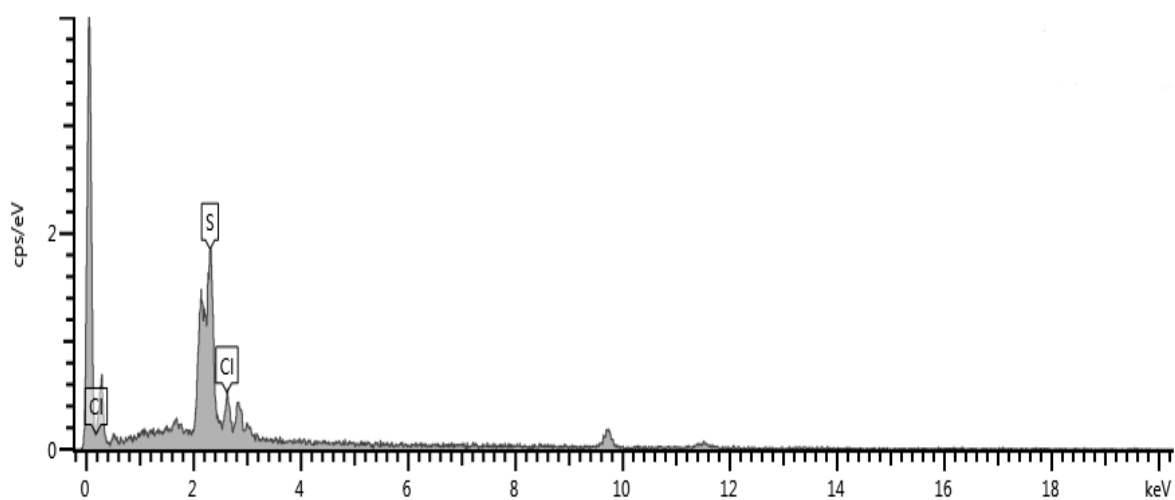


Figure A11: EDS spectrum of polysulfone dissolved in DCM

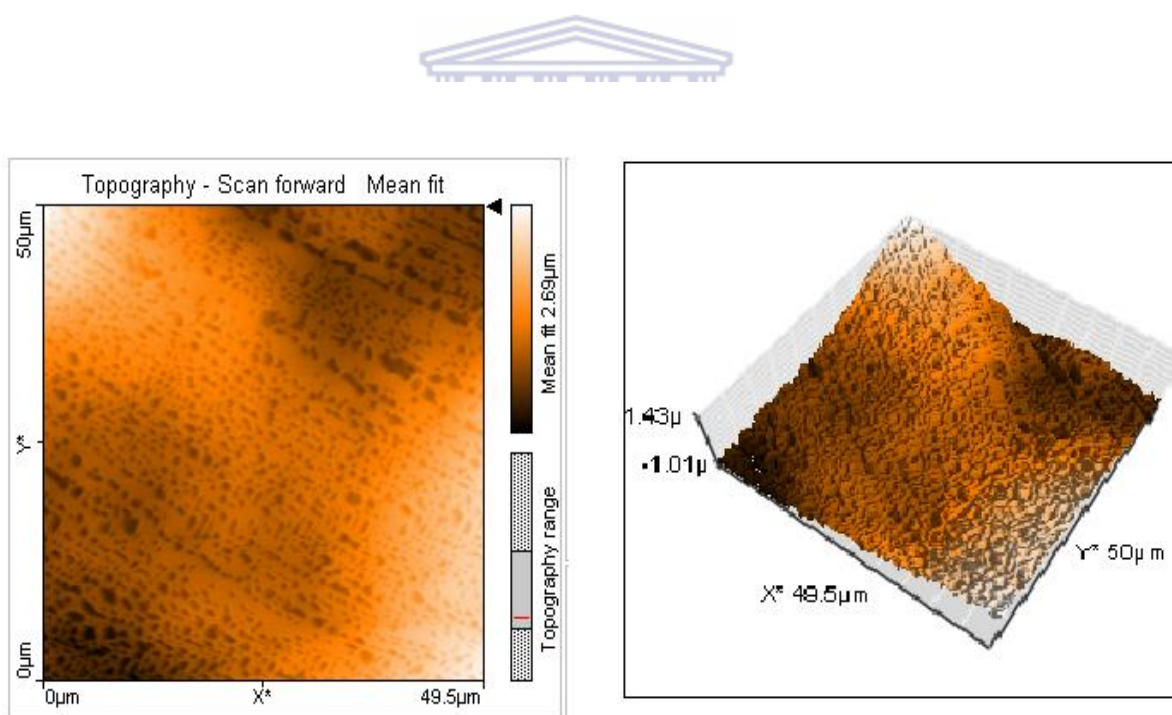


Figure A12: AFM image of polysulfone dissolved in DCM

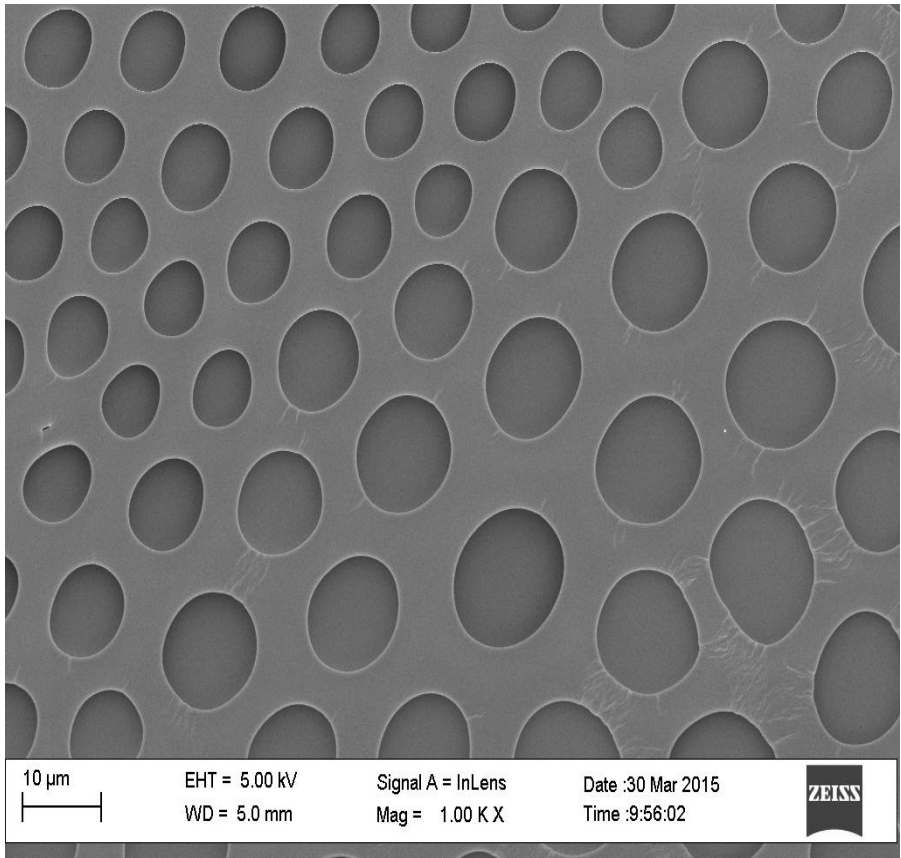


Figure A13: SEM image of polysulfone mixed with graphene oxide in DCM

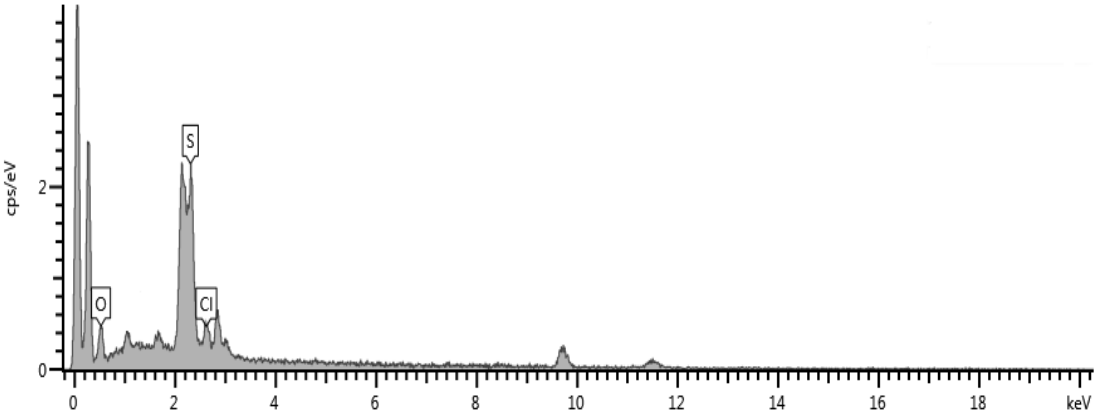


Figure A14: EDS spectrum of polysulfone mixed with graphene oxide in DCM

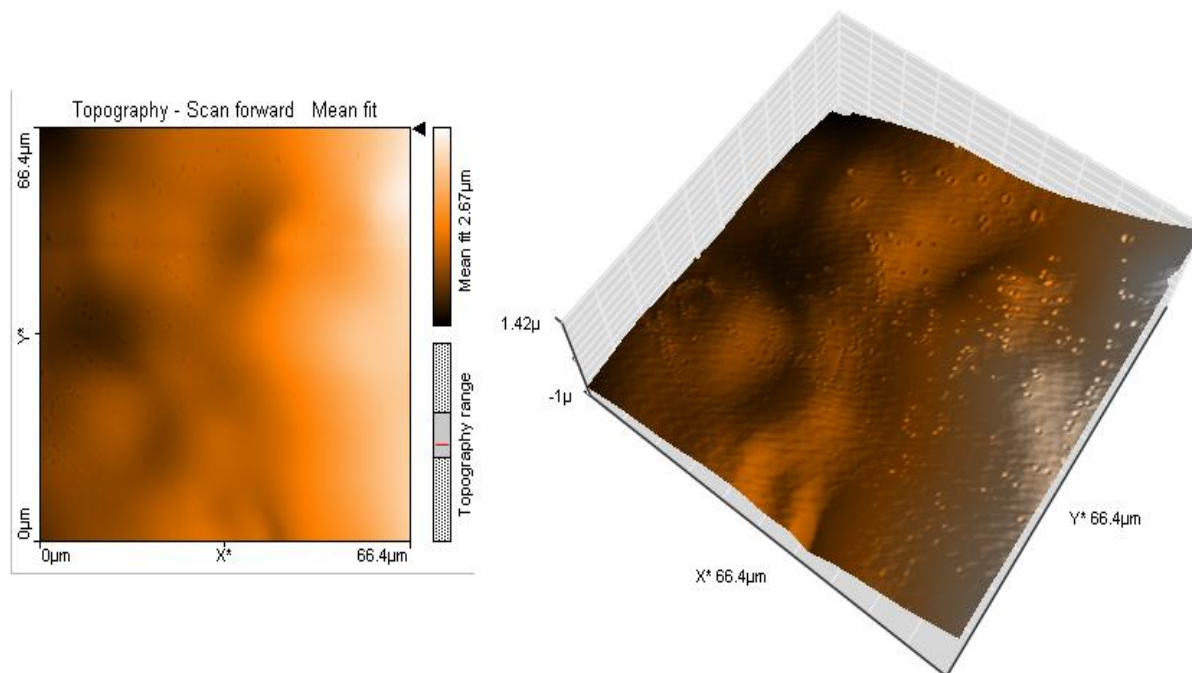


Figure A15: AFM image of polysulfone with graphene oxide in DCM

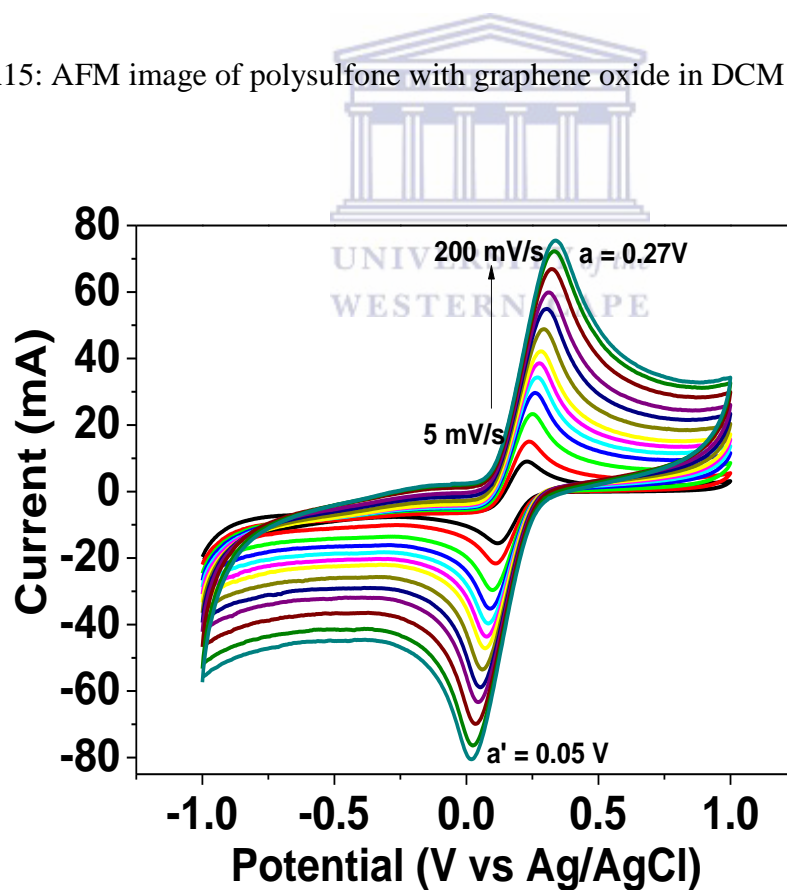


Figure A16: Characterisation of 5mM $K_3[Fe(CN)_6]$ at GO/BDD electrode by CV

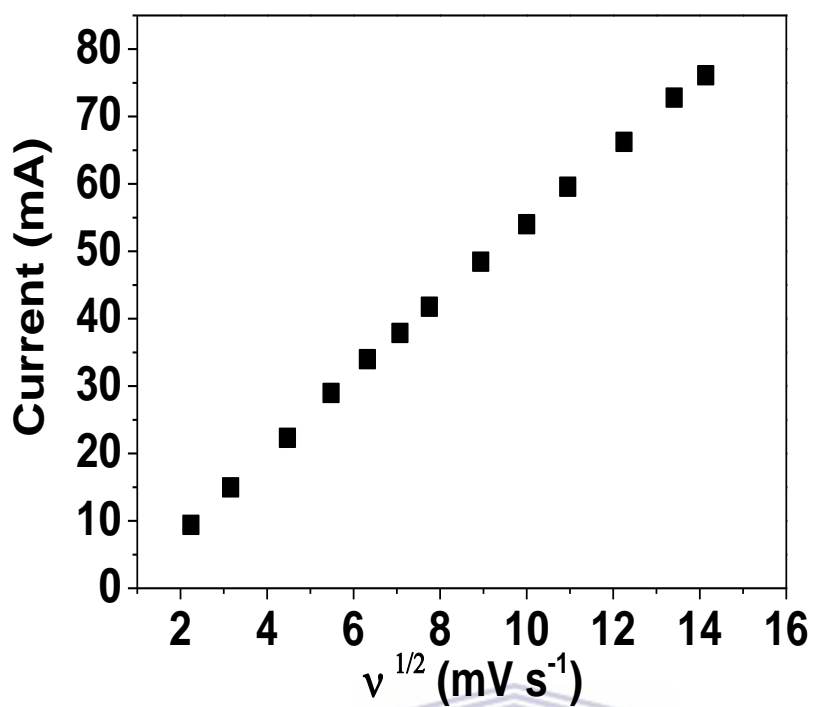


Figure A17: Current vs. square root of scan rate plot for 5mM $K_3[Fe(CN)_6]$ at GO/BDD electrode

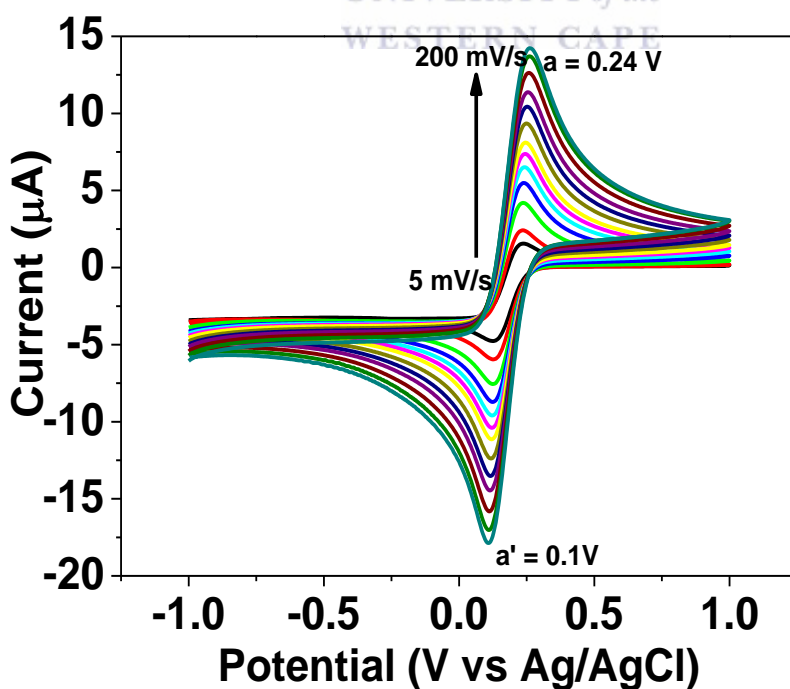


Figure A18: Characterisation of 5mM $K_3[Fe(CN)_6]$ at PSF/BDD electrode by CV

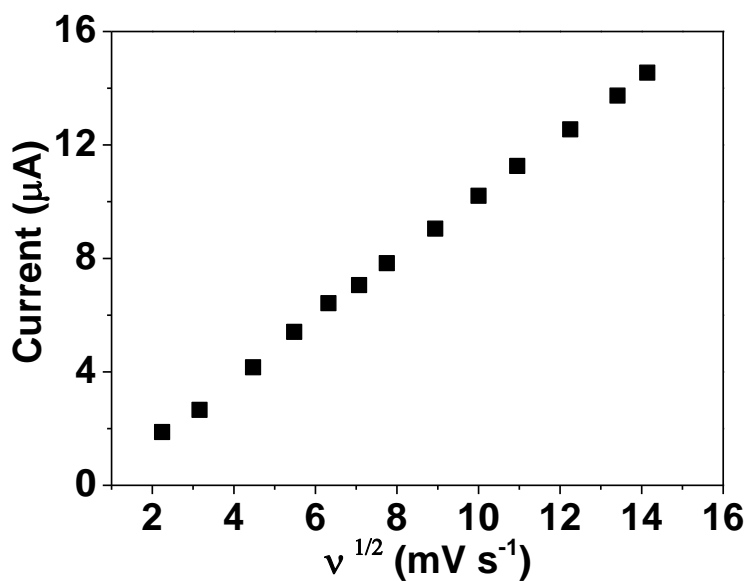


Figure A19: Current vs. square root of scan rate plot for 5mM $K_3[Fe(CN)_6]$ at PSF/BDD electrode

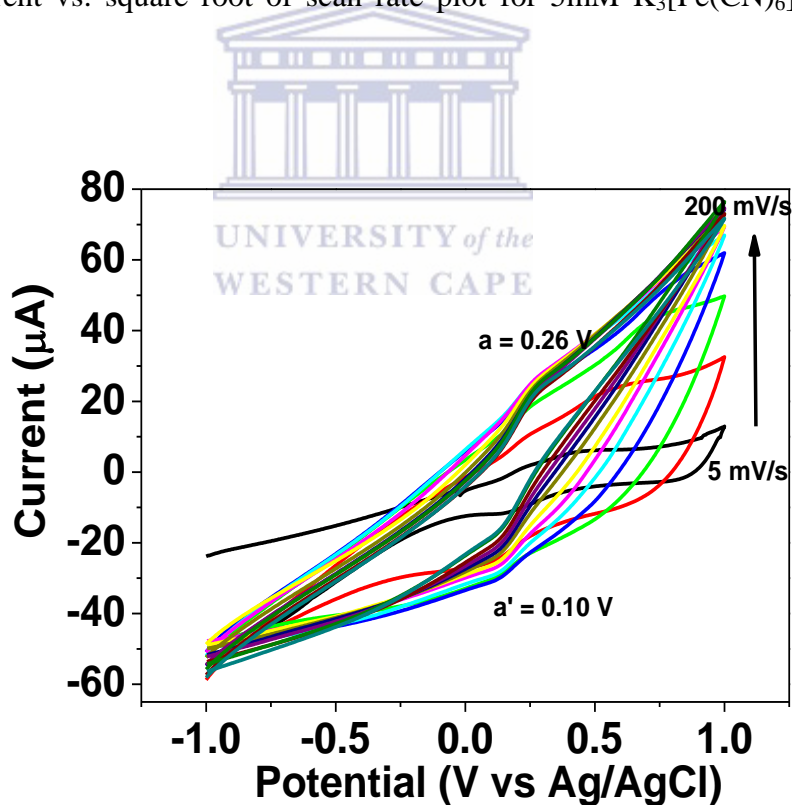


Figure A20: Characterisation of 5mM $K_3[Fe(CN)_6]$ at PSF-GO/BDD electrode by CV

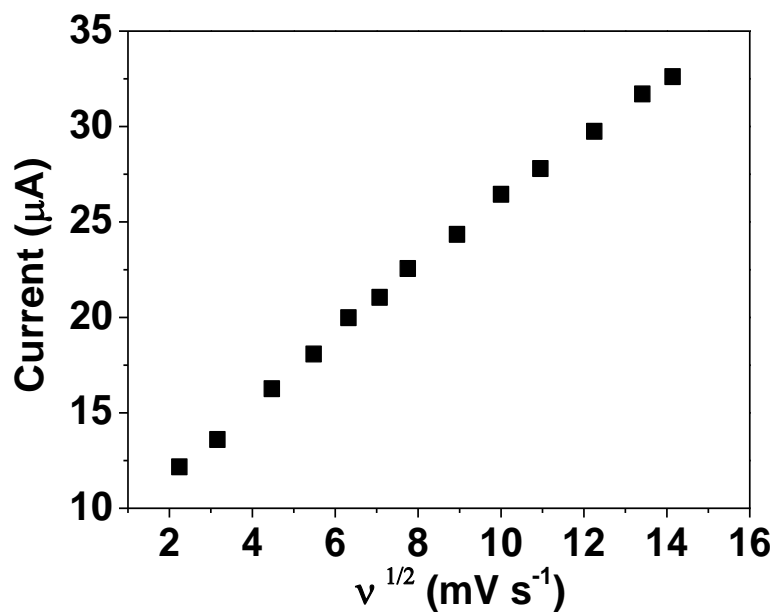


Figure A21: Current vs. square root of scan rate plot for 5mM $K_3[Fe(CN)_6]$ at PSF-GO/BDD electrode

Table A1: Diffusion Coefficient and formal potential of 5mM $K_3[Fe(CN)_6]$ at GO/BDD, PSF/BDD and PSF-GO/BDD electrode

Electrode	Diffusion Coefficient ($cm^2 s^{-1}$)	Formal Potential (mV)
Graphene Oxide / BDD electrode	$I_{pa} = 7.667 \times 10^{-3}$ $I_{pc} = 7.434 \times 10^{-3}$	173.5
PSF in DCM / BDD electrode	$I_{pa} = 1.058 \times 10^{-4}$ $I_{pc} = 1.060 \times 10^{-4}$	180
PSF/GO in DCM / BDD electrode	$I_{pa} = 1.349 \times 10^{-4}$ $I_{pc} = 7.893 \times 10^{-5}$	200.6

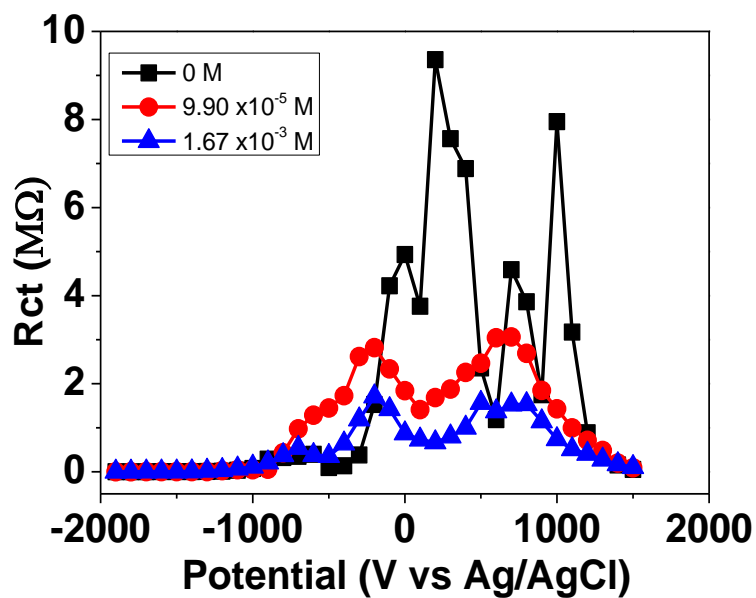


Figure A22: Rct plot of neomycin at PSF-GO/BDDE measured at different potentials

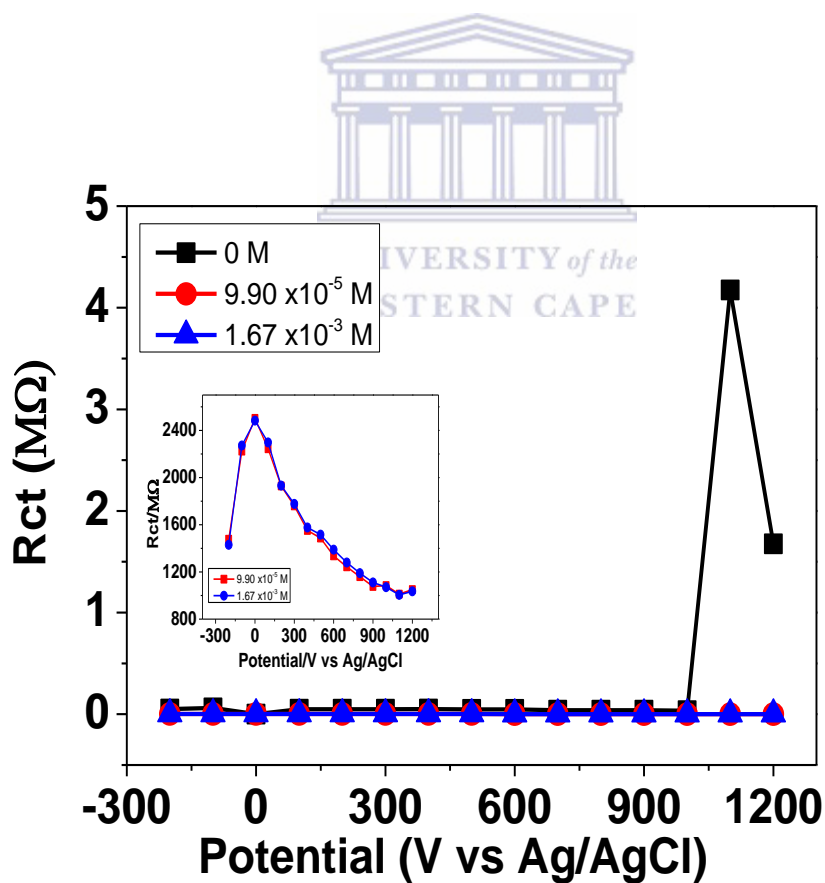


Figure A23: Rct plot of penicillin G at bare BDDE measured at different potentials

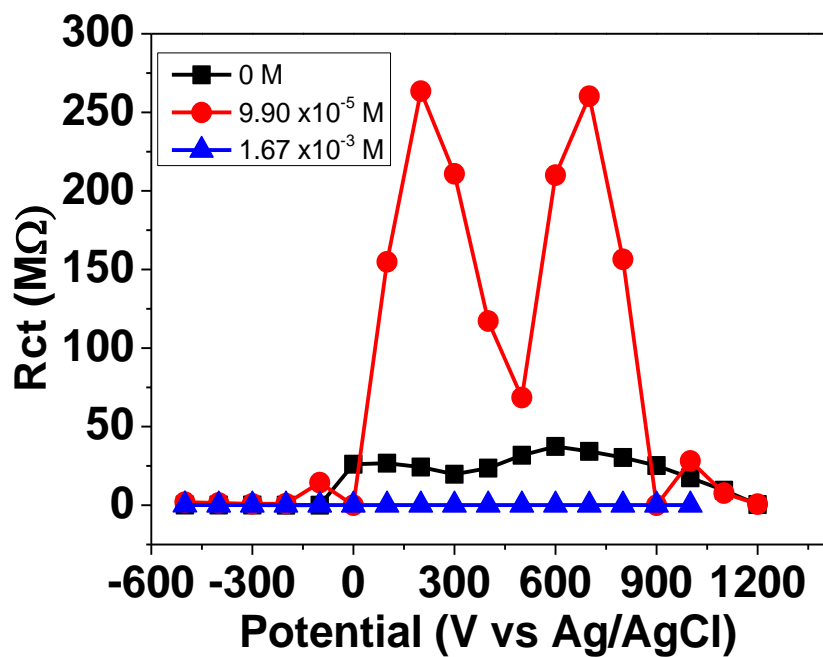


Figure A24: Rct plot of norfloxacin at unmodified PSF/BDDE measured at different potentials

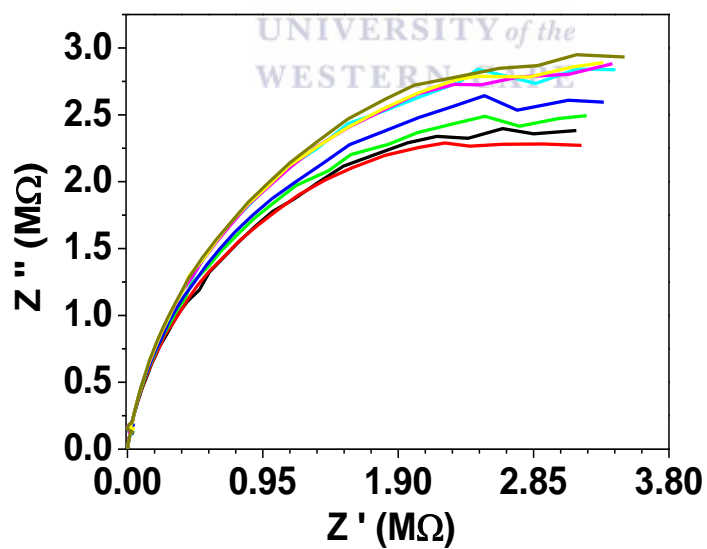


Figure A25: (a) Detection of neomycin by EIS at low frequency range.

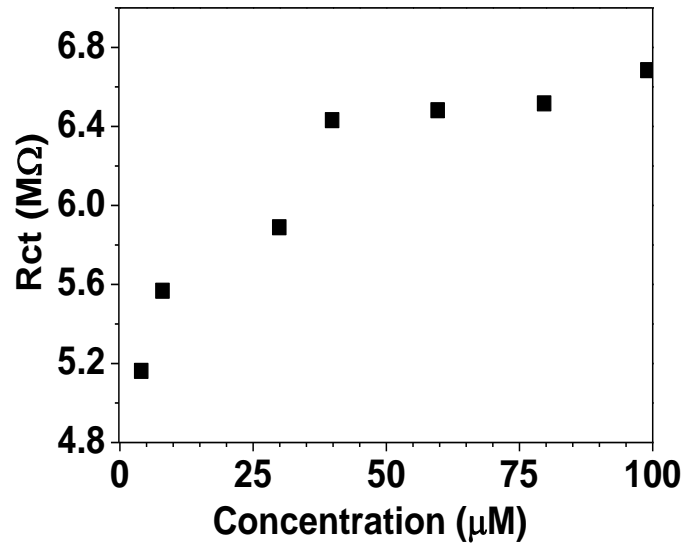


Figure A25: (b) Calibration curve of neomycin using R_{ct} extracted from Nyquist plot

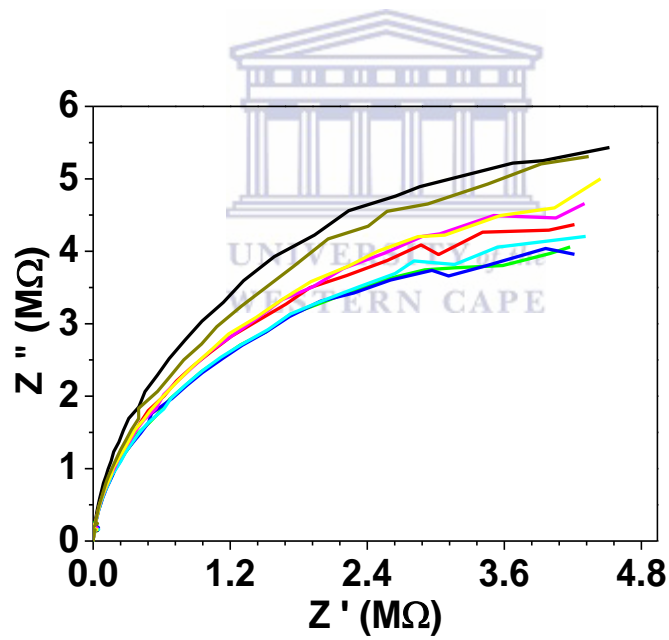


Figure A26: Detection of penicillin G by EIS at low frequency range.

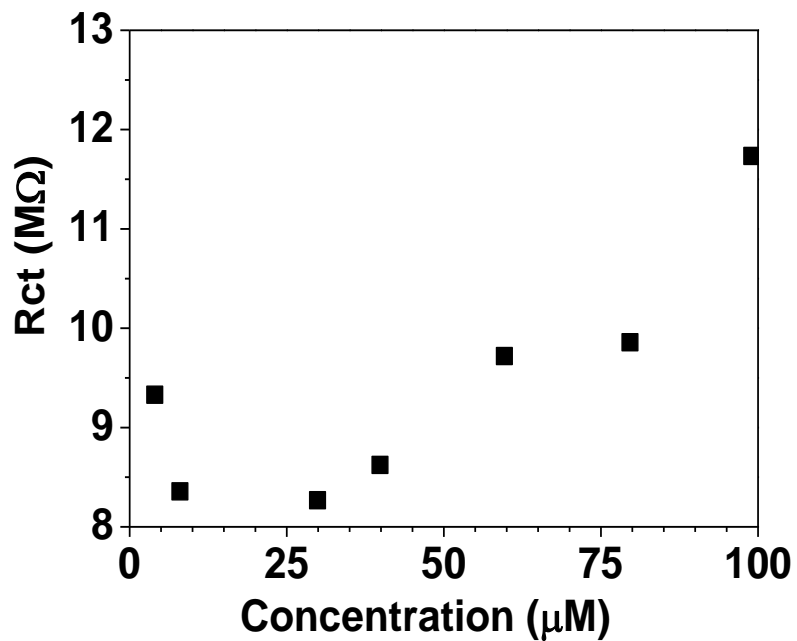


Figure A26: (b) Calibration curve of penicillin G by EIS using Rct extracted from Nyquist plot

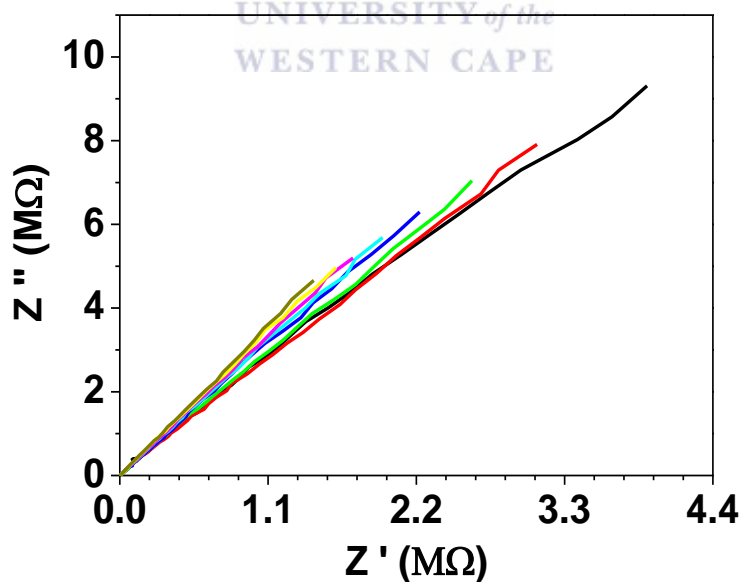


Figure A27: (a) Detection of norfloxacin by EIS at low frequency range.

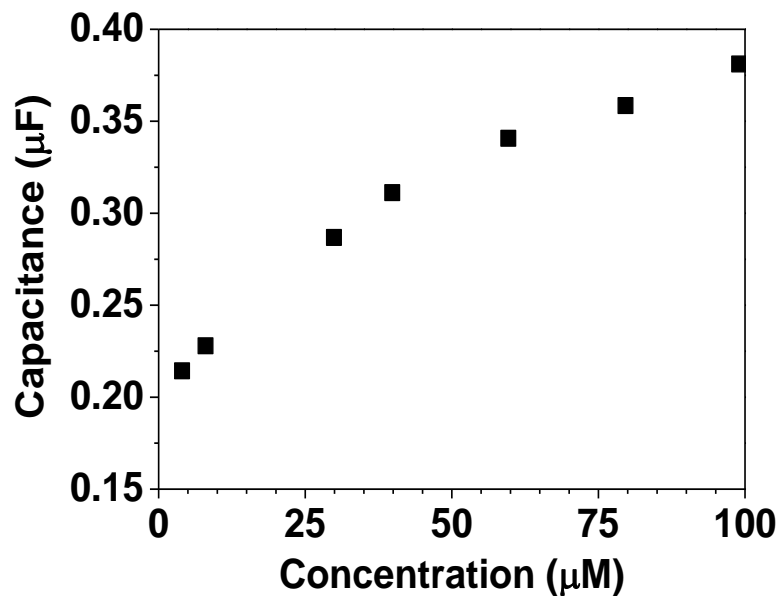


Figure A27: (b) Calibration curve of norfloxacin using R_{ct} extracted from Nyquist plot

